1970

The Formation and Reactivity of BORON CARBIDE and related materials

JONES, JAMES ALFRED

The Formation and Reactivity of

BORON CARBIDE and related materials

A Thesis presented for the Research Degree of

DOCTOR OF PHILOSOPHY

of the

COUNCIL FOR NATIONAL ACADEMIC AWARDS

London

by

JAMES ALFRED JONES

Department of Chemistry
Plymouth Polytechnic
Plymouth, Devon.

February, 1970.

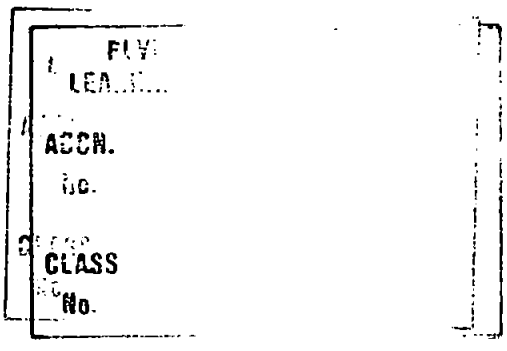

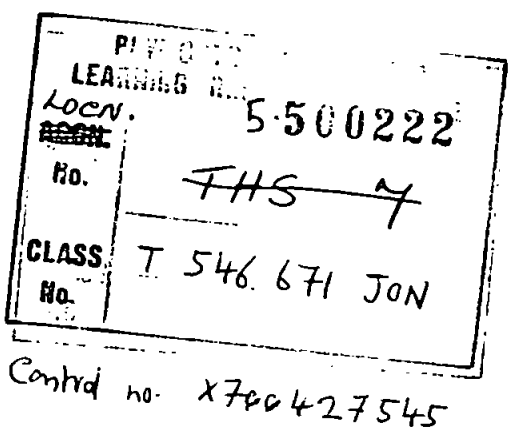

Control no. X700427545

A B S T R A C T

The formation of boron carbide, $(CBC)^{+}B_{11}C^{-}_{3}(B_4C)$ is reviewed with special reference to newer production methods and fabrication techniques. Its crystal structure and the nature of its bonding are discussed in relation to those of other borides and carbides.

Information so far available on the sintering of this material is summarised in relation to its reactivity. Sintering into monolithic components can only be achieved by hot pressing at pressures between 200 and 300 $Kgcm^{-2}$ and at temperatures above 2000°C preferably at about 2,300°C for the most rapid achievement of theoretical density, i.e. pore free.

High purity, stoichiometric boron carbide produced by the magnesium thermal reduction of boric oxide in the presence of carbon, and of submicron average particle size, has been oxidised by heating in air. The work indicates that there is preferential oxidation of boron at temperatures below 800°C; any oxidation of the resultant carbon is inhibited by the product B_2O_3 phase. The measured activation energy of 23.9 Kcals per mol supports this view.

Formation of mixed systems of titanium borides are described, including both orthorhomic and cubic monoboride together with the hexagonal diboride. These are formed when titanium alloys (alpha, beta, and mixed alpha and beta) are coated with boron carbide and heated to 1400°C under vacuum or inert atmosphere.

A C K N O W L E D G M E N T S

The author wishes to express his sincere thanks to Dr. D.R. Glasson for his supervision and guidance throughout the course of this work.

He is grateful to Mr. L. Bullock, Managing Director, Bullock Diamond Products Ltd., Torpoint, Cornwall, and to Dr. A.B. Meggy, Head of the Chemistry Department, Plymouth Polytechnic, for the use of facilities and the supply of materials. His thanks are also due to Noel Pearman, Andrew Johnson and Margaret Sheppard for their technical assistance and to Miss Loraine Ash who typed the manuscript.

He is indebted to his wife, Dorothy, for her constant help and encouragement.

****

C O N T E N T S

SECTION 1, INTRODUCTORY SURVEY AND REVIEW

I.I. General discourse.

In spite of early historical applications, long history of investigation and use, boron and its compounds have not been extensively investigated until recent years. Studies of their inorganic chemistry and metallurgical science have been limited by the relatively low concentration of the element in the earth's crust, the specifity of its raw material sources. Also there are difficulties in conducting the appropriate investigations due to the unique character of boron which occupies an intermediate position between the metals and nonmetals in the Periodic classification.

Boron, Latin name borax, is already mentioned in the ancient works on chemistry and metallurgy dating from 800 A.D. in connection with its use as a flux. In 1702, V. Goldberg described the production of an acid from borax (sodium tetraborate) but believed this acid to be a salt. In 1748, F. Baron proved that borax is a salt of boric acid. In 1777, this boric acid was discovered by G. Hoeffer in one of the lakes of Tuscany.

The high affinity of boron for numerous elements, especially for oxygen, made it impossible to isolate pure boron and its alloys. Ultimately, elementary boron was obtained, independently in 1808, by Sir Humphry Davy and by the French chemists Gay-Lussac and Thenard.

By far the most important investigations of boron and its compounds were by Henri Moissan. In 1892, Moissan developed a method for producing boron by reducing boric anhydride with magnesium, a method which is still in use at the present time. In

1899, he obtained a compound of boron with carbon, viz., boron carbide, and subsequently the borides of chromium, titanium and tungsten and those of silicon and boron steels.

In 1909, Moissan's research was continued by Weintraub who discovered the semiconductor properties of boron, and by Wedekind and Kroll who produced all the refractory borides known at present.

A number of works on boron and borides were conducted in the 1930's and 1940's by Becker, Agte, Moers and Andrieux. These investigations developed the production of boron and borides by deposition from the dissociated gaseons halides and by the electrolysis of fused media. However, the basic research on boron and borides has been stimulated over the past two decades, by the interest in heat resistant alloys containing boron and refractory borides; fundamental work has been done by Kiessling (Switzerland) Kieffer, Benesovsky, Hovak, Nowotny (Austria), Glaser, Schwarzkopf, Binder, Blumenthal, Moskowitz, Post, Brewer (United States), and Samsonov, Neshpor, Umanskii, (U.S.S.R.).

The compound of boron with carbon produced by Moissan on smelting boric anhydride with sugar charcoal in an electric arc furnace was assigned the formula B_6C from analytical results. It was one of a number obtained by Podzus (1933), viz., BC, B_2C_2, B_3C, B_4C and B_6C. The product called <u>boron carbide</u> which had been on the market some years as a metallurgical source of boron had roughly the composition BC. However, Ridgway (Chipawa Plant, Ontario, of the Norton Company of America) patented a process in 1934 for the production of a definite crystalline compound having

an average composition closely approximating the formula, B_4C, for use as an abrasive. This outstanding contribution laid the foundations on which are built our present knowledge of the boron-carbon system and of the related metal borides with all their complexity and profuseness.

Studies of metal and nonmetal borides have been mainly concerned with their preparation, characterisation, structure, and physical properties; bonding has received some attention but comparatively little is known about their chemistry. A number of reviews have dealt in some detail with particular aspects such as structure, preparation, and physical properties for example, Schwartzkopf and Kieffer (1953), Aronsson et al. 1965), Post (1964), Hoard and Hughes (1967) and Thompson and Wood (1963), but only those of Samsonov and Markovskii (1960), Greenwood et al. (1966) and the recent review of Glasson and the Author (1969) covers aspects of their chemistry as well.

The present work carried out during the period 1964 to 1969 in the John Graymore Chemistry Laboratories of The College of Technology, Plymouth, and at the Works of the Bullock Diamond Products Limited, Torpoint, Cornwall, concerns the production on a semi-technical scale of boron carbide of a particularly high purity and in a highly crystalline state. Its reactivity is studied with regard to (a) its homogeneous sintering with and without additives, (b) its application to the formation of transition metal refractories and (c) the resistance of these materials to oxidation, nitridation and hydrolysis. This stimulates from a need to produce abrasive-resistant surfaces on

machine tools and similar articles for application in a large number of industrial concerns.

I.2. The classification of borides, carbides and related materials

Data for the properties of many refractory borides, carbides, silicides, etc., have been collated and reported by a number of workers in their respective fields, namely Schwarzkopf and Kieffer (1953), Campbell (1956), Gangler (1949), Warde (ca. 1950), Finlay (1952), Bradshaw (1958), Hiester (1957), Lange (1960) and others. However, the most truly comprehensive collations are by Shaffer (1964) and Samsonov (1964); in particular the latter is extremely valuable as it covers otherwise unpublished or obscure material by the author and other workers in the U.S.S.R.

It is difficult to define the term 'refractory compound' since any subdivision into refractory and non-refractory compounds is arbitrary and presupposes the fixing of some melting-point boundary, above which, chemical compounds are considered to be refractory. Such a boundary has been repeatedly established and has gradually been shifted to regions of higher and higher temperature, from 1000°C in the second half of the last century, to 2000°C in the first half of this century, and often currently is assumed to be 3000°C.

Nevertheless, the expression 'refractory compound' is now gradually losing its original meaning and is becoming deeper and more fundamental, encompassing a whole complex of properties, including high hardness, brittleness, and heat of formation, as well as specific electrical and magnetic properties as determined by the electronic structure of the corresponding compounds and the

position of their components in the periodic system of the elements. Thus, a refractory compound need not always be one of high melting point, but may denote a substance possessing a combination of other properties, e.g. high hardness, low vapour pressure and rate of evaporation, and resistance to chemical attack. The principal tenor of the concept of 'refractiveness' is increasingly becoming the character of the chemical bond between the component atoms of the compounds, which is mainly metallic or covalent with a small degree of ionic bonding. Such types of bond occur as a rule (i) in compounds of metals (mainly transition metals or metals similar to them, according to a number of criteria) with non-metals of the type boron, carbon, silicon, nitrogen, sulphur, phosphorus, etc., not having ionization potentials high enough to produce ionic bonds, (ii) in compounds between nonmetals and (iii) in certain intermetallic compounds.

Compounds of the first class are conveniently called 'metal-like' refractories; a necessary condition for the formation of metal-like refractories is the participation of incomplete d and f electron levels, i.e. a transition metal characteristic. As a qualitative criterion, Samsonov (1953, 1964) proposed the use of the quantity, $1/Nn$, where n is the number of electrons in the n incomplete level, signified by the principal quantum number N; another factor is the ability of atoms of the nonmetal to donate valence electrons, given by the magnitude of their ionization potentials. The electron density between the atom cores in the crystal lattice and its distribution depend on the values of n, N and I.P. nonmetal; an increase in $1/Nn$ (acceptor capacity of the metal) produces a

displacement of the electron concentration towards the metallic atom for a constant donor, whereas an increase in ionization potential of the nonmetal for a constant acceptor produces a displacement towards the nonmetal with a corresponding increase in ionic character. Thus, variations in the values of 1/Nn and I.P. nonmetal produce diversity, but for a binary system the number of combinations are not infinitely large. This in turn determines the continually discrete character of the variation in the type of bond, and, correspondingly, of the physical and chemical properties of this class of compounds in which the chemical bonds are heterodesmic.

Borides, where the boron atoms are isolated from each other (M_2B), have the boron valence electrons predominantly in the free d levels of the metal atom. In the more complex structures, having chain and network structures of boron, the nonmetal valence electrons are mainly expended in the formation of covalent catenated bonds and a smaller proportion is transferred to the general electron aggregate, symptomatic with metallic bonding. Conversely, in carbides the proportion of metallic bond increases as the result of the higher ionization potential of carbon, and they possess typical metallic properties. Silicides follow more closely the behaviour of borides, while nitrides tend to be ionic and compare more closely with oxides.

The second class of refractory compounds is formed by compounds of nonmetals with each other or the so-called nonmetallic refractory compounds; all of these compounds, like the metal compounds, are characterised by a heterodesmic character of the bond,

but with predominance of the covalent bond, and they have semiconductor properties as well as high electrical resistance at room temperature; as a rule, these compounds have a structure with layer, chain or skeletal structural groups, and either melt with decomposition or decompose before reaching the melting point.

Table I.2.1 shows a number of currently known compounds of this class.

T A B L E I.2.1.

Element	Ionisation potential, ev.	Si	B	S	P	C	N
Si	8.14	Si	Si_xB	Si_xS	SiP	SiC	Si_3N_4
B	8.28	B_xSi	B	B_xS	B_xP	B_xC	BN
S	10.42	S_xSi	B_xS	S	S_xP	-	-
P	10.43	SiP	B_xP	S_xP	P	-	-
C	11.24	SiC	B_xC	-	-	C (diamond)	-
N	14.51	Si_3N_4	BN	-	-	-	-

In crystals of the elements situated along the diagonal, indicated by the arrows, the width of the energy gaps increases in the direction of the arrows, while in the compounds formed between these elements it may be assumed that there will be an increase in the proportion of ionic bond with increase in the difference in ionisation potentials of the components (from Si_xB to Si_3N_4, from Si_3N_4 to BN, etc.). Finally, three elements of the periodic system occupy an intermediate position with regard to the ability to form refractory metal-like and nonmetallic compounds, despite their low melting

point and high vapour pressure. These elements, beryllium, magnesium and aluminium, are capable of forming fairly refractory semiconductor compounds, with nonmetals, for example, beryllium, magnesium, aluminimum borides, aluminium nitride, magnesium silicides, etc.

The third class of refractory compounds of metals with each other - intermetallic compounds, has recently been discussed in depth by Westbrook (1966), and include beryllide, magnide and aluminide systems of other metals.

On the basis of this classification, it is possible to explain a number of the properties of refractory compounds and also the direction of their variations, such as their thermal and chemical stability, their mechanical properties such as hardness and strength, and of course their electrical and optical properties.

In the present work only data of certain compounds of the second class are considered, unless there is a specific need to compare such data with that of compounds of the other two classes.

I.3. The structural properties of the boron carbides and related materials and their application

The covalent radius of an element coupled with its ionisation potentials serve as a qualitative indication of the nature of its bonding in both catenate and alternate modes. Both parameters must be treated with reserve. Covalent radii are average values from a number of compounds or are a specific value for the element in a particular allotropic form, e.g. carbon in graphite or in diamond, and indicate the contribution of the element, in

terms of bond length, to the covalent bond formed between two elements. The term "ionisation potential" is the energy for the removal of the outer-most electron to infinity, from an atom in the gaseous state; nevertheless, they show the contribution, in terms of electron density, to the covalent bond.

The use of the covalent radius of an element to give a definitive indication of an 'interstitial' compound from its ration with the host element, has been applied rigorously by Hägg et al (1930). In the case of refractory compounds of the second type formed by atoms of comparable size and ionisation potential, such a classification has no relevance.

Table I.3.1. shows the accepted covalent radii for related elements and the ratio of these values to one another.

T A B L E I.3.1.

The covalent radii of some light elements forming refractory compounds

B			A1	C	Si	N
covalent radius / atomic weight		0.82	1.18	0.77	1.11	0.75 Å
B	10.811	1.000	1.439	0.939	1.354	0.915
A1	26.9815	0.695	1.000	0.653	0.941	0.636
C	12.0111	1.065	1.532	1.000	1.442	0.974
Si	28.086	0.739	1.063	0.694	1.000	0.676
N	14.0067	1.093	1.573	1.027	1.480	1.000

Table I.3.2. gives the composition of the refractory compound under discussion as represented by 'ideal' stoichiometric formulations, and it should be noted that many of these compounds exist in a form having the same crystal structure (Table I.3.3.) for a wide range of compositions, i.e. the so-called homogeneity range.

TABLE I.3.2.

The compositions of some related refractory compounds

Phase	Formula weight	'metalloid' * % atomic	content % weight
AlB_{10}	135.18 g/mole	90.91	80.05
AlB_{12}	156.82	92.31	82.80
Al_4C_3	143.95	42.86	25.03
AlN	40.99	50.00	34.18
$B_{13}C_2$	164.68	86.67	85.40
$B_{12}C_3$	165.87	80.00	78.68
B_6Si	92.95	14.29	30.22
'B_4Si'	71.37	20.00	39.36
B_3Si	60.52	25.00	46.39
BN	24.83	50.00	43.57
SiC	40.07	50.00	70.05
Si_3N_4	140.22	42.6	60.06

* the most electropositive element

i.e. the foremost element in the phase formulation

T A B L E I.3.3.

Crystal Structures of some refractory compounds

Phase	Unit Call	Space group	Structure Type	a Å	b Å	c Å	α	c/a	Reference	Year
AlB_{10}	Rhombic	---	---	8.881	9.100	5.690	--	--	Cohn et al	1948
AlB_{12}	Tetrag.	D_4^4 - $P4_12_1$	---	10.161	--	14.283	--	1.41	"	"
AlB_{12}	Rhombic	D_{2H}^{48} - Imma	---	12.34	12.631	10.161	--	--	"	"
Al_4C_3	Rhombohed.	D_{3d}^5 - R3m	Al_4C_3	8.53	--	--	28°17'	--	Stackelberg	1934
AlN	Hexagonal	C_{6v}^4 - C6mC	ZnS	3.104	--	4.965	--	1.600	Bokii	1954
$B_{13}C_2$	Rhombohed	D_{3d}^5 - $R\bar{3}m$	B_4C	5.598	--	12.12	--	2.165	Zhdanov	1954
$B_{12}C_3$	"	D_{3d}^5 - $R\bar{3}m$	B_4C	5.630	--	12.19	--	2.16	"	1954
B_6Si	Rhombic	---	---	14.392	18.267	9.88	--	--	Cline	1959
B_4Si	Hexagonal	D_3^7 - R32	B_4C	6.330	--	12.736	--	2.012	La Place	1961
B_3Si	Tetragonal	---	---	2.829	--	4.765	--	1.63	Samsonov	1955
BN	Hexagonal	D_{3h}^1 - $P6m^2$	Graphite	2.504	--	6.674	--	2.665	Popper	1958
SiC IV	Rhombohed.	C_{3v}^5 - $R\bar{3}m$	---	17.718	--	--	9°58'	--	Bokii	1954
SiC VI	"	C_{3v}^5 - $R\bar{3}m$	---	27.759	--	--	6°21.5'	--	Bokii	1954
SiC	Cubic F.C.	T_d^2 - $F\bar{4}3m$	ZnS	4.358	--	--	--	--	Bokii	1954
Si_3N_4	Hexagonal	C_{3v}^4 - H3C	---	7.76	--	5.64	--	0.725	Narite	1959
Si_3N_4	Hexagonal	D_3^2 - P63/m	---	7.59	--	2.92	--	0.385	Narite	1959

The crystal structures of the refractory compounds given in Table I.3.3. are discussed in more detail in Section I.4, and their indexing by X-ray diffraction in ~~Appendix II~~ Section 2.2.

Table I.3.4 gives the temperature stability range of these phases, unless a range of values is actually given, the temperature given is the maximum of the stability range.

TABLE I.3.4.

Temperature stability ranges

Phase	Temperature stability range, °C	Reference	Year
AlB_{10}	1660 - 1850	Serebryanskii	1961
Al_4C_3	2100	Slavinskii	1952
AlN	2230	-	1958
$B_{13}C_2$	2480	Vuillard	1959
$B_{12}C_3$	2350	"	1959
αSiC	2100	Samsonov	1959
βSiC	2650	"	1959
αBN	3000	Sindeband	1950
αSi_3N_4	1900	-	1958
βSi_3N_4	1900	-	1958
B_4Si	1370	Matkovich	1960
B_6Si	1370	"	1960
C pyrographite	3652	-	1959

I.4. The crystallo-chemical structure of the boron carbides

To understand the complex structures found in these materials requires a detailed knowledge of the element itself. Boron has an extra-nuclear structure of five electrons. In the ground state two of these are in the K-shell and the remaining three valence electrons occupy four low-lying orbitals which are available for bonding; the boron atom is thus electron deficient.

B.5 

In the solid form the element does not assume the usual metallic state encountered in such cases, but rather it crystallizes into a variety of polymorphic forms, all of which are extremely hard semiconductors.

In the majority of the nonmetallic elements where catenation of like atoms or alternation of dissimilar atoms take place, viz., two-centre bonding, the bond consists of an orbital embracing the two atomic nuclei and containing the maximum of two electrons. It is often necessary to invoke 'hybridisation' of the atomic orbitals to explain the co-ordination maxima and stereochemistry of these elements. However, in the case of boron, polycentred bonds are the rule both in catenation and alternation; e.g., three boron atoms in a trigonal plane are bonded together by a three-centred orbital embracing the nuclei and filled by only two electrons; such economy allows for further bonding by each atom. The wave mechanical operation (after Lipscomb 1958) takes a linear combination of the available 2s and 2p atomic orbitals, viz :-

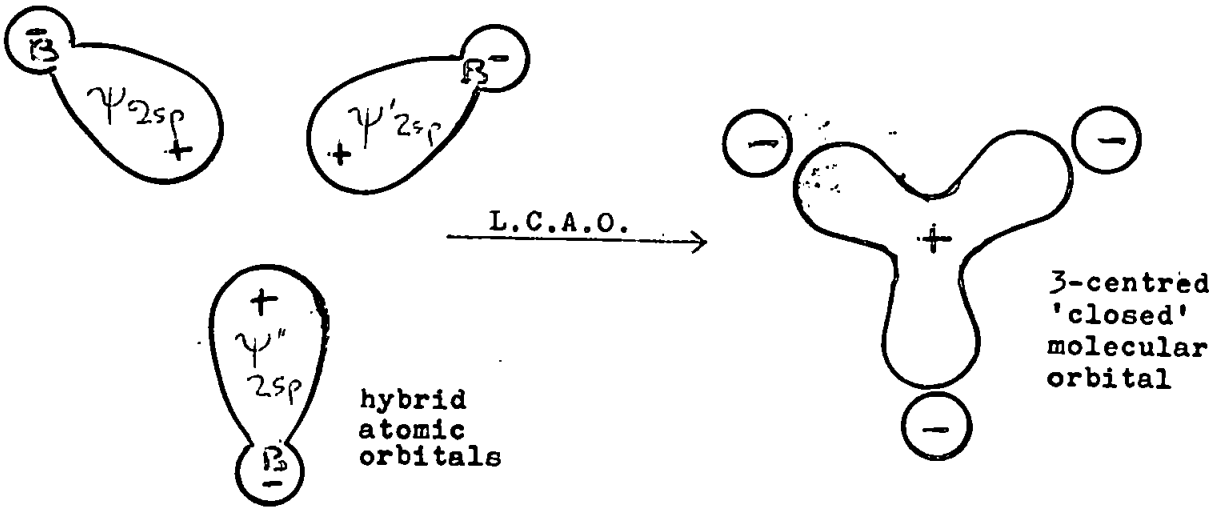

Higher-centred bonds are possible involving four, five, six and even twelve boron atoms; e.g., in the common B_{12} structural unit the atoms are located at each vertex of an almost regular icosahedron (Fig. I.4.1); each boron atom is involved in three-centre bonding with its five immediate neighbours and in a twelve-centre bonding with these and the remaining six atoms, requiring 26 of the 36 electrons available for the intra-icosahedral bonding. In the simpler rhombohedral form of boron, the ten remaining electrons are required for extra-icosahedral bonding of the twelve atoms to neighbouring icosahedra (six in three-centre bonding and six in two-centre bonding). In cases where the extra-icosahedral bonding are all of a two-centre kind, donation of two electrons to give a B_{12}^{2-} anion is needed (e.g. B_{12}^{2-} CBC^{2+}).

Fig. I.4.1.

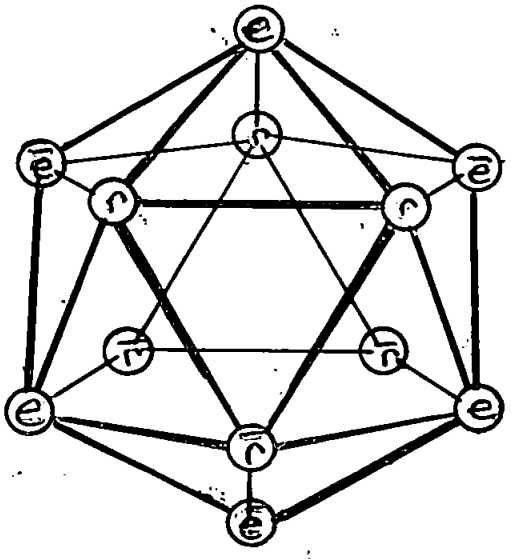

The icosahedron shares with the tetrahedron, the octahedron and the dodecahedron the distinction of being one of the five regular convex Platonic polyhedra; all are ~~icosa~~iso hedral with regular polygons as faces and possess a set of equivalent vertices which lie on the surface of a circumscribed sphere. The icosahedron has twelve vertices with five edges and five faces at each vertex, the thirty edges defining twenty equilateral triangles. It is a highly symmetric structure element, endowed with considerably more symmetry than can be utilised in a three-dimensional crystallographic array, having 31 rotational symmetry axes, 15 twofold axes connecting centres of opposite edges, 10 threefold axes connecting centres of opposite faces, 6 fivefold axes linking opposite vertices, 15 mirror planes passing through opposite edges and is centrosymmetric. Eliminating redundancy leaves a collection of symmetry of order 120; this constitutes a non-

crystallographic point group comparable to the crystallographic point group of highest symmetry Oh - m3m of order 48, which describes the symmetry of the cube and the regular octahedron. Fivefold rotation is not utilised in two or three-dimensional periodic networks. A molecule or group possessing this symmetry can use any other crystallographic symmetry it might possess or it can be propagated as an antisymmetric element in a general position by the translation symmetries; in either case, the extent to which it simulates fivefold symmetry is a measure of its internal rigidity while interacting with external neighbours must induce some distortions. Since these are small in even strong intericosahedral linkage it is possible to discuss the structures in terms of dimensionally regular icosahedra. They are not only complex because of the various detailed accommodations that must be made, but are also characteristically rather open networks, with regularly spaced holes large enough to contain metal and other impurity atoms. Moreover, the structures are susceptible to modification by inclusion in the three-dimensional frameworks of additional boron or other atoms in positions that relieve the strains imposed by the difficulty of propagating the pentagonal structure elements. An icosahedron provides an extremely efficient way of packing twelve spheres about a point very little different from the packing a twelve spheres around a central sphere as in cubic close-packing except that the cavity in an icosahedron has a diameter of 0.90 that of the sphere, rather than unity. This reduction of the interior volume (by about 30%) results in a serious loss of external three-dimensional packing efficiency.

Within a B_{12} icosahedron each boron atom forms five bonds symmetrically disposed to a fivefold axis of symmetry. In three-dimensional framework structure each boron atom characteristically forms one additional bond directed outwards towards an atom in another icosahedron or towards an interposed framework atom giving a co-ordination number of six for each atom; the preferred co-ordination polyhedron for a boron atom is a pentagonal pyramid (Fig. I.4.2.) the bond to the five atoms in the base are 60° apart and are inclined at $121^{\circ}43'$ to the bond along the unique axis. The length of the unique bond varies between structures.

Fig. I.4.2.

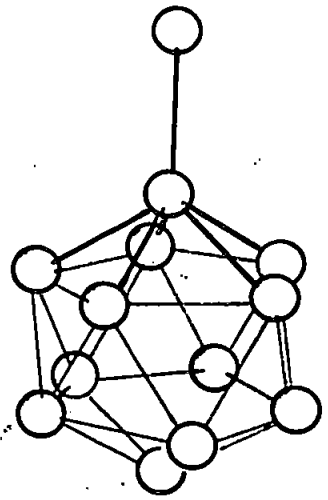

According to the results of X-ray diffraction analyses by Zhdanov and Sevastyanov (1941), and by Clark and Hoard (1943), the original description of the boron carbide structure was based upon single crystals with a stoichiometric composition B_4C corresponding to the traditional formulation of the principal compound in the boron-carbon system. This B/C ratio was satisfactorily achieved with two structural elements - a B_{12} icosahedron and a linear C_3

group in a primitive rhombohedral unit cell. All essential features of the structure remain intact over a wide composition range; variations in composition are accommodated by interchange of boron and carbon atoms at appropriate points in the framework and perhaps in some cases by inclusion of extra atoms in the open structure. Moreover, it appears that the only congruently melting compound in the system is not in fact $B_{12}C_3(B_4C)$, but is rather the thermally more stable $B_{12}(CBC)$ where the linear C_3 group is replaced by a linear C - B - C group. Recent work indicates the B_4C composition to be in fact $(B_{11}C)(CBC)$, nevertheless this refinement does not affect a discussion of the basic structure.

The icosahedron depicted (Fig. I.4.1.) in a projection along the threefold axis is labelled to distinguish between two classes of atoms (vertices) rhombohedral and equatorial. The rhombohedral atoms r and their centrosymmetric mates $\bar{r}$ subtend at the centre of a vector triplet which will be used to define the direction of the rhombohedral axes. The vectors are of equal length and directed along the icosahedral fivefold axes and are all inclined to each other at the angle $63^\circ 26'$ (more precisely arctan 2). It should be noted that a rhombohedral lattice defined by an angle of exactly 60° corresponds to a face-centred cubic array of lattice points. The remaining six atoms in the equatorial positions, e and $\bar{e}$, link in a staggered belt around the equator of the icosahedron. The atoms lie at the vertices of a flat triangular antiprism, the fivefold axes traversing the vertices are only slightly inclined ($10^\circ 50'$) to the equatorial plane.

In the boron carbide structure (primitive rhombohedral unit, space group $R\bar{3}m$) a B_{12} icosahedron is centred at each lattice point, appropriately oriented with respect to the cell axes to conform with the required symmetry $\bar{3}m(D_{3d})$. In each B_{12} the r atoms lie almost directly along the rhombohedral axes and are bonded to the equivalent atoms, $\bar{r}$ of the unit centred at the adjacent lattice points. The resulting rigid three-dimensional framework involves exactly half of the boron atoms in direct inter-icosahedral bonds each formed along quasi-fivefold axes of icosahedra.

No direct lateral connections exist between equatorial atoms in adjacent icosahedra; all such bondings must be effected through additional interposed atoms which are required to complete the framework. With this arrangement of icosahedra a substantial cavity is created at the centre of the cell along the threefold axis; the cavity is surrounded by an octahedral array of B_{12} units, three above the centre and three below. The quasi-fivefold axes traversing the equatorial atoms, $\bar{e}$, of three of these adjacent icosahedra meet precisely at a point on the threefold axis about 1.6 Å from the equatorial atoms and 1.4 Å above the centre of the cell; a corresponding intersection involving the equatorial atoms, e, in the other three icosahedra occurs 2.8 Å away, below the centre of inversion. An atom placed at or near this intersection not only stabilizes the rhombohedral framework but also satisfies the preferred coordination geometry for all the equatorial atoms. It is required only to form three bonds to boron at a reasonable distance of 1.6 Å and at approximately tetrahedral angles and to link across the 2.8 Å span, if necessary through a collinear third atom at the centre.

The geometric constraints specified above play a prominent role in determining the possible structural modifications of the boron carbide structure, they are satisfied by not only a C - B - C chain but by a variety of other nonmetal atoms.

A number of secondary considerations also permit variations in the structure without violating the basic framework. For example, the framework encloses two holes per unit cell each large enough to accommodate an extra atom. They are located on the threefold axis just above and below the central chain. Density and stoichiometry can be modified by partial inclusion of extra boron, carbon and other atoms in these holes particularly for systems prepared under conditions far from equilibrium. Another structural degree of freedom involves the partial substitution of a limited number of icosahedral boron atoms by such divergent elements as carbon, silicon and perhaps beryllium, the substitution is driven by electron deficiencies in the icosahedral framework as well as geometric constraints.

The foregoing description of the boron carbide structure has been idealised in terms of perfectly regular icosahedra; in fact, the approximations are quite good, but a number of small deviations do occur. The essential features of the framework are shown in Fig. I.4.3. which represents a section of the structure viewed down a threefold axis. Regular icosahedra with 1.80 Å edges bonded rhombohedrally at 1.80 Å would be separated by 5.22 Å at an angle of $63^{\circ}26'$. The rhombohedral lattice constants of boron carbide are $a = 5.167 \pm 0.003$ Å and $\alpha = 65.60^{\circ} \pm 0.05^{\circ}$ or

Fig. I.4.3.

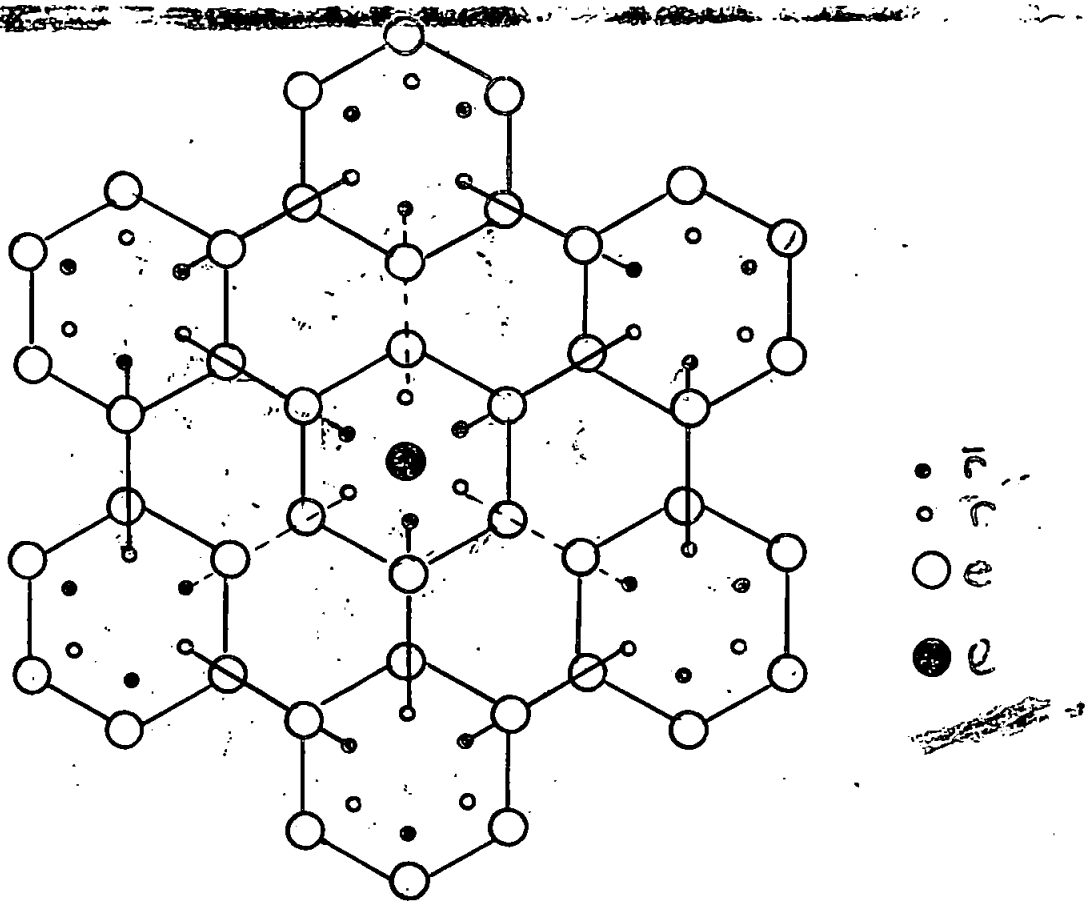

a_o = 5.58 Å and C_o = 12.00 Å for its hexagonal cell containing three rhombohedral unit structures, (Fig. I.4.4.) and the observed boron-boron distances range from 1.72 to 1.80 Å.

The intra-icosahedral bonds are all very close to 1.80 Å except for a slight constriction around. The rhombohedrally directed inter-icosahedral bonds are 1.72 Å considerably longer than the 1.60 Å equatorial bonds to the carbon atoms (covalent

Fig. I.4.4.

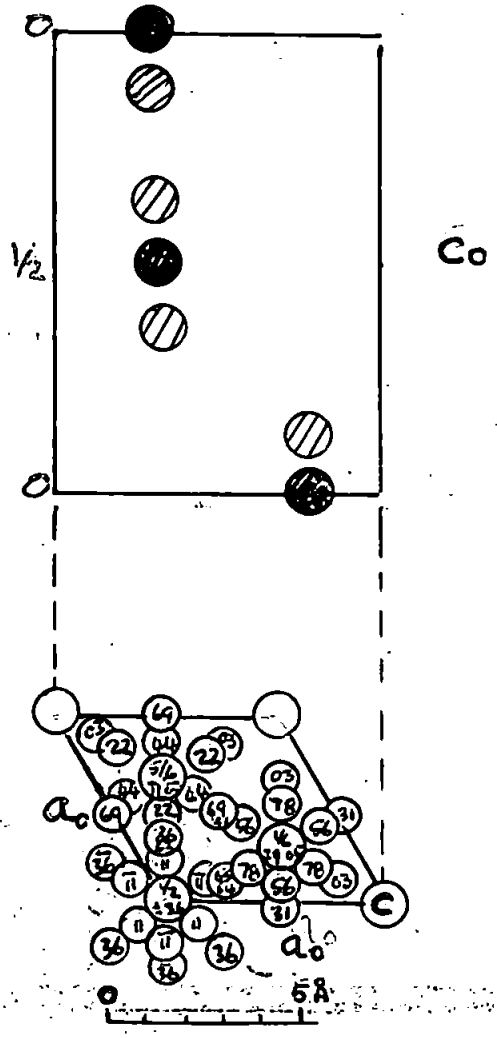

(a) Two projections of the hexagonal unit of $B_{12}C_3$

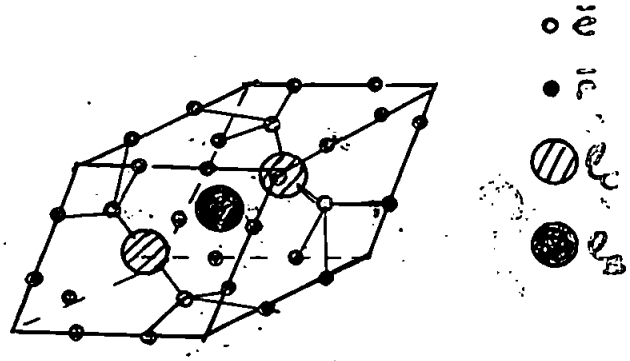

(b) Rhombohedral unit cell of $B_{12}C_3$

radius carbon (Sp^3) = 0.77 Å, covalent radius of boron (equatorial) = 0.86, the calculated boron-carbon bond becomes 1.63 Å).

I.5 BORON-CARBON system in detail

The various structural data so far reported must be considered carefully, as it is already quite evident that the thermal treatment accorded to a reacting mixture of specified composition is of major consequence in determining the nature of the product. The role too

of possible critical impurities, for example, aluminium, requires detailed investigation. Thus, Glasser et al (1953) report on the products obtained by heating various mixtures of boron and carbon to approximately 2000°C involving sintering into composites. Hoard and Hughes are critical of their results as the temperature probably falls short of fusion for any composition in the boron-carbon system; thermodynamic equilibria were not achieved and the composition range of interest, 4 to 28 atom % of carbon, extended at both ends beyond the range of thermodynamic stability. Allen (1953) recorded density and X-ray powder data for three compositions; B_4C, $B_{17}C_3$ and B_7C, and took the composition B_4C to represent the unique choice for a true compound. He assumed substitutional solid solution, i.e. boron for carbon in the ideal $B_{12}C_3$ framework in the phases $B_{17}C_3$ and B_7C. Samsonov et al (1960) describe a still evolving phase diagram for the boron-carbon system; in the composition range, 0 to 28 atom % of carbon, two compounds are reported, $B_{13}C_2$ melting congruently at about 2450°C and $B_{12}C_3$ melting incongruently at about 2350°C. More recent work by Vuillard (1968) using more refined techniques gives the values as 2480°C for the melting point of $B_{13}C_2$ and states that B_4C is completely fused at 2360°C. The phase diagram for the boron-rich part of the system has been established by Dolloff (1960) and refined by Elliot (1961) (Fig. I.5.1.); it is reduced from 4-28 atom % of carbon (Glasser 1953) and 6-24 atom % of carbon (Samsonov 1956, 1960) to approximately 8-20 atom % of carbon, corresponding to a mean value equivalent to $B_{13}C_2$ and to an upper limit of B_4C, for the composition range of the rhombohedral boron carbide phase.

Figure I.5.1.

Projected phase diagram
boron-carbon

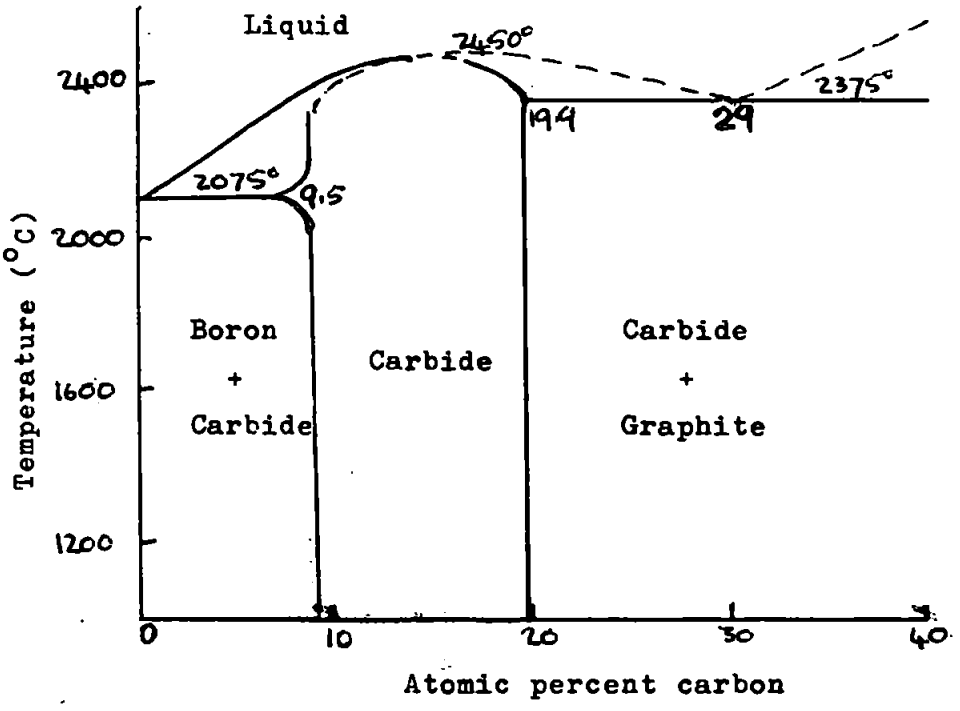

It should be noted that the rhombohedral alpha boron which has the simple boron carbide structure is not stable at these elevated temperatures, and it is the complex beta form of the element which exists, and that the eutectic containing only 3 atom-% of carbon melts at 2100°C only a little lower than the 2370°C for pure B-rhombohedral boron (Vuillard 1963).

The possibility of another compound (presumably as a peritectic) being interpolated between the eutectic and the

$B_{12}C_2$ compositions, is tentatively put forward by Samsonov et al (1960) on the following basis.

A plot of electrical resistivity against composition shows a series of maxima at $B_{12}C_3$, $B_{13}C_2$ and $B_{13}C$, of which the second is by far the most prominent; a similar plot of thermal E.M.F. shows a sharp deep minimum at $B_{13}C_2$ accompanied by maximum at $B_{12}C_3$ and $B_{13}C$ (probably a necessary consequence of the minimum at $B_{13}C_2$). The data carry conviction for the $B_{13}C_2$ composition, but are only suggestive of possible compound formation in the other two cases.

In their re-investigation of crystalline B_4C, Scott et al (1964) have utilized three-dimensional counter-recorded X-ray data comprising the larger part of that measurable with $MoK\alpha$ radiation. The density of 2.52 g./cc. and the lattice constants a = 5.167 $\pm$ 0.003 Å, = 65.60 $\pm$ 0.05°, are typical of a B_4C composition. Fourier difference synthesis shows that true interstitial holes are not used by extra atoms; it shows also that there is a deficit of electron density associated with the central position in the triatomic chain that amounts to rather more than one electron for occupancy of this position by a neutral carbon atom. The integrated electron densities for all peaks in the Fourier synthesis are suggestive of either of two theoretically significant formulations: I. $C_3^{2+}B_{12}^{2-}$ - or - II. $(CBC)^+(B_{11}C)^-$; in either case the icosahedron is formally assigned 38 valence shell electrons, the chain 10. The analysis generally speaks for a transfer of negative charge from the central atom of the chain to the icosahedron, very roughly estimated as 1.8 to 0.8 electrons according

to whether the central atom of the chain is a carbon or a boron. The nearly insignificant anisotropy in the apparent thermal motions of the terminal carbon atoms in the chain strongly suggests that the chains approach structural and consequently chemical homogeneity - that the chains are predominantly either C_3 or CBC, with little mixing of the two. Interpretation of the structural data on the basis of CBC chains and $B_{11}C$ icosahedra (in which the carbon atoms are randomly distributed among the twelve positions) is quite straightforward and unforced as compared with the classic alternative using C_3 chains and B_{12} icosahedra (the latter being inconsistent with the N.M.R. results obtained by Silver and Bray (1959) for similar material). Consequently, it appears that an ordinarily well-annealed boron carbide of B_4C composition is structurally to be formulated, at least in first approximation, as $(CBC)^+(B_{11}C)^-$ to indicate probable charge transfer and is considered to be energetically preferred.

Revision of the theoretical discussions of electron distribution is not required; the electron counting of a boron carbide of B_4C composition, written as $C_3^{2+}B_{12}^{2-}$ after Longuet-Higgins and Roberts (1955), or as the more probable $(CBC)^+(B_{11}C)^-$ after Scott et al is 2 + 2 (4) + 38 = 48 electrons. The formal charge transfer is in either case from the central atom of the chain to the icosahedron, although this does not mean that the central atom of the chain is thereby limited to a pair of opposed collinear sigma bonds. Either theoretical model is compatible with the predicted and observed semi-conducting behaviour of a B_4C composition (Yamazaki, 1957); in fact, the model which

minimises the charge transfer should be energetically preferred.

In contrast, $B_{13}C_2$ is the one boron carbide composition which as $(CBC)^+B_{12}^-$ enjoys unambiguous status as a realisable ordered chemical compound; the electron count is inevitably one electron short of the theoretical requirement for a closed shell or filled bond configuration. Therefore, theoretically $B_{13}C_2$ should display metallic conduction by 'positive holes', but in fact it is shown by Samsonov et al (1960) to have a higher resistivity than B_4C. This suggests the inference can be made that the 'holes' are non-conductive by being trapped within the icosahedra, restricting conductivity to n-type (electron conduction).

Studies by Tucker and Senio (1954, 1955) of neutron irradiated boron carbide (of B_4C composition) demonstrate the extraordinary resistance of the three-dimensional framework to extreme maltreatment. Virtually all the B - 10 nuclei are transmuted by neutron irradiation to He - 4 and Li - 7 nuclei (15% of all atoms present) yet the more fundamental characteristics of the boron carbide structure are clearly preserved, although there is expansion of the a_o axis of 0.89% and contraction of the C_o axis of 1.38% as well as an intensification of the anisotropic thermal effect which is six times as strong in the C_o-direction as in the a_o direction together with changes in the average positions of certain of the lattice atoms and very heavy diffuse scattering. Nevertheless, most of the damage to the residual framework is repaired by rather mild annealing at 700 to 900°C.

That the boron carbide structural type, aided perhaps by a partial filling of interstitial holes and/or a rather free use of framework vacancies, should accommodate a variety of compositions ranging from the highly boron-rich to the moderately carbon-rich extremes, appears rather less surprising in view of the Tucker and Senio studies. As noted by Clark and Hoard (1953) carbon in excess of the 20 atom-% required for B_4C occurs as graphite, and it is suggested that only quenched compositions might retain a higher content of carbon in the boron carbide phase. Lowell (1966) has shown that at the carbon-rich end of the boron-carbon system over a temperature interval of 1800 to 2500°C, boron occupied one of two possible sites: (1) an interstitial position in the centre of the hexagon formed by the carbon atoms -or- (2) a substitutional position replacing a carbon atom. The maximum solubility of boron in graphite is given as 2.30 atom % at 2350°C (the fusion maximum of B_4C) and a tentative phase diagram (Fig. I.5.2) shows solid solution over only a very small area. The effect of boron dissolved in graphite on the lattice constants of the latter, are summarised by the following equations :-

$$a_o = 2.46023 + 0.00310K_B, \text{ Å}$$

$$C_o = 6.71163 - 0.00594K_B, \text{ Å}$$

where K_B is the atomic fraction of dissolved boron.

Hence, it appears that the range of solid solution formation extends principally to boron-rich compositions.

Figure I.5.2.

Phase diagram boron-carbon
(carbon rich region)

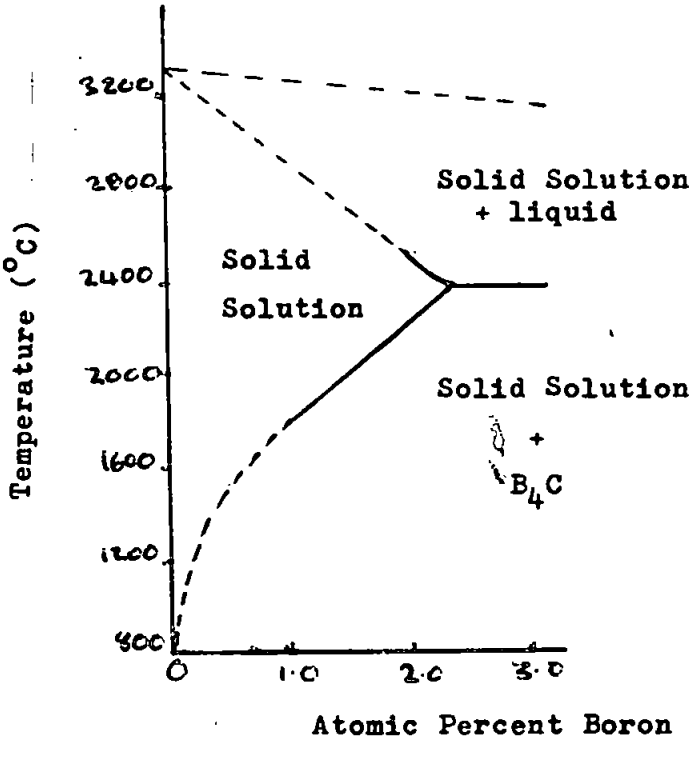

I.6(a) Compounds of General Boron Carbide Structure type

The materials listed in Table I.6.1, are sometimes called 'interstitial compounds of α-boron'. This is grossly inaccurate as by the concept formulated by Hägg (1929) and scrupulously observed by the Uppsala workers to this day, requires that the lattice constants and the volume of the host phase (in this case boron) remain virtually unaltered; the small holes - the interstices - which geometrically interleave the crystalline arrangement of quasi-spherical atoms of the host, are filled partially or wholly

TABLE I.6.1

CRYSTALLINE MATERIALS OF GENERAL BORON CARBIDE STRUCTURE TYPE (HOARD, 1967)

	Rhombohedral Cell		Hexagonal Cell		Relative Volume	
Material	a, Å		a_o, Å	c_o, Å	V/V	V/V_M
α-RhB	5.057	58° 4'	4.908	12.567	ONE	0.855
Model	5.12	63°26'	5.38	12.23	1.17	ONE
$B_{6.6}O$	5.14	62°56'	5.37	12.31	1.17	1.00
B_4C	5.174	65°30'	5.598	12.12	1.25	1.07
$B_{13}C_2$	5.204	65°29'	5.630	12.19	1.28	1.09
'$B_{12}S$'	5.19	67°56'	5.80	11.90	1.32	1.13
$B_{12}P_{1.8}$	5.248	69°31'	5.984	11.850	1.40	1.20
$B_{12}AS_2$	5.319	70°32'	6.142	11.892	1.48	1.26
$B_{2.89}Si$	5.592	68°49'	6.319	12.713	1.67	1.43

by the sufficiently small atoms of the interstitial component. This is wholly at variance with the boron carbide structure, where the effective volume of an 'interstitial' chain atom is fully as large as that of a 'host' atom. Even more important is that the required continuity of phase between α-rhombohedral boron and the boron carbide compositions is lacking; instead, the composition range for solid solution on the equilibrium diagram terminates at the boron-rich end in a eutectic with β-rhombohedral boron at a temperature some 900°C higher than that at which the thermal instability of the α-rhombohedral polymorph is manifest.

I.6.1. BORON-OXYGEN system

For the material described as $B_{6.6}O$ (Table I.3.1) La Placa and Post (1961) prefer the formulation O_2^{2+} B_{12}^{2-} rather than the apparent $(OBO^{2+}B_{12}^{2-})$ on the basis of density measurements. The former is more in keeping with the Longuet-Higgins criteria for electron counting and suggests that the oxygens, while filling the 'carbide' lattice site, are not bonded to one another but each form three bonds to icosahedral boron atoms.

I.6.2. BORON-SILICON system

The preparation of B_6Si and B_3Si as definite compounds was first reported by Moisson and Stock (1900), Cline (1959) and Adamsky (1958) have characterised the orthorhombic B_6Si; the compound is black, opaque and very hard with a density of 2.43 g/cc. and is semiconductive. The orthorhombic structure is thought to contain 40 B_6Si's in the unit cell. The detailed study of B_3Si by Magnusson and Brosset (1962) not only supports

the Moisson and Stock formula, but strongly suggests that this compound is representative of the numerous preparations to which other investigators (Colton 1960, 1961); Matkovich (1960) and Rizzo et al (1960 a) have assigned the formula, B_4Si. A careful chemical analysis, by Rizzo and Bidwell (1960 b) and phase equilibrium studies by Knarr (1960) give the empirical formula B_3Si. The compound melts incongruently at about 1400°C to give B_6Si + Si.

The atomic arrangement is crystalline B_3Si is of generalised boron-carbide type, with Si_2 replacing C-B-C chains and with $B_{10.5}Si_{1.5}$ as the composition on the average, of the icosahedral groups, silicon atoms substitute for boron only in the icosahedral r and $\bar{r}$ positions since substitution in the equatorial positions with Si-Si bond lengths of 2.34 Å would produce intolerable distortion of the framework if used to link icosahedra to chains. The value reported for the actual Si-B crosslinks, 2.002 ± 0.029 Å agrees with the sum of the tetrahedral bond radius of silicon (1.17 Å) and that of the equatorial boron (0.83 Å). For electron counting, it is the $(B_{10}Si_2)$ Si_2 (or B_5Si_2) which obeys exactly the Longuet-Higgins and Roberts (1955) criteria for closed shell or filled bond configuration.

Whereas the frequently reported B_4Si would be $(B_{11}Si)$ Si_2, the B_3Si composition some halfway in between requires the use in equal proportions of $B_{11}Si$ and $B_{10}Si_2$ icosahedra.

If the supposition is made that in a $B_{10}Si_2$ icosahedron the two silicon atoms occupy non-contiguous positions (i.e. one on r and the other on $\bar{r}$) a numerous family of statistically

equivalent frameworks in which there are no Si-Si bonds excepting in the chains, can be constructed. However, if the proportion of $B_{10}Si_2$ icosahedra is greater than half, there must be Si - Si bonds in de-stabilizing position, thus B_3Si appears to be at the silicon-rich limit for stability of the phase. On the other hand, a $B_{12}Si_2$ (B_6Si) composition having a boron carbide type structure would be two electrons short of the theoretical counting for a filled bond configuration, so that a more complex orthorhombic structure is preferred for the B_6Si composition (compare the α - tetragonal form of elemental boron).

I.6.3. System BORON-CARBON-SILICON

Samsonov et at (1955, 1960) and Meerson et al (1961) describe two ternary compositions $B_5Si\ C_2$ and $B_3Si_2\ C_2$; both are extremely hard, semiconductive materials prepared by the action of silicon carbide or silicon on boron-carbide or boron, or by a mixture of the three elements. Taking a hypothetical composition of $(B_{10}\ C_2)\ Si_2$, $(B_5\ SiC)$, as ideal, with regard to electron counting, by analogy with B_6Si and B_3Si, the 'boron rich' taking C = B, $B_5Si\ C_2$ should be orthorhombic and the silicon-rich $B_3Si_2\ C_2$ should be rhombohedral. Lipp and Röder (1966) describe substitution compounds of the formulation $B_{12}(C, Si, B,)_3$ (produced by heating boric oxide, sand and graphite, in an electric arc furnace) having rhombohedral structures and lattice constants (hexagonal) of a_o = 5.65 Å and C_o = 12.35 Å. The system B_4C-SiC has been considered as having a quasi-binary eutectic (at 15 atom% carbon) at 2300°C. The mutual solubility is less than 2% and

in silicon-rich compositions the hexagonal alpha-SiC is present, and in boron-rich compositions the cubic beta-SiC is present.

I.6.4. System BORON-CARBON-NITROGEN

Boron carbonitride has been reported by Samsonov et al (1962). Degtyarev et al (1966) describes a preparation by the nitriding (N_2) of B_4C at 1800-1900°C. Its electrical properties are almost that of an insulator and it is probably a mixture of boron-nitride (80%) and graphite (20%). It has a high thermal shock resistance.

I.6(b). Compounds of boron with other nonmetals having low boron content

I.6.1(b) BORON-OXYGEN

Boron trioxide (boric anhydride) is obtained by the dehydration of boric acid and by the oxidation of borides. It occurs in a crystalline or vitreous state depending on the method of production. In the crystalline state it has a rhombohedral structure which can be indexed as hexagonal with, a = 4.325 Å and, c = 8.317 Å. In the vitreous state it possesses a structure with short-range order depicted in Figure 1.6.1., after Zachariasen (1932) and consisting of individual groups of networks of triangular complexes of $[BO_3]$. The distance of B - O is 1.39 Å and O - O, 2.40 Å. The vapour at 1500°C consists of the monomer B_2O_3.

Figure I.6.1.

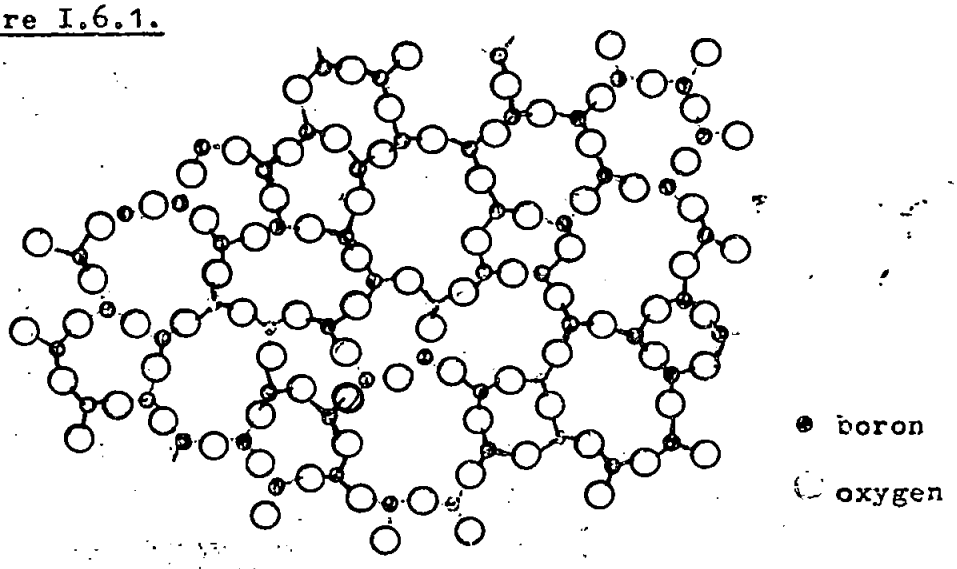

A lower oxide of formula $(BO)_x$ is formed when B_2O_3 is heated with the correct proportion of elemental boron at a temperature between 1050° and 1350°C; it has an amber-coloured vitreous form and reacts vigorously with water liberating hydrogen with traces of boranes and is sometimes pyrophoric. In the vapour phase at temperatures in excess of 2000°C it exists as a mixture of the monomer and dimer.

I,6.2(b). BORON-NITROGEN

Boron nitride is obtained as the hexagonal or 'graphitic' white form by direct synthesis from the elements, pyrolysis of boron-nitrogen compounds or by the action of nitrogen or ammonia on a variety of boron compounds under reducing conditions. Boron nitride differs from graphite by having the layers stacked immediately above one another but still maintaining the B-N alternation, Figure I.6.2.

Figure I.6.2.

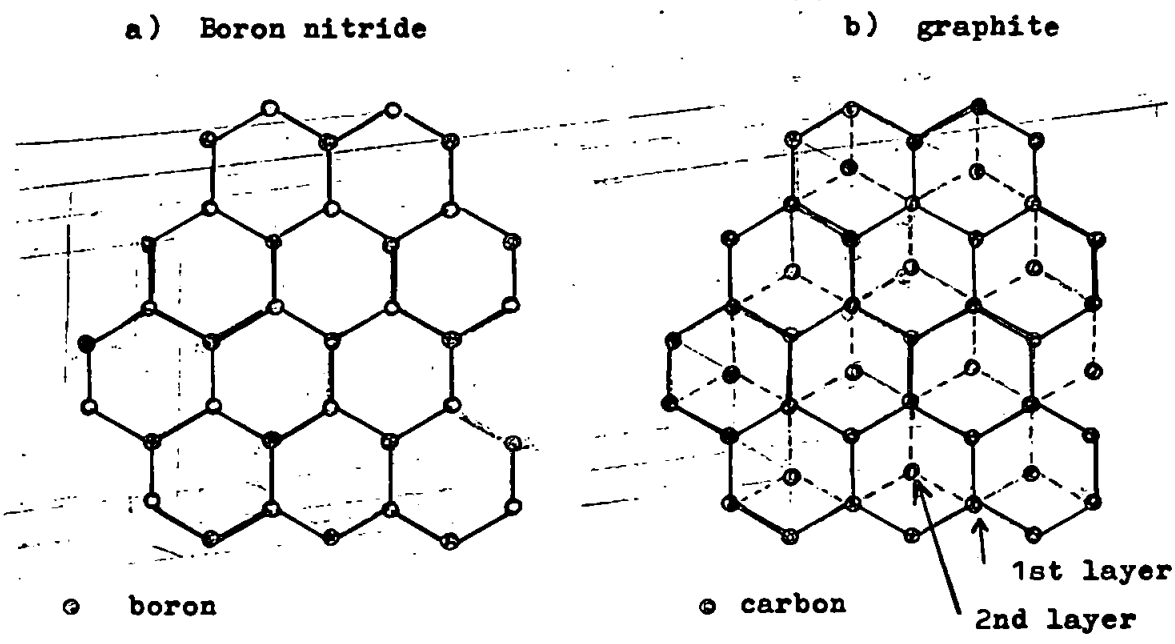

As carbon exists in two main allotropic forms so does boron nitride; following the synthesis of diamond by Bundy (1955), Wenthorf (1957) produced the cubic analogue 'borazon' by converting the graphite form at 1600°C at a pressure of 60 kilobars. As formed it has the zinc blende structure of diamond, but, as with diamond, a hexagonal wurtzite form is known.

I.7. Systems of boron with metals

(a) Lower borides

The boron frameworks of three-dimensionally linked polyhedra that typify the true higher borides are replaced in the metal diborides by quasi-infinite networks of two dimensionally linked boron atoms. The structure type of the atypical AlB_2, is utilized by most of the better-characterised diborides. The versatility of this simple hexagonal structure (Figure I.7.1) in its ability to accommodate metal atoms that differ widely in metallic radius and in electronic configuration is made evident by the listing of diborides in Table 1.7.1; the significant departures from exact diboride stoichiometry and ideal lattice are not indicated although such departures are quite general. Diborides of the transition metals from the fourth group and increasingly from latter groups of the Periodic Table must be formed in competition with still lower borides in which the special nature of the metal atoms plays an ever more prominent role. The rather involved structural chemistry of the lower borides (and of the related silicides) is discussed in detail by Aronsson et al. (1965).

Figure I.7.1.

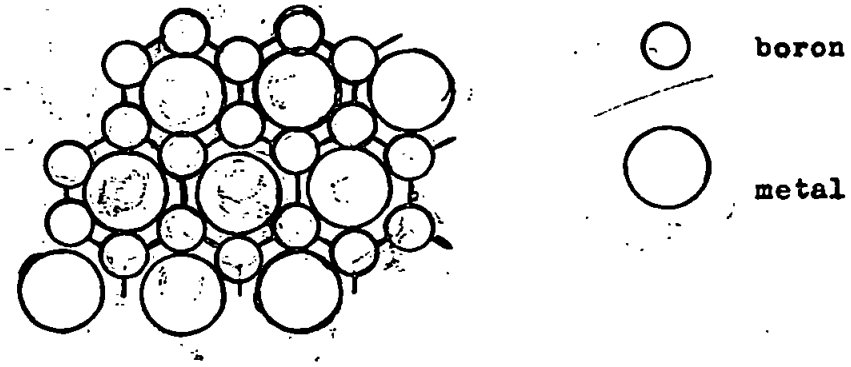

The AlB_2 structure type has a hexagonal unit cell containing just one metal and two boron atoms in positions wholly fixed by the space group, P6/mmm. In geometrical terms the crystalline arrangement is completely statified along the hexagonal axis, c, that is, layers of metal atoms alternate layers of boron atoms. The close packing of metal atoms is typically metallic, however, the direct superposition of these layers to give a simple hexagonal lattice is quite atypical for pure metal, thus the eight-coordinate polyhdron of each metal is a hexagonal bipyramid, and each atom has a graphite-like with a B-B bond distance of a/3. Each atom of metal is in contact with twelve boron atoms and 'sees' eight others at a distance comparable with the metallic diameter, so that, in fact, twenty coordination is shown. The metal diameters 2R, of the listed diborides, varies widely yet the B-B distance varies little, from 1.71A in CrB_2 to 1.91A in GdB_2. It can be concluded that the lattice spacing, a, is largely determined as a compromise between the conflicting dimensional demands of M-M binding within the metal-layers and the B-B binding within the boron net, with the latter favoured. It can be surmised that the B-B bond length of 1.75A observed in TiB_2 represents minimum strain of the boron net. The structure type approaches maximum thermal stability in the diborides of titanium, niobium, tantalum and hafnium; they are significant in that they have melting points some 1000° above those of the pure metals.

T A B L E 1.7.1.

Structural data for the metal diborides

Metal Boride	Distance, A							Density	
	c/a	c	a	2Rm	B-B	M-B	Rm+Rb	g./cc calc.	expt.
GdB_2	1.19	3.94	3.31	3.61	1.91	2.74	2.68	7.96	
YB_2	1.16	3.84	3.30	3.60	1.90	2.70	2.68	5.54	
TbB_2	1.19	3.86	3.28	3.56	1.89	2.70	2.66	8.34	
DyB_2	1.17	3.84	3.28	3.55	1.89	2.70	2.66	8.53	
HoB_2	1.17	3.82	3.27	3.53	1.89	2.68	2.65	8.80	
ErB_2	1.16	3.79	3.28	3.51	1.89	2.68	2.64	8.89	
LuB_2	1.14	3.74	3.25	3.47	1.87	2.64	2.62	9.76	
ScB_2	1.12	3.52	3.15	3.28	1.82	2.53	2.52	3.67	
PuB_2	1.24	3.95	3.19	3.28	1.84	2.68	2.52	12.85	
ZrB_2	1.11	3.53	3.17	3.21	1.83	2.54	2.48	6.10	6.17
MgB_2	1.14	3.52	3.08	3.20	1.78	2.50	2.48	2.63	2.67
HfB_2	1.10	3.47	3.14	3.16	1.81	2.51	2.46	11.2	10.05
UB_2	1.27	3.99	3.13	3.16	1.81	2.68	2.46	12.70	
TaB_2	1.04	3.23	3.10	2.97	1.79	2.41	2.36	12.2	11.7
NbB_2	1.05	3.27	3.11	2.96	1.79	2.43	2.36	6.92	6.60
TiB_2	1.06	3.23	3.03	2.93	1.75	2.38	2.34	4.48	4.38
MoB_2	1.01	3.06	3.04	2.83	1.75	2.33	2.30	8.01	
WB_2	1.01	3.05	3.02	2.85	1.74	2.32	2.31	14.2	
AlB_2	1.08	3.26	3.01	2.86	1.74	2.38	2.31	3.16	3.17
VB_2	1.02	3.05	2.99	2.73	1.73	2.30	2.25	5.05	
CrB_2	1.03	3.07	2.97	2.60	1.71	2.30	2.18	5.20	
MnB_2	1.01	3.04	3.01	2.58	1.74	2.31	2.17	5.35	

(b) Higher borides

(i) The system BORON-ALUMINIUM

Kohn et al (1958, 1961, 1965) in a series of studies of the higher aluminium borides, concluded that there are three polymorphs of AlB_{12}; the α-, β- and γ- forms. The most common phase, α - AlB_{12} is tetragonal, pseudocubic, with lattice constants a = 10.16 Å and c = 14.28 Å. The diffraction symmetry and the systematic absences correspond to the uniquely determinable enantiomorphic pair of space groups $P4_1\,2_1\,2$ and $P4_3\,2_1\,2$ with the possibility that the observed 4_1 symmetry results from a polytypic ordering of identical layers and that the correct space group should be $P4_2\,2_1\,2$. The high symmetry of the quasi-spherical icosahedral structural units favours the formation of alternative frameworks systematically related to a basic framework structure. Such twinning, which preserves all of the essential features of icosahedral stereochemistry, owes its origins to detailed bonding requirements of relatively small amounts of the secondary component of the boride. The β- AlB_{12} is reported by Kohn et al (1958) as being intricately twinned on (110) and $(1\bar{1}0)$ and indexed on an orthorhombic, pseudo-tetragonal cell, a = 12,34 Å, b = 12.63 Å and c = 10.16 Å, in the space group I2/m2/m2/a. Matkovich et al (1965) suggests that carbon is required for this phase. Kohn and Eckart (1961) emphasise twinned space groups in their formulation of γ- AlB_{12} (an orthorhombic phase with a = 16.56 Å, b = 17.53 Å, c = 10.16 Å in $P2_1\,2_1\,2_1$) as a polytypic derivative of the alpha. From analysis it appears that the γ- phase derives from the α - phase

by a cell twinning operation involving a rotation of 180° around the normal to (101) after every (101)α layer.

The role of aluminium in driving these transformations is unknown; it probably substitutes for boron in generating some framework links, but the possibility of partial occupancy of some framework holes cannot be ignored. Further evidence is provided by Giese et al (1964) who show a reversible 'martensitic' transformation of alpha to gamma (C.C.P. ⟶ H.C.P.). The gamma form is the stable one at lower temperatures.

(ii) The system BORON-ALUMINIUM-CARBON

The ternary compound Al B_{26} C_4 appears as a secondary product in the Al B_{12} preparations of Kohn et al (1958) and was characterised as Al B_{10}. Matkovich et al (1964) formulated the phase Al $B_{24}C_4$ and Wills (1963) demonstrated by X-ray diffraction that nearly regular icosahedra are dominant features of the structure. Hoard and Scott (1966) have reformulated the structure for a 62-atom cell containing 2 Al atoms, 4 B_{12} icosahedra and 4 linear C-B-C chains to give an empirical composition of Al $B_{26}C_4$. The effective volume of the B_{12} CBC sub-grouping in Al $B_{26}C_4$ is about 4% greater than that in B_4C. The structure is derived from the boron-carbide framework by a cell-twinning operation of a mirror reflection in the twinning plane. The carbon atoms are precisely located in each rhombohedral sub-cell at the usual terminal sites of the three-atom chain, and bond equally to three icosahedra. Again the role of the aluminium atoms is not clear, but their presence is certainly required for stability of the phase.

Giese et al (1964) report that at approximately 2000°C, Al $B_{26}C_4$ transforms by loss of aluminium to a rhombohedral boron carbide, probably B_{12} CBC, and have decided to call the ternary phase 'beta boron carbide', and B_4C 'alpha boron carbide'.

Elektroschmelzwerk Kempton G.m.b.H (1964) have patented a process for the production of a hard material formed by heating boron carbide with aluminium to between 1400-1500°C in an inert atmosphere. The composition of the final product is not given but is probably the ternary compound, Al $B_{26}C_4$.

I.8. Chemical thermodynamics and kinetics of the production of BORON-CARBIDE and related materials

Although the extensive properties, enthalpy and free energy of elements and their compounds cannot be measured in absolute terms, it is possible to determine the change in these properties attending a chemical reaction. The standard free energy change, ΔG°, for a chemical reaction affords a direct quantitative measure of the extent to which the reaction may proceed, related to the equilibrium constant for the reaction, by the expression:-

$$\Delta G^\circ = - R T \ln K \text{ ---------- (i)}$$

For the general reaction between an element (a metal) and another element (a nonmetal) e.g. the formation of a metal oxide :-

$$M_{(s)} + O_{2(g)} \rightleftharpoons MO_{2(s)}$$

the standard free energy change at a particular temperature is equal to the standard free energy of formation of the compound, in this case the metal oxide. If data is compiled for the reactions of a number of elements with one element, e.g. oxygen, the relative affinities of these elements for the one element can

be ascertained by plotting the standard free energy change per gram equivalent of the element as a function of temperature ($^{\circ}$Kelvin). This graphical method of presentation, the Ellingham diagram (1944), is extremely valuable in extractive metallurgy and preparative chemistry in indicating the feasibility of a reaction over a particular temperature range and also the compatibility of materials at high temperature. The general diagrams drawn by Ellingham showed a plot of standard free energy change (invariably negative) against temperature ($^{\circ}$C) for the formation of a number of oxides under standard conditions; gases participating in the reactions being at one atmosphere pressure.

A pressure correction for the departure from nonstandard conditions is calculated from the Van't Hoff equation (1886) :-

$$\Delta G_T = \Delta G^{\circ}_T + RT \ln \frac{P \text{ products}}{R \text{ reactants}} \quad \text{--------- (ii)}$$

The Richardson (1948) nomographic scale on the Ellingham diagram allows the equilibrium gas compositions to be read directly at any temperature. Thus for oxide reduction by carbon and hydrogen, CO/CO_2 and H_2/H_2O (vap.) ratios are relevant, and for nitride reduction by hydrogen the N_2/NH_3 ratio is required. In the case of the borides and carbides, where the reactants and products are refractory, the vapour pressures of the components concerned are only significant at high temperatures and only slightly modify the standard free energy change. At moderate temperatures the standard free energy change plotted as a function

of temperature (^{o}K) is linear and has generally a positive slope providing there is no net volume change (increase) on going from reactants to products; this is in spite of the temperature dependent of the related extensive properties, enthalpy and entropy

ΔH^{o} and ΔS^{o}, but since

$$\Delta G^{o} = \Delta H^{o} - T\Delta S^{o} \qquad \text{---------- (iii)}$$

the two terms are almost self-balancing. At higher temperatures, fusion and evaporation of the reactants and products give more significant changes in the enthalpy and entropy, causing inflections in the linearity of the plots especially for evaporation. At the temperature when ΔG^{o}_{T} is equal to zero, products are at equilibrium with reactants under standard conditions. Hence, above this temperature (the decomposition temperature), the products are thermodynamically unstable and, vide infra, below this temperature reaction is feasible, providing the ΔG^{o}_{T} value is negative, i.e. the plot has positive slope. When two or more such plots are compared to show their relative affinities for a particular element, oxygen, the oxide products can co-exist with either of the reacting elements at the point where the plots cross, i.e. have the same value of ΔG^{o}_{T} as f (T). Outside this temperature, should the slopes differ, one product will have a more negative free energy change and hence is the more stable; in turn, the element forming this product (oxide) will reduce the less stable product of the other element. This position is reversed on going to a temperature the opposite side of the cross-over point.

There are a number of disadvantages in the application of these $\Delta G^{\circ}_{T}/T$ diagrams, principally these are:-

(i) the free energy changes refer to standard states only, conditions never realised in dynamic systems.

(ii) The assumption is made that the compounds are of definite composition although in practice for many refractories this may not be so.

(iii) the distribution of the reactants and products between the different phases is not taken into account.

(iv) the formation of intermetallic compounds and other mixed phases between products and reactants is a possibility.

(v) they indicate only whether a process is thermo-dynamically possible, but do not indicate the kinetics of the process.

Their main advantage lies in their simplicity and ready evaluation. Reliable data for their compilation are available from a number of sources, e.g. U.S. Bureau of Standards Publications (1952, etc.), Janaf Thermochemical Tables and Supplements (1960-5), and Schick (1966) (Appendix I), although much of the data for the higher temperatures have been obtained by extrapolation.

Diagrams for a number of oxide, boride, carbide and chloride systems have been compiled (Figures I.8.1, I.8.2, I.8.3, and I.8.4). The data for oxides and chlorides are necessary as most borides and carbides are produced by the reduction of oxides and halides by carbon or hydrogen. Having determined the feasibility of a process, the net enthalpy change, ΔH°_{T} must be evaluated to determine whether the process on going from reactants to products is exothermic or endothermic and if gaseous reactants and products are formed, on this basis the efficacy of a 'closed' or an 'open' system can be assessed. Thus in the production of boron carbide by the reduction of boric oxide with carbon according to the reaction:-

$$(a)\quad 2B_2O_{3(c)} + 7\,C_{(s)} = B_4C_{(c)} + 6CO_{(g)}$$

the reaction is thermodynamically feasible over the temperature range 1880 - 3100 $^{\circ}K$ (i.e. ΔG°_{T} is negative) is ENDOTHERMIC (i.e. ΔH°_{T} is positive) and the operating free energy change is given by:-

$$\Delta G_T = \Delta G^{\circ}_{T} + RT \ln p_{CO} \qquad \text{---------- (iv)}$$

i.e. is favoured by an open system, however if account is made of the volatility of the boric oxide so that:-

$$\Delta G_T = \Delta G^{\circ}_{T} - RT \ln p_{B_2O_3} + RT \ln p_{CO} \qquad \text{----(v)}$$

this may not be the case, particularly at very high temperatures. When producing boron carbide by the magnesium thermal reduction

Figure 1.8.1. Ellingham diagram of standard free energy change for OXIDES

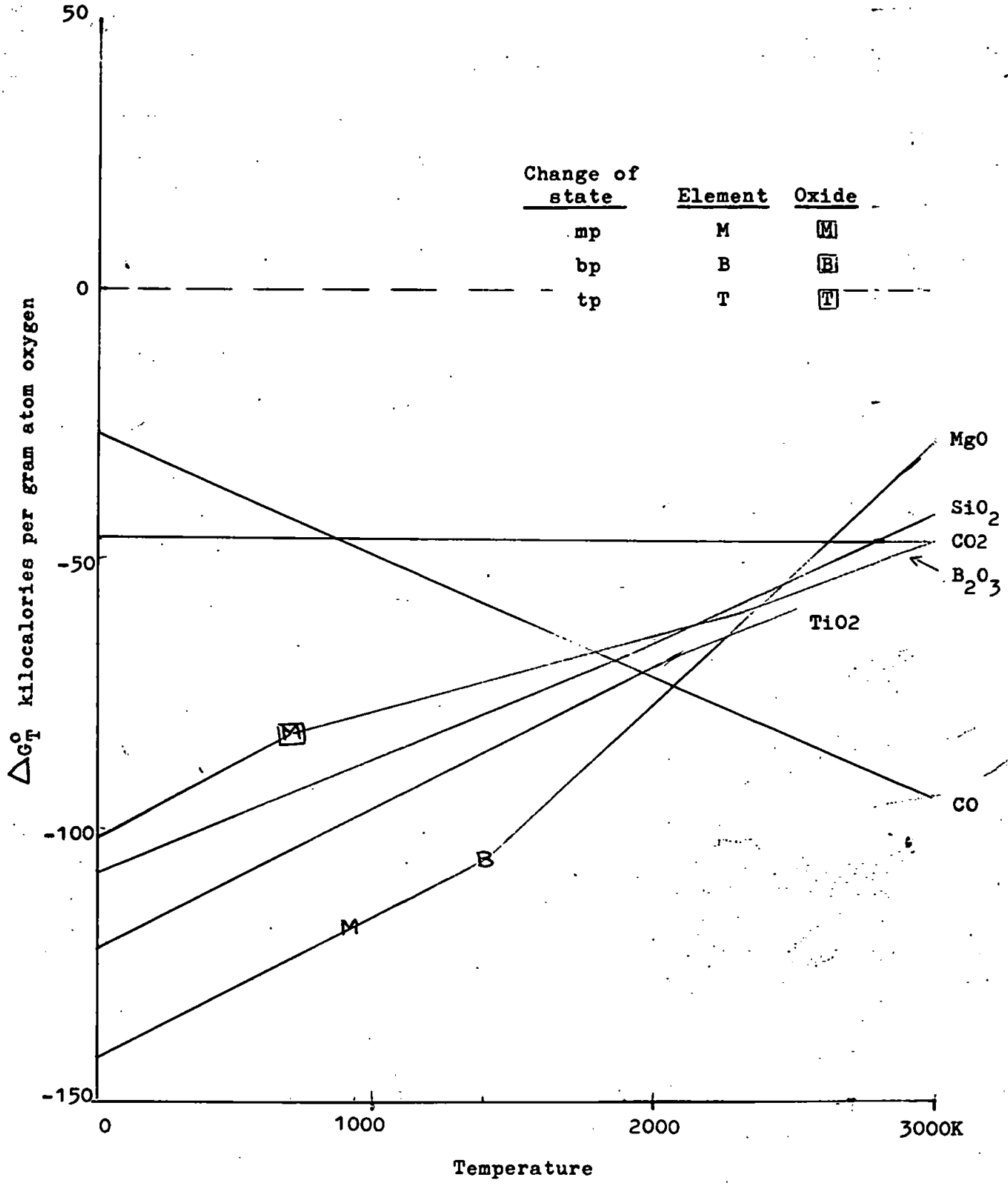

Figure 1.8.2. Ellingham diagram of standard free energy change for BORIDES

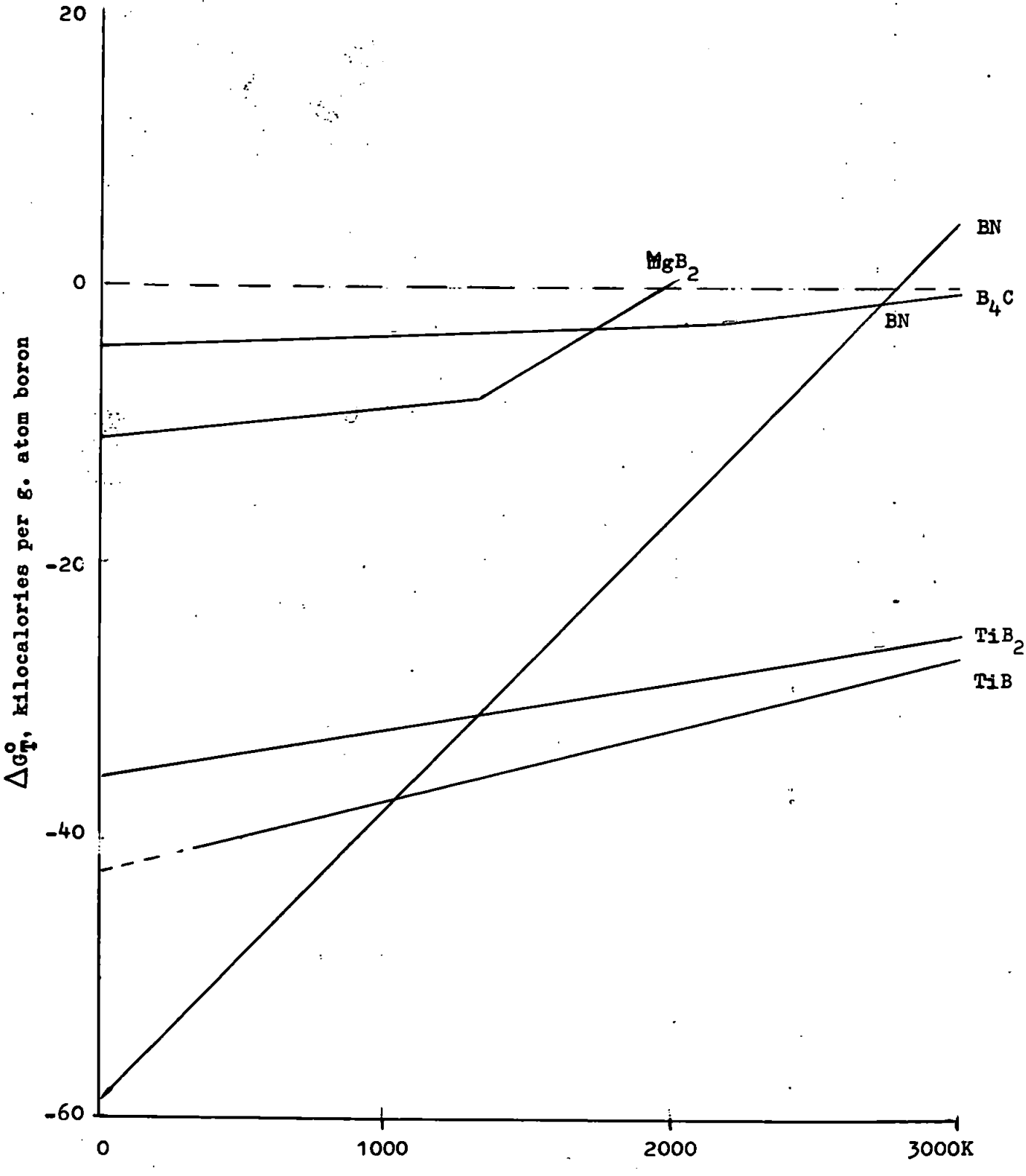

Figure 1.8.3. Ellingham diagram of standard free energy change for CARBIDES

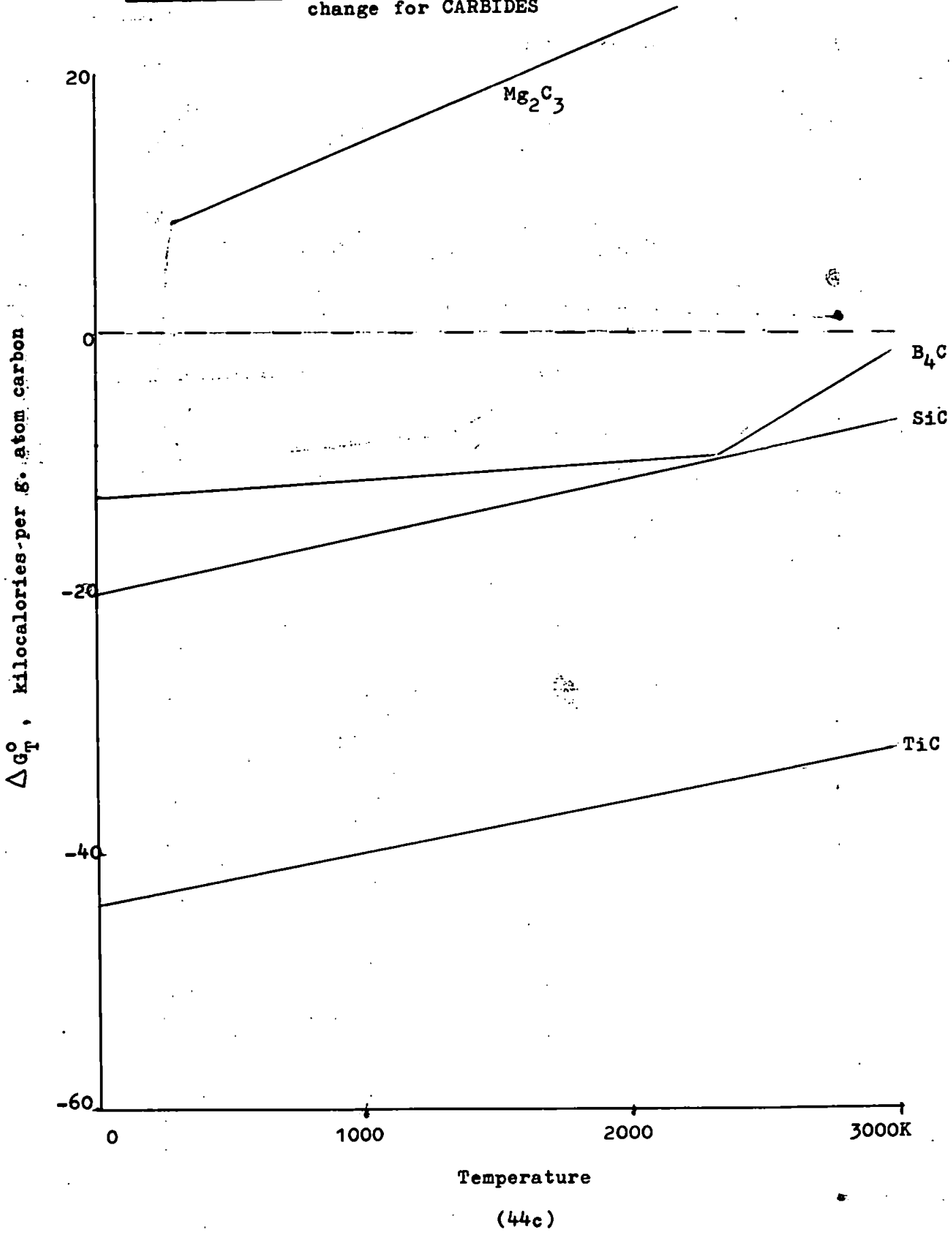

Figure 1.8.4. Ellingham diagram of standard free energy change for CHLORIDES

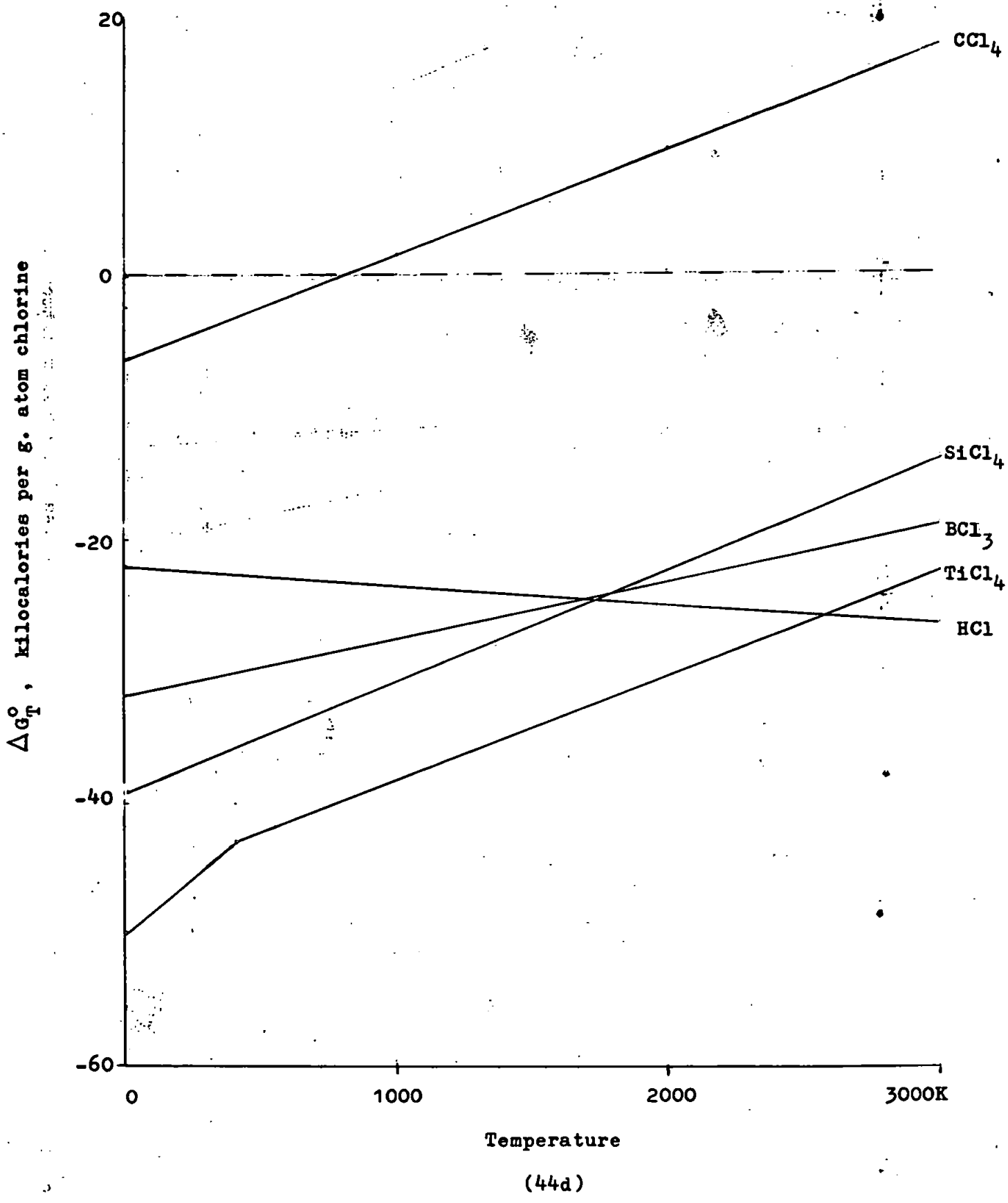

(44d)

of boric oxide in the presence of carbon according to the equation :-

$$(b)\quad 2B_2O_3 + 6\,Mg + C = B_4C + 6\,MgO$$

the reaction is thermodynamically feasible over the temperature range 0 - 2400 ^{o}K (i.e. ΔG^{o}_{T} is negative) is EXOTHERMIC (i.e. ΔH^{o}_{T} is negative); and the operating free energy change is given by :-

$$\Delta G_T = \Delta G^{o}_{T} - RT \ln p_{B_2O_3} - RT \ln p_{Mg} \quad \text{---- (vi)}$$

suggesting that a 'closed' system is preferred, having in mind the kinetics of the process.

The remaining method of production, that of the gas phase reduction of a boron trihalide by hydrogen in the presence of methane, carbon-tetrachloride or carbon, viz :-

$$(c)\quad 4\,BCl_3 + 4\,H_2 + CH_4 = B_4C + 12\,HCl$$

$$(d)\quad 4\,BCl_3 + 8\,H_2 + CCl_4 = B_4C + 16\,HCl$$

$$(e)\quad 4\,BCl_3 + 6\,H_2 + C = B_4C + 12\,HCl$$

are all thermodynamically feasible over a wide temperature range (> 1700 ^{o}K) and are highly EXOTHERMIC, the operating free energy change is given by :-

$$\Delta G_T = \Delta G^{o}_{T} - RT \ln p_{BCl_3} - RT \ln p_{H_2} - RT \ln p_{CH_4 \text{ or } CCl_4} + RT \ln p_{HCl} \quad \text{------- (vii)}$$

as there is an overall increase in volume on going from reactants to products, the reaction is favoured by a reduction of pressure.

The formation of boron carbide from the elements - β rhombohedral boron and graphite is feasible up to a temperature of 3100°K (Figure I.8.2) and is moderately EXOTHERMIC, however the difficulty of achieving thermodynamic equilibrium when both reactants are refractory solids must be emphasized. Formation by hot pressing (Glasser et al 1953; Kranz 1963) can give a wide range of composition probably having dispersed phases of boron or graphite in the only two definitive compounds $B_{13}C_2$ and $B_{12}C_3$ (see Section I.2).

The chemical kinetics and mechanism of formation of boron carbide cannot be readily assesed except possibly for the vapour phase production from the hydrocarbon-hydrogen reduction of the halide (Pring and Fielding 1909; Powell et al 1966). Samsonov et al (1950, 1960) have demonstrated that there are two consecutive processes in the reduction of boric oxide by an excess of carbon :-

$$(f)\quad B_2O_{3vap.} + 3\ CO_{(g)} = 2B_{(g)} + 3\ CO_{2(g)} \quad \text{(above } 1640^{\circ}K\text{)}$$

$$C_{(s)} + CO_{2(g)} = 2\ CO_{(g)}$$

and

$$(g)\quad 4B_{(g)} + C_{(s)} = B_4C_{(s)}$$

The newly-formed boron diffuses through the boron carbide layers progressively formed on the surface of the graphite particles,

finally giving boron carbide particles retaining the original shape of the graphite. The coefficient of diffusion of boron in graphite is given empirically, as :-

$$D = 3.02\ e^{-28,625/T} \qquad \text{----------(viii)}$$

(Samsonov et al 1968; Lowell 1967), which indicates that the diffusion of carbon in boron is correspondingly much slower. This is to be expected from the magnitude of the lattice energy as indicated by the relative melting points and boiling points of boron and carbon (boron, m.p. 2450°K, b.p. 3931°K; carbon m.p. 4000°K, b.p. 4500°K); although the boron atom is the much larger of the two (covalent radius, 0.86 Å for boron, 0.77 Å for carbon), the former has the higher polarisability (first ionisation potential boron, 8.28-electron volts; carbon 11.41-electron volts) and is more readily distorted.

Magnesium reduces boric oxide, by a similar mechanism at temperatures where both the oxide and magnesium are in a liquid or vapour state, B_2O_3 m.p. 723°K, b.p. 2316°K; Mg m.p. 922°K, b.p. 1378°K, and form boron by the reaction :-

$$\text{(h)}\quad B_2O_{3(vap)} + 3\,Mg(g) = 2\,B(g) + 3MgO_{(s)}$$

and the newly-formed boron diffuses into the added carbon :-

$$\text{(i)}\quad 4\,B_{(g)} + C_{(s)} = B_4C_{(s)}$$

It appears improbable that the carbon does not react with some of the boric oxide, but the net reaction is the same, since :-

(j) $Mg + CO \longrightarrow MgO + C$

Effusion studies of the volatilisation of boron from boron carbide solid solutions below their fusion temperatures 2200 to 2600°K by Robson and Gilles (1964) and Hildenbrand and Hall (1964) show the preferential loss of boron to the vapour phase regardless of the composition of the sample. The vapour pressure of the boron is given by :-

$$\log P_{(atm)} = 7.506 - (29,630/T) \quad \text{---------- (ix)}$$

Verhaegen et al (1962) identified B_2C and BC_2 as well as boron in the vapour, by mass spectrometry, the first being a minor constituent but the pressure ratio $p(B)/p(BC_2) = 15$ at 2500°K.

The Hitachi workers in Japan (1966) report that production of boron carbide by the magnesium thermal reduction process is possible at temperatures as low as ca 1000°K when certain 'catalysts' are present, namely, magnesium oxide and other 'inert' materials.

Considering that the formation of boron carbide takes place in two consecutive processes by chemical equations (f) and (g), it appears likely that at moderate temperatures the latter process involves boron in the solid state rather than as a vapour, as judged from the vapour pressure given by equation (ix). Assuming that the magnesium or carbon (monoxide) reduction of the boric oxide is rapid, the rate-determining step for the overall reaction is the diffusion of boron into the graphite grains. Budnikov and Ginstling (1965) have constructed a model for reactions of this type based on Ficks law of diffusion.

Figure I.8.5.

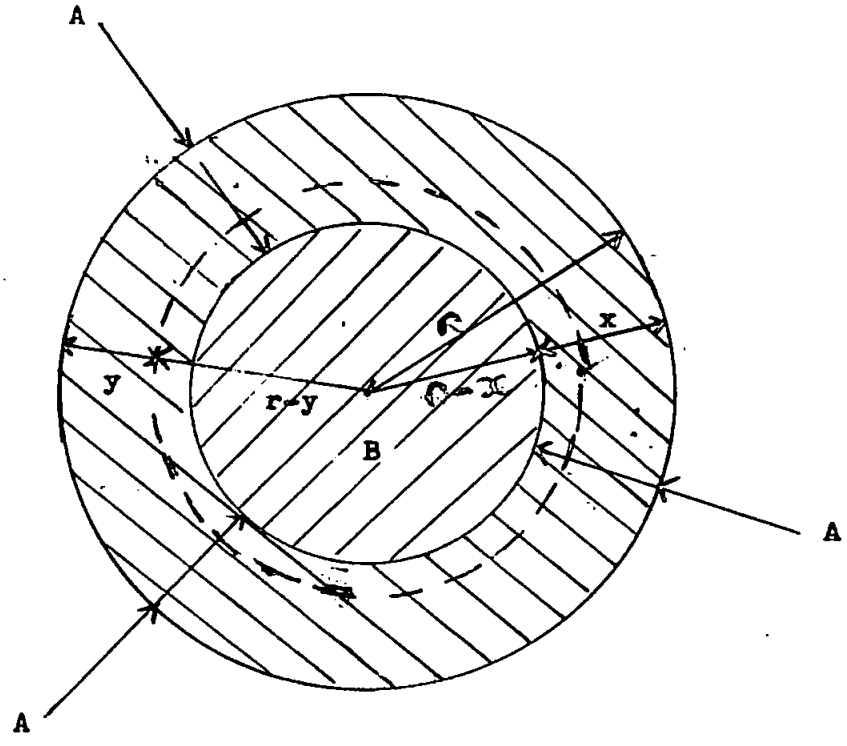

In the general type of reaction $A + B \longrightarrow AB$, (Figure I.8.5), the thickness of the product layer, x, continuously increases. The rate of diffusion of A through AB is very much less than the rate of reaction between A and B, so that the concentration of A at the surface dividing AB and B is zero; also the concentration of A at the surface of the grain is constant, as the external resistance of diffusion is much

less than that experienced in the product AB. Applying Ficks Law to a grain of spherical symmetry, Budnikov and Ginstling obtain an expression for the rate of growth of the product layer AB :-

$$\frac{dx}{dt} = \frac{K}{x/_r(1 - x/_r)} \qquad \text{-------- (x)}$$

x = thickness of layer AB

t = t i m e

K = rate constant = $\frac{D}{\epsilon} C$

D = diffusion coefficient of A through AB

C = molar concentration of A at the surface of the grain

ϵ = proportionality coefficient = $\rho\, n/\mu$

ρ = density of AB

n = stoichiometric coefficient of the reaction expressed as the number of moles of A reacting with one of B.

μ = formula weight of AB

r = radius of the spherical grain

Esin and Gel'd (1954) note that dx/dt has a minimum when $x/r = 0.5$ i.e. $x = r/2$.

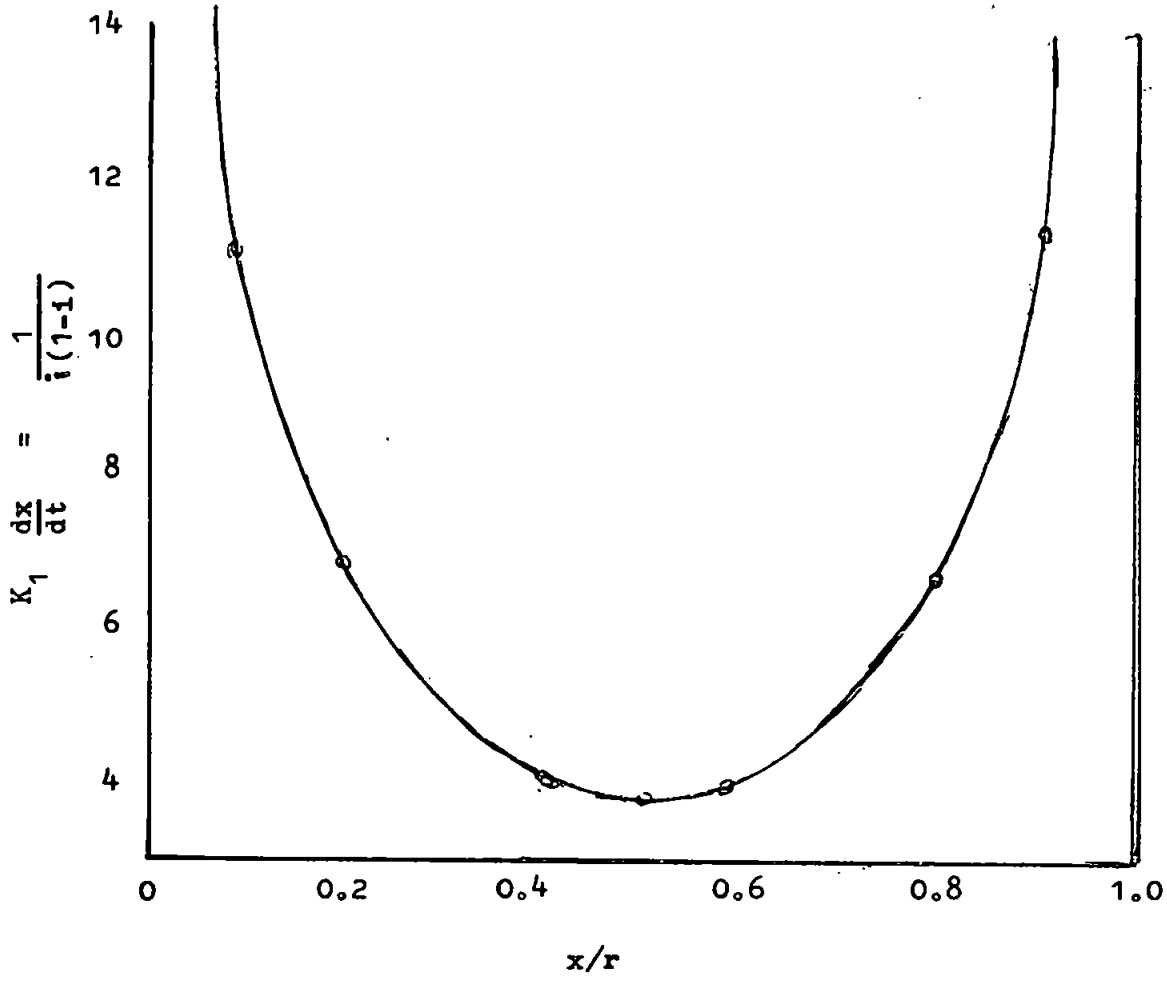

Figure I.8.6. Relationship between rate of increase in thickness of product ratio x/r

The relationship between the rate of increase in thickness of product layers and the ratio x/r is shown in Figure I.8.6, from the graph it is seen that the rate dx/dt for thickening of the product AB continuously falls with a change in the magnitude x/r from 0 to 0.5 and then symmetrically increases from the minimum value to infinity with a change in x/r from 0.5 to 1.

It should be noted that when $x/r \longrightarrow 0$, and $x/r \longrightarrow 1$, the rate of thickening is not infinite, since in these cases the value dx/dt is determined by the rate of chemical reaction between A and B and not by the diffusion process. The equations derived express the relationship between the thickness of the layer of product with time. In practice, it is much more interesting to obtain equations for calculating the degree of conversion of the substance.

Let the particles of reagent B forming the product AB during reaction with reagent A, have respectively at the initial moment and at a certain time from the start of the reaction, a volume V_o and V_t, a mass $V_o\rho$ and $V_t\rho$, and as surface area So and S_t. If during time, dt, the reaction occurs over a thickness, dx, in the grains of B corresponding to a mass of dV_t , then :-

$$dV_t\rho = S_t d\,x\rho \qquad \text{---------- (xi)}$$

$$\text{or} \quad \rho(V_o - V_t) = \rho \int_o^{\infty} F dx$$

$$\text{hence} \quad dV_t = F dx \quad \text{and} \quad V_o - V_t = \int_o^{\infty} S_t dx \quad \text{--- (xii)}$$

The degree of conversion of the reagent B may be expressed as :-

$$\alpha = \frac{V_o - V_t}{V_o} = \frac{\int_0^x S_t dx}{V_o} \qquad \text{-------(xiii)}$$

differentiating gives:

$$\frac{d\alpha}{dt} = \frac{d\left(\frac{(Vo - Vt)}{Vo}\right)}{dt} = \frac{St}{Vo} \circ \frac{dx}{dt} \qquad \text{-------(xiv)}$$

$$\text{or } \frac{d\alpha}{dt} = \frac{So}{Vo} \circ \frac{St}{So} \frac{dx}{dt} \qquad \text{----------(xv)}$$

since

$\frac{St}{So} = f(\alpha)$ and the explicit form of this function varies with the geometrical shapes of the grain. Thus for a sphere :-

$$f(\alpha) = (1 - \alpha)^{2/3}$$

$$\alpha = 1 - \frac{(r - x)^3}{r} \qquad \text{----------(xvi)}$$

for a solid cylinder:

$$f(\alpha) = (1 - \alpha)^{1/2}$$

$$\alpha = 1 - \frac{(r - x)^2}{r} \qquad \text{----------(xvii)}$$

The ratio S_o/V_o may be expressed as follows :-

$$\frac{So}{Vo} = \frac{1}{\Psi\ 1} \qquad \text{----------(xviii)}$$

Ψ = shape coefficient (sphere $^1/3$, cube $^1/6$, etc.)

1 = least thickness of the grain

Equation (xv) can be rewritten :-

$$\frac{d\alpha}{dt} = \frac{1}{\Psi 1} \cdot \frac{dx}{dt} \quad f(\alpha) \qquad \text{----------(xix)}$$

to give a general expression :

$$\frac{d\alpha}{dt} = \chi f(\alpha) \qquad \text{----------(xx)}$$

χ = reaction coefficient

$f(\alpha)$ = shape factor for the grain

Under certain conditions the kinetic equation may indicate a pseudo-monomolecular reaction (one of first order). Thus, if the solid A reacts with a liquid B to produce a solid AB, forming with reagent B a mixture which melts at the reaction temperature, then the diffusion layer of the product AB continuously increases from the side A and passes into the liquid phase from the side B. In this case, the thickness of the diffusion layer of product AB may have very low values, but is constant over a long period. Such a condition may be the state when boron carbide is oxidised by moist air.

Finally, it should be noted that diffusion coefficient D from Ficks Law is temperature dependent. Hevesy established that:-

$$D = Ae^{-E/RT} \qquad \text{----------(xxi)}$$

where A = pre-exponential coefficient of diffusion at a temperature of infinity. (connected with the frequency of the atomic oscillations).

E = the energy of activation of diffusion (or the energy of opening up the lattice).

R = the gas constant

T = temperature $^{\circ}K$.

This equation, analogous to the Arrhenius equation for the velocity of mono-molecular reactions, is correct for most conditions and mechanisms of diffusion so far investigated.

Therefore the rate constant, K, in equation (x) should follow a similar relationship. It is also pertinent to state that the equation for the variation of viscosity with temperature during hot-pressing is, according to Koval'chenka and Samsonov (1961), governed by a similar expression (see Section I.9).

I.9 The sintering of boron carbide and other refractory materials

General principles of the mechanism of sintering

In any discussion of sintering processes two systems have to be distinguished, homogeneous, consisting of a single component or components which give continuous series of solid solutions, or heterogeneous for multiple component systems. It is unlikely that in pure homogeneous systems any significant sintering is ever achieved; even very small fractions of another component assist in their consolidation and are often of the utmost necessity. Nevertheless, discussion of a pure homogeneous system provides insight into the general principles of sintering mechanism. Homogeneous systems are taken as being 'binder free' and are exemplified by borides, carbides, nitrides, silicides and single phase metal powders.

In the homogeneous sintering of a powder, distinction can be made between two overlapping stages of sintering. The first stage is characterised by the formation and growth of bonds, that is, contact areas between adjacent powder particles. The growth of these contact areas takes place during the early stages of sintering, and is manifested by improved cohesion of the compact; where the material is electrically conducting there is rapid increase of conductivity. During the second stage, the material is densified and the pore volume decreased. Under favourable conditions the latter is practically eliminated.

At present, surface-free energy is generally recognised as the driving force in both stages of sintering. The energy required for sintering is supplied by the decrease of surface areas or by the replacement of interfaces of high energy by those of lower energy (e.g. grain boundaries).

Calculations have shown that the surface free energy is sufficient to account for sintering, provided a suitable mechanism is available for the transport of atoms involved in the consolidation of powder compacts. The following five mechanisms are possible in the case of homogeneous materials :-

(1) Evaporation followed by condensation

(2) Surface diffusion

(3) Volume diffusion

(4) Viscous flow (Newtonian flow characterized by a linear relationship between strain rate and stress

(5) Plastic flow (Bingham flow characterized by the existence of a yield stress).

The first attempt to develop a quantitative theory was by Frenkel (1945) who assumed that with both amorphous and crystalline powders viscous flow would occur under the variation influence of the capillary forces associated with the curved surfaces of the pores with time. The viscosity may be represented by the equation :-

$$\eta = k T / D\Omega_o \qquad \text{----------(i)}$$

Where η = viscosity

D = coefficient of self-diffusion

T = absolute temperature

k = constant

Ω_o = atomic volume

The mechanism of deformation of solids by viscous flow and the role of diffusion in the deformation of crystalline solids was evolved further by Shaler and Wulff (1948), Nabarro (1948) and Herring (1950). Frenkel's postulate holds for the sintering of glasses.

At high temperatures crystalline solids can deform at stresses below the yield point. The rate law and stress-dependence governing their deformation agree with the laws of viscous flow, so that their behaviour can be described by a material constant which has the dimensions of viscosity. However, the actual mechanism of deformation is considered to be the migration of individual vacancies or atoms, i.e. volume diffusion. The driving force for this migration is the gradient in chemical potential resulting from differences in stress.

The sources and sinks of this diffusion vacancy or atom migration are grain boundaries and the surfaces of pores, as well as the outer surface of the solid. The first demonstration that mass flow by volume diffusion occurs during sintering, was provided by Kuczynski (1950). Earlier, Pines (1946) had recognized that the concentration of the lattice vacancies (Schottky defects) would be greater under concave pore surfaces than under a plane surface and had concluded that pores could be eliminated by the diffusion of vacancies away from the pore in the resultant vacancy concentration gradient. Yet Kuczynski was the first to provide quantitative proof of this by comparing the observed time dependence of neck growth with the time dependences predicted for viscous flow, evaporation-condensation, volume diffusion and surface diffusion. He showed that in all four cases, the sintering time, t, to produce a neck of radius, x, should be given by the form :-

$$\left(\frac{x}{a}\right)^n = \frac{A(T)\,t}{a^m} \qquad \text{----------(ii)}$$

Where a = particle radius

$A(T)$ = a function of temperature only

and

$n = 2,\ m = 1$ for viscous flow

$n = 3,\ m = 2$ for evaporation-condensation

$n = 5,\ m = 3$ for volume diffusion

$n = 7,\ m = 4$ for surface diffusion

$n = 6,\ m = 4$ for grain boundary growth

Measurements of neck growth between spheres and planes of copper and silver showed that the neck diameter increased as $t^{1/5}$, indicating that volume diffusion was the predominant mechanism operating. With very small spheres of copper (less than 30 micron) however, a deviation from the relationship was observed at the lowest sintering temperatures used, which he interpreted as being due to the increased contribution of surface diffusion at these particle sizes and temperatures. Kuczynski's model for neck-growth by volume diffusion is shown in Figure I.9.1, which shows two spheres in contact, sectioned through their centres. The capillary suction in the neck is then :-

$$\frac{1}{r} - \frac{1}{x} = \frac{\gamma}{r} \qquad \text{----------(iii)}$$

γ = surface tension

r = radius of curvature of the neck surface in the plane of the section

When a vacancy is formed under the surface of the neck, a quantity of work, $\frac{\gamma \zeta^3}{r}$, is therefore done by the capillary suction, where ζ^3 is the volume of the vacancy, and the thermal energy, w, required to form the vacancy is decreased by this amount. Hence :-

$$\frac{\Delta C}{C} = \frac{C^1 - C}{C} = \frac{\gamma \zeta^3}{rkT} \ll 1 \qquad \text{-----(iv)}$$

C = concentration of vacancies in the unstressed crystal

C^1 = concentration of vacancies in the neck

This expression is identical with that for the increase in the vacancy concentration around a cylindrical pore of radius r_o. To obtain an expression for the vacancy flux away from the neck, Kuczynski assumed in effect that the surface of the latter could

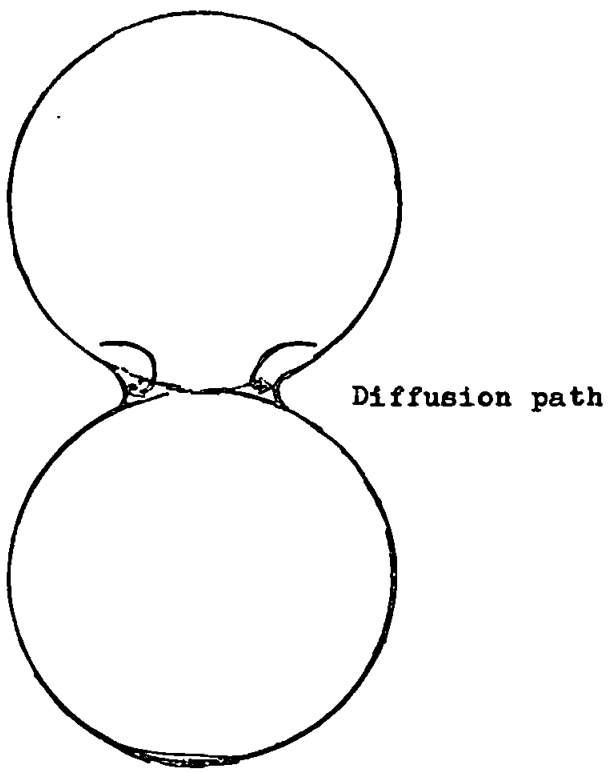

Figure I.9.1. Kuczynski model for initial sintering by vacancies being eliminated at the surface of spheres.

be considered as forming one half of the surface of a cylindrical pore from which there was radial diffusion to sinks on the surfaces of the sphere. For this case, the vacancy concentration gradient adjacent to the surface is $\frac{\Delta C}{r \ln d/r}$ where d is the distance at which $C^1 = C, \ln d/r$ was assumed to be unity, and an equation could thus be set up for the rate of increase in the volume of the neck :-

$$\left(\frac{x}{a}\right)^5 = \frac{40\gamma\delta^3 Dt}{a^3 k T} \qquad \text{----------(v)}$$

a = particle radius

D = coefficient of volume diffusion

Alexander and Baluffi (1950) observed that in copper, only pores in the vicinity of grain boundaries closed rapidly, which accords with the theoretical deduction of Nabarro (1948) and Herring (1950) that the grain boundaries can act as sources and sinks for vacancies and are considered necessary for rapid sintering. Two alternative mechanisms have been suggested to account for this action of grain boundaries :-

(1) that they act as 'pipe lines' for rapid diffusion of vacancies to free surfaces

(2) that they act as sinks for the destruction of vacancies as envisaged in the Nabarro-Herring mechanism

The densification of compacts by the former process exclusively would require that vacancies should diffuse to the outside of the compact. This, it would start from the outside and be a function of compact size, contrary to general experience. However, grain boundary diffusion will be expected to contribute to mass transport over a short distance during sintering, as evident in the sintering of alumina (Coble (1958)). The second mechanism provides a means for the destruction of vacancies within the compact. Kuczynski's original model assumed that vacancy sinks are confined to the particle surfaces and could only account for densification so long as the pores remain open and inter-connected. Kingery and Berg (1955) showed that the observed rates were too rapid to be accounted for by neck growth due to volume diffusion, and proposed a model (Figure I.9.2.) in which a grain boundary existing between two spherical particles is considered to act as the vacancy sink.

Atoms would then flow from the vacancy sinks to the neck surface, as indicated by the arrows, and thus, by spreading out of material at the neck, cause the particles to coalesce. Subsequently Coble and Ellis (1958, 1963) concluded that the deformation produced by plastic flow is limited to a fixed value determined by the hot hardness of the material, limited as a mechanism to $< 84\%$ theoretical density. Further densification is ascribed to a diffusion process similar to that of heat transfer. Vasilos

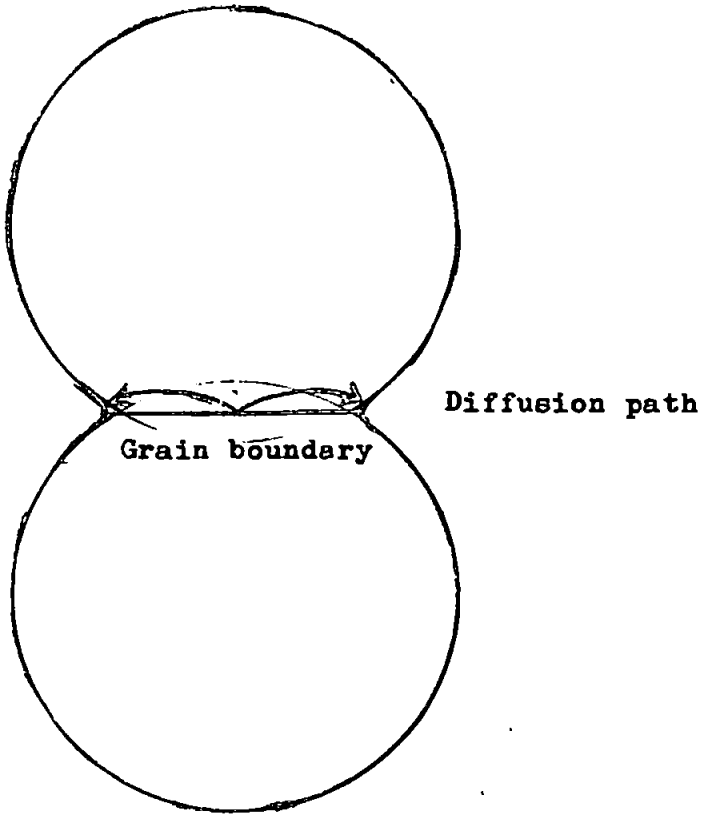

Figure I.9.2. Kingery and Berg model for vacancies eliminated at grain boundary at neck

and Spriggs, (1963) have applied the Coble model for the hot pressing of magnesia and find a logarithmic time law of densification :-

$$\rho = 1 - kD \ln \frac{t_f}{t} \qquad \text{----------(vi)}$$

ρ = relative density

t_f = time at which pores vanish, valid up to relative densities of $> 90\%$

Figure I.9.3. Mackenzie and Shuttleworth model

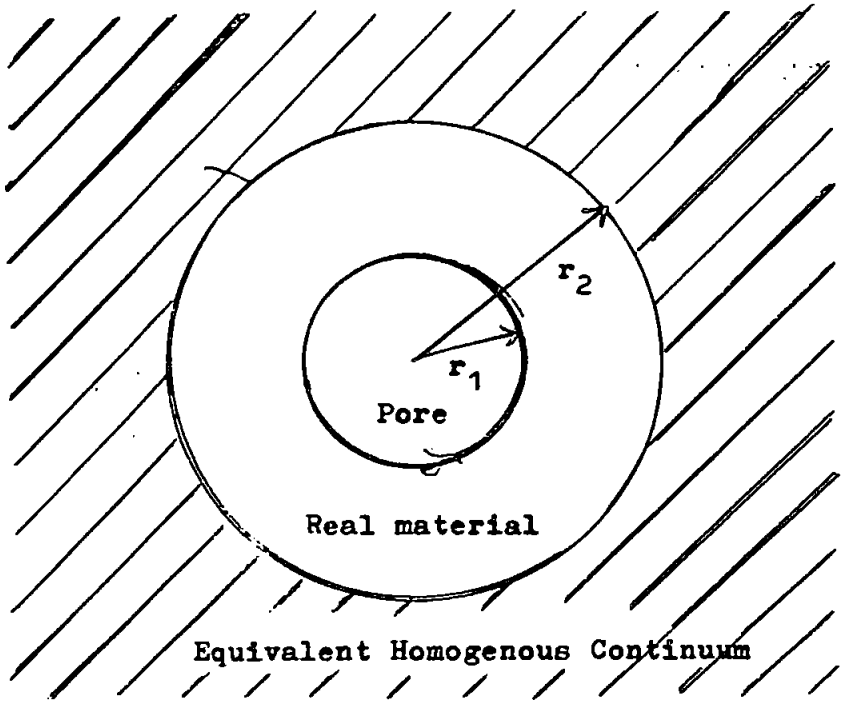

The Mackenzie and Shuttleworth theory (1949) rests on a model consisting of closed pores in a homogeneous matrix (Figure I.9.3). This theory is really only valid for the final stage of sintering where closed pores first appear ($<$10% porosity), however, the theory agrees with experimental results for sintering stages at even 35% porosity, i.e. when the pores are inter-connected. They obtained the following expression :-

$$\frac{d\rho}{dt} = \frac{3}{2}\left(\frac{4\pi}{3}\right)^{\frac{1}{3}} \frac{\gamma_n}{\eta_0} (1-\rho)^{\frac{2}{3}} \rho^{\frac{1}{3}} \left[1 - a\left(\frac{1}{\rho} - 1\right)^{\frac{1}{3}} \ln\left(\frac{1}{1-\rho}\right)\right] \quad \text{------- (vii)}$$

ρ = relative density = $1 - \left(r_1/r_2\right)^3$

γ = surface tension

n = number of pores per unit volume of material

η_∞ = coefficient of viscosity

$a = \sqrt{2}\left(\frac{3}{4\pi}\right)^{\frac{1}{3}} \circ \frac{\tau_c}{2\gamma\,\eta_\infty^{\frac{1}{3}}}$

τ_c = yield stress

It can be shown that:-

$$n = \left(\frac{1-\rho}{\rho}\right) \circ \frac{3}{4\pi} \circ \frac{1}{r_I^3} \qquad \text{-------- (viii)}$$

r_I = pore radius

so that for pressureless sintering :-

$$\left(\frac{d\rho}{dt}\right)_{P=0} = \frac{3}{2} \circ \frac{\gamma}{\eta_\infty\, r_I}\left[(1-\rho)\right]\circ\left[1 - \frac{\sqrt{2}\,\tau_c\, r_I}{2} \ln\left(\frac{1}{(1-\rho)}\right)\right]$$

---- (ix)

For pressureless sintering, the driving force is the pore pressure $2\gamma/r_I$. For hot pressing there is an additional external pressure P. It can be shown that :-

$$\left(\frac{d\rho}{dt}\right)_{\rho>0} = \left(\frac{d\rho}{dt}\right)_{P=0} + \frac{3P}{4\eta_\infty}(1-\rho) \qquad \text{----(x)}$$

$$P \gg 2\gamma/r_I \qquad \text{(xa)}$$

$$\text{and} \qquad \gg \tau_c \qquad \text{(xb)}$$

For instance, if the radius of the pores r_I is 1 micron (10^{-4} cm.) and the surface tension of the material, γ, is 1000 ergs/cm^2, then the material pore pressure is 2 x 10^7 dynes/cm^2 —— 20 Kg/cm^2. A normal value for P is 500 Kg/cm^2.

Using relationship (xa) and (xb), the hot-pressing equation may be simplified, as the terms contained $2\gamma/r_I$ and T can be eliminated so that the rate law of the hot-pressing process may be written as :-

$$\frac{d\rho}{dt} = \frac{3}{4} \frac{P}{\eta_{ss}} (1 - \rho) \qquad \text{---------- (xi)}$$

or, integrated with respect to time :-

$$\ln \frac{1-\rho}{1-\rho_o} = -\frac{3}{4} \cdot \frac{P}{\eta_{ss}} t \qquad \text{---------(xii)}$$

when $\rho = \rho_o$ when $t = 0$

The plastic flow theory succeeded in accounting for several experimental characteristics of the hot-pressing process. The theory explains the effect of external pressure in reducing the sintering temperature necessary for densification. It further explains the effect of pressure on the end point density at constant temperature, the effect of pressure on the sintering rate and the influence of particle size on the end-point density. At the end point $\left(\frac{d\rho}{dt}\right)_{p>o} = 0$.

The hot-pressing equation (xii) given by Murray et al (1954) has been verified by Mangsen et al (1960) hot-pressing alumina, by Vasilos (1960) for silica and by Jaeger et al (1962) on

other ceramics. From their studies of binder-free hafnium, zirconium and tantalum, Lersmacher and Scholz (1961) state that the plastic flow theory can describe the early stages of hot-pressing, but that deviations occur at longer times, particularly at higher temperatures. They conclude that the density after long sintering times (e.g. 60 mins.) does not continuously increase with temperature, but reaches a maximum at a specific temperature. This is related to grain growth during sintering; grain growth is directly controlled by impurities such as the binder metals, iron, cobalt and nickel in heterogeneous sintered ceramics.

Again it was clear from the many experimental results that the initial sintering rate is often greater than that predicted from the plastic-flow equation.

A completely new approach was made when Koval'chenko and Samsonov (1961) proposed their hot-pressing equation, based upon the mathematical framework of the rheological behaviour of a dispersed system; later, a correction for grain growth was introduced.

Their model is a system consisting of a gaseous phase in the form of globules dispersed in an incompressible viscous medium. In addition, the concentration of the dispersed phase, Q, (equivalent to $1 - \rho$), is so small that terms involving Q^2 need not be considered. In such a system :-

$$\frac{1}{Q} = \frac{V_2}{V_1} + 1 \qquad \text{----------(xiii)}$$

Where Q = porosity

V_2 = the volume of the viscous medium

V_1 = the volume of the dispersed phase, i.e. the volume of the pores.

$V = V_1 + V_2$ = total volume of the system

The following relation between the material constants η and ζ is valid for a porous fluid system :-

$$\zeta = 4\eta \frac{(1 - Q)\ (1 - 2Q)}{Q(3 - Q)} \qquad \text{---------- (xiv)}$$

Where η = viscosity of the medium = 1st coefficient of viscosity

ζ = 2nd coefficient of viscosity

Since Q is small, the rate at which work (W_d) must be done to deform the system, may be written :-

$$W_d = \zeta \left(\frac{dV}{Vdt}\right)^2 \qquad \text{---------- (xv)}$$

and equated to the external work (W_{ext}) supplied for the compression of the system, i.e. :-

$$W_{ext} = -P \frac{dV}{Vdt} - \frac{\gamma ds}{Vdt}$$

$$= \zeta \left(\frac{dV}{Vdt}\right)^2 = W_d \qquad \text{---------- (xvi)}$$

Where P = external pressure

γ = surface tension

S = total pore Area

dV/V = relative volume change of the system

Neglecting the surface tension term, as in the Murray theory, gives :-

$$-P = \zeta \left(\frac{dV}{Vdt} \right) \qquad \text{----------(xvii)}$$

$$\text{h e n c e} \quad \frac{dV}{V} = \frac{dQ}{1 - Q} \qquad \text{----------(xviii)}$$

$$\text{a n d} \quad \frac{dQ}{dt} = -\frac{P}{4\eta} \cdot \frac{Q\,(3 - Q)}{(1-2\,Q)} \qquad \text{----------(xix)}$$

Since η for a viscous body is constant with respect to time, we have upon integration :-

$$\frac{Pt}{4\eta} = \frac{\ln\,(3 - Q_o)^{5/3}\, Q_o^{1/3}}{(3 - Q)^{5/3}\, Q^{1/3}} \qquad \text{----------(xx)}$$

Where $Q = Q_o$ for $t = 0$

According to Nabarro (1948) and Herring (1950) the viscosity is a function of the grain size, R, since the viscous flow of a poly-crystalline body depends upon the self-diffusion between grain boundaries subject to tensile and compressive stress. Thus :-

$$\eta = \frac{k\,T\,R^2}{10\,D\,\Omega_o} \qquad \text{----------(xxi)}$$

Where k = Boltzmann's constant

R = average grain radius

D = coefficient of self-diffusion

Ω_o = atomic volume

for metals and metal carbides the grain-growth is time dependent as (Burke and Turnbull (1952) Lersmacher et al (1962));

$$R^2 = R^2_o (1 - bt) \qquad \text{----------(xii)}$$

R_o = grain radius a t = 0

b = rate constant $\left(= \frac{K\ V}{R^2_o}\right)$

$K = K_r e^{-E/RT}$

The time-dependence of the viscosity becomes :-

$$\eta (t) = \frac{R^2_o (1 + bt)\ kT}{10D\Omega_o} \qquad \text{----------(xxii)}$$

$$\eta (t) = \eta_o (1 + bt) \qquad \text{----------(xxiv)}$$

Where $\eta = \eta_o$ for t = 0

Equation (xix) may now be written:

$$\frac{dQ}{dt} = -\frac{P}{4\eta_o (1 + bt)} \cdot \frac{Q\ (3 - Q)}{(1 - 2Q)} \qquad \text{----------(xxv)}$$

or integrated with respect to time :-

$$\frac{P}{4\eta_o b} \ln (1 + bt) = \ln \frac{(3 - Q_o)^{5/3}\ Q_o^{1/3}}{(3 - Q)^{5/3}\ Q^{1/3}}$$

$$= F(f) \qquad \text{----------(xxvi)}$$

The plots of F(f) versus ln(1 + bt) for tungsten carbide hot-pressed at 2500^{0}C and various pressures are linear.

As pointed out by Scholz and Lersmacher (1964) this last equation may be simplified to 'Murray form' noting the relation:-

$$\zeta = \frac{4}{3} \eta \frac{(1 - aQ)}{Q} \qquad \text{----------(xxvii)}$$

a = constant (varies between different authors)

i.e. does not contain any second-order term in Q as in equation (xxvi)

$$\frac{dQ}{dt} = \frac{3P}{4\eta} \cdot \frac{(1-Q)\,Q}{1 - aQ} \qquad \text{----------(xxviii)}$$

for $a = 1$

$$\frac{dQ}{dt} = \frac{3P}{4\eta} \cdot Q \qquad \text{----------(xxix)}$$

so that equation (xxvi) becomes :-

$$\ln \frac{Q\,(1 - Q_o)}{Q_o(1 - Q)} + a \ln \frac{1 - Q}{1 - Q_o} = -\frac{3P}{4\eta} ob \ln (1 + bt) \qquad \text{-------(xxx)}$$

for $a = 1$

$$Q = Q_o(1 + bt)^{\frac{-3P}{4\eta_o b}} = Q_o(1 + bt)^{\frac{-D\Omega_o 15}{kt\ 2R^2_o b}}$$

$$= Q_o(1 + bt)^{-exp.} \qquad \text{----------(xxxi)}$$

The densification process during hot-pressing is thus described by a hyperbolic rate equation based on the Nabarro-Herring mechanism.

In applying the above theory to a polycrystalline, porous body, r_2, (figure I.9.4) stands for the average distance from the pore centre to the surrounding grain boundaries. The apparent viscosity of such a body increases with the square of grain size as (1 + bt) to a final value, the diffusional viscosity of a single crystal. This is known to be extremely small. Therefore densification by the Nabarro-Herring mechanism can operate at useful rates only for a moderate grain size.

This last equation has been established empirically by Scholz and Lersmacher (1964) in studies on the hot-pressing of pure metallic carbides. Theyput :-

$$Q = Q_o(1 + Bt)^{-n} \qquad \text{----------(xxxii)}$$

where B is an empirical constant. The exponent n in equation (xxxii) is a constant of the material and is obtained from the slope of a plot of ln Q versus ln(1+ Bt), they found a linear relationship between ln Q and ln t, i.e. :-

$$\frac{dQ}{dt} = -k\frac{Q}{t} \qquad \text{----------(xxxiii)}$$

As pointed out by Scholtz (1963) equation (xxxii) is not satisfied at t = 0 where Q must equal Q_o unless an additional constant is used. In a plot of lnQ versus ln t, there should be an asymptopic approach to Q_o, this was evident in McElland and Whitney's (1962) work on tin powder.

I,10. The chemical reactivity of boron carbide and related compounds

The paucity of information on the reactivity of these compounds and the often conflicting available data results from the general inertness of these materials, particularly to non-oxidizing reagents, and the significance of the state of sub-division and the purity of the materials under examination. When considering the suitability of these refractiories for application, the reactions of greatest importance are those of oxidation, nitidation, and their degree of compatibility with metals and other refractory materials. In materials highly re-

sistant to chemical attack, e.g. oxididation, the reaction is extremely slow, even when the process is shown to be thermodynamically feasible, (see Section I.8). The apparent resistance to attack often results from the low volatity and refractoriness of the oxidation products or from the impervious nature of the oxide film, which inhibits further reaction, e.g. when metal carbides suffer oxidation, carbon is removed as the gaseous oxide and resistance to attack depends on the protective nature of the metal oxide layer. However, when a boride or a silicide is oxidised by air, oxygen or other oxidative gas, a vitreous phase of the nonmetal oxide covers the material and inhibits attack. Thus, boron carbide shows an increase in weight when heated in dry air to temperatures below 1000°C, but above this temperature there is progressive loss in weight as the boric oxide shows significant volatity. In moist air, loss of weight occurs at a much lower temperature due to the removal of boron as the more volatile boric acid. It follows that a study of weight change has little value unless cogniscence is taken of the exact composition and state of the reaction products.

Oxidative attack by acidic and basic fused media and solutions is assisted by the removal of the reaction products into solution; boron carbide and most borides react spontaneously with fused alkaline metal hydroxides, nitrates and persulphates. The action of elemental halogens on boron carbide (and other borides) is a highly exothermic process after initiation giving the volatile boron trihalide and carbon (or the metal halide).

Niridation by the element or ammonia gas is only significant at very high temperatures. It was reported in 'New Scientist', 1963, that boron carbide forms boron nitride and graphite when hot-pressed in a nitrogen atmosphere to 2000°C; metal borides form the metal nitride and boron nitride.

The reaction of boron carbide and other borides with molten metals is controlled by the contact angle the metal makes with the surface of the sintered compact. A zero contact angle, complete wetting of the surface, shows high reactivity between the two phases, whereas, a large angle indicates little or no reaction. Table 1.10.1. gives the contact angles of some refractory phases with metals in the molten state (Figure I.10.1.)

Figure I.10.1. Surface energy relationship between solid, liquid and vapour interfaces (after Sutton).

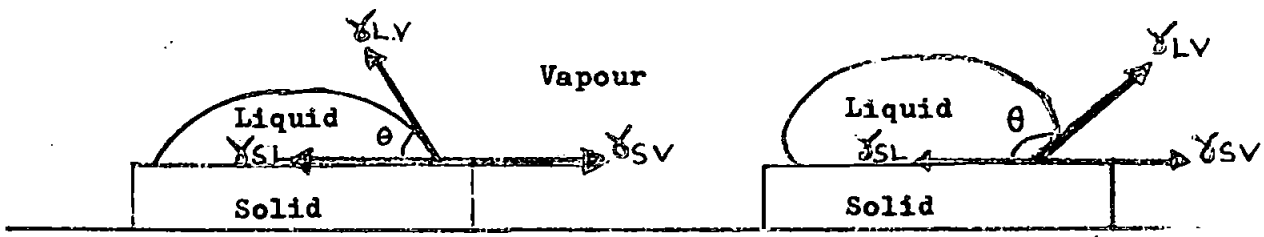

a) Wetting $\theta < 90^\circ$ b) Non-wetting $\theta > 90^\circ$

γ_{SL} surface energy solid liquid interface
γ_{SV} " " solid vapour "
γ_{LV} " " liquid vapour "

$$SL = SV - LV \cos \theta$$

T A B L E 1.10.1.

Contact angles of some molten metals with refractory boron compounds.

Phase	Metal	Temperature	Θ°	Reference
B_4C	Zn	540-620	121.5 - 119	Samsonov 1960
"	Cu	995-1090	130 - 17	"
"	Al	600-670	117 - 118	"
"	Pb	225-395	121 - 113	"
"	Brass	905-950	54.5 - 30	"
"	Fe	1780	strong reaction	Hamijan 1952
"	Co	1780	90	"
"	Cr	1820-1830	0	Janes + Nixdorf
"	Cr/Ni	1400-1410	0	1966
"	Ni	1470	41	"
TiB_2	Cu	1100-1500	158 - 154	Eremenko 1958
"	Ni	1480	100 - 38.3	"
CrB_2	Cu	1450	50	"
"	Ni	1480	11	"
ZrB_2	Cu	1160-1400	123 - 36	"

I.11. The applications of Boron Carbide and related refractories.

The principal applications of these materials result from their two main properties 1) refractoriness and 2) favourable mechanical strength and hardness. For example, boron carbide is the hardest and most abrasion-resistant material available in massive form. For some 25 years it has been used for sand-blasting nozzles, mortars for grinding, as a grit in grinding polishes and wheels, and for die, spinnerets and gauges. A recent application has been the production of light-weight armour on account of its hardness combined with high strength, high elasticity and low density. Since boron has a high nuclear cross-section the carbide has been used for control and shield materials and as burnable poisons in nuclear reactors. Boron carbide with a boron content of 78 wt-%, has the interesting anomalous property of a higher boron density than elemental boron itself; it is also more economical to produce. Another feature of the material is its electrical conductivity, suitable for its applications as a thermocouple, electrodes in cells and spark-erosion and for resistances. One serious disadvantage possessed by boron carbide, which limits its application, is its poor thermal shock resistance, one-half of the heating cycle, it shatters when cooled rapidly; composite materials containing silicon carbide show greater promise. Whiskers of boron carbide, single-crystal fibres, show extremely high strength and modulus and have been investigated as a possible reinforcement for metal and resin matrices.

The utilization of other borides has been limited by their poor oxidation resistance. Nevertheless, their use in mixed systems with silicides has been proposed in aircraft components at high temperatures. Both titanium and zirconium diborides have electrical resistivities comparable to copper and extensive tests have been made of these borides as electrodes for aluminium reduction although intergranular corrosion and their brittleness has caused failure. Many metal borides have application as heterogeneous catalysts in organic syntheses involving hydrogenation.

The present work has been stimulated by the need to produce boron carbide of a controlled quality for use as an abrasive grit by growing it to size, and for a material capable of sintering with a minimum of pressure and temperature. Also consideration has been given to the formation of wear-resistant surfaces on metal bases such as titanium by the in situ formation of their borides from boron carbide.

SECTION 2 - EXPERIMENTAL TECHNIQUES FOR THE PRODUCTION AND SUBSEQUENT ANALYSIS OF BORON CARBIDE.

The section covers the semi-technical production of boron carbide by the magnesium thermal reduction process and the experimental techniques used in determining the phase composition, crystallite and aggregate sizes of the material; and the principles underlying them.

2.1. The production of boron carbide - $B_{12}C_3$

Boron carbide, $B_{12}C_3$, was prepared by the magnesium thermal reduction process first described by Grey (1951) and later developed by Samsonov et al (1960). The starting materials were; anbydrous boric oxide, B_2O_3 (Borax Consolidated 20 Mule Team Technical Grade), granular magnesium turnings (Magnesium Elektron) and carbon black (Cabot, Sterling SO fluffy).

The boric oxide and the carbon black were mixed together in the ratio of their stoichiometric proportions (17.5 kg B_2O_3 + 1.25 kg C.) by milling in a steel ballmill having 'hardmetal' spheres for 24 hours to ensure complete blending. A stoichiometric amount of magnesium (18 kg) was blended gradually with the other components. Trials had indicated the difficulty of reacting large charges of the mixture (~40 kg) owing to the powders sifting and the reaction propagating slowly when initiated by a hot-wire fuse. It was found necessary to bind the reactants together by mixing in a small quantity of kerosene, this served to bind the components together in their correct stoichiometric proportions and also provide a blanket of vapour so preventing oxidation of the hot products by the air. Successive runs were com-

pleted with a high degree of control, unlike the experiences of the Hitachi workers (1966) who reported explosive reactions and added a diluent to the reactants, e.g. magnesia, MgO.

Temperatures in excess of 1600°C were measured within the charge. When cool, the charge was removed from its iron crucible, the crust was discarded and the remainder crushed down to a coarse powder. The crushed powder was added to an excess of diluted sulphuric acid (25 vol.%. 1.84 SG. H_2SO_4) to dissolve out the magnesium oxide and decompose magnesium boride and any unreacted boric oxide. It was found possible to decant off the liquor together with any unreacted carbon from the boron carbide sediment. Successive washings were made with warm water, decanting off the bulk of the liquor and finally filtering through a filter-paper supported on cloth (Whatman No1) and washed with copious amounts of water until free of sulphate ion. The boron carbide cake was dried in an oven at 120°C for several hours and then milled to a fine powder.

2.2(a) The chemical analysis of boron carbide and related compounds

As indicated in Section 1.10 the refractory compounds of boron resist attack by many chemical reagents, particularly in aqueous media. Therefore, fairly drastic methods are required for their dissolution before chemical analysis for boron and other elements, Blumenthal (1951) describes methods for the analysis of many of these compounds.

For the determination of boron the sample is first mixed with anhydrous sodium carbonate in the ratio of 1 part to 20 parts of the alkali, the mixture is heated to fusion in a platinum dish, previously lined with sodium carbonate to prevent attack on the metal by elemental boron. A powerful exothermic reaction normally occurs through the oxidation of the boron and other components, but it is sometimes necessary to add some sodium nitrate to the melt to assist the oxidation. On cooling the fused melt is leached with dilute hydrochloric acid and the solution made up to volume. The borate ion in an aliquot is determined either titrimetrically with sodium hydroxide by the mannitol method or by flame photometry using an atomic absorptiometer. In both techniques it is necessary to remove interfering cations by ion exchange. In the present work both methods of analysis were employed.

The titrimetric method of analysis for boron is based on the method of Kramer (1955) using a cation exchange in the hydrogen form (Permutit Zeocarb 225 meshrange 40-80) and determining the equivalence point of neutralisation with a pH meter (Pye). Firstly the stronger hydrochloric acid is neutralised with sodium hydroxide to pH = 7.00, then excess mannitol is added to release hydrogen ions by the following reaction:

$$\underset{\text{Orthoboric acid}}{H_3BO_3} + \underset{\text{mannitol}}{C_6H_{14}O_6} = H_2BO_3{\cdot}\text{mann}^- + \underset{\text{hydrogen ion}}{H^+} + H_2O$$

The titration is then continued to the same pH value.

Alternatively, the eluate from the ion exchange column is analysed for boron by atomic absorption spectroscopy using a Hilger and Watt Atomspek spectrophotometer. The solution is excited in an acetylene/nitrous oxide flame. Using a boron lamp the wavelength is set at 2498 Å and the attenuation of the radiation is observed for samples and for standard solutions of boron.

Other elements were determined qualitatively by emission spectrography using a Hilger and Watt Large Quartz spectrograph, and quantitatively, (with the exception of carbon) by atomic absorption using the appropriate element lamp. Emission spectrography has application in the detection of most elements, only those light elements having high ionisation potentials, e.g. nitrogen, oxygen, the chalcogens and the halogens are not detected when excited in the usual manner. (The solid sample is excited in the usual manner.) The solid sample is excited by arcing between copper or graphite eletrodes (Johnson-Matthey-specpure) and recording the spectra on a photographic plate (Ilford Ordinary N30), exposures being taken at two spectral ranges; viz, above 2760Å and above 2200Å to record all of the most sensitive emission lines of the elements in question.

Quantitative analyses were carried out for the various elements detected by qualitative analysis, by measurement with the atomic absorption spectrophotometer (Hilger-Watt Atomspek) of the solutions obtained from either alkaline or acid fusion (potassium pyrosulphate), comparison being made with prepared standards.

2.2(b) X-ray diffraction identification of phases

A comprehensive summary of the theory and practice of X-ray diffraction techniques is given by Peiser et al (1960). A crystal consists of a regular three-dimensional array of atoms in space. Points having identical surroundings in the structure are called lattice points, and collection of such points in space forms the crystal lattice. If neighbouring lattice points are joined together the unit cell is obtained, i.e. the smallest repeating unit of the structure. Sometimes it is more convenient to choose a larger repeating unit, for example a centred cell. In general the shape of the unit cell is a parallelepiped, but, depending on the symmetry of the crystal, it can have a more regular shape, e.g. cubic or rectangular. The shape of the unit cell is completely described by the lengths of its three edges or axes and the angles between them. Conventionally, the axes are termed $\underline{x}$, $\underline{y}$, $\underline{z}$ or $\underline{a}$, $\underline{b}$, $\underline{c}$, and the angles α, β, γ ; α being between the $\underline{y}$ and $\underline{z}$ axes, etc.

Crystals can be classified into seven classes according to their symmetry as shown in Table 2.2.1.

T A B L E 2.2.1

Crystal Glass	Conditions limiting cell dimension	Minimum symmetry
Triclinic	$a = b = c$ $\alpha \neq \beta \neq \gamma = 90^\circ$	None
Monoclinic	$a = b = c$ $\alpha \neq \gamma = 90^\circ, \beta = 90^\circ$	One 2-fold axis or 1 pps*
Orthorhombic	$a = b = c$ $\alpha = \beta = \gamma = 90^\circ$	Two 2-fold axis or 2 pps*
Tetragonal	$a = b = c$ $\alpha = \beta = \gamma = 90^\circ$	One 4-fold axis
Hexagonal	$a = b = c$ $\alpha = \beta = 90^\circ$ $\gamma = 120^\circ$	One 6-fold axis
Rhombohedral	$a = b = c$ $\alpha = \beta = \gamma = 90^\circ$	One 3-fold axis
Cubic	$a = b = c$ $\alpha = \beta = \gamma = 90^\circ$	Four 3-fold axis

* pps perpendicular planes of symmetry

Various sets of parallel planes can be drawn through the lattice points of a crystal. Each set of planes in identified by a set of three integers, namely, the Miller indices, h, k, l corresponding to the three axes a, b, c, respectively. The index, h, is the reciprocal of the fractional value of the intercept made by the set of planes on the a axis, etc. When a crystal interacts with an incident beam of X-rays, the lattice can act as a diffraction grating, because the lattice's dimensions are of the same order of magnitude as the wavelength of the X-rays. The diffracted beam which emerges, in phase, from a particular set of lattice planes obeys Bragg's Law.

$$\lambda = 2d \sin \theta \quad \text{---------- (i)}$$

where λ = wavelength of the incident X-ray beam

$\underline{d}$ = interplanar spacing

θ = angle of incidence (diffraction)

When the crystals are large and have a large number of lattice planes in each set the diffracted beam appears at a sharp angle. With aggregates of small crystals broadening occurs and the extent serves as a measure of crystallite size. The interplanar spacing, $\underline{d}$, is related to the unit cell dimensions of the crystal and to the Miller indices of the set of planes. Thus, measurement of Bragg angles leads to the determination of the lattice constants.

If a single crystal of a substance is rotated in a beam of monochromatic X-radiation, the diffraction pattern forms a series of spots on a photographic plate. However, if the sample is in the form of a crystalline powder or a sintered compact, the crystals in which show random orientation, the diffracted beams lie along the surfaces of a set of coaxial cones. The pattern can be recorded using either an X-ray diffractometer with electronic ionisation detector and chart recorder, or a powder camera with photographic film which gives a series of concentric rings.

The distribution with respect to the Bragg angles and intensities of the diffracted beams is characteristic of a particular structure and can be used as a means of identification, as a fingerprint. The X-ray powder diffraction patterns

of most crystalline substances in their various allotropic forms, are recorded (A.S.T.M. Powder Diffraction File in a card form). The powder pattern of a mixture of crystalline structures consists of the superimposed patterns of the individual structures. It should be noted that due to instrument characteristics, and orientation effects displayed by the sample, the relative intensities of the lines forming these patterns do not always correspond with those of the A.S.T.M. card.

In the present work, X-ray powder diffraction patterns were determined using a Berthold diffractometer fitted with a gas filled proportional counter fitted to a combined discriminator/ratemeter and EHT supply and having a chart recorder output. The source of X-radiation, copper KX of wavelength 1.542Å, was an Hilger and Watt's constant voltage generator fitted with a sealed tube Philips copper target having nickel filters to remove the Kβ component. The generator was operated at a standard 40 Kilo volts potential, and a filament voltage of 20 milliamps.

Loose powders were examined by mixing with a cellulose acetate cement and coating a suitable amorphous (X-ray transparent) material such as a glass cover slide. Sintered materials and metal samples were machined with a flat face and mounted directly on to the goniometer. Phases were identified by reference to the appropriate A.S.T.M. tables or to reference samples measured in the same manner.

2.2(c) Electron microscopy and diffraction

Comprehensive accounts of the theory and practice of electron diffraction and its application to high level magnifications (microscopy) are given by Zworykin et al (1945) Kay (1965) and Hirsch et al (1965).

A beam of electrons possesses wave properties similar to those of a beam of electromagnetic radiation, the wavelength being given by the de Broglie relationship:

$$\lambda = \frac{h}{p} = \frac{h}{mv} \qquad \text{---------- (i)}$$

where λ = wavelength

h = Planck's constant

m = electron mass

v = velocity

p = momentum

If the accelerating potential difference is V, the energy, E, of an electron is given by

$$E = \tfrac{1}{2} mv^2 = Ve \qquad \text{---------- (ii)}$$

where, e = electrostatic charge.

Combining equations (i) and (ii) and eliminating V gives:

$$\lambda = \frac{h}{\sqrt{2meV}} \qquad \text{---------- (iii)}$$

A relatively small correction has to be applied to equation (iii) to account for the variation in the mass of the electron with velocity, which depends on the voltage. In practice, however, the wavelength, if required, is determined by recording the diffraction pattern of a substance with known unit cell dimensions and calculating a single factor, the camera constant, $L\lambda$, where L is the effective camera length. If the same instrument is used at the same accelerating voltage, then $L\lambda$ remains constant. At an accelerating voltage of 100 kilo volts the wavelength of an electronic beam is 0.037 Å.

The electron microscope is constructed on similar principle to the optical microscope, but its optics or lens system is comprised of a series of magnetic or electrostatic fields of varying intensity and direction through which the beam passes. The shorter wavelength of electrons compared with that of visible light enables a much greater resolution to be achieved by the electron microscope; the theoretical limit of resolution of a microscope is given by half the wavelength of the radiation used - .02A for the electron microscope and 2000 Å for the optical microscope, a gain of 10^5. Figure 1 gives the general layout of a typical electron microscope. The object to be studied, by transmission, is placed in the focal plane of the instrument and its magnified image viewed directly on a phosphor screen or recorded on to photographic film held in a cassette within the instrument. Normally, both facilities are employed, one to align and select, the other to record. The energy of electrons is reduced when they are scattered readily on collision

with gas molecules. Hence, the microscope has to be operated at a sufficiently low pressure to increase their mean free path, thus a vacuum of about 10^{-6} mm Hg is required.

Diffraction patterns of the samples viewed on the electron microscope can be obtained by interposing a special lens system between the objector and the projector. (Figure 2.2.1) such diffraction is possible only when the crystals or their aggregates are very thin and/or are composed of elements of low mass number as the electrons are highly absorbed by matter. The diffraction pattern of a single crystal consists of reflections from a plane of reciprocal lattice point, here, electrons, because of their very short wavelength differ from X-rays. Nevertheless for a polycrystalline specimen in random orientation, the diffraction pattern consists of the typical concentric rings.

Figure 2.2.1.

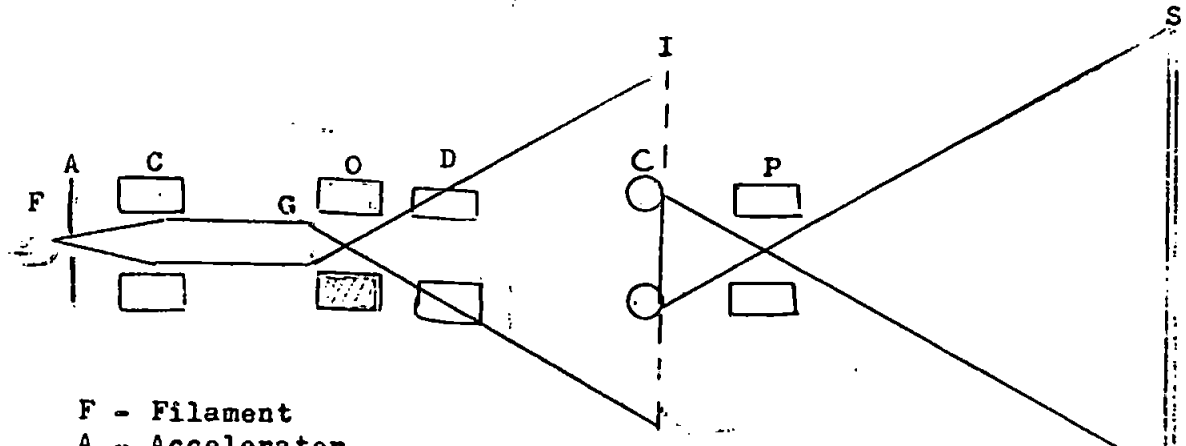

F - Filament
A - Accelerater
C - Condenser Lens
G - Sample Grid
O - Objective Lens
D - Diffraction Lens
I - Image
C - Camera
P - Projector Lens
S - Screen

In the present work, direct transmission and diffraction micrographs of powdered materials and transmission micrograph surface replicas of sintered refractory materials were made using a Philips E.M.100B electron microscope, see Van Dorsten, Nienwdorf and Verhoeff, (1950.)

Specimens were supported by a carbon film laid on a copper grid. The carbon film was produced initially by evaporation from a pair of carbon electrodes struck by a D.C. Arc on to a clean mica surface inside the vacuum belljar of an Edwards Speedivac High Vacuum Coating Unit 12E6. The carbon film of roughly 200Å thickness was floated on to distilled water and each copper grid coated with the film. A copper grid consists of a 3 mm diameter of # 200 square mesh foil, each hole has side length of 100 μm, the width of the sashes forming the window vary in size to give a pattern which assists in the location of a particular area of the grid.

Samples for direct transmission were prepared by dispersing the powder in water or other unreactive liquid medium together with a suitable deflocculating agent, for boron carbide addition of ammonium hydroxide solution (10% vol./vol.) proved to be adequate for dispersion. A portion of the solution was placed on the prepared grid and evaporated to dryness under an infra-red heat lamp.

Samples prepared as replicas were prepared by pressing a gob of melted clear polystyrene polymer or by coating with a PVA emulsion on to the sintered surface, an initial impression served

to remove any adherent material from the surface, until it solidified. The film replica so produced was then shadowed, i.e. coated with a film of platinum in the coating unit in such a manner as to 'highlight' the surface structure. The polymer was dissolved away, using chloroform for polystyrene and dilute HCI for P.V.A., and the film placed directly on to a copper grid. The grids were placed in the sample holder and placed in the microscope through a vacuum seal at the focal plane of the lens system. After selection of an area of interest at the required magnification the film was exposed for a number of seconds depending on the intensity of the image. Magnification is determined by reference to the voltage applied to the focussing optics and a calibration chart. On completion of a set of exposures the film camera was removed from the microscope and the film, 35mm (Kodak Fine Grain Reversal) developed in a fine grain developer to give optimum contrast. Prints were made from the 'negative' on to Kodak bromide paper noting the magnification factor of the enlargement from its negative, in this manner magnifications of over 70,000 times the original size were obtained.

2.2(d) Surface area measurement by gas sorption

The amount of a gas adsorbed by a substance depends, inter alia, on the specific surface, i.e. the surface area per unit mass.

Therefore, gas sorption measurement provide a means of determining the average particle size of a powder of regular shape and simple geometry. A general account of the technique is given by Gregg and Sing (1967).

The method most widely used is that due to Brunauer, Emmett and Teller (1938). The B.E.T. equation states :-

$$\frac{p}{x(po-p)} = \frac{C-1}{XmC} \cdot \frac{p}{po} + \frac{1}{XmC} \qquad \text{---------- (i)}$$

where p = pressure of adsorbate vapour in equilibrium with absorbent

po = saturated vapour pressure of vapour adsorbed

x = amount of vapour adsorbed

xm = capacity of filled monolayer

c = a constant

Figure 2.2.2.

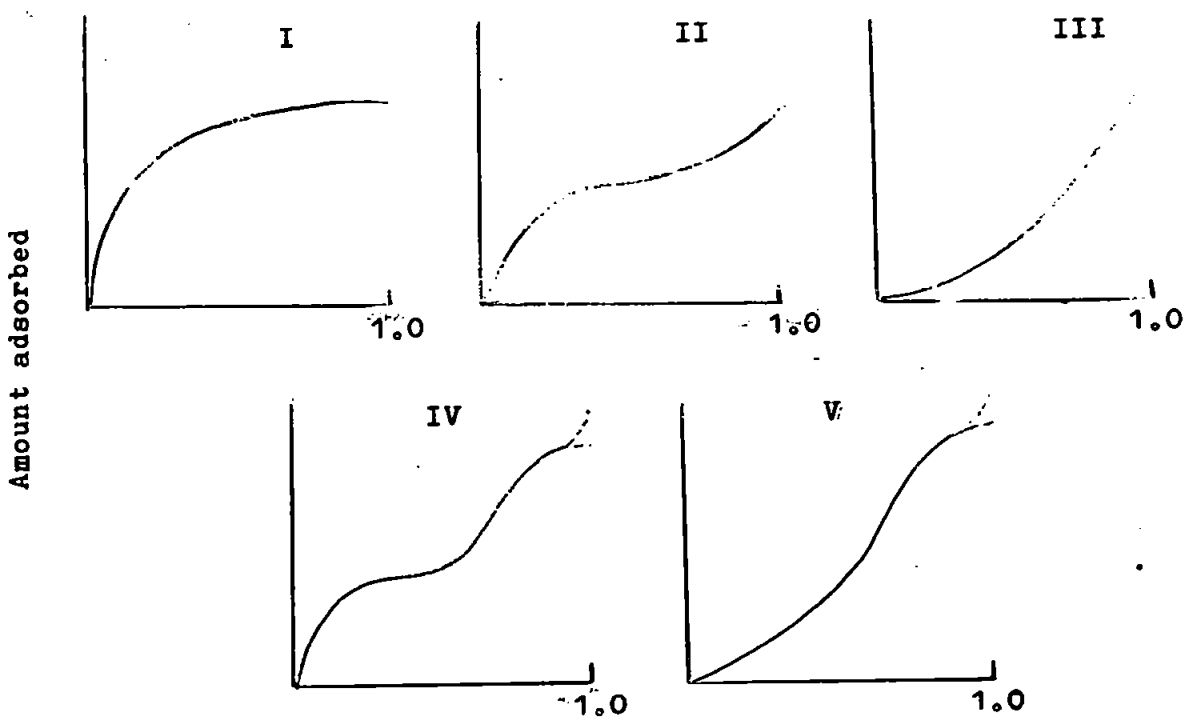

Five types of adsorption isotherm in the B.E.T. classification

Adsorption isotherms are classified into five types as proposed by Brunauer, Deming, Deming and Teller (B.E.T. classification. See Figure 2.2.2. Of these, only Types II and IV can be used to calculate the specific surface of the adsorbing solid and only Type IV for making an estimate of pore size distribution. However, Type II isotherms give best agreement with the B.E.T. equation over limited ranges of relative vapour pressure (Gregg (1961), p.31,56). Thus a plot of $\frac{p}{x(po-p)}$ versus $\frac{p}{po}$ results in a straight line graph of slope $\frac{C-1}{XmC}$ and intercept $\frac{1}{XmC}$. Elimination of c from these two expressions gives Xm. The adsorbate can be measured either gravimetrically or volumetrically (tensiometrically) (Gregg and Sing, 1967, p.310).

The specific surface, S, is related to Xm by the equation:-

$$S = \frac{Xm}{M} \cdot N \cdot Am \qquad \text{---------- (ii)}$$

where M = molecular weight of adsorbate

N = Arogadros number

Am = cross-sectional area of an adsorbate molecule in a completed monolayer

For a substance consisting of cube-shaped crystallites, the average particle size, l, is related to S by :-

$$S = \frac{6}{Pl} \qquad \text{---------- (iii)}$$

where P = density of the adsorbent

The same relationship is valid for calculating the equivalent spherical diameter, similar relationships can be derived for plate and needle-shaped crystallite powders.

The sorption balance used in the present work is based on the design by Gregg (1946, 1955.) The balance used for low temperature nitrogen adsorption as described by Glasson (1956) and B.S. 4359, Part I (1969) and is shown in Figure 2.2.3.

The whole assembly is encased in glass allowing it to be evacuated and filled with any desired gas. Balancing of the beam is affected by applying a current to the external solenoid. The instrument is calibrated by measuring the current required to observe the null-point for known loadings on the balance pan.

The samples for which surface areas were to be measured, were placed, in turn, into the bucket and outgassed to remove physically adsorbed vapour, this was undertaken at 200°C to remove possible moisture (Glasson, 1964). The adsorbate was nitrogen gas and the coolant, boiling liquid oxygen, so that the isotherms were measured at -183°C. The weight of the sample was determined in vacuo, and aliquots of nitrogen gas were introduced into the system. Simultaneous readings of sample weight and the nitrogen gas pressure were taken when equilibrium was reached. A final reading was recorded at room temperature and one atmosphere pressure of nitrogen. The IBM Programme for computing the surface areas was that devised by P.O'Neill and Denise Harris (Plymouth Polytechnic) and is detailed in Appendix II.

Figure 2.2.3.

The gas sorption balance

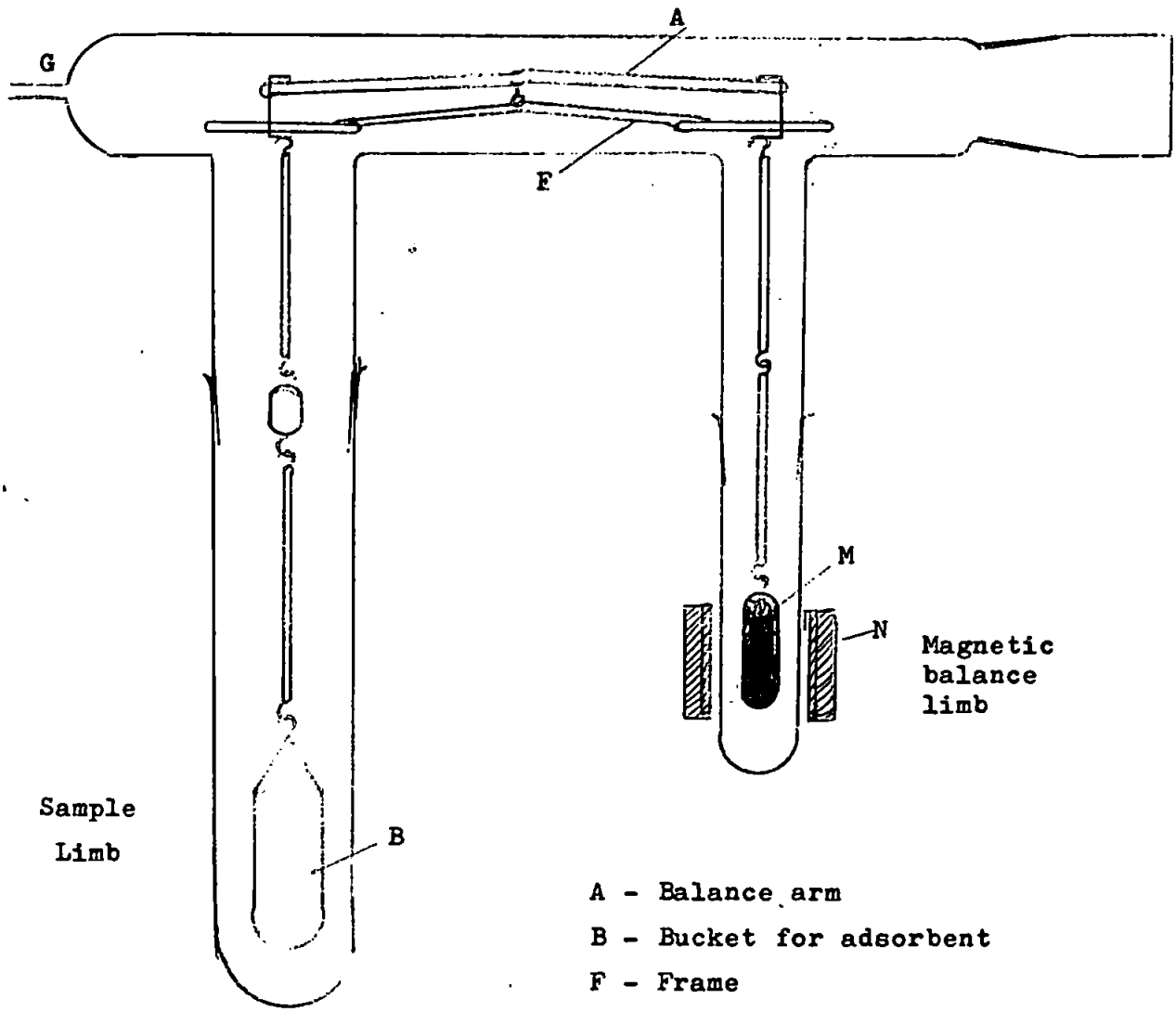

A - Balance arm

B - Bucket for adsorbent

F - Frame

G - Connection to gas handling system

M - Permanent magnet or solenoid

N - Solenoid

2.2(e) Thermometric analysis

There are a number of analytical techniques which come under the title of thermometric analysis of these perhaps two of the most widely applied. One, thermogravimetric analysis (T.G.A.) is a technique whereby the weight of a sample can be followed over a period of time while its temperature is being changed, usually it is increased at a constant rate; it is particularly suited for measuring the loss of weight on the decomposition of a solid to a solid residue and to a gas, and also indicates the termal stability of a compound in both inert and in reactive atmospheres.

A thermobalance consists of a modified single or double pan analytical balance (Gregg and Winsor, 1945). In the present work, a Stanton balance was used having a crucible suspended into an electric furnace, via a nichrome wire support from the weighing pan. The furnace winding was energised through a linear variable programmer (Stanton-Redcroft) and temperature was measured using a Pt/Pt.-13%Rh thermocouple attached to a millivolt meter. (Baird and Tatlock-Resilia). The general set up is shown in Figure 2.2.4.

0.5g of the powder under test were accurately weighed into an alumina crucible (Thermal Syndicate Thermal Alumina), attached to the balance and the weight noted. The thermal programmer was set to give a linear rise (20°/min) from the ambient to the set temperature for the run, and the weight of the crucible recorded at known intervals of time. In the present work the reacting gas was air, the relative humidity and the ambient

Figure 2.2.4. Thermal gravimetric analysis apparatus

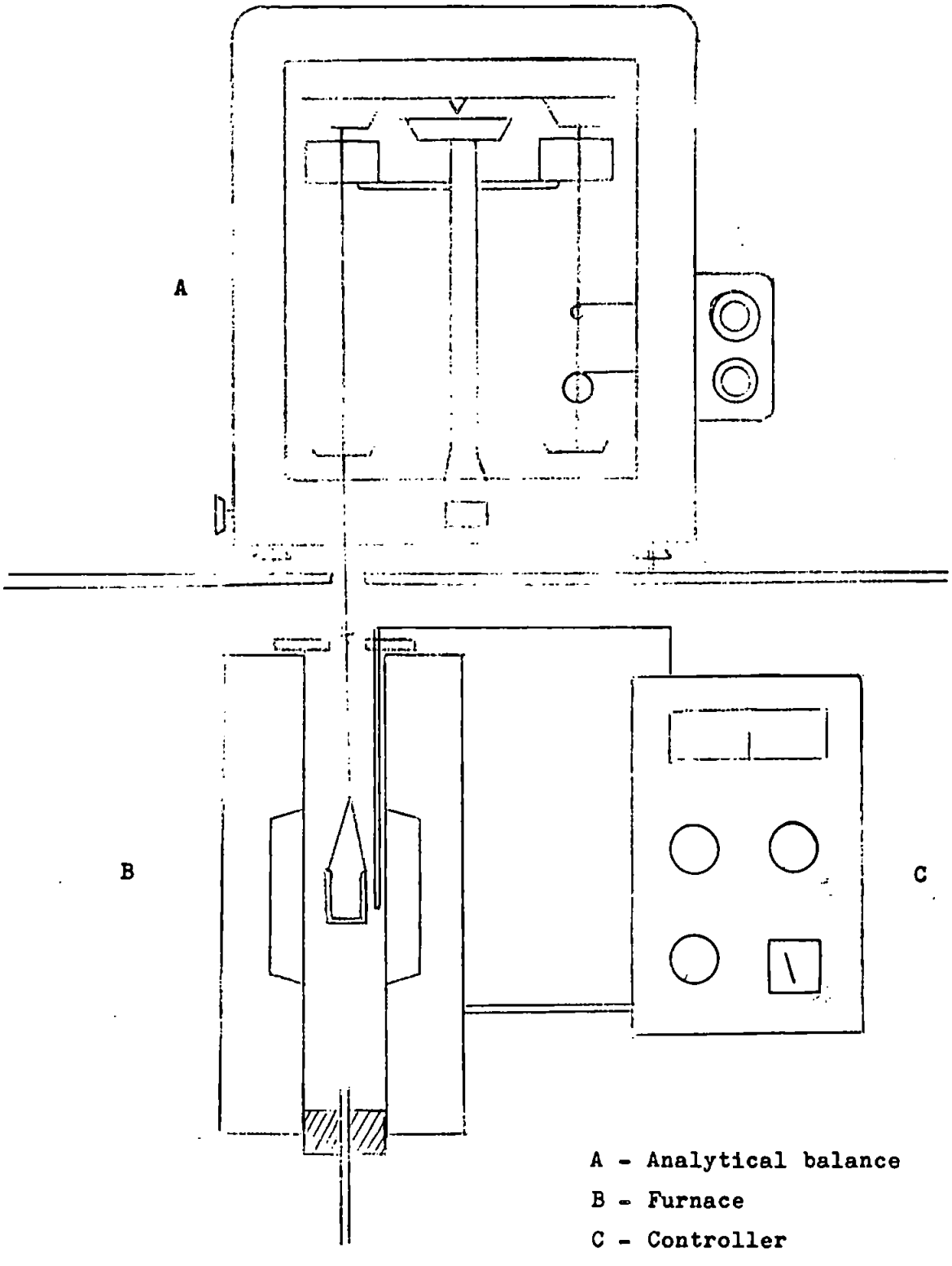

A - Analytical balance
B - Furnace
C - Controller

temperature being recorded throughout the run. Samples of boron carbide and other borides were heated between 20° and 1100°C; isotherms being studied in the temperature regions showing pronounced weight change in the specimen. The reaction kinetics were determined from the slope of logarithmic weight changes plotted against the logarithmic time as discussed in Section I.8. The activation energy of the oxidation by air of boron carbide was estimated by the Arrhenius equation.

A second method of thermometric analysis is that of differential thermal analysis, D.T.A., it was first applied by Houldsworth and Cobb (1922-3). Thermocouples embedded in the test and inert materials were connected in opposition so that any appreciable E.M.F. set up during the heating resulted from the evolution or absorption of heat in the test sample and the temperatures at which such changes occured were noted. In the present work, D.T.A. equipment based on the design described by Grimshaw, Heaton and Roberts (1945) was employed - Figure 2.2.5. 0.5g of the sample was packed alongside the reference material, recrystallized Al_2O_3 in a ceramic block. The block was heated in an electric furnace (Griffin and George) controlled by a linear programmer, (Stanton-Redcroft) heated at a rate of 10 to 20°/min. The temperature of the block and the temperature differential were recorded automatically over the temperature range of 250 to 1000°C in order to determine the temperature required for the onset of oxidation of boron carbide and related materials by air.

Figure 2.2.5. - D.T.A. apparatus

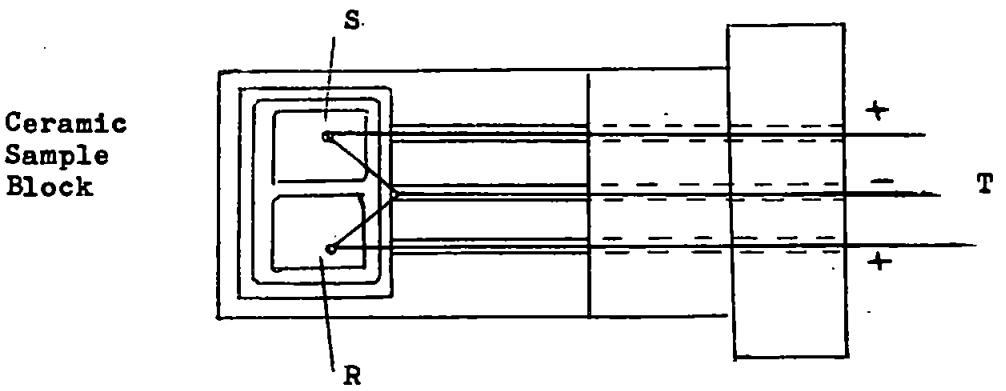

R - Reference
S - Sample
T - Thermocouples

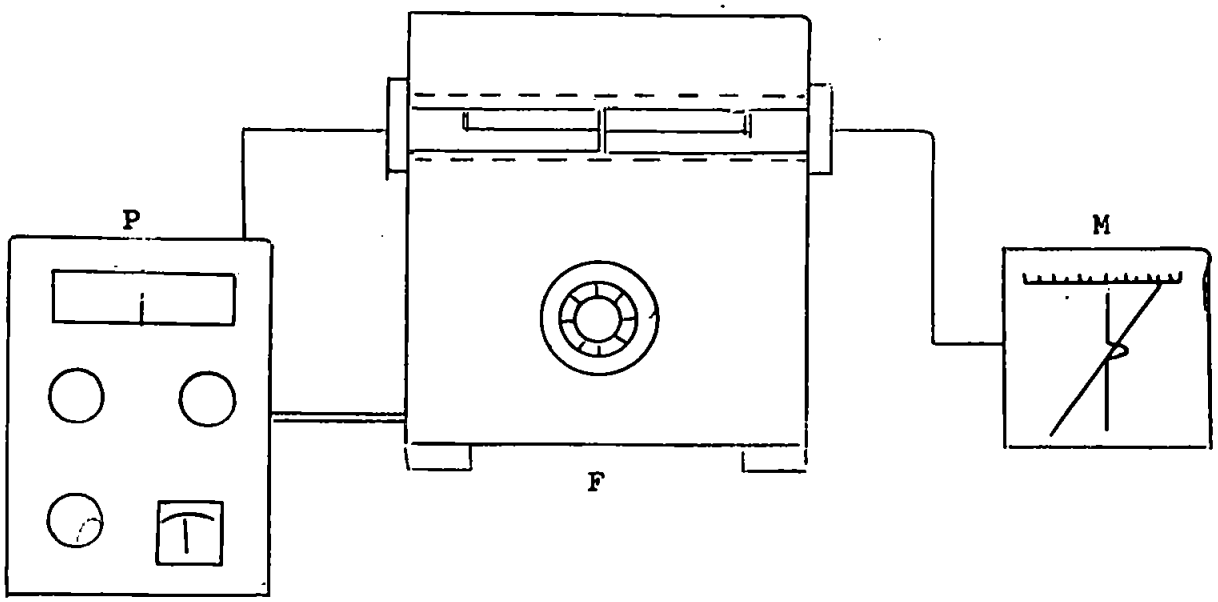

F - Furnace
P - Linear programmer
M - Multipen recorder

SECTION 3 - EXPERIMENTAL RESULTS OBTAINED ON THE PREPARED BORON CARBIDE AND ON RELATED MATERIALS

The section includes results of the analysis and the subsequent treatment of the prepared boron carbide to determine its changes in surface activity, crystallite and aggregate sizes on sintering.

3.1. The analysis of the prepared boron carbide

3.1(a). The chemical analysis showing the composition of the boron carbide with regard to its stoichiometry and to its purity is given in Table 3.1.1.

TABLE 3.1.1.

Element \ Sample No.	1.		2.	
	wt. %	at. %	wt. %	at.%
boron **	76.2	77.6	74.3	75.6
carbon	20.8	19.6	20.3	18.9
free carbon	2.8		5.4	
free B_2O_3 **	0.1		0.1	
oxygen	-		-	
nitrogen	-		-	
silicon *	0.1		0.1	
magnesium *	0.4		0.15	
iron *	0.05		0.05	
others *	n.d.		n.d.	

n.d. not detected

* spectrophotometrically ** volumetrically

3.1(b) Phase identification of boron carbide by X-ray diffraction

Data obtained from the diffractometer trace of the prepared boron carbide (Figure 3.1.1.) is compared with that obtained from a commercial sample of boron carbide (Norton Norbide) (Figure 3.1.2.) and the date given in A.S.T.M. Card 6-0555. (Table 3.1.2.)

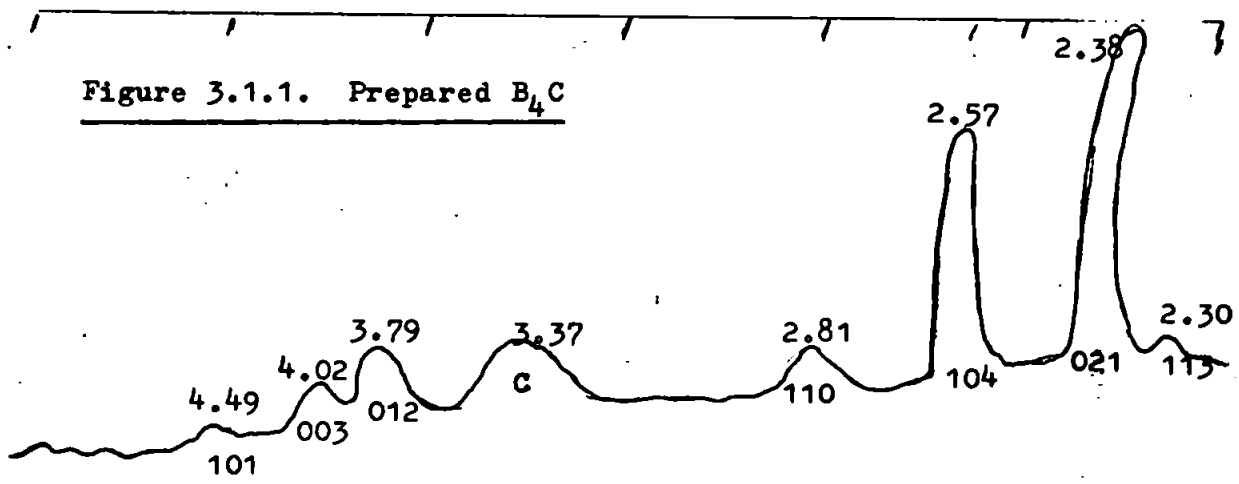

Figure 3.1.1. Prepared B_4C

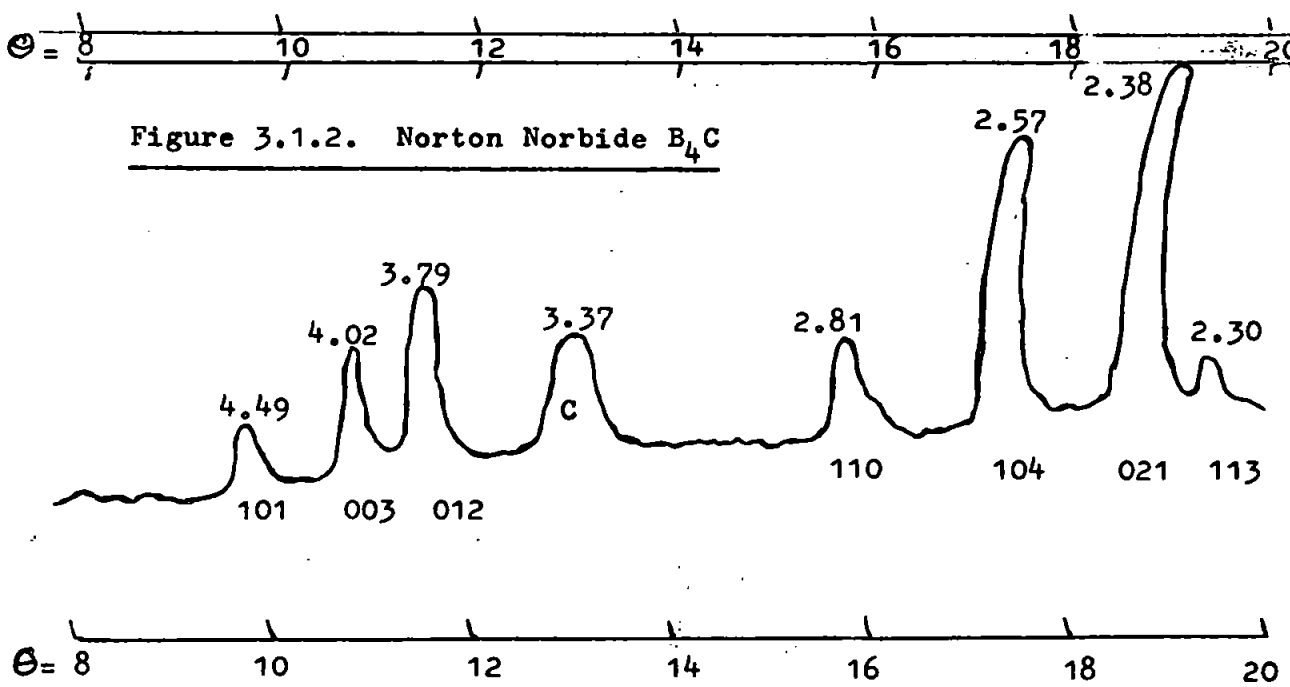

Figure 3.1.2. Norton Norbide B_4C

TABLE 3.1.2.

B_4C (Figure 3.1.1.)		B_4C (Figure 3.1.2.)		A.S.T.M. CARD 6-0555		
I/I_1	d(Å)	I/I_1	d(Å)	I/I_1	d(Å)	(hkl)
v.w.	4.49	20	4.49	30	4.49	101
w	4.02	30	4.02	40	4.02	003
60	3.79	65	3.79	70	3.79	012*
15	3.37	20	3.37	100	3.35	001
w	2.81	15	2.81	30	2.81	110
80	2.57	80	2.57	80	2.57	104
100	2.38	100	2.38	100	2.38	021
w	2.30	w	2.30	10	2.30	113
w	2.02	20	2.02	10	2.02	006
w	1.87	10	1.87	10	1.87	211
10	1.71	20	1.71	30	1.714	205
v.w.	1.63	v.w.	1.63	10	1.637	116
—	-	-	-	10	1.628	107
w	1.50	15	1.50	20	1.505	303
w	1.46	20	1.46	30	1.463	125
w	1.45	20	1.45	30	1.446	018
w	1.41	20	1.41	30	1.407	027
w	1.35	w	1.35	20	1.345	009
w	1.34	w	1.34	20	1.342	113
w	1.33	w	1.33	20	1.326	223
v.w.	1.29	v.w.	1.29	10	1.286	208
w	1.26	w	1.26	20	1.261	306
v.w.	1.19	v.w.	1.19	10	1.191	042

I/I_1 - relative intensity taking (021) = I_1 = 100

* Spacing for Carbon (graphite)

3.1(c) Particle size analysis

Sedimentation methods for particle size analysis, e.g. Andreasen pipette method, indicated that when samples of the prepared boron carbide were dispersed in water the terminal velocities given by:-

$$V = \frac{2\,gr^2(d_1-d_2)}{9\eta} \quad \text{cm./sec}$$

where V = terminal velocity

g = 981 cm/sec^2

r = Stokes diameter (cm)

d_1 = density of boron carbide, g/cm^3

d_2 = density of water, g/cm^3

η = viscosity of water

showed, that 70% of the sample consisted of 'particles' with radii above 30 μm and the remainder displaying a maximum distribution at or below 1 μm radius (Figure 3.1.3.). Further dispersion (by subjecting the sample to ultrasonic vibration) altered the distribution curve, and it was evident that the larger particles were, in fact, aggregates of smaller particles. On the assumption that aggregation was due to an acidic oxide layer on the surface of each particle of boron carbide, the experiments were repeated using a dilute solution of ammonium hydroxide (1 molar) to disperse the samples; results now showed the majority of the particles to be below 1 μm in size. These methods do not function accurately below 1 μm radius as

the terminal velocities are extremely slow, so that such dispersions are virtually stable. For this reason, other methods of particle size analysis were investigated.

It was noted that there was some broadening of the X-ray diffraction lines produced by the prepared boron carbide (Figure 3.1.1.). The lines obtained by X-ray diffraction have a finite width due to the collective effect of X-ray beam width, the aperture of the detector and mechanical imperfection of the instrument, e.g. recorder response. The instrumental broadening can be determined readily by examining the diffractometer traces of a large perfect crystal of calcite ($CaCO_3$). Superimposed on the instrumental line width there may be an intrinsic line broadening arising from lattice distortions, stacking faults or from the sample being composed of very small crystallites; the effect becomes significant at dimensions $< 0.1 \mu m$. The line width is related to the crystallite size; one commonly-used relationship is :-

$$\beta = \frac{\text{integrated intensity of the line}}{\text{intensity of peak}} = \frac{K \lambda}{t . \cos\Theta}$$

where K = constant ($\sim$ unity)

λ = wavelength of the radiation

Θ = Bragg angle

t = a linear dimension = $\sqrt[3]{V_m}$

V_m = mean crystallite volume

β = line width (in terms of 2Θ)

β is estimated either from the recorder trace as the peak width at half the peak maximum after subtraction of the background radiation, or using the scaler and printout to give optimum statistical accuracy. This formula can only be used experimentally when there is insignificant instrumental line broadening. As it is not possible to correct by simple subtraction the contribution of the instrument broadening in cases where such broadening is significant, the method due to Jones (1938) is used. The observed integral breadths of the lines are first corrected for the fact that they are produced by the $\alpha_1\alpha_2$- doublet of the copper X-radiation using the graph, Figure 3.1.4. of b/Bo against Δ/Bo, where Bo is the observed line broadening, b is the corrected width for the sharp, s-line of calcite ($14^{o}43'$) Δ is the doublet separation measured in the same units, calculated from the formula :-

$$\Delta = 0.285 \tan\Theta \quad \text{(Copper } K_{\alpha}\text{)}$$

The corrected width B, for the broadened m-line of the (104) spacing for boron carbide ($17^{o}31'$) is obtained from the same graph. β, the intrinsic broadening, is obtained from the graph β/B against b/B Figure 3.1.5. In a typical calculation of the average crystallite size of the prepared boron carbide (batch # 1) the following results were obtained.

Figure 3.1.4.

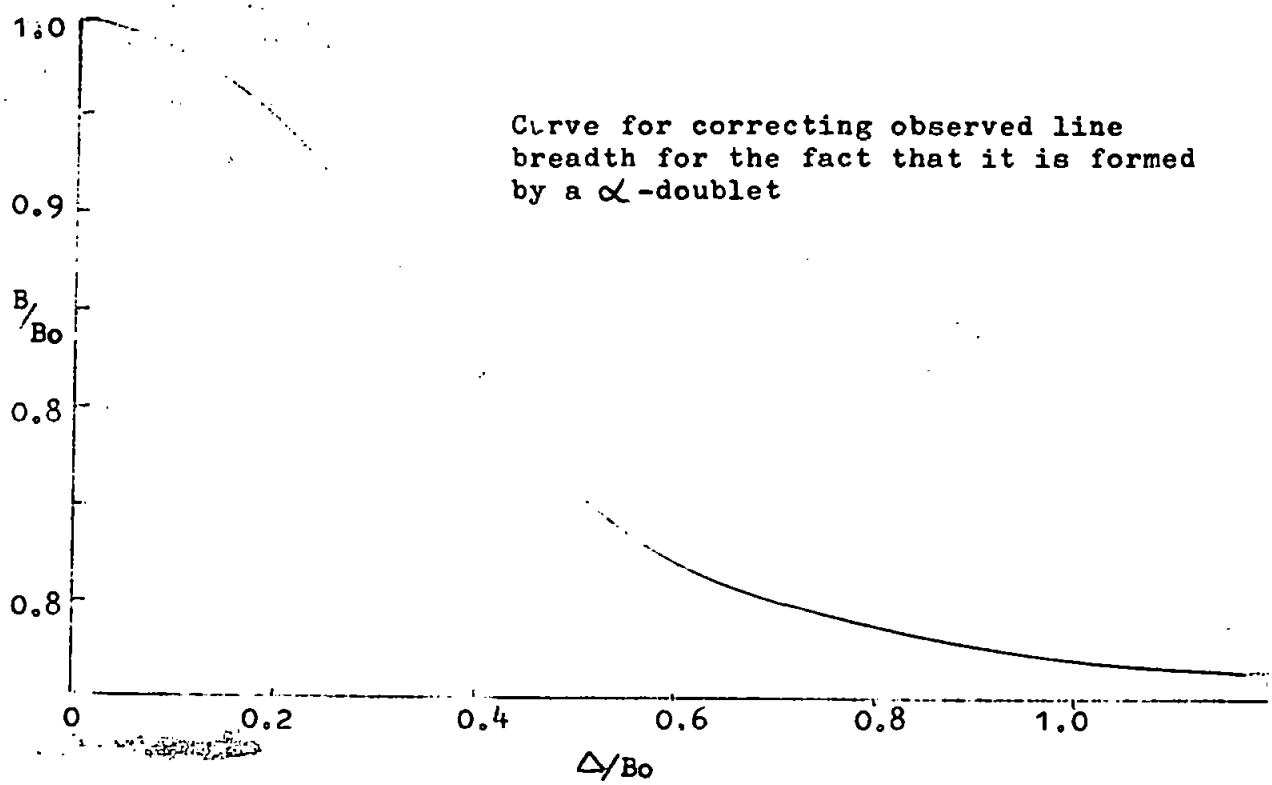

Curve for correcting observed line breadth for the fact that it is formed by a α-doublet

Figure 3.1.5.

Curve for correcting line breadth for the effect of instrumental broadening

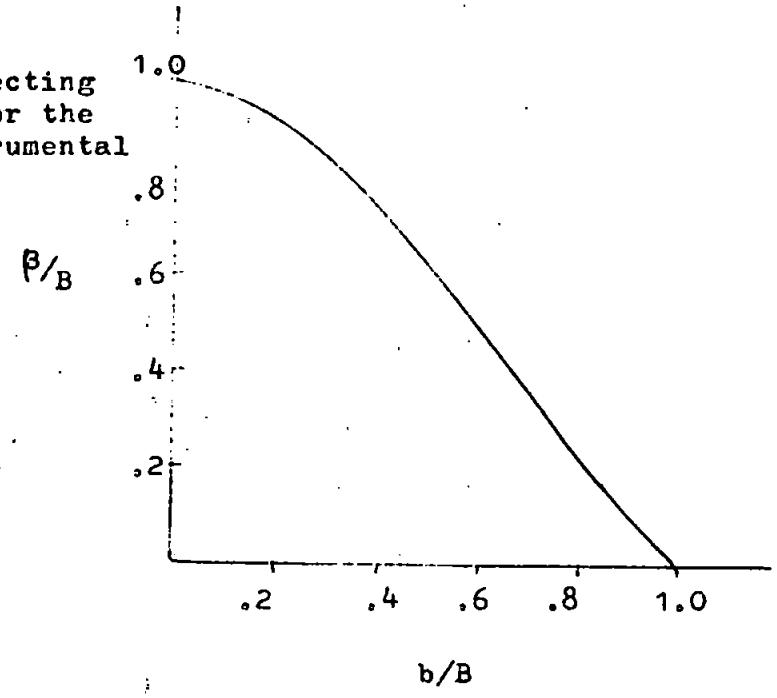

Boron carbide m - line $B = 0.307^{\circ}$ from Figure 3.1.1.

Calcite s - line $b = 0.240^{\circ}$

m - line $\triangle = 0.2.85 \tan 17^{\circ}31' = 0.090$

$\therefore \quad \triangle/Bo = 0.293$

from Figure 3.1.4. $B/Bo = 0.90 \quad B = 0.276^{\circ}$

s - line $\triangle = 0.285 \tan 14^{\circ}43' = 0.075$

$\therefore \quad \triangle/Bo = 0.313$

from Figure 3.1.4. $b/Bo = 0.887 \quad b = 0.213^{\circ}$

$\therefore \quad b/B = 0.772$ from Figure 3.1.4. $\beta = 0.28$

hence $\beta = 0.0773^{\circ} = \frac{.0773 \times 2\pi}{360}$ radians

$$\therefore \quad t = \frac{1.54 \times 360}{.0773 \times 2\pi \cos 17^{\circ}31'} = 1,200 \text{ Å}$$

(or $0.12 \mu m$)

Line-broadening determinations were carried out on samples obtained from the Andreasen method having maximum aggregate size between 5 μm and 65μm. Measurements were made on the diffraction lines for (110), (104), and (021) spacings and are shown in Figure 3.1.6., together with their corresponding average crystallite size values which ranged between 200 and 2000Å.

The (104) spacing in the hexagonal indexing of the rhombohedral boron carbide lattice corresponds to the (200) spacing where the rhombohedron is regarded as a deformed cube.

Thus, the line broadening for this reflection should afford a measure of average crystallite size nearest to the equivalent spherical diameter. The results gave useful confirmation of those found by gas sorption and electron microscopy.

Measurement by the B.E.T. method of surface sorption gave a specific surface of 20 m^2g^{-1} and the average crystallite size (or equivalent spherical diameter) as 0.1μm (1000 Å) based on the assumption that the crystallites are cube-shaped (or spherical).

Study by electron microscopy showed that the largest single crystals were about 1μm in size and to have regular shape being very few in number. These crystals were seen against an almost uniform background of very fine particles whose average diameters were somewhat less than 0.1μm.

A typical sequence of electron micrographs showing the particle size range of the boron carbide and the attendant aggregation and sintering is shown in Figure 3.1.7.

Figure 3.1.6.

Graph of values of average crystallite size by line-broadening for samples fractionated by sedimentation.

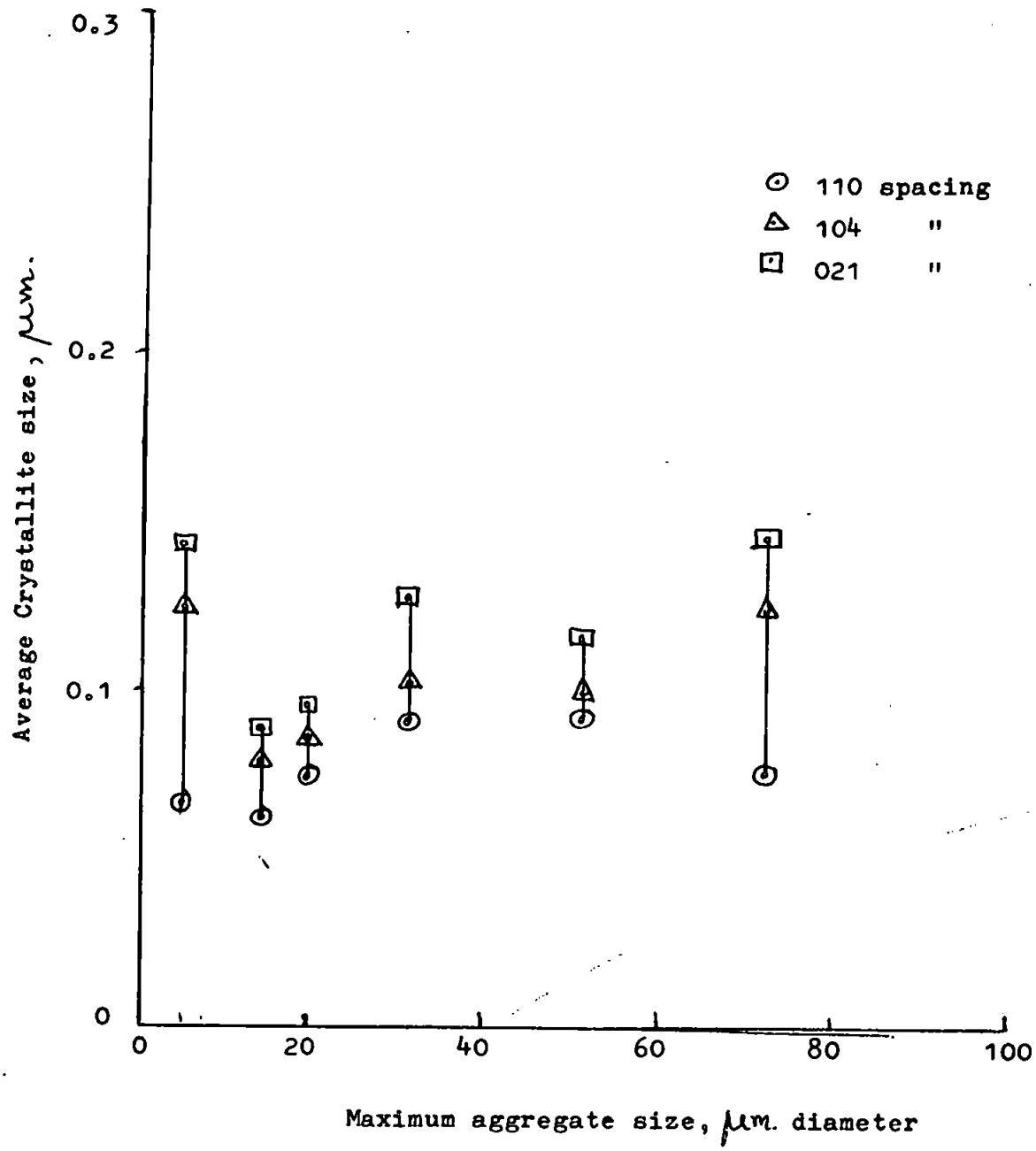

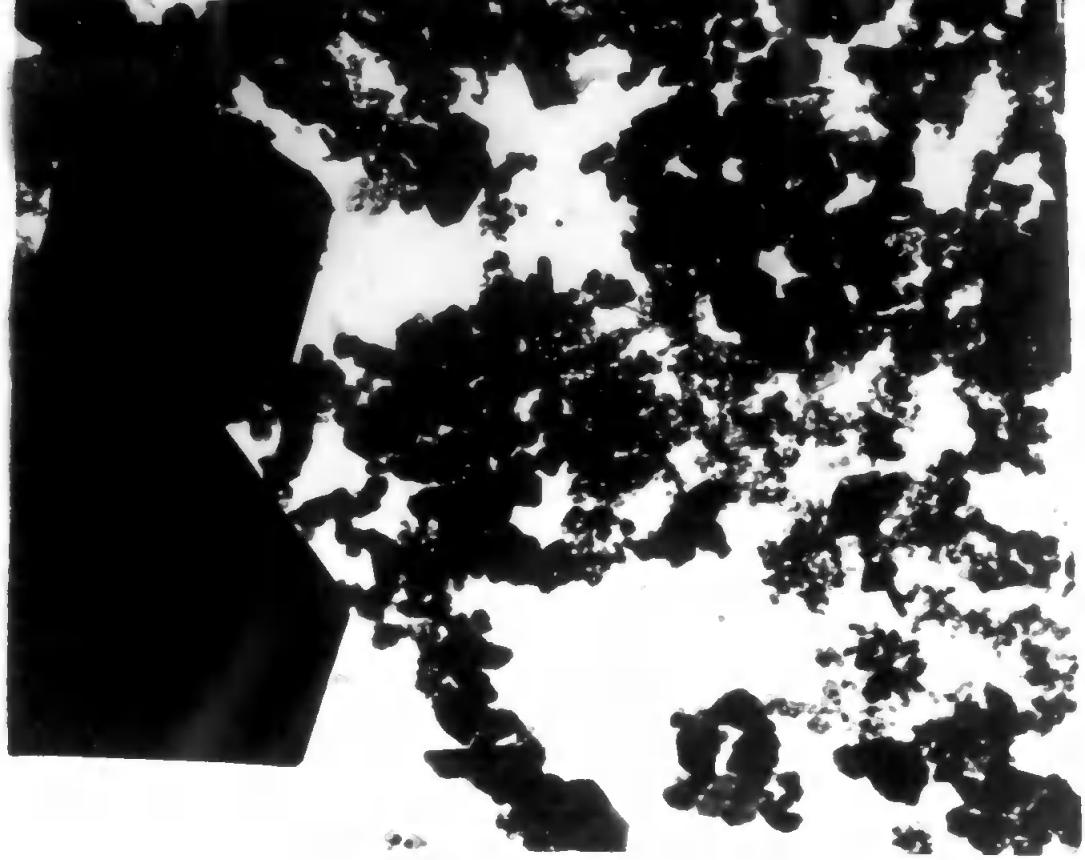

Figure 3.1.7. Electron micrographs of the prepared DURUM CARBON.

40,000 X magnification

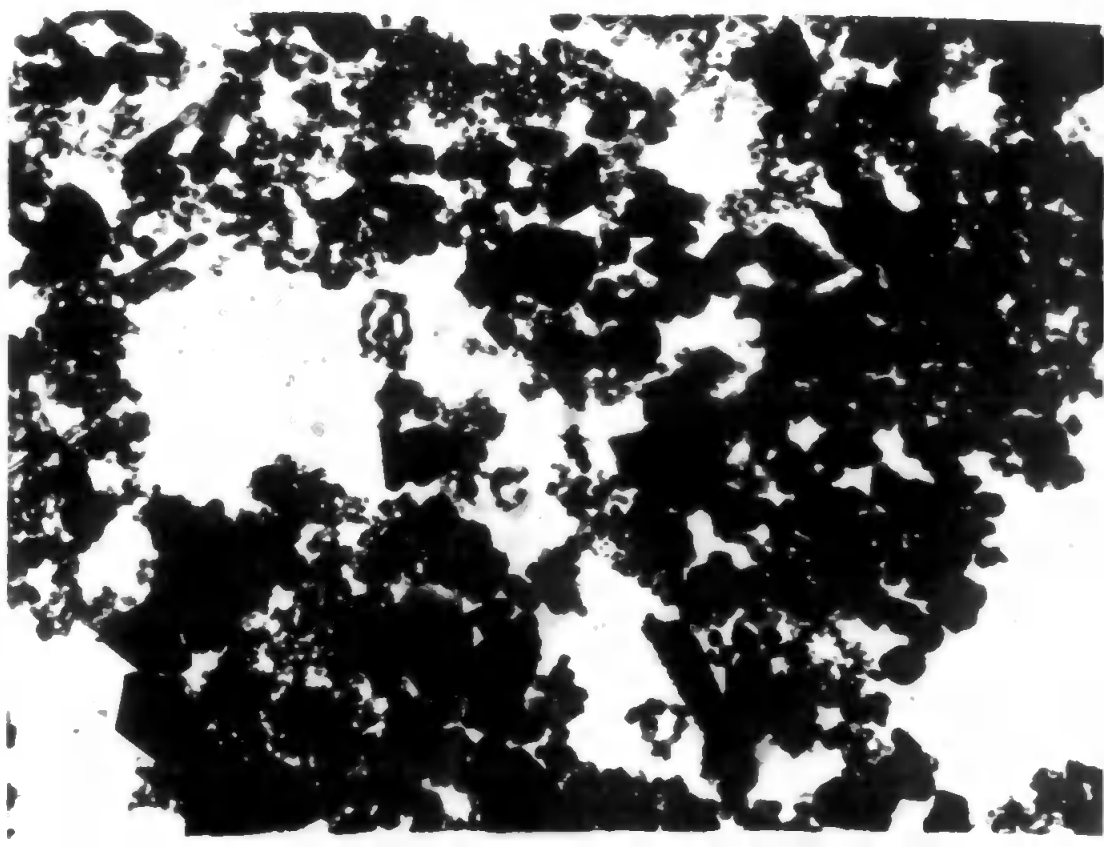

To distinguish between the relative sizes of the particles, a sizing graticule based on the design by Fischmeister (1961), shown in Figure 3.1.8., was placed over the image recorded on photographic paper; the size of each particle was estimated and the number of such particles recorded. The graticule contains sets of circles and ellipses of equal area forming a geometrical progression of the form $Ao2^n$. The ellipses have their major axes twice the lengths of their minor axes. Both sets of shapes were untilized depending on the orientation of the crystallite on the grid. A typical estimation gave an observable particle size range of 1μm to 0.01μm with the mean ranging between 600 and 1,000 Å (0.06 - 0.1μm) based on sample weight. After allowing for the problems of obtaining a representative sample and of dispersing the aggregates, it was considered that this last method gives the most satisfactory way of determining particle size range in the submicron region, particularly when used in conjunction with gas sorption.

Figure 3.1.8.

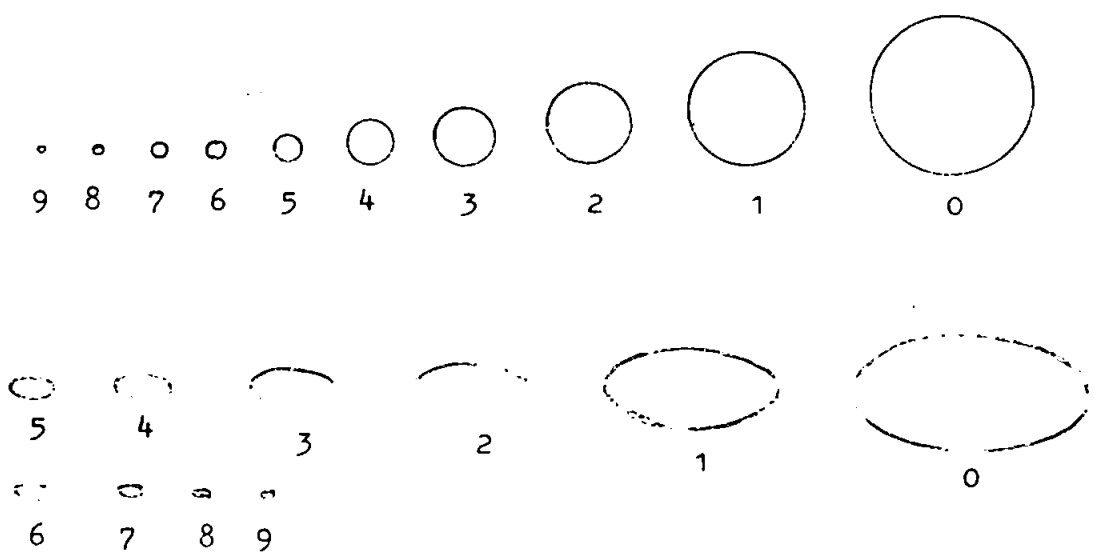

Electron diffraction patterns of single crystallites gave little correlation with the observed X-ray diffraction data owing to the impossibility of orientating the crystal, with respect to the electron beam, along a known axis. The phenomenon of Kikuchi lines observed on many of these samples was ascribed to lamellar layers of boric anhydride (or hydrate) produced on evaporating the boron carbide dispersions.

3.2. The vacuum sintering of boron carbide

A vacuum furnace was constructed, being powered by a four kilowatt radiofrequency induction heater (Delapena E 4KW) with the wound coil external to a 1 in. diameter fused silica tube (Thermal Syndicate Purox). The tube was evacuated by a single stage rotary pump (Edwards Speedivac ISI50) backing a two stage oil diffusion pump (Edwards Speedivac 403A); vacua of between 10^{-5} to 10^{-6} mm Hg. were achieved.

About 4g of the prepared boron carbide were pressed into a pyrolytic graphite crucible (Le Carbonne), supported on a ceramic pedestal inside the tube furnace and heated to temperatures ranging from 1000-1800°C. Temperatures were measured with a disappearing filament pyrometer (Foster) the crucible being viewed through a window at the end of the tube, correction being made for the spectral emissivity of boron carbide at the measured temperature (Kingery 1959). The maximum temperature achieved was limited by the tendency for the crucible and the tube walling to react; alumina proved unsatisfactory as it became porous on heating and failed completely after a

few runs. The general arrangement of the apparatus is shown in Figure 3.2.1. Samples were heated for periods from one to five hours; some outgassing was observed when fresh boron carbide was heated to $> 1000^{\circ}C$, but not when such samples were reheated. The initial outgassing was probably due to a surface oxide layer which was removed as the volatile boric anhydride, B_2O_3. Surface area and average crystallite size measurements were made on each sample after heating. Results are shown in Figure 3.2.2. and pronounced sintering of the powders is indicated particularly at the upper temperature regions; however, such sintering was confined to the smaller crystallites as the samples remained in powder form and showed no tendency to bind. X-ray diffraction patterns ~~Figure 3.3.3.~~ ~~and Table 3.3.1.~~ show an increase in the amount of free carbon as the samples sinter. The effect of adding fine chromium powder (10% by weight) was to further increase the degree of sintering, as indicated by an increase in the average crystallite size. X-ray diffraction confirmed the presence of a mixture of chromium carbide and diboride in samples heated above $1600^{\circ}C$.

3.3. Hot pressing of the prepared boron carbide

Samples of the boron carbide were compressed in a graphite mould set between hydraulic rams and heated to temperatures above $2000^{\circ}C$ by a 36 kilowatt R.F. induction heater (Wild - Barfield). Figure 3.3.1. Burnt lime, CaO, was used to contain the heat of the die set (more recent work shows that graphite wool or carbon black are better media for heat retention).

Figure 3.2.1. High temperature vacuum furnace for sintering studies.

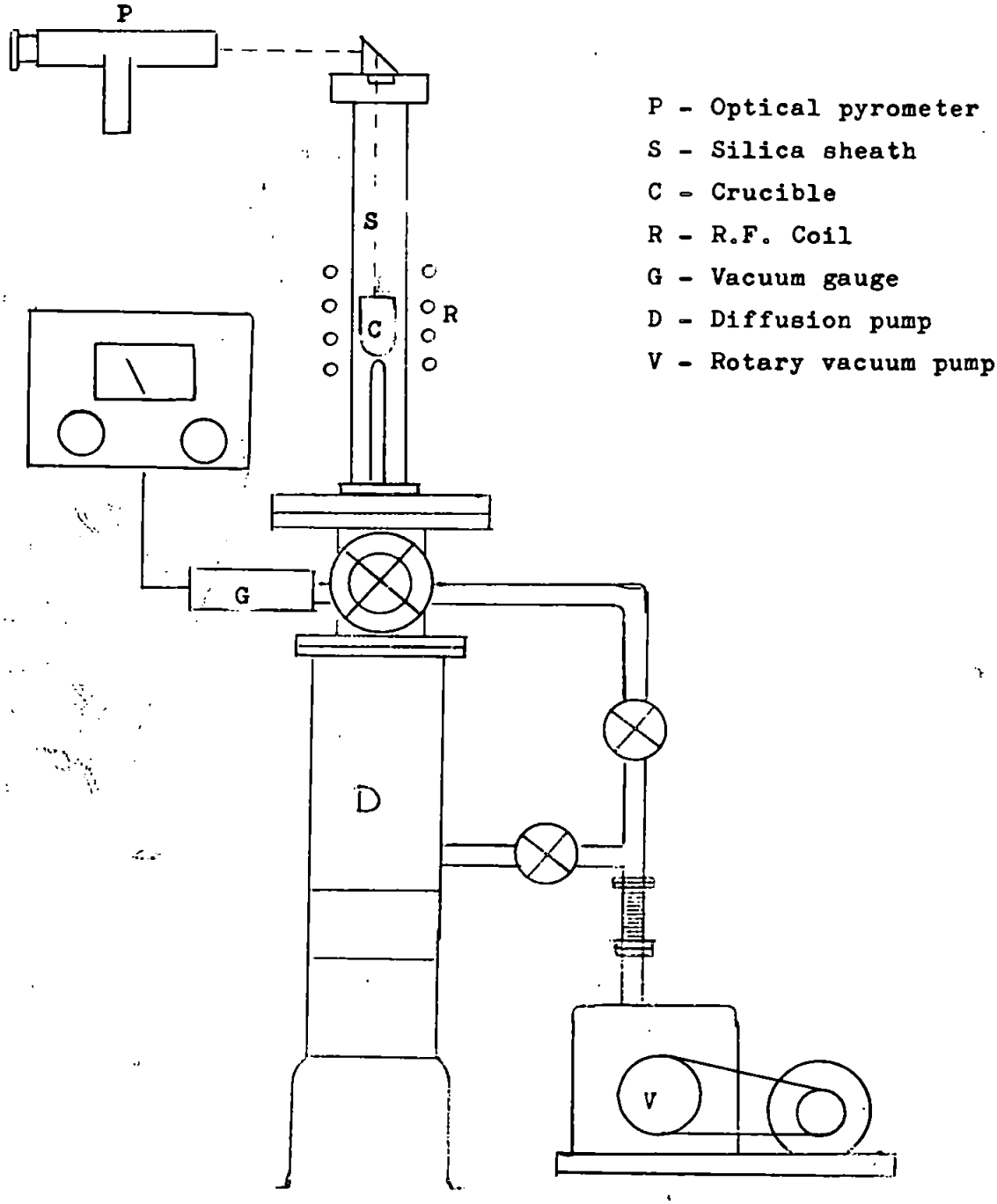

Figure 3.2.2(a)

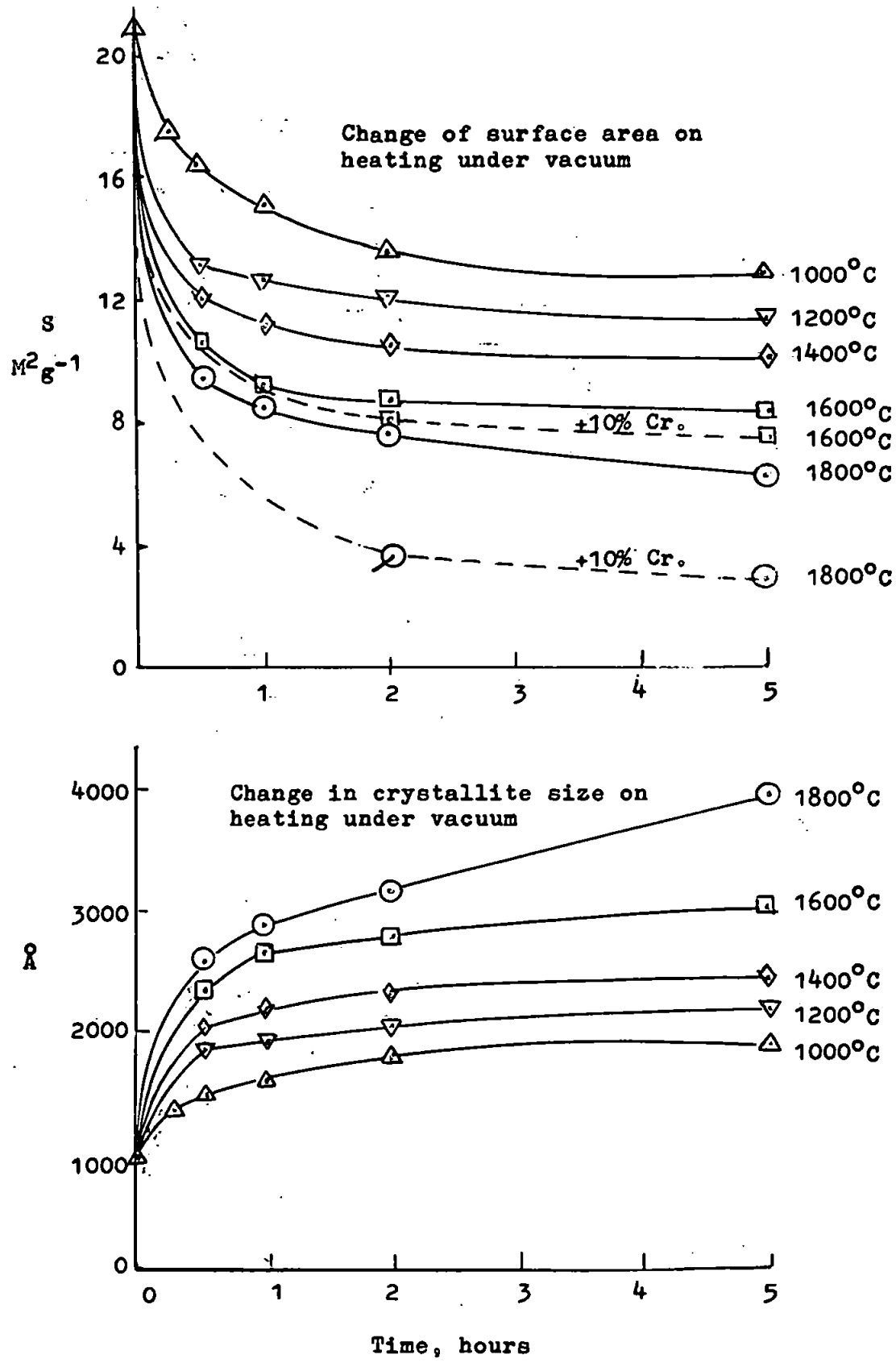
Change of surface area on heating under vacuum
S
M^2g^{-1}
20
16
12
8
4
0
1
2
3
4
5
1000°C
1200°C
1400°C
1600°C
±10% Cr.
1600°C
1800°C
+10% Cr.
1800°C
Change in crystallite size on heating under vacuum
Å
4000
3000
2000
1000
0
1800°C
1600°C
1400°C
1200°C
1000°C
Time, hours

Figure 3.2.2(b)

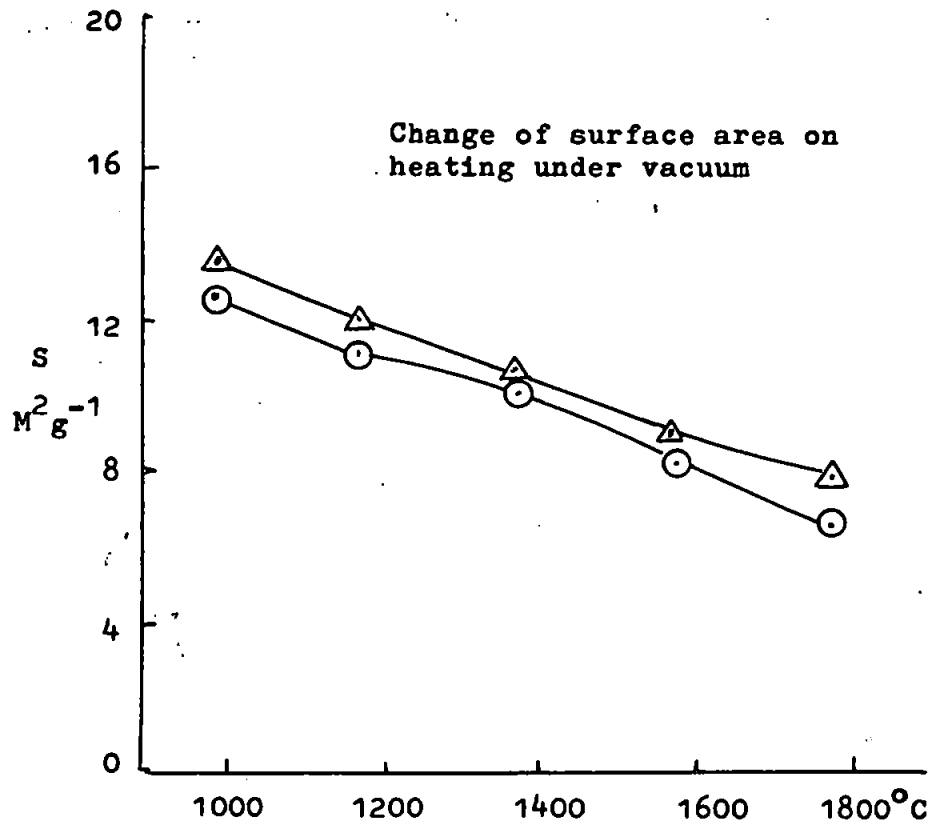
Change of surface area on heating under vacuum
S
M^2g^{-1}
20
16
12
8
4
0
1000
1200
1400
1600
1800°C

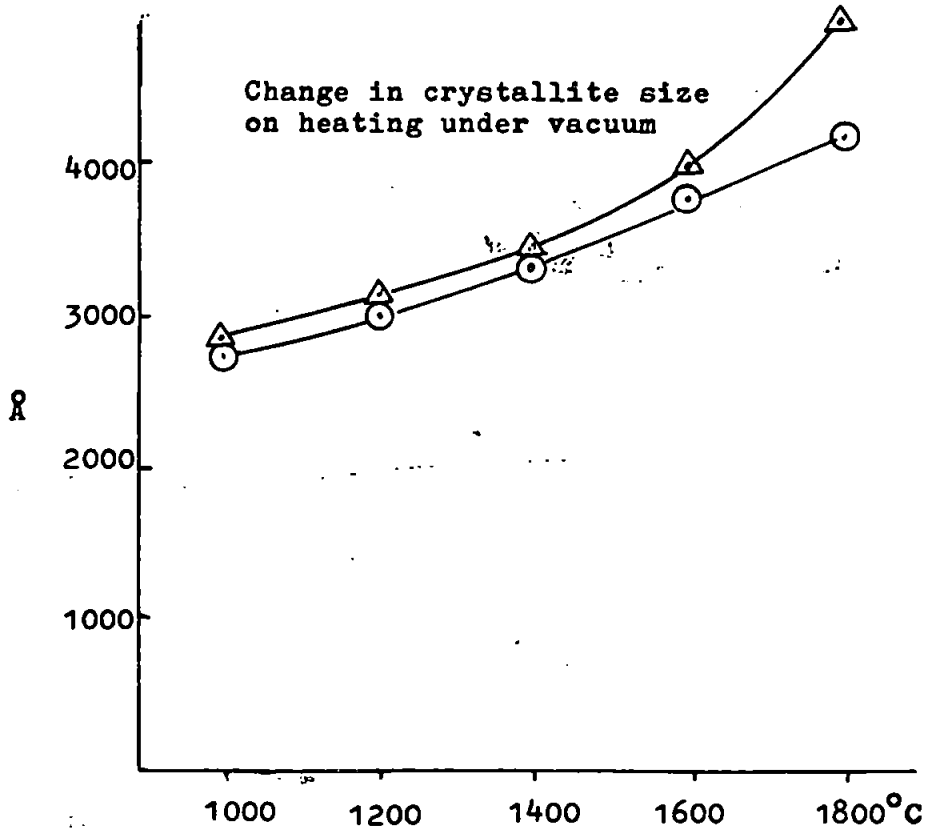
Change in crystallite size on heating under vacuum
Å
4000
3000
2000
1000
1000
1200
1400
1600
1800°C

Figure 3.3.1. Hotpressing set up for compaction of boron carbide.

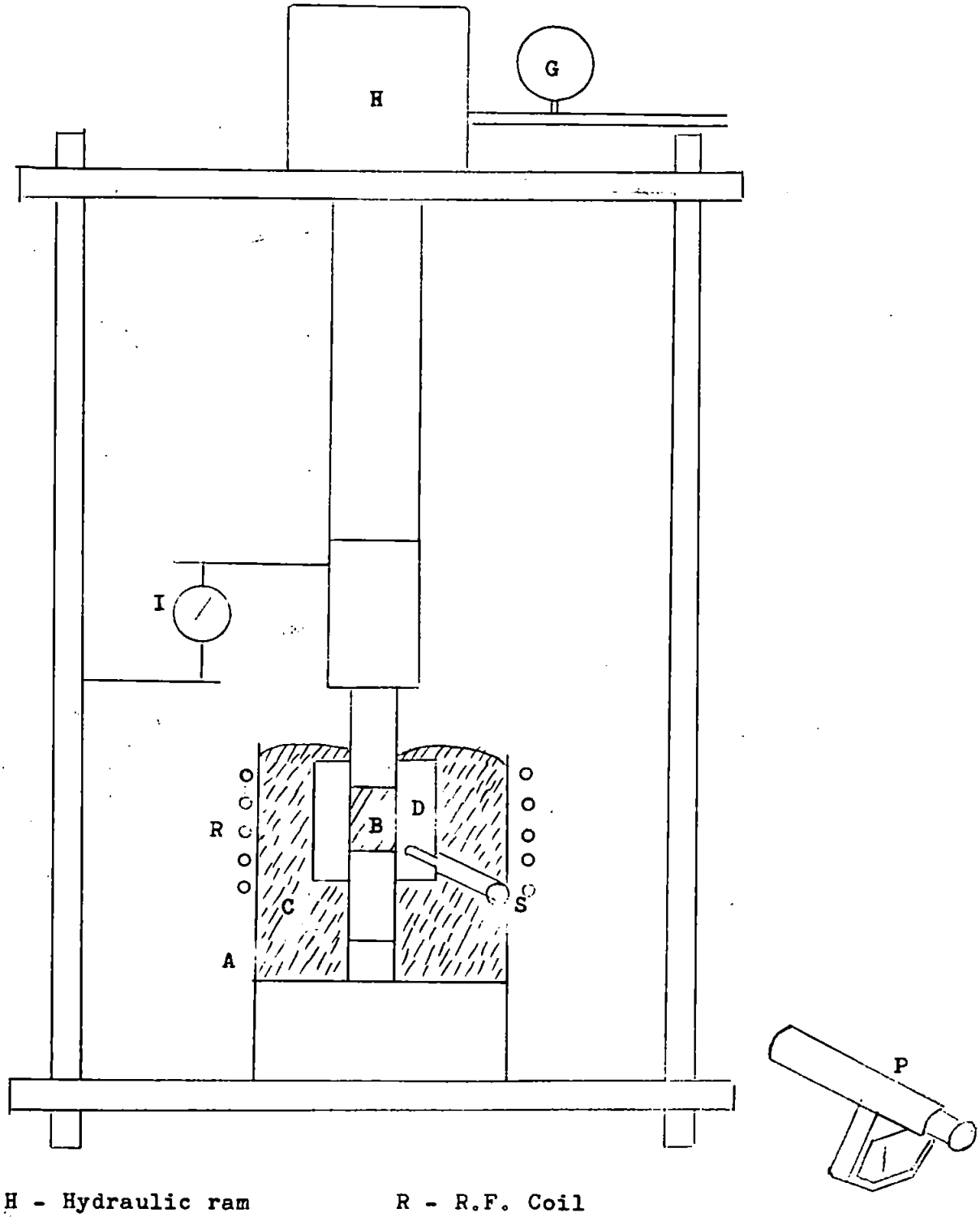

H - Hydraulic ram
G - Pressure gauge
I - Ram-Travel indicator
C - Carbon black
B - Boron carbide
R - R.F. Coil
A - Asbestos shield
D - Graphitedie
P - Optical pyrometer
S - Sighting tube

A constant pressure of 300 Kg/cm^2 was applied to the compact; at cold, consolidation of the powder amounted to 40% of the theoretical density, which increased to about 70% when the temperature reached 1000°C although no binding occurred, and remained so until a temperature above 2000°C was achieved. (an estimated temperature of 2300°C was achieved on one run). Temperatures were measured using a disappearing filament pyrometer (Foster Instrument). When cool, the compact was removed from the mould; the majority of the specimens showed good surface finish and extreme hardness. The sintered boron carbide was sectioned on a diamond grit wheel (Bullock Diamond Products). Sections were examined for their density by high density media (Sym. tetrabromoethane and carbon tetrachloride mixed in various proportions) and the phase identified by X-ray diffraction Table 3.3.1.

3.4. The ball-milling of the prepared boron carbide.

6g. samples of the powder were ball-milled under standard condition, i.e. a constant ratio of sample weight to number and sizes of the porcelain balls, in a porcelain mill for different lengths of time. Changes in specific surface, S, and average crystallite size determined by gas sorption (Section 2.2(d)) are shown in Figure 3.4.1. The specific surface, S, remained practically constant during the first 5h. after which it progressively increased. While the average crystallite sizes, as determined by gas sorption, remained constant, X-ray line broadening (section 3.1(c)) showed development of strain within the crystallites as

T A B L E 3.3.1.

B_4C		A.S.T.M. CARD 6-0555		
I/I_1	d(Å)	I/I_1	d(Å)	(hkl)
15	4.49	30	4.49	101
40	4.02	40	4.02	003
70	3.79	70	3.79	012
50	3.38(carbon)	100	3.35	001 *
25	2.81	30	2.81	110
80	2.57	80	2.57	104
100	2.38	100	2.38	021
10	2.30	10	2.30	113
7	20.2	10	2.02	006
10	1.87	10	1.87	211
30	1.714	30	1.714	205
7	1.637	10	1.637	116
5	1.628	10	1.628	107
5	1.56			
30	1.505	20	1.505	303
40	1.463	30	1.463	125
35	1.446	30	1.446	018
40	1.407	30	1.407	027
20	1.345	20	1.345	009
20	1.342	20	1.342	113
20	1.326	20	1.326	223
7	1.286	10	1.286	208
20	1.261	20	1.261	306
7	1.191	10	1.191	042

I/I_1 - relative intensity taking (021) = I_1 = 100

* ASTM 13.148 spacing for graphite

there was additional line broadening in excess of that due to the particle size of the material. Further milling decreased the average crystallite size and further strain developed as indicated in Table 3.4.1.

TABLE 3.4.1.

Milling time, h,	Average cryst. size, Å,	Intrinsic (104 reflection) broadening caused by Cryst. size β_1	Cryst. strain β_2	Internal* strain e,	Apparent* strain η
0	1160	0.080°	--	--	--
10	730	0.127°	0.108°	0.0030	0.0060

* $\beta = -2e \tan\theta$ (see Klug and Alexander 1954)
and $\eta = \beta \cot\theta$

In the course of milling, the material became porous, as indicated by the development of some hysteresis in the adsorption isotherms. As noted in Section 3.1. the original material consisted of large crystals of about 1 μm and below in size and aggregates of smaller crystals all below 0.1 μm. Electron micrographs of the milled samples, Figure 3.4.2. indicated that during the earlier stages of milling only the larger crystals are reduced in size and hence the average crystallite size was not decreased markedly. Compaction of the aggregates lead to the development of porosity, with the type II isotherms tending towards type IV and showing some hysteresis even at very low relative pressures.

Table 3.4.1. Ball milling of boron carbide

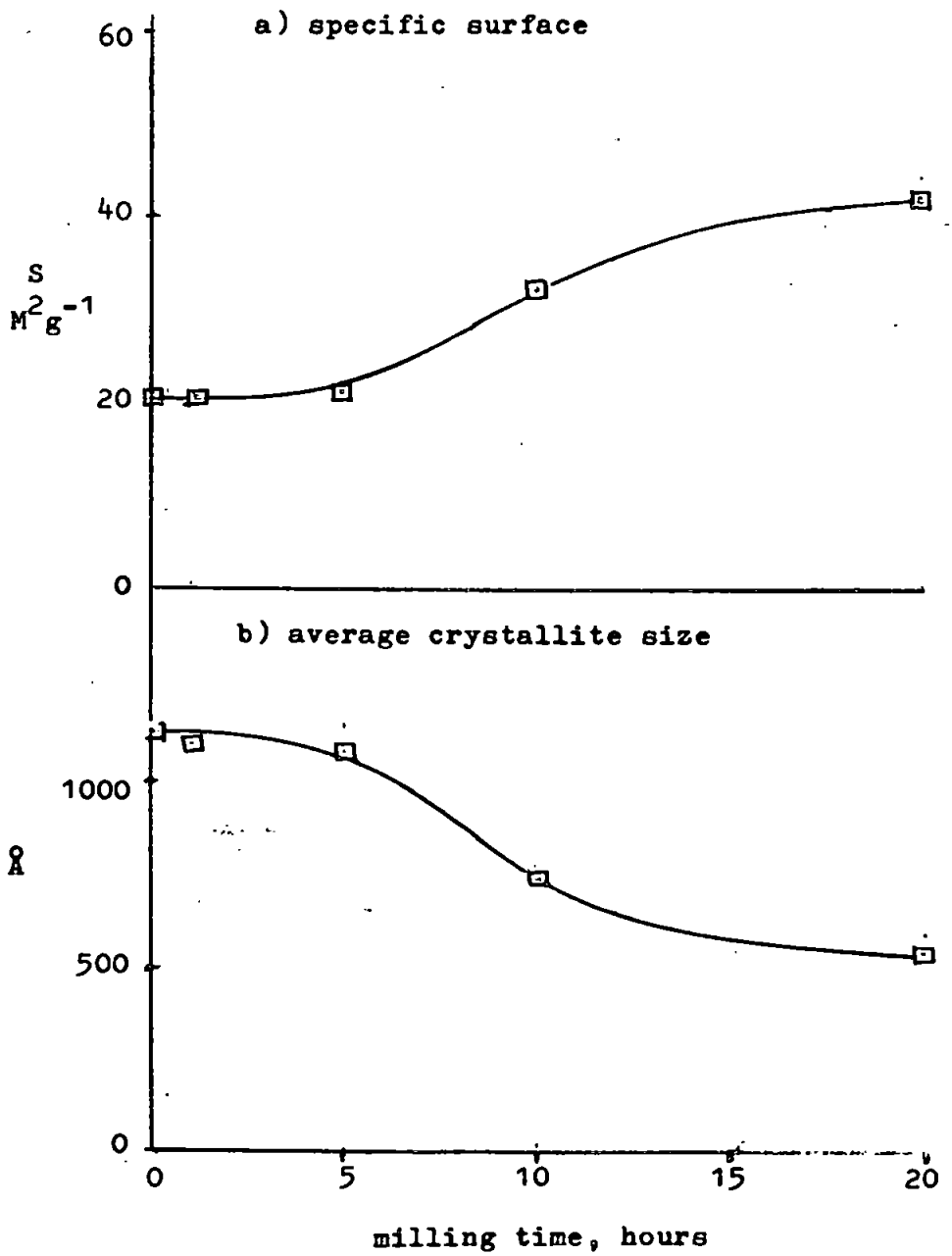

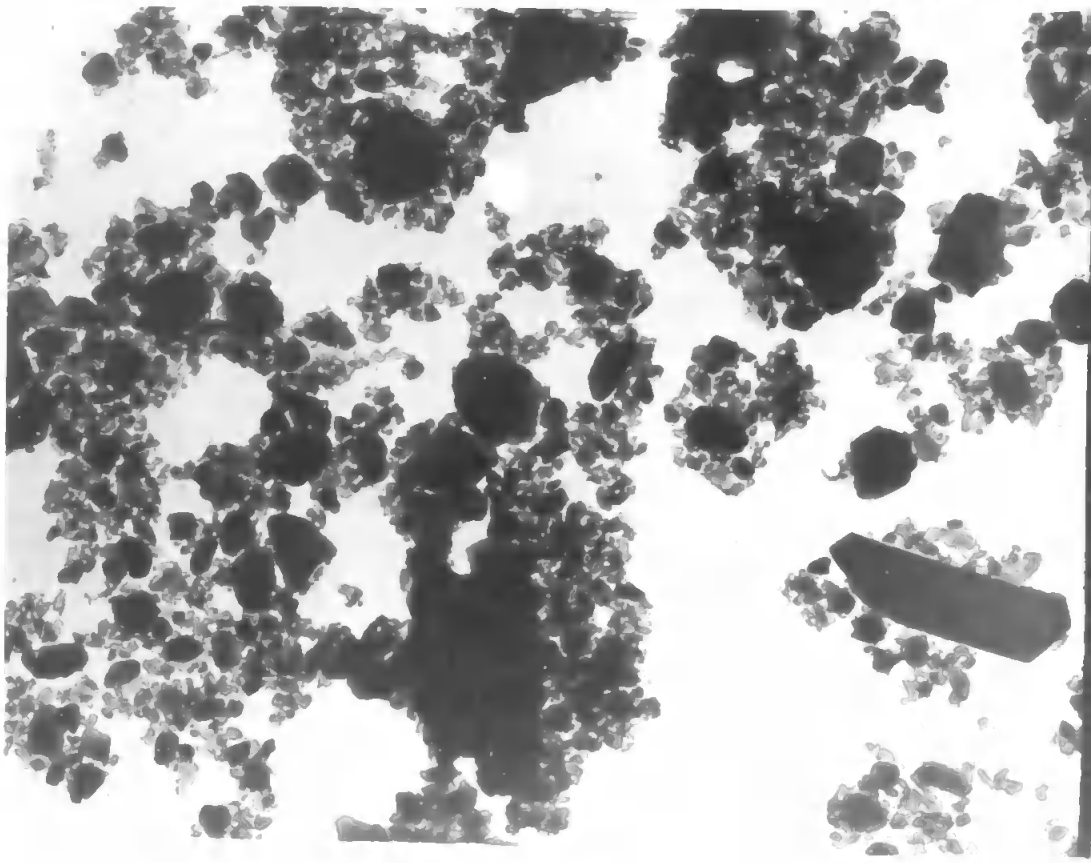

Figure 3.4.1. The prepared BORON CARBIDE ball-milled for 10 h.
40,000 X magnification.

The prepared BORON CARBIDE ball-milled for 20 h.
40,000 X magnification.

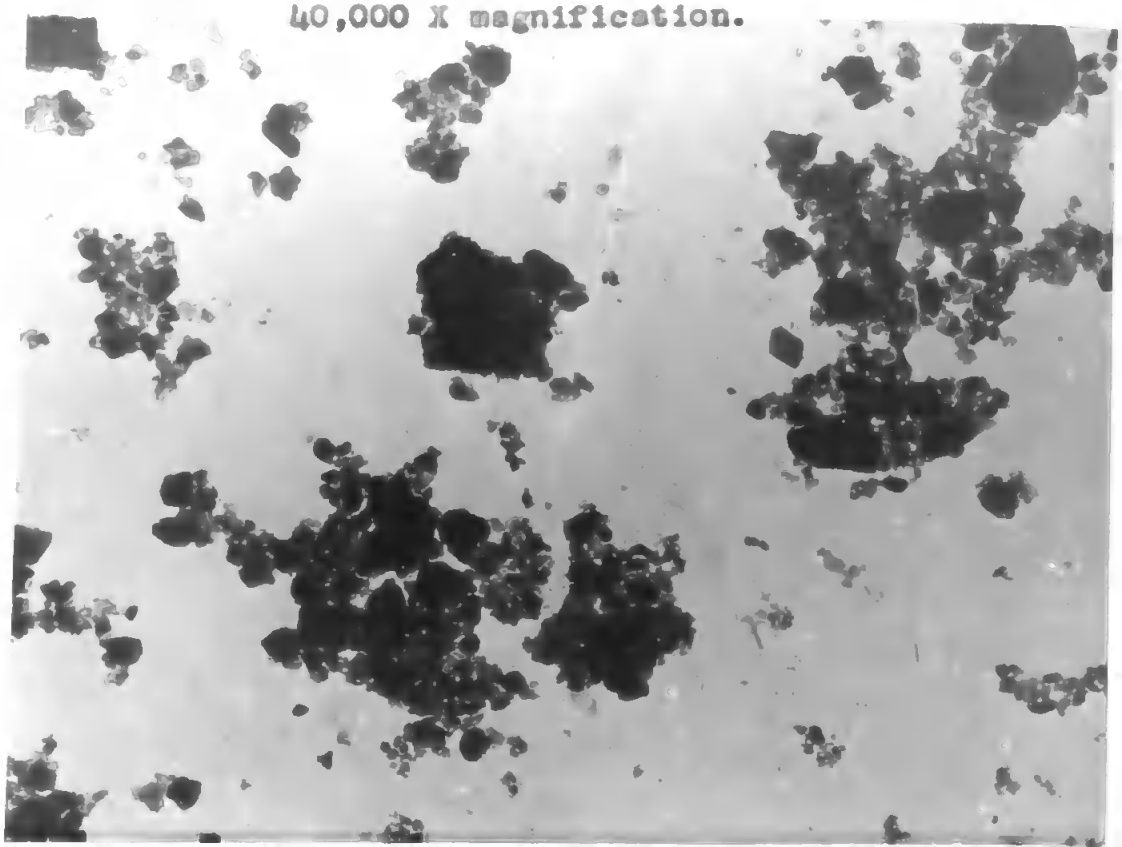

SECTION 4. THE OXIDATION OF BORON CARBIDE

The section concerns the behaviour of the prepared boron carbide in reactive atmospheres, for example, air, at high temperature.

4.1. The kinetics have been studies for the oxidation of boron carbide with (i) carbon dioxide over the temperature range 600 to 750°C by Davies and Phennah (1959), (ii) air and water vapour between 200 and 750°C by Litz and Mercuri (1963), (iii) pure oxygen between 515 and 646°C by Harvey (1965) and (iv) in dry air between 503 and 527.5°C by Dominey (1968). The following reactions are proposed :-

1. Dry CO_2

a) $B_4C + 7CO_2 \longrightarrow 2B_2O_3 + 8CO$

or b) $B_4C + 3CO_2 \longrightarrow 2B_2O_3 + 4C$

2. Dry air and oxygen

a) $B_4C + 4O_2 \longrightarrow 2B_2O_3 + CO_2$

or b) $B_4C + 3\frac{1}{2}O_2 \longrightarrow 2B_2O_3 + CO$

or c) $B_4C + 3O_2 \longrightarrow 2B_2O_3 + C$

3. Water vapour

a) $B_4C + 8H_2O \longrightarrow 2B_2O_3 + CO_2 + 8H_2$

or b) $B_4C + 6H_2O \longrightarrow 2B_2O_3 + C + 6H_2$

with associated B_2O_3 transport via

c) $B_2O_3 + H_2O \longrightarrow 2HBO_2$ (g)

In all cases, study of the kinetics of the above reactions was made using thermogravimetric analysis with, generally, some analysis of the reaction products. The percentage weight <u>increase</u> for complete oxidation via reactions 1(a), 2(a) and 2(b) is 152%; via 1(b) 245%; via 2(c) 174%; and the percentage weight <u>decrease</u> for reaction via 3(a) is 100% and via 3(b) is 88% when transport of B_2O_3 occurs via 3(c).

Complete reaction is rarely achieved, being dependent on the temperature and the phases present during reaction. Nevertheless, all appear to be principally controlled by the rate of diffusion of the oxidant, e.g. O_2, through a viscous layer of boric anhydride, B_2O_3, except in reactions 3(a) and 3(b) at low temperature, $450^{\circ}C$, when the product B_2O_3 layer is removed by water vapour as it is formed. At temperatures in the region of $650^{\circ}C$ and above the liquid viscosity and surface tension of the B_2O_3 influence the reaction rate in causing the separate aggregates to coalesce into a glassy compact. The volatility of B_2O_3 is insignificant at these temperatures.

In the present work, samples of the prepared boron carbide were heated in the thermogravimetric balance described in Section 2.2(e) at 500, 600, 650, 700, 750 and $800^{\circ}C$ in an atmosphere of air and the change in weight of the sample over a period extending to several hours. The results obtained are shown graphically as a direct plot and as a logarithmic plot, Figure 4.1.1. In this way the slope of the tangent of the graph serves to indicate the order of reaction, since

$$-\frac{dc}{dt} = kc^n$$

where c = concentration at any time t, and is proportional to the change in weight.

n = order of reaction

Figure 4.1.1. Weight change on oxidation of B_4C in air.

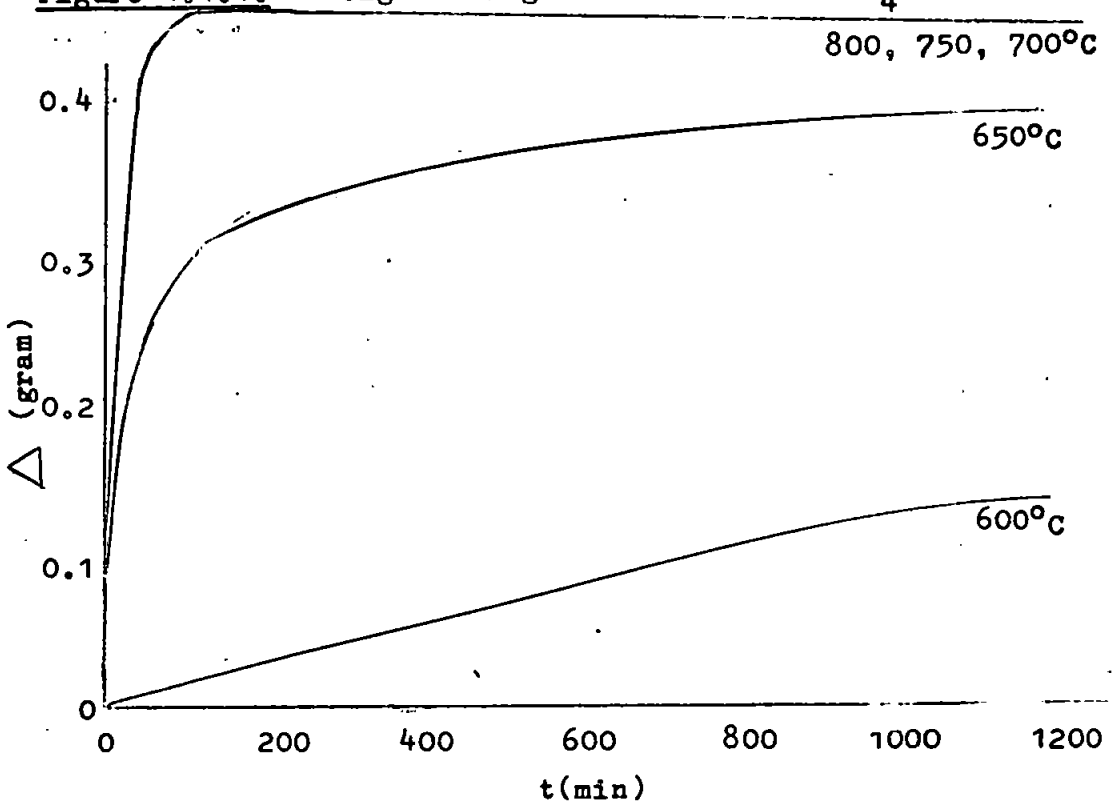

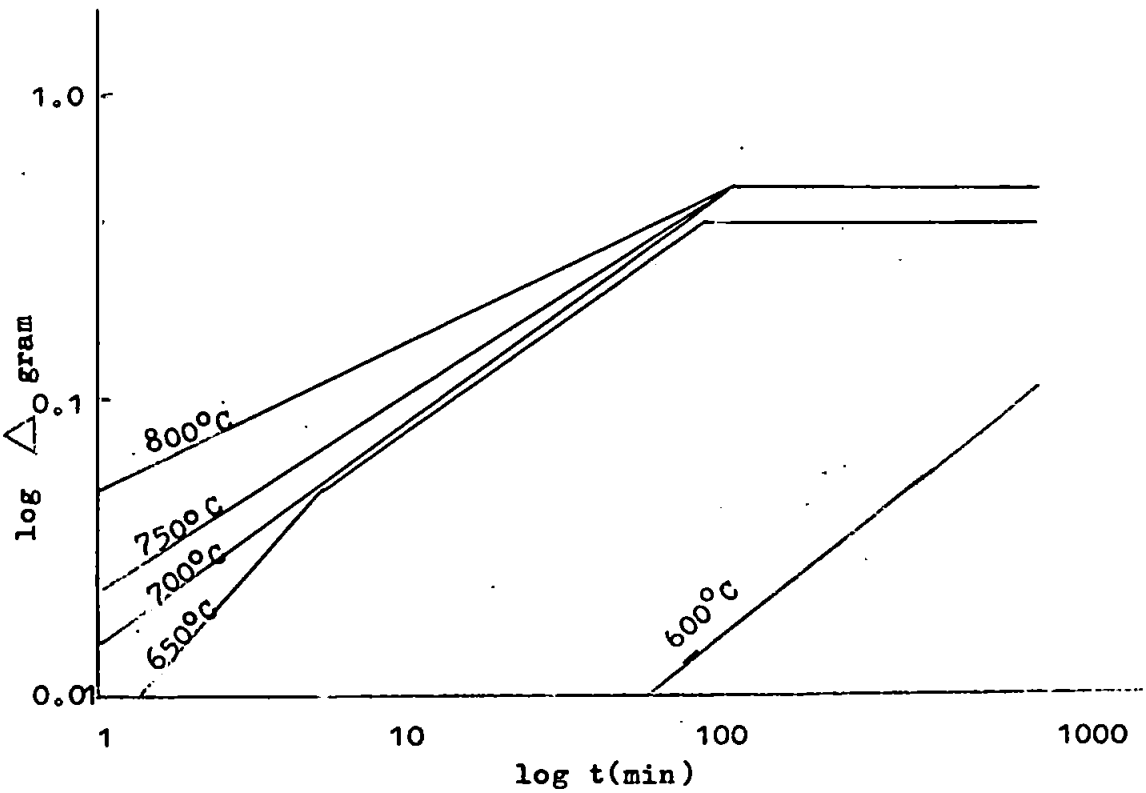

Thus, at 500°C there appeared to be little reaction on the basis of weight change, a situation which was maintained until the temperature was raised to 600°C when oxidation occurred as a first order reaction. At higher temperatures, the order of reaction changes being 2/3 at 650°C and $\frac{1}{2}$, or parabolic above 650°C. In all cases, after a sufficient interval of time, the reactions came to a standstill with less than 50% of the material oxidised on the basis of weight change. Determination of the water soluble boric oxide by titrimetric analysis, Section 2.2(a), on completion of the thermogravimetric analysis, indicated, that in fact more than 70% of the boron carbide had been oxidised. It was evident that some loss of B_2O_3 had occurred due to presence of moisture in the atmosphere, maximum humidity being recorded as 70%RH at 20°C during the oxidation (equivalent to 1.75 vol. % or 12.3 mm.Hg pressure of water vapour).

According to Litz and Mercuri (1963), reaction would be favoured at the lower isotherms, which is evident from the results for 650°C when B_2O_3 is being removed almost at a rate by which it is being formed.

The energy of activation for the oxidation of boron carbide was determined by the Arrhenius method of plotting the logarithm of the rate of oxidation against reciprical temperature (°K) as in Figure 4.1.2.

Figure 4.1.2.

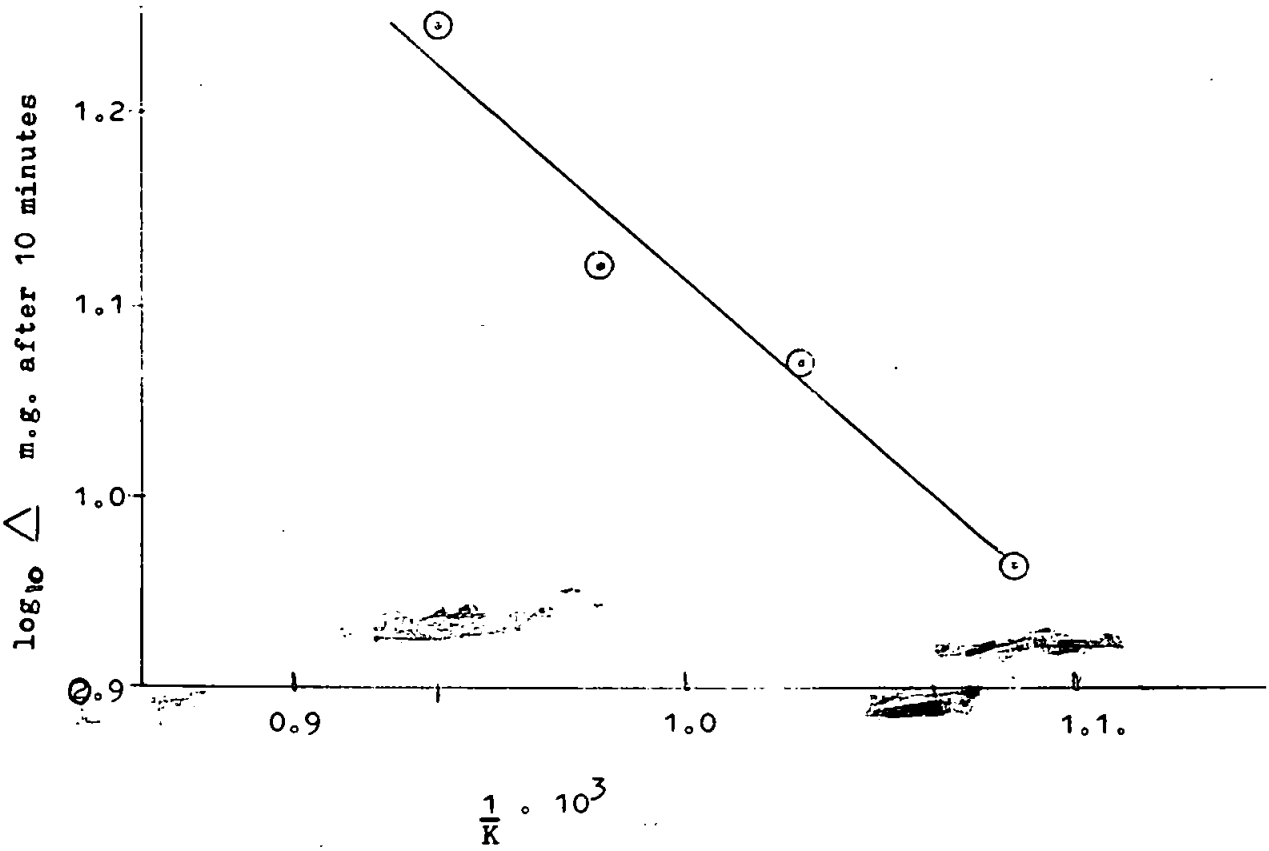

The value obtained of 23.9 kilo-calories per gram molecule of B_4C is in accord with the values of 11 kilocalories per mol. obtained for reaction 3(a) and 47 kilocalories per mol. for reaction 2(a) by Litz and Mercuri (1963).

4.2. Supplementary to the above work, 5g samples of the boron carbide were heated in a furnace at 700°C in air, for $\frac{1}{4}$, $\frac{1}{2}$, $\frac{3}{4}$, 1, 2 and 4 hour intervals of time to estimate the extent of sintering during oxidation. Determination of the surface area by gas sorption analysis, Section 2.2(d), on the cooled samples

freshly oxidised, and following washing with hot water to remove the boric acid gave the results tabulated in Table 4.2.1.

T A B L E 4.2.1.

Boron carbide oxidised in air at 700°C

Time hours	% wt increase	% oxidation eqn 2(a)	% oxidation eqn 2(c)	S, $m^2 g^{-1}$ before washing	S, $m^2 g^{-1}$ after washing
0	0	0	0	20.6	—
$\frac{1}{4}$	16.7	11.0	9.6	4.4	35.7
$\frac{1}{2}$	22.1	14.5	12.7	4.1	42.6
$\frac{3}{4}$	30.9	20.3	17.8	3.4	—
1	41.8	27.5	24.1	2.0	56.8
2	53.8	35.4	30.9	0.8	74.8
4	68.2	44.8	39.2	0.3	—

The expected reduction of surface area on heating is due to (i) preferential oxidation of the smaller crystallites, and (ii) aggregation of the remaining crystallites and sealing of the pores by the liquid B_2O_3. However, none of these mechanisms correlate with the marked increase of the surface area of the unreacted carbide following leaching, unless the larger crystallites undergo splitting. Phase identification by X-ray diffraction, Section 2.2(b) showed a pronounced increase in the free carbon present in

these samples, Figure 4.2.1., which was significantly broadened,

Figure 4.2.1.

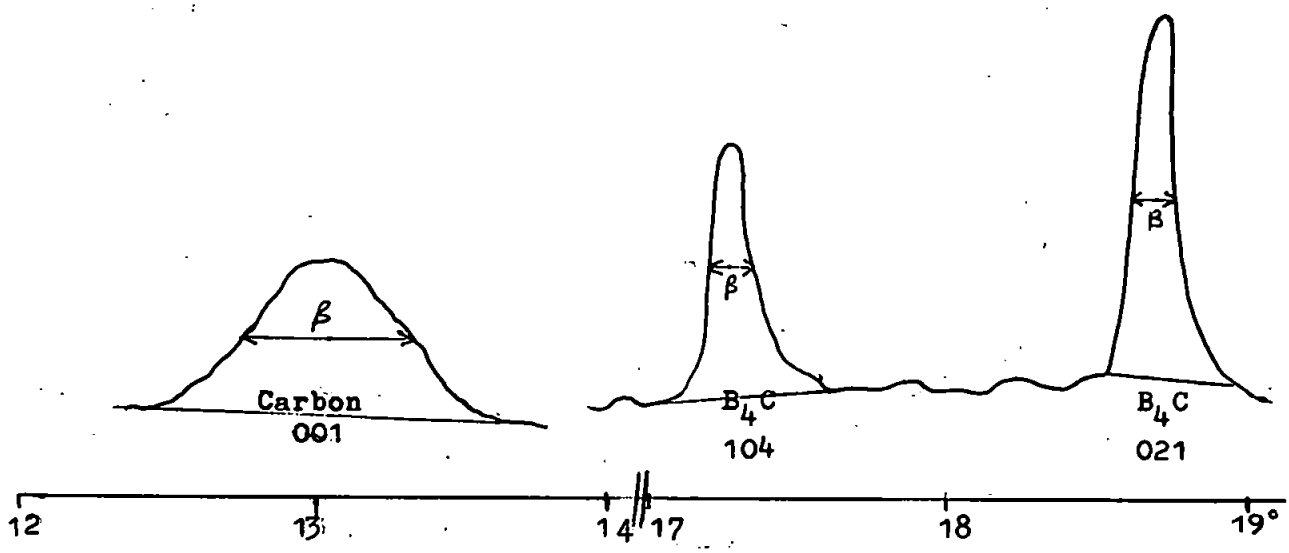

where as the peaks for the (104) and (021) spacing of the boron carbide showed no appreciable changes in half peak broadening but had modified profiles. Should splitting of the unchanged boron carbide crystallites have occurred through spalling at the carbide-oxide interface when the samples were cooled then re-heated samples would not have proceeded to give oxidation rates similar to those of samples which had been continuously heated. In practice, there was no distinction between these samples.

Assuming that the boron carbide and carbon are separate phases their individual surface areas were estimated on the basis of reaction 2(c), viz,

$$B_4C + 3O_2 \longrightarrow 2B_2O_3 + C$$

and are given in Table 4.2.2.

T A B L E 4.2.2.

Surface areas and average crystallite sizes produced on oxidizing boron carbide

Time hours	% wt increase	% oxidation	wt fraction B_4C	wt fraction C	Surface area (m^2g^{-1}) B_4C+C	Surface area (m^2g^{-1}) B_4C	Surface area (m^2g^{-1}) Δ	Surface area (m^2g^{-1}) C	Average crystallite Size Å
0	0	0	1	0	20.6	20.6	-	-	-
$\frac{1}{4}$	16.7	9.6	0.904	.021	35.7	19.2	16.4	783	34
$\frac{1}{2}$	22.1	12.7	0.873	.028	42.6	23.8	23.8	850	31
1	41.8	24.1	0.759	.052	56.8	39.6	39.6	762	35
2	53.8	30.9	0.691	.067	74.8	58.7	58.7	876	30

The X-ray broadening of the carbon peak gives the dimension along the C-axis of 82Å, assuming a uniform hexagonal crystal habit, where the edge of the prism base is a multiple of the C-C distance of 1.42Å and the prism height, a multiple of the interplanar spacing, 3.35Å, the edge dimension is:

$$82 \times \frac{1.42}{3.35} = 34.75 \text{ Å}$$

compared with the average crystallite size from gas sorption determination of 32.5Å. Hysteresis was shown by the sorption isotherms of the more oxidised samples, Figure 4.2.2, indicating that the carbon has porosity and lacks crystallinity. The method of computation of the B.E.T. isotherm by digital computer (I.B.M. 1130) is given in the Appendix.

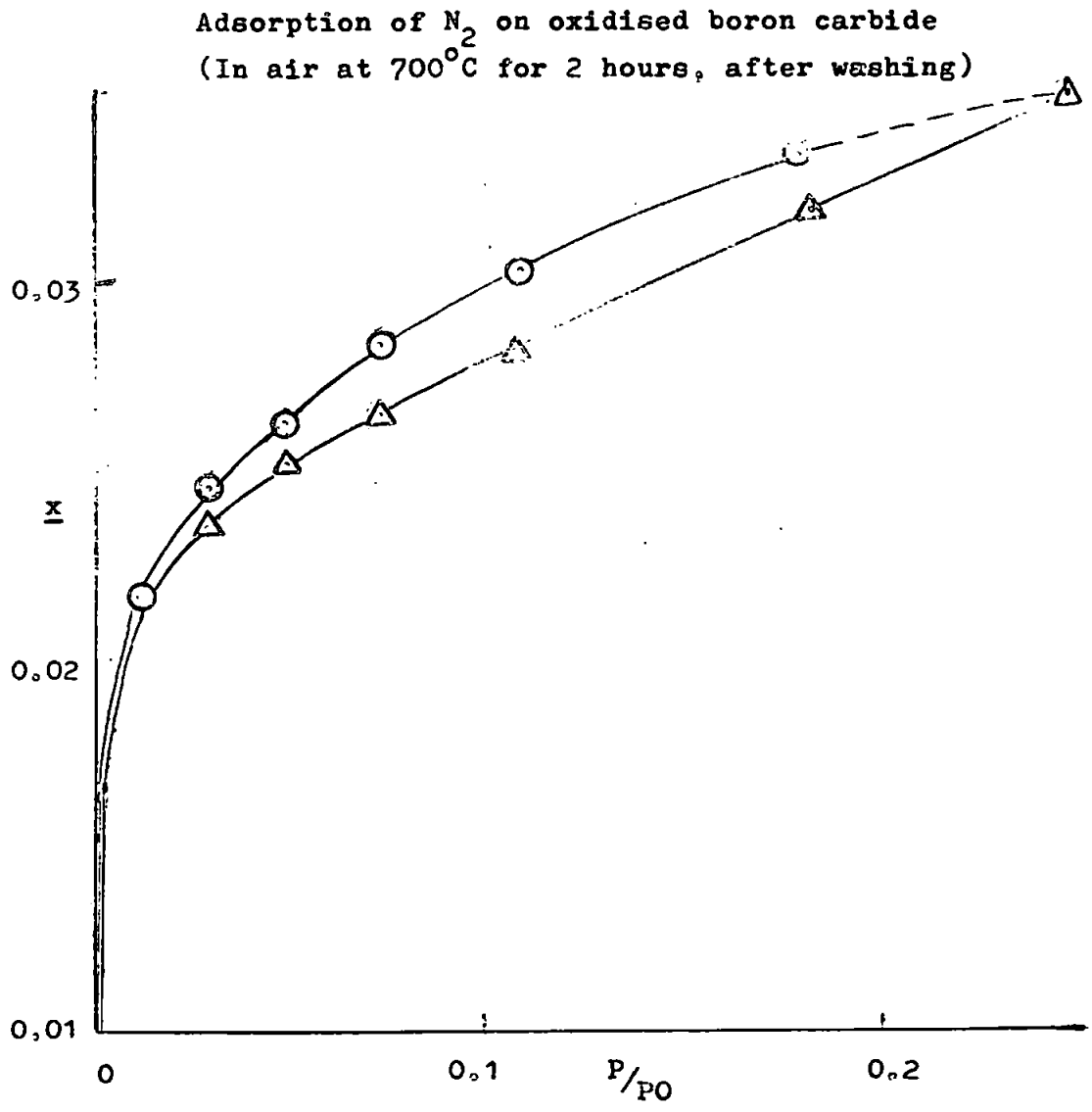

4.3. Chemical analysis and electron microscopy were employed to indicate the composition and appearance of the boron carbide following oxidation, Sections 2.2(a) and (c), the results are tabulated in Table 4.3.1. for the chemical analysis and in Figure 4.3.1. for the microscopy.

TABLE 4.3.1. The chemical analysis of the products of oxidation of boron carbide in air at 700°C

Time of oxidation h,	B_2O_3 water soluble	% B_4C oxidised	Residue after washing			
			% B	% C	% B_4C	% free carbon
$\frac{1}{4}$	14.7	7.0	74.2	25.8	94.4	5.6
$\frac{1}{2}$	23.9	12.5	72.9	27.1	92.7	7.3
1	40.1	23.6	71.4	28.6	90.8	9.2
2	54.2	35.0	70.9	29.1	90.2	9.8
4	67.8	50.1	68.4	31.6	87.0	13.0

4.4. Differential thermal analysis, D.T.A., as described in Section 2.2(e) was used to determine the minimum temperature for the onset of oxidation of boron carbide in air. The boron carbide was diluted with the alumina powder before placing in the sample holder and with alumina as the reference, heated between 600 and 700°C at the rate of 5°C per minute. The leading edge of the D.T.A. curve was registered at 637°C; reaching a maximum at 640°C; due to the highly exothermic oxidation of boron carbide (Smith et al. 1955) a deflection was maintained to above 700°C.

Figure 4.3.1. Boron carbide oxidised in air $\frac{1}{2}$ h. at 700 °C
(a) unleached, 10,000 X magnification.

(b) Boron carbide oxidised in air, 4 h. at 700 °C
unleached, 10,000 X magnification.

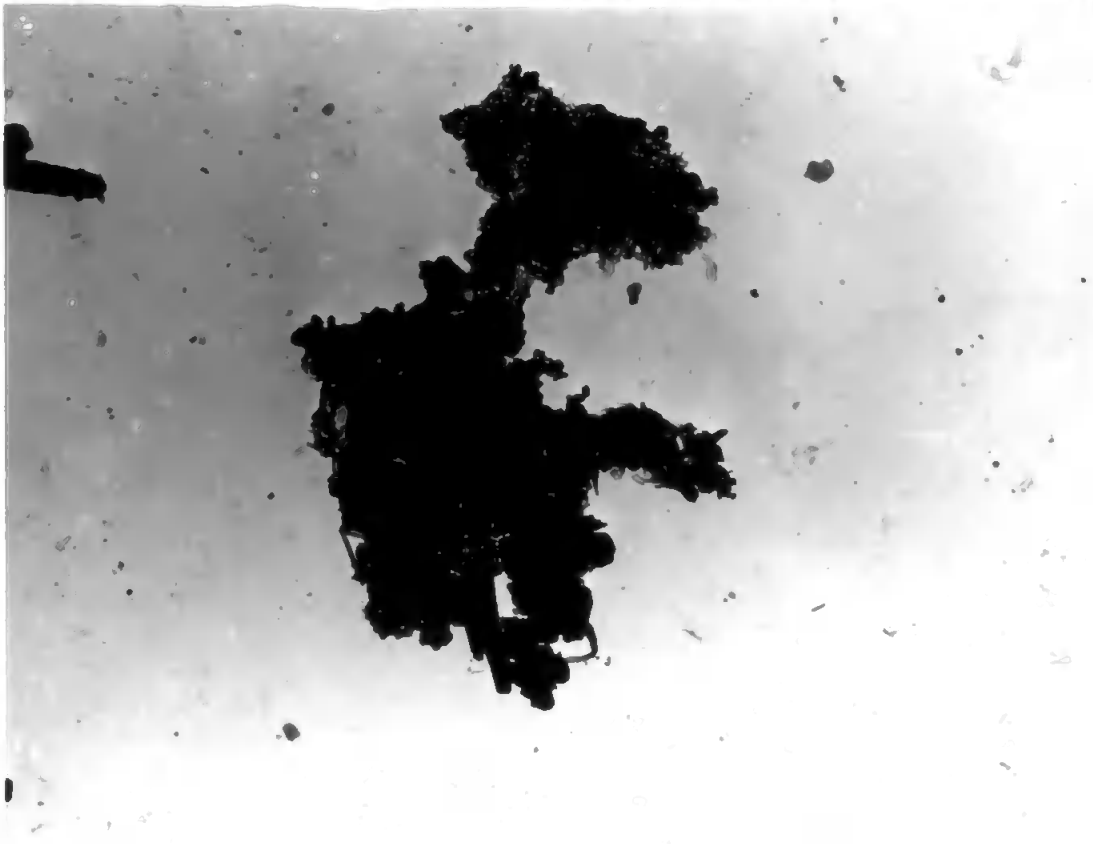

Figure 4.3.1. Boron carbide oxidised in air for 1 h. at 700 °C
(c) leached with water, 10,000 X magnification.

(d) Boron carbide oxidised in air for 1 h. at 700 °C
leached with water, 40,000 X magnification.

SECTION 5. THE FORMATION OF TITANIUM BORIDE

The section covers the formation of titanium boride on to a substrate of titanium alloy by reaction with boron carbide.

5.1. Titanium, one of the lightest of the transition elements, has other desirable properties of strength and toughness as well as resistance to corrosion. In the pure state it exists as the alpha, hexagonal, form which transforms to the beta, body-centred cubic form at a temperature of 882°C. Alloy additions are either alpha- or beta-stabilizing depending on whether they raise or lower the transformation temperature; there are three basic types of alloy according to McQuillan and McQuillan (1956). The first, alpha alloys, contain only alpha stabilizers, or a predominance of them, namely O, N, C, and many nontransitional elements, e.g. Al, Sn, Cn. Some have a small amount of the beta form in the structure at room temperature and are known as 'near' or 'super' alpha alloys. The second type, alpha-beta, contain additional elements which stabilise the beta phase to such an extent that the microstructure, at room temperature, consists of a mixture of the alpha and beta phases. The beta phase is stabilized by the addition of transition elements such as Fe, Cr, Mo, Mn and V. These alloys are of immense value as they can have their mechanical properties controlled by precipitation hardening. The third type, beta, are all beta at room temperature and contain a large proportion of beta-stabilizing elements, Mo, V and Cr. These have limited applicability. The constitutions of a number of alloys of all three types are summarised in Table 5.1.1.

T A B L E 5.1.1.

The composition and phases of commercially available titanium (I.M.I. Limited)

I.M.I.	B.S. Spec.	Composition	Phase	Class	Density g/cm^3	Remarks
130	--	Commercially pure	Alpha	I	4.51	(become succes-
160	TA, 7,8,9,	" "	"	I	4.51	(sively mechani- (cally stronger
230	TA,21,22,23,24	Ti - 2.5 Cu	"	I	4.56	Ductile, medium strength
314	--	Ti - 4 Al-4Mn	Alpha-beta	III(2)	--	--
315	--	Ti - 2 Al-2Mn	Alpha-beta	III(2)	4.51	low strength
317	TA,14,15,16,17,	Ti - 5 Al-2.5Sn	Alpha-beta	III(1)	4.46	medium "
318	TA,10,11,12,13,28,	Ti - 6 Al-4V	Alpha-beta	III(2)	4.42	" "
205	--	Ti - 15 Mo	beta	II	--	high "

Figure 5.1.1. Titanium-Boron Phase Diagram

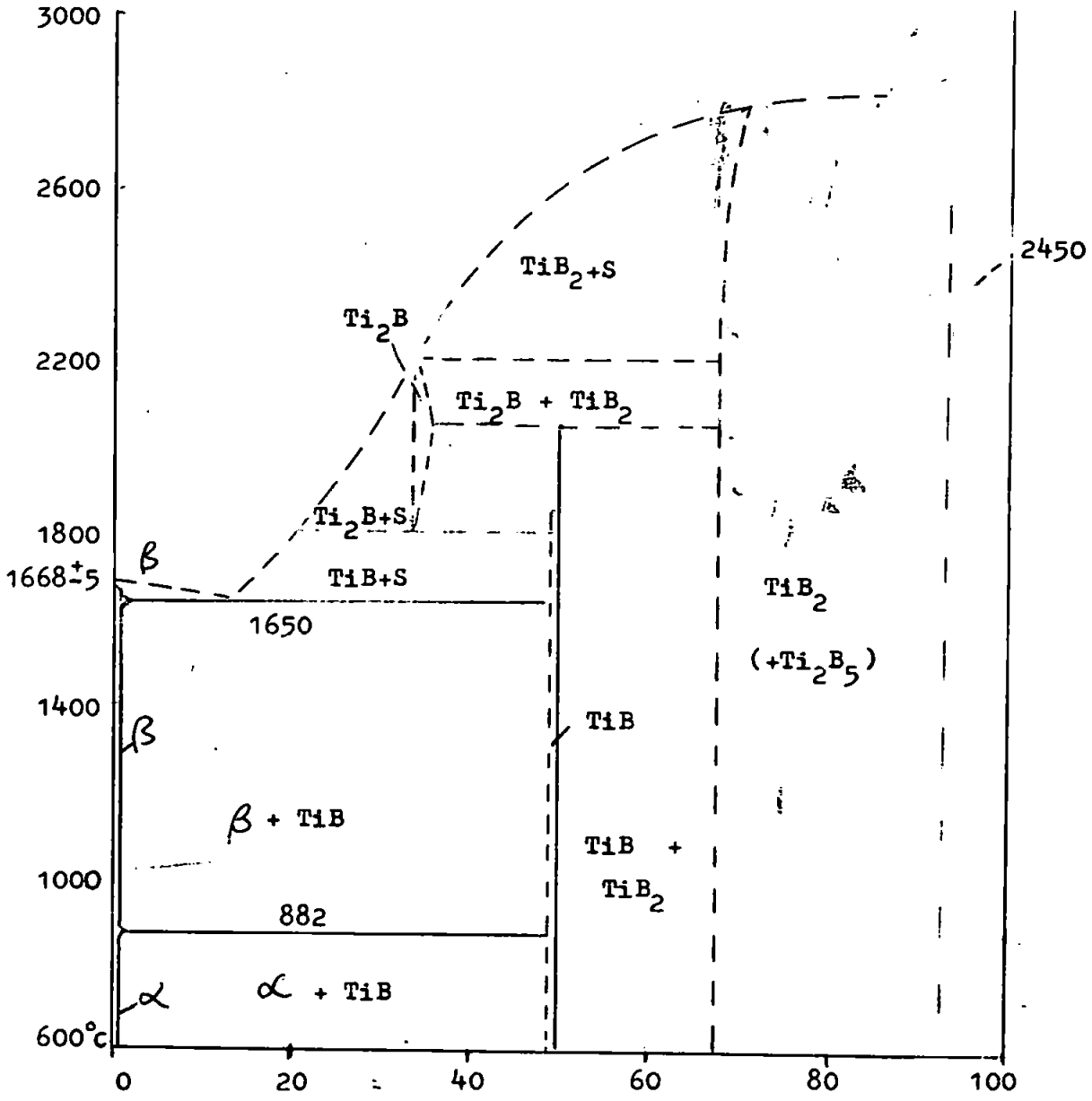

Titanium readily forms a series of binary compounds with the light elements, boron, carbon, nitrogen and oxygen, which are refractory and often of extreme hardness. The phase diagram for the titanium-boron system is shown in Figure 5.1.1. Of the compounds, Ti_2B, TiB, TiB_2, Ti_2B_5, and TiB_{12}, only TiB_2 is stable at room temperature according to Samsonov (1960); both Ti_2B and TiB disproportionate to TiB_2 and Ti according to Palty et al (1954), the same workers have shown that the solubility of boron in titanium does not exceed 0.05% between 750 and 1300°C and is only 0.1% at the eutectic temperature ($\sim$ 1650°C).

5.2. Moissan (1895, 1896) and Wedekind (1913) first obtained titanium diboride by sintering compacted powders of the two elements. Andrieux (1948) produced TiB_2 by the electrolysis of fused mixtures of TiO_2, B_2O_3, CaO and CaF_2 at temperatures of about 1000°C. Gas phase production of a compound approximating to TiB_2 was carried out by Moers (1931) heating $TiCl_4$ and BBr_3 between 1400 and 1800°C. Other methods depend on the reduction of the metal oxide and boric anhydride by carbon by the following reaction :-

$$TiO_2 + B_2O_3 + 5C \longrightarrow TiB_2 + 5CO$$

but in the proportions 1:4:7 as against 1:1:5 demanded by stoichiometry nevertheless the product still contains 2% free carbon (Blumenthal 1956). Kieffer et al (1952) have developed a 'borocarbide' method of production which consists of the reactions :-

$$Ti + B_4C + B_2O_3 \longrightarrow TiB_2 + CO$$

or $$Ti + TiO_2 + B_4C \longrightarrow TiB_2 + CO$$

carried out in a Tammann furnace at between 1800-2000°C. An alternative method developed by Samsonov (1956) was based on the reaction :-

$$2\ TiO_2 + B_4C + 3C \longrightarrow 2\ TiB_2 + 4CO$$

conducted under a vacuum of 10^{-1} to 10^{-2} mm Hg. and at a temperature of 1400 to 1450°C and contained a carbon content of between 0.01 - 0.3% of carbon after one hour. Thermodynamic data (Section 1.7) indicates that the reaction :-

$$2\ Ti + B_4C \longrightarrow 2\ TiB_2 + C$$

is feasible over the temperature range 0 to 4000°K and is exothermic and that TiB_2 is formed in preference to TiC.

5.3. In the present work, various alloys of titanium (Imperial Metal Industries (Kynoch) Ltd.) were sectioned by a diamond grit wheel (Bullock Diamond Products) and polished. Each section was coated to a thickness of about 0.1 mm with the prepared boron carbide powder by evaporating a suspension of the material in water to dryness under an infraheat lamp. The specimens about 1 cm in diameter, were placed in fused alumina crucibles (Thermal Syndicate) and loaded into the high temperature vacuum furnace (Metals Research P.C.10).

Figure 5.3.1. High temperature Laboratory Furnace (Metals Research, Type PCA10)

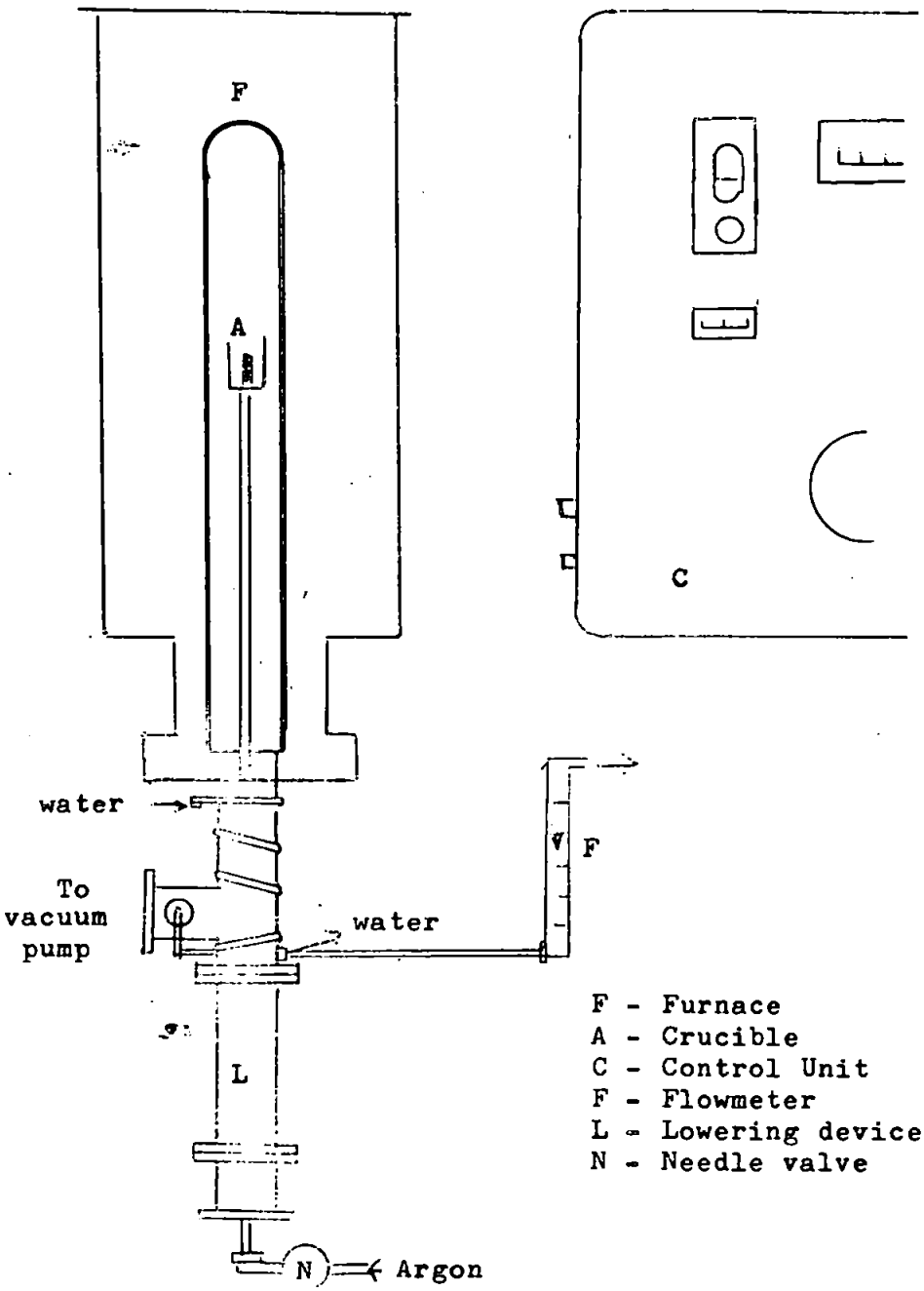

For vacuum and inert atmospheres (argon) a small amount of titanium hydride, TiH_2 was placed in the furnace to getter any residual O_2 and N_2 in the system. Specimens were heated to temperatures between 1000° and 1600°C for a period of one hour, and were cooled slowly allowing the titanium phases to equilibriate. The specimens were surface-etched by immersing quickly in a 1:1 mixture of HCl and HNO_3 and washing under water. The phases on the surface of the titanium metal substrate were examined by X-ray diffraction and by electron micrography of replicas.

5.4. The lattice spacings, for coated specimens heated at various temperatures, obtained from X-ray diffraction traces, are tabulated in Tables 5.4.1(a), 5.4.1(b), 5.4.1(c) and 5.4.1(d), alongside the published data for B_4C, C (graphite), alpha Ti, beta Ti, TiB_2, TiB, TiC, TiN, TiO, TiO_2 and any alloying element in order to establish concordance.

TABLE 5.4.1(a)

X-ray diffraction d-spacings, Å, obtained from the boron coated titanium-Comm. Pure (I.M.I. 130) heated to 1400°C for two hours under argon

Boron Coating	Base Alloy	Ti	B. Ti	Alloy	Ti_2B	TiB		TiB_2	TiC	TiN	TiO	TiO_2	B_4C
						cubic.	ortho						
		5.0682	calc.		Palty	calc.	5.0700	8.121	6.0614	6.0642	8.117	4.0551	5.0555
3.18w					3.67		3.053m	3.22w				4.05	4.49
2.98m	2.98m											3.245s	4.02
	2.83w							2.62m					3.79s
2.585m	2.58m	2.557m											2.81
2.51s	2.56m				2.538s		2.543s	2.51s					2.57s
2.46s						2.46s				2.44s		2.489	
					2.343s		2.346s				2.407		2.38s
2.31s	2.36m	2.342m	2.310s										
	2.33s											2.297	2.30w
2.24w	2.24vs	2.244s			2.263w								
2.14s					2.157m		2.161m		2.179s			2.188	
2.12vs						2.13s	2.140s			2.12s			
											2.085s	2.054	2.02w
2.03vs								2.033s					
1.93w	1.91m				1.950m		1.956m						
1.85w					1.856m		1.863m						1.87w
1.75	1.72m	1.726w			1.748m		1.755m						1.714m
1.63			1.63m					1.613w					1.637
													1.628
1.515		1.475w					1.528w	1.514w	1.535m			1.687	1.505
	1.467m	1.332w	1.33m		1.362s		1.461w			1.496	1.475		1.463
	1.327m					1.28w	1.362s		1.311m				1.446
		1.247w				1.23m			1.255w	1.277	1.259		1.407
										1.223	1.205		

*A.S.T.M. Card Index: w - weak, m - medium, s - strong, vs - very strong

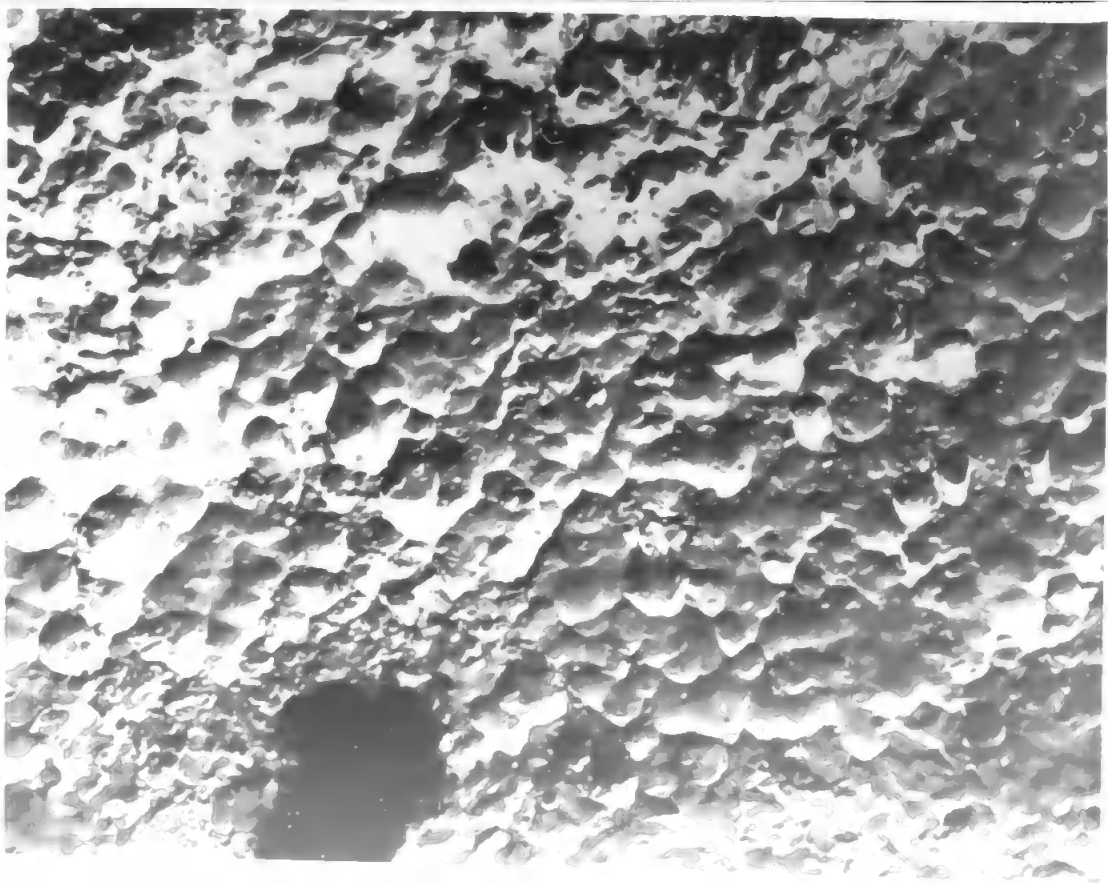

Figure 5.4.1.(a) I.M.I 130, Boride coated, 20,000 X magnification.

I.M.I. 130, untreated, 10,000 X magnification.

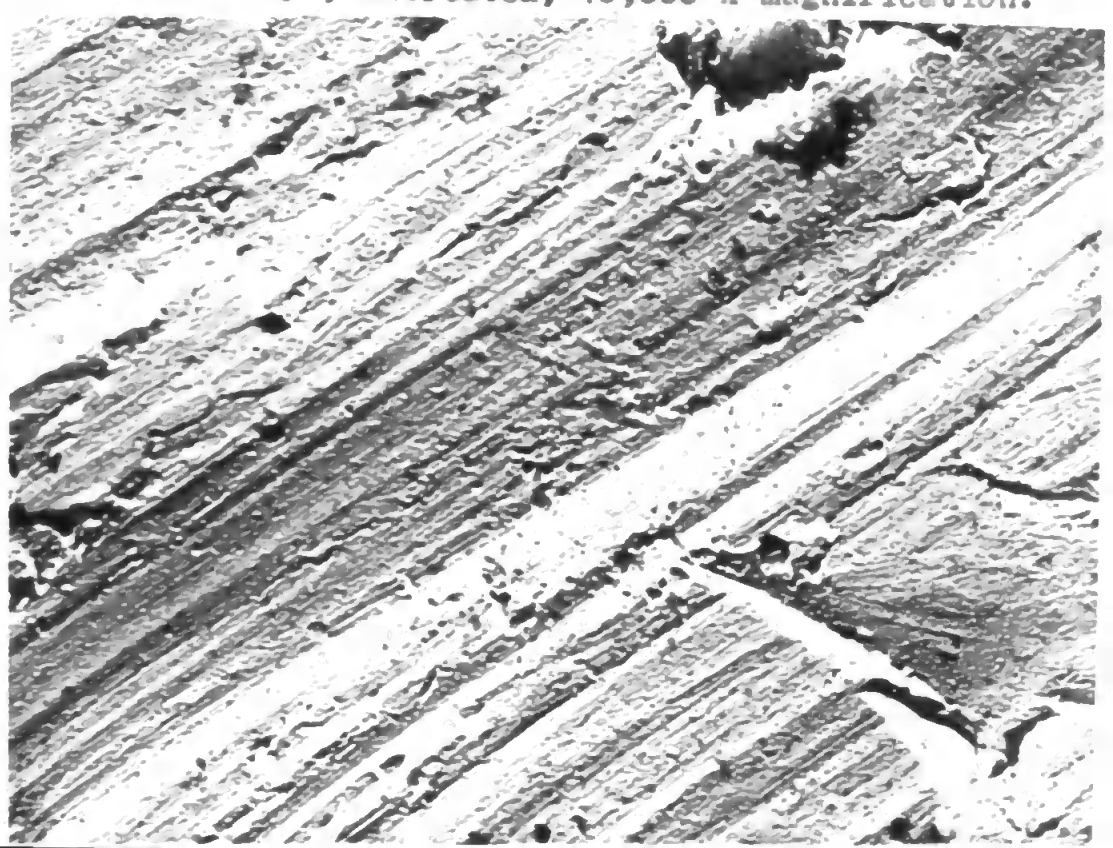

TABLE 5.4.1(b)

X-ray diffraction d-spacings, Å, obtained from the boron coated titanium, 2.5 Cu, (I.M.I. 230) heated to 1400°C for two hours under argon

Boron Coating	Base Alloy	Ti	B_o Ti	Alloy	Ti_2B	TiB cubic.	TiB ortho	TiB_2	TiC	TiN	TiO	TiO_2	B_4C
		5.0682	calc.	Copper	Palty	calc.	5.0700	8.121	6.0614	6.0642	8.117	4.0551	5.0555
3.18w				4.0836	3.67		3.053m	3.22w				4.05	4.49
2.98m												3.245s	4.02
								2.62m					3.79s
2.585m	2.54m	2.557m											2.81
2.51s					2.538s		2.543s		2.51s				2.57s
2.46s						2.46s				2.44s		2.489	
					2.343s		2.346s				2.407		2.38s
2.31s	2.33m	2.342m	2.310s										
												2.297	2.30w
2.24w	2.24vs	2.244s			2.263w								
2.14s					2.157m		2.161m		2.179s			2.188	
2.12vs						2.13s	2.140s			2.12s			
				2.088s							2.085s	2.054	2.02w
2.03vs								2.033					
1.93w				1.808m	1.950m		1.956m						
1.85w					1.856m		1.863m						1.87w
1.75	1.72m	1.726w			1.748m		1.755m						1.714m
1.63			1.63m					1.613w					1.637
													1.628
1.515	1.47m	1.475w					1.528w	1.514w	1.535m			1.687	1.505
	1.303m	1.332w	1.33m		1.362s		1.461w			1.496	1.475		1.463
				1.278w		1.28w	1.362s		1.311m				1.446
		1.247w				1.23m			1.255w	1.277	1.259		1.407
										1.223	1.205		

* A.S.T.M. Card Index: w - weak, m - medium, s - strong, vs - very strong

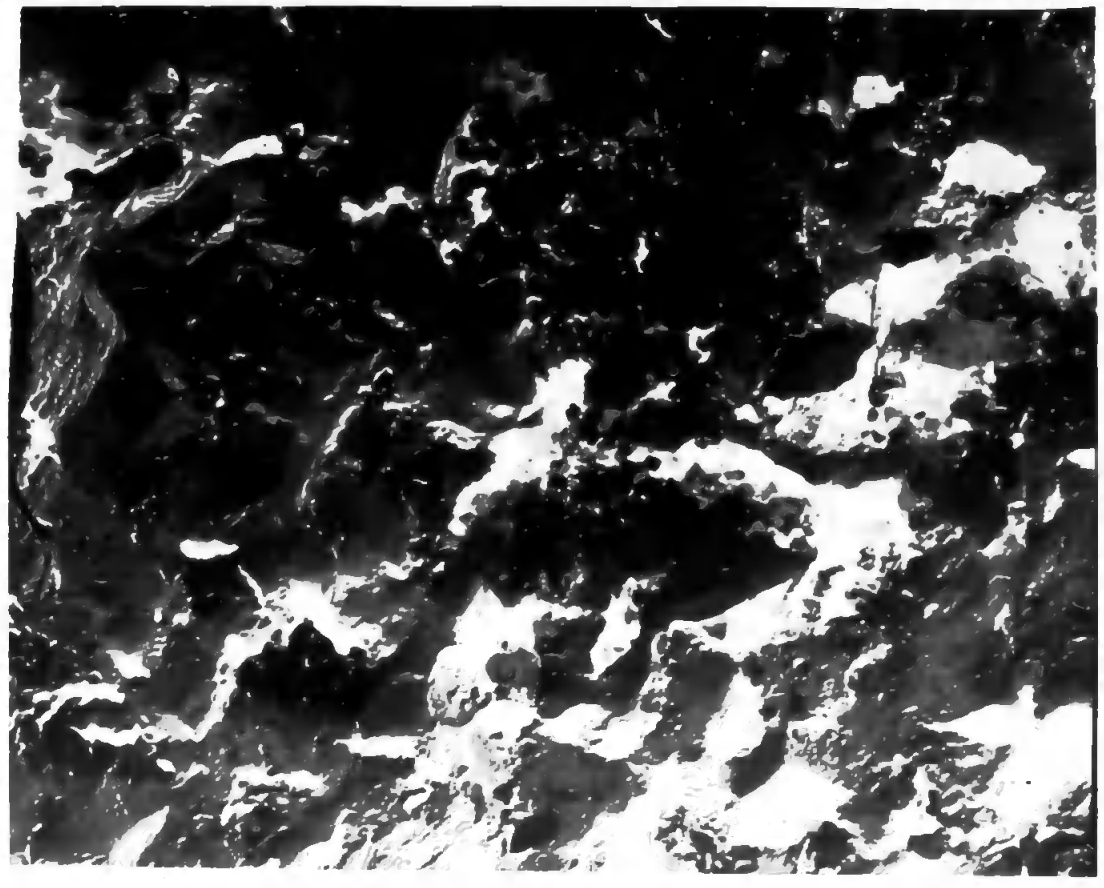

Figure 5.4.1 (b) I.M.I. 230 Boride coated, 20,000 X magnification.

I.M.I. 230, untreated, 20,000 X magnification.

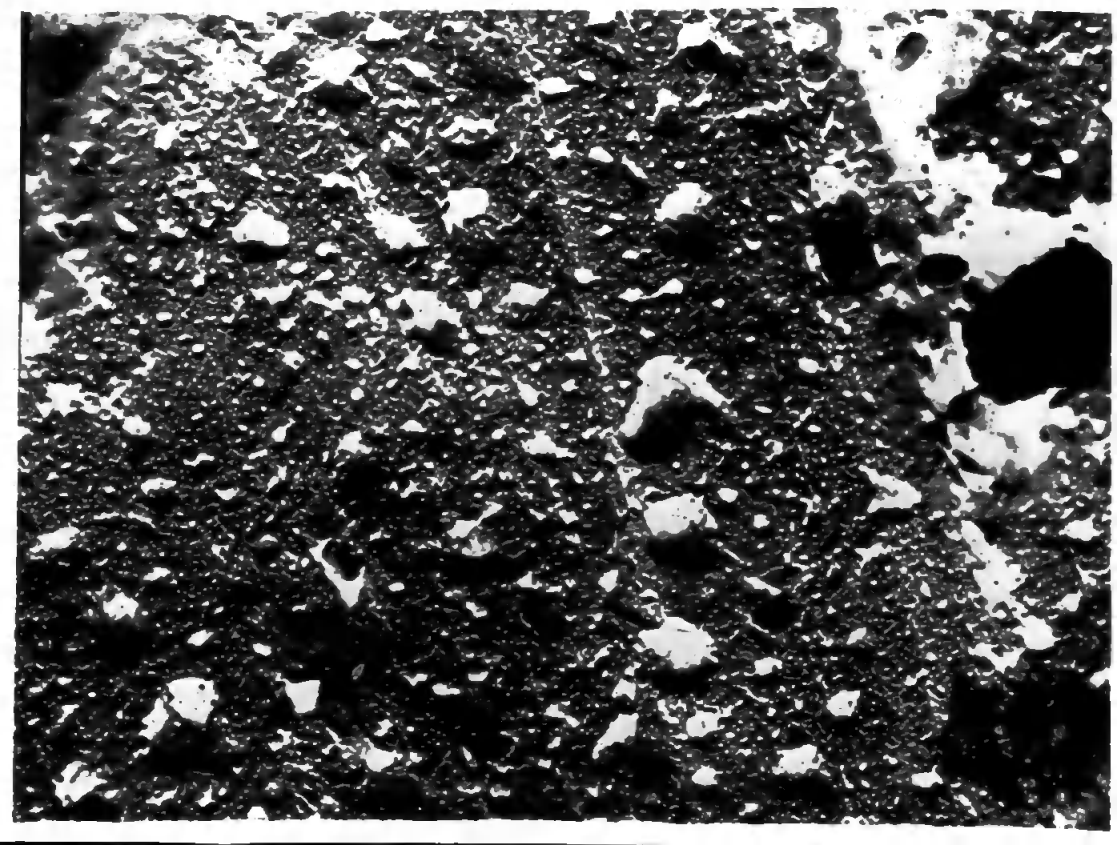

TABLE 5.4.1(c)

X-ray diffraction d-spacings, Å, obtained from the boron coated titanium - 15 Mo (I.M.I. 205) heated to 1400°C for two hours under argon

Boron Coating	Base Alloy	Ti	B. Ti	Alloy	Ti_2B	TiB		TiB_2	TiC	TiN	TiO	TiO_2	B_4C
		5.0682	calc.	Mo	Palty	cubic. calc.	ortho 5.0700	8.121	6.0614	6.0642	8.117	4.0551	5.0555
3.18w					3.67		3.053m	3.22w				4.05	4.49
2.98m												3.245s	4.02
								2.62m					3.79s
2.585m		2.557m											2.81
2.51s	2.51m				2.538s		2.543s		2.51s				2.57s
2.46s						2.46s				2.44s		2.489	
					2.343s		2.346s				2.407		2.38s
2.31s	2.31s	2.342m	2.310s										
2.24w	2.23s	2.244s		2.225	2.263w							2.297	2.30w
2.14s					2.157m		2.161m					2.188	
2.12vs						2.13s	2.140s			2.12s			
											2.085s	2.054	2.02w
2.03vs								2.033					
1.93w					1.950m		1.956m						
1.85w					1.856m		1.863m						1.87w
1.75		1.726w			1.748m		1.755m						1.714m
1.63	1.63m		1.63m					1.613w					1.637
													1.628
1.515		1.475w		1.574m			1.528w	1.514w	1.535m			1.687	1.505
		1.332w	1.33m		1.362s		1.461w			1.496	1.475		1.463
	1.33m					1.28w	1.362s		1.311m				1.446
		1.247w				1.23m			1.255w	1.277	1.259		1.407
				1.285m						1.223	1.205		

* A.S.T.M. Card Index: w = weak, m = medium, s = strong, vs = very strong

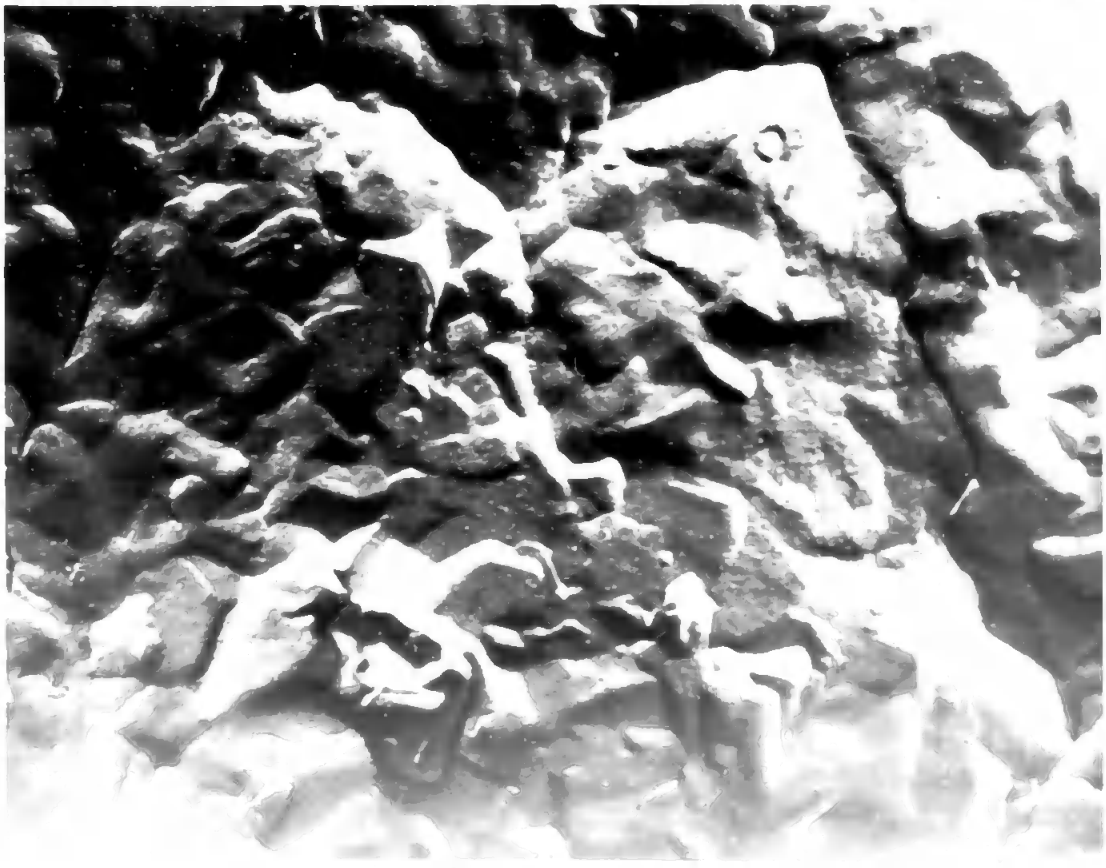

Figure 5.4.1.(c) I.M.I. 205, boride coated, 20,000 X magnification.

I.M.I. 205, untreated, 20,000 X magnification.

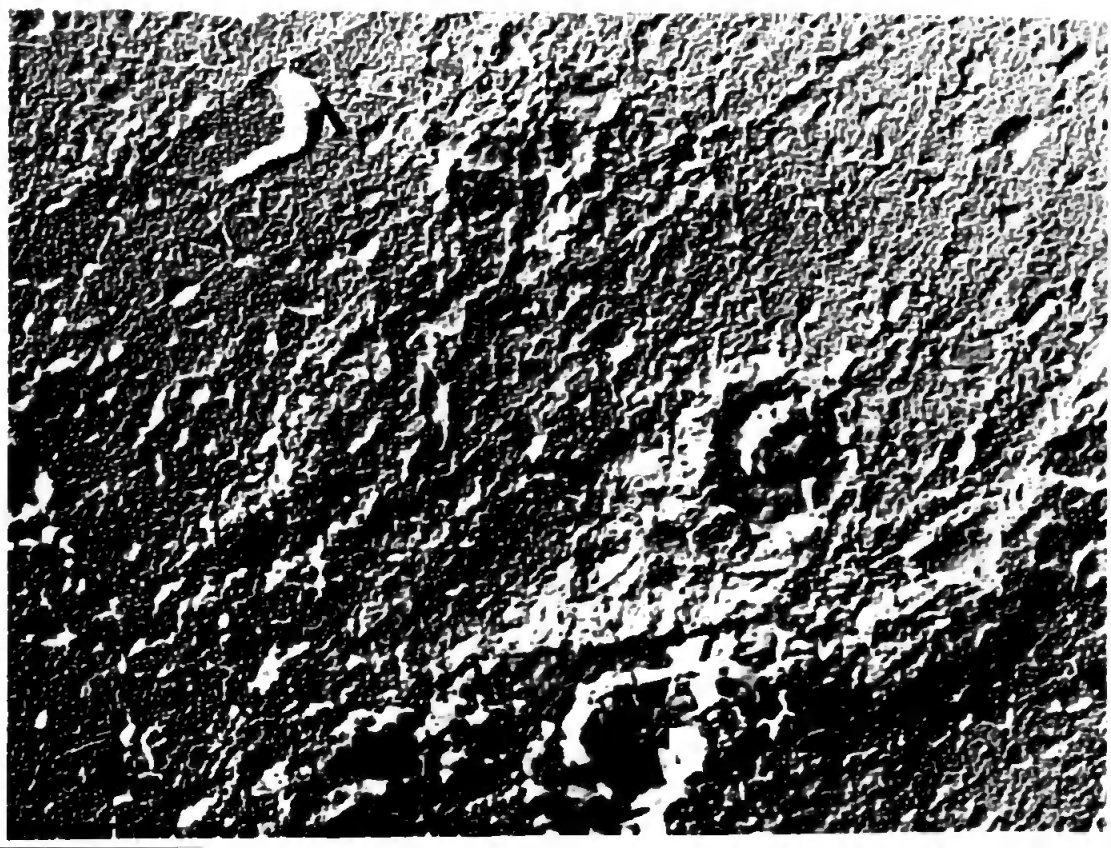

T A B L E 5.4.1(d)

X-ray diffraction d-spacings, Å, obtained from the boron coated titanium 6Al 4V($\frac{\alpha}{\beta}$) (I.M.I. 318) heated to 1200°C for two hours under argon

Boron Coating	Base Alloy	Ti 5.0682	B. Ti calc.	Alloy Al/V	Ti_2B Palty	TiB cubic. calc.	TiB ortho 5.0700	TiB_2 8.121	TiC 6.0614	TiN 6.0642	TiO 8.117	TiO_2 4.0551	B_4C 5.0555 *
3.18w					3.67		3.053m	3.22w				4.05	4.49
2.98m												3.245s	4.02
								2.62m					3.79s
2.585m		2.557m											2.81
2.57													
2.51s	2.51m				2.538s		2.543s		2.51s				2.57s
2.46s						2.46s				2.44s		2.489	
2.38					2.343s		2.346s				2.407		2.38s
2.31s	2.31s	2.342m	2.310s	2.338s									
2.24w	2.23s	2.244s			2.263w							2.297	2.30w
2.14s				2.14s	2.157m		2.161m					2.188	
2.12vs						2.13s	2.140s			2.12s			
											2.085s	2.054	2.02w
2.03vs				2.024m				2.033					
1.93w					1.950m		1.956m						
1.85w					1.856m		1.863m						1.87w
1.75		1.726w			1.748m		1.755m						1.714m
1.63	1.63m		1.63m					1.613w					1.637
													1.628
1.515		1.475w					1.528w	1.514w	1.535m			1.687	1.505
		1.332w	1.33m	1.431w	1.362s		1.461w			1.496	1.475		1.463
	1.33m			1.238w		1.28w	1.362s		1.311m				1.446
		1.247w		1.221w		1.23m			1.255w	1.277	1.259		1.407
										1.223	1.205		

* A.S.T.M. Card Index: w - weak, m - medium, s - strong, vs - very strong

Figure 5.4.1.(d) I.M.I. 318, boride coated, 10,000 X magnification.

I.M.I. 318, untreated, 20,000 X magnification.

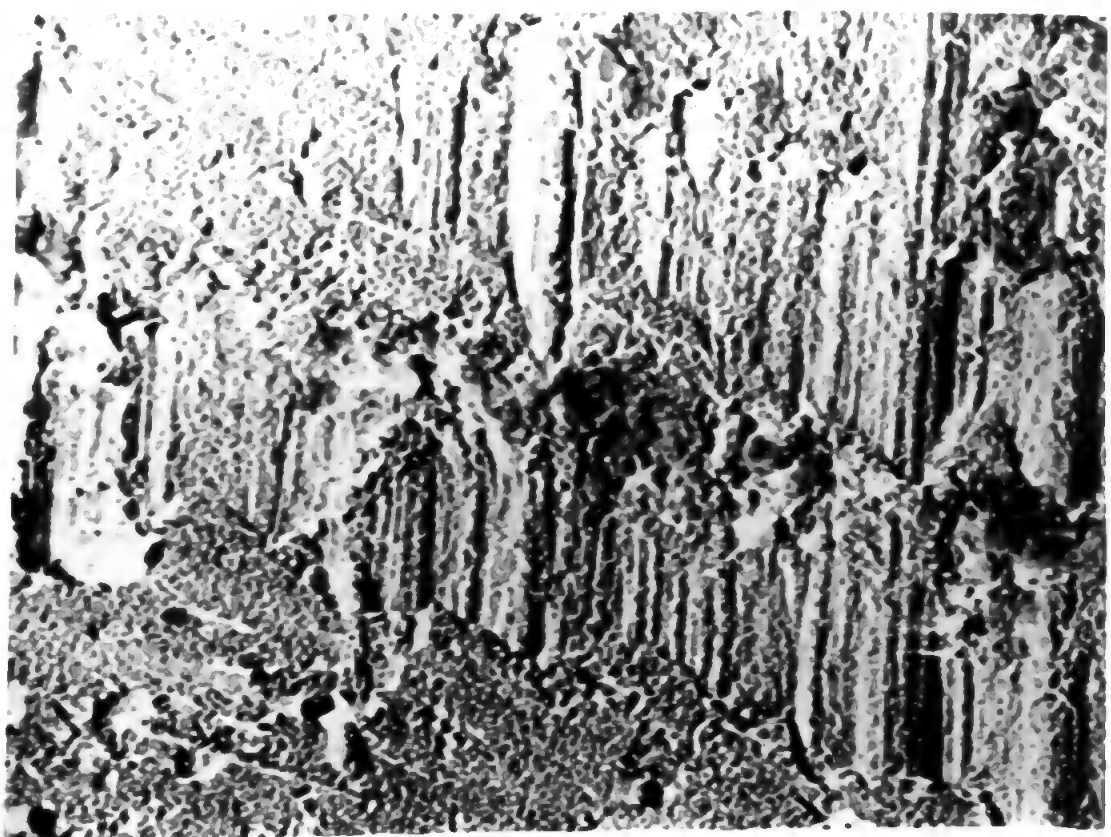

The X-ray diffraction intensities indicated that the final surface coatings had depths of some 100μm and had the same composition and phase irrespective of the composition and phase of the titanium alloy substrate. It was found that the principal phases were TiB, cubic and orthorhombic, TiB_2, and beta Ti and very little alpha Ti even when the substrate was pure alpha (I.M.I. 130, Table 5.4.1(a). Specimens heated above 1400°C were uncontaminated by any carbide or free carbon phase; this is in accord with Mercuri et al (1959) who showed that the oxygen and carbon content of metal borides can be reduced by heating above 1400°C under partial vacuum. A possible tetragonal phase of a lower boride was not discounted, however, it was impossible to resolve it from the almost identical spacings of the orthorhombic TiB (a = 6.10Å, c = 4.53Å, and a = 6.12Å b = 3.06Å, c = 4.56Å respectively).

5.5. When transition metals are combined with light nonmetals (carbon, nitrogen, hydrogen) so called interstitial phases of these atoms in the pores of the metallic lattices are formed. The interstitial phases are formed, according to Hägg (1931), under the condition that the ratio of the radius of the nonmetal to the radius of the metal atom does not exceed 0.59. They have simple structures, F.C.C., H.C.P. and B.C.C. Above this ratio, more complex structures are formed but titanium and boron give the limiting ratio of 0.59. As a result, pure alpha titanium accommodates boron (from boron carbide) giving, initially, a lower boride TiB_x which has a tetragonal lattice when

$x \triangleq 0.2$. (Palty et al, 1954). This boride disproportionates peritectoidally into beta Ti and TiB at a temperature above 900°C. The monoboride is normally of the orthorhombic-P, FeB type when near stoichiometric, TiBy ($y = 1 \pm 0.1$) (Decker and Kasper (1954) (Taylor and Kagle (1963)), a cubic, NaCl, form of TiB, a = 4.21Å(Ehrlich, 1949), a = 4.26Å(Glaser, 1952), exists when some C, N or O is present for stabilisation; excess carbon causes disproportionation to TiB_2 and TiC but formation of the latter is precluded by the presence of excess boron. Below 680°C TiB also disproportionates to TiB_2 and presumably alpha Ti (Palty et al (1954)); Samsonov (1956), reporting on the saturation of annealed specimens of high purity titanium with boron, indicates that the only phase evident at room temperature is the hexagonal TiB_2. In the present work, as indicated, there is a mixture of phases, despite slow cooling under argon. It is considered noteworthy that the spacings for (110) of the beta titanium, B.C.C. and for (111) of the orthorhombic TiB occur at 2.31Å thus giving mutual stabilisation when a specimen is quenched resulting in 'freezing-in' the metastable phases. The surfaces of the untreated and treated metals were polished and etched metallographically; direct photomicrographs and electron-micrographs of replicas of these surfaces are shown in Figures 5.5.1. and 5.5.2. respectively.

5.6. Attempts to polish the coated specimens by the normal metallographic techniques proved difficult as the surface was extremely hard. Hardness tests by the usual indenter were

impracticable owing to the thinness of the surface and the relative low hardness of the titanium. The surface withstood the abrasion of carborundum, SiC, and corundum, Al_2O_3; only with diamond was it possible to remove the surface. Titanium alloys show a pronounced tendency to gall, i.e. metals in contact binding together; attempts at case-hardening titanium and its alloys by either surface heat treatment of an age-hardened alloy, or, by a superficial layer of metal containing O, N or C, have been of limited success. Titanium heated in O_2 or N_2 at 1000°C has a layer which exhibits spalling and gas carborization yields a carbide surface of between 25 μm and 1 μm thick, however the presence of any hydrogen is most undesirable during the fabrication and use of titanium and its alloys. The case-hardening of titanium and its alloys by boron appears to offer the control lacking in the other techniques and is the basis of a patent application by the Author (1969).

SECTION 6

The section summarises the conclusions derived from the results obtained in the previous sections and suggests a theory for the phenomenalogical formation of boron carbide and a number of related compounds.

6.1. The preparation of boron carbide

The material produced by the magnesium thermal reduction of boric oxide, B_2O_3, in the presence of carbon black, described in Section 2.1., was of composition corresponding to the stoichiometric formula B_4C, but contained some free carbon. The unusual feature of this reaction is the fact that both reaction products - boron carbide and magnesium oxide - are refractory compounds, in which case, each boron carbide particle is separated by magnesium oxide which precludes grain growth and results in the extremely small crystallite size. Further crystallite growth can only be achieved by reheating the separated boron carbide to 1800°C or grain growth by ball milling for several hours (Samsonov, 1960, p.186).

6.2. Sintering of boron carbide

The sintering of boron carbide, inasmuch that the crystallites grow in size, was achieved by heating the prepared boron carbide, under vacuum, at temperatures between 1000-1800°C. Phase studies indicated some loss of boron, particularly at the higher temperatures; there was no tendency for the particles to adhere. Thus, the Tammann temperature, which indicates the ratio of the

temperature at which particles begin to aggregate and adhere compared with their melting point, kelvin, for boron carbide is much greater than the 50-70% found for many ceramic oxides and nitrides. It was reported by Jackson (1961) that for most borides and carbides, including B_4C, final consolidation of the material is not achieved until a temperature of about 90% of the melting point is reached. This can be explained in terms of the increased covalency of these compound, compared to many oxides, inhibiting the diffusion at the surface and at the grain boundaries characteristic of many oxides and ionic nitrides. For this reason it is not possible to compact either diamond or borazon (cubic BN) by sintering (with or without pressure) to a pore-free state, as these represent the ultimate in three-dimensional pure covalent bonding of the constituent atoms.

Compaction of boron carbide to almost theoretical densities was achieved only by hot-pressing to a temperature above 2,300°C (m.p. B_4C 2,450°C) and at pressures between 200 and 300 Kg cm^{-2} (limited by the working pressure of the graphite mould sets), despite a rapid consolidation of the powder to about 30% pore density at a temperature of 1000°C. These results confirm those of Hashimoto and Toibana (1969) which show the mechanism of sintering of boron carbide to occur via a process of plastic flow as a result of the temperature and load causing deformation of asperities and consequent adherence according to the Murray Model equation for pressure sintering: $\frac{dD}{dt} = \frac{3P}{4\eta} \cdot (1 - D)$, where $\frac{dD}{dt}$ is the densification rate, P is the applied pressure, η is

the viscosity and D is the relative density. It should be noted that a similar result for alumina, Al_2O_3, where T_m = 94% of the melting point was obtained by Mangsen et al (1960).

Compacts of boron carbide, B_4C, having little porosity (the X-ray density is 2.52 g/cc), represent the hardest material available in a massive compacted form.

6.3. The oxidation of boron carbide in air.

The high-purity, near stoichiometric boron carbide of submicron size, produced as described in 6.1., was oxidised by heating in air. Changes in phase composition, surface area, crystallite and aggregate size have been correlated with the time and temperature of the oxidation. The boric oxide, B_2O_3, formed, acted as a matrix for the remaining boron carbide and the newly-formed carbon and progressively retarded the rate of oxidation. The activation energy of 24 kilocalories per mole was somewhat lower than the value of 47 kilocalories per mole obtained by Mercuri et al, on material of larger particle size, due, it is believed, to the selective oxidation of the boron under the influence of the vitreous B_2O_3 phase.

6.4. The formation of an adherent coating of mixed titanium borides to a titanium alloy was achieved by heating the metal and its layer of very fine boron carbide to temperatures above 1000°C under a inert atmosphere, or in a vacuum. Only when heated above 1400°C was the surface free of unreacted B_4C and carbon. The carbon which appears to stay free of the boride

phase was assumed to have been oxidised to carbon manoxide by traces of oxygen or water vapour in the system. There was no evidence that the titanium boride, or the base metal, suffered oxidation during the period of heating of two hours. The beta phase titanium, rather than the expected alpha phase was present even when the chosen base metal was pure alpha. This could be explained by the peritectoidal decomposition of the lower boride of titanium initially formed to the orthorhombic TiB and the body centred beta titanium, these metastable phases were frozen in on cooling. The second phase of TiB, cubic, which was present was assumed to be stabilised by carbon in the system and the final product identified was the stable hexagonal diboride TiB_2. The surface so produced was extremely hard compared with the ductile titanium alloy and represented a method for producing a gall-resistant surface on these alloys.

6.5. The formation and stability of boron carbide and related compounds can be considered phenomenalogically on the basis of their crystallochemical structure. Scott et al (1967) in their re-evaluation of the X-ray data for $B_{12}C_3$ (B_4C) as being in fact $(CBC)^+ (B_{11}C)^-$ indicate a possible mechanism for its formation besides its likely stoichiometry; a priori, the reaction for the formation of boron carbide involves the diffusion of boron atoms into the graphite lattice causing breakage of the intercalated carbon bonds. This results in a alternate structure as in boron nitride. Subsequently, aided by multicentred bonding, many more

boron atoms are accommodated into the structure as icosahedra. It should be noted that, statistically, the formula, $(CBC)^+(B_{11}C)^-$, represents the highest carbon content, 20 atomic %, for a structure with no two carbon atoms contiguous where the intraicosahedral carbon is not in an equitorial position to bond to the linear grouping C-B-C. Also significant is the fact that BN represents the highest boron compound of the B-N system, suggesting that elements of a greater number of valence electrons than carbon are able to saturate the electron deficiency inherent in boron. This would cast doubt on the reported structures $B_{6.6}O$, $'B_{12}S'$, $B_6P_{0.9}$ (Martkovich 1963) unless supported by small percentages of carbon in their structures. In borides, where the metals are themselves electron deficient, the complexity of the boron structure is unaffected unless the metal is present in amounts indicated by the lower borides, viz. M_2B, MB, etc. Then the valence electrons of both the metal and the nonmetal occupy the conduction band of the metal. These lower borides have simple structures similar to those of the metals in displaying maximum coordination.

6.6. The present work has indicated the paucity of information available which relates the observed physical data for these compounds with their crystallo-chemical structure, due mainly to the difficulties in the technology involved in their production in a pure and defined state. Further work is indicated into the mechanism of formation of these compounds and to the influence

of contaminants on the final products. Parallel work to that on borides and carbides, is being undertaken in this Department in the field of nitrides (Glasson et al (1968, etc). Jayaweera (1969), I. Ali (1970) and N.G. Coles (1970)).

REFERENCES

R.F. Adamsky, Acta Cryst. 11, 744, (1958)

R.D. Allen - J.Am.Chem.Soc. 75 3582 (1953)

B.M. Alexander and R.W. Baluffi - J.Metals 2, 1219, (1950)

L. Andrieux, Ann.Chem.Phys. 12, 42, (1929)

B. Aronsson 'Borides' in H. Hausner, Ed. Modern Materials, Vol. 2, Academic Press N.Y.(1960)

B. Aronsson, T. Lundstrom and S. Rundquist - Borides, Silicides and Phosphides 'Methuen', London, (1965)

L.F. Athy - Bull Amer.Assoc.Petrol.Geol. 14, 1, (1930)

J. Baxter, A. Roberts, Powder Metallurgy Symposium, Iron and Steel Inst., London, (1954) p. 63.

H. Blumenthal, Powder Metallurgy Bull, 7, 79, (1956)

H. Blumenthal, Anal.Chem. 23, 992, (1951)

G.B. Bokii, Introduction to Crystallography, Izd. MGU Moscow (1954)

W.G. Bradshaw and C.O. Matthews, 'Properties of Refractory Materials, collected data and references', LMSD-2466 (1958)

S. Brunauer, P.H. Emmett and E. Teller, J.Amer.Chem.Soc. 60, 309, (1938)

P.P. Budnikov and A.M. Ginstling - 'Reaktsii v Smesyakh Tverdykh', trans. K.Shaw, Maclaren, London, (1968)

F.W. Bundy, J.Chem.Phys. (1955)

F.W. Bundy and R.H. Wentorf, Jr. J.Chem.Phys. 38, 1144 (1963)

J.E. Burke and D. Turnbull, Progress in Metal Physics, 3, 220, (1952)

I.E. Campbell, 'High Temperature Technology', J. Wiley, N.Y. (1956)

H.K. Clark and J.L. Hoard - J.Am.Chem.Soc. 65, 2115, (1943)

C. Cline, J.Amer.Electrochem.Soc. 106, 52 (1959)

C. Cline, J.Amer.Electrochem.Soc. 106, 322, (1959)

R.L. Coble, J.Amer.Ceram.Soc. 41, 55, (1958)

R.L. Coble and J.S. Ellis - J.Amer.Ceram.Soc. 46, 493, (1963)

E. Colton - J.Am.Chem.Soc. 82, 1002, (1960)

E. Colton - J.Inorg.Nucl.Chem. 17, 108, (1961)

M.W. Davies and P.J. Phennah - J.Appl.Chem. 9, 213, (1959)

H. Davy, Phil.Trans. 99, 37, (1809)

E. Decker and J. Kasper, Acta Cryst. 7, 77, (1954)

V.S. Degtyarev et al, Ogneupory, 31, (5), 52, (1966)

R.T. Dolloff, WADD Tech.Rept.No 60-143, Contract No. AF33(616)-6286 July, (1960)

D.A. Dominey - J.Chem.Soc. A.712 (1968)

P. Ehrlich, Z.anorg. Chem. 4, 1, (1949)

Elektroschmelzweek Kempton G.M.B.H. Patent 1,070,325 (1964)

H.J.T. Ellingham, J.Soc.Chem. Ind. London, 63, 125, (1944)

R.P. Elliott, Final Tech.Rept. ARF-2200-12 (U.S.A.E.C.) Contract No. AT(11-1)-578, (May, 1960 - April 1961)

O.A. Esin and P.V. Gel'd, Metallurgizdat, 1, II, 1949, (1954)

V.N. Eremenko and Yu V. Naidich, 'Wetting of the surfaces of refractory compounds by the rare metals'. Vid.Akad.Nauk.Ukr.S.S.R., Kiev, (1958)

J. Frenkel - J.Phys. U.S.S.R., 9, 385, (1945)

G.R. Findlay, Chemistry in Canada, 4, 41 (1952)

H.F. Fischmeister, C.A. Blande and S. Palmqvist, Powder Met. 7, 82, (1961)

J.J. Gangler, C.F. Robards and J.E. McNutt, NACA-TN-1911, (1949)

J. Gay-Lussac and C. Thenard, Recherches Physico-Chimique, 9, 276, (1811)

R.F. Giese, Jr., J. Economy and V.I. Matkovich, Chicago Meeting of Amer.Chem.Soc. (Physical Chemistry) Paper No. 34, Aug-Sept. (1964)

F.W. Glaser - J.Metals, 4, 391, (1952)

F.W. Glaser, D. Moskowitz and B. Post - J.Appl.Phys. 24, 731, (1953)

D.R. Glasson, J.Chem.Soc. 1506, (1956)

D.R. Glasson, S.C.I. Monographs No. 18,401, (1964)

D.R. Glasson, J.Appl.Chem. 14, 121, (1964)

D.R. Glasson and S.A.A. Jayaweera, J.Appl.Chem. 18, 65, (1968)

D.R. Glasson and S.A.A. Jayaweera, J.Appl.Chem. 18, 77, (1968)

D.R. Glasson and J.A. Jones, J.Appl.Chem. 19, 125, (1969)

D.R. Glasson and J.A. Jones, J.Appl.Chem. 19, 137, (1969)

E.G. Gray, B.P. 687, 946

N.N. Greenwood, R.V. Parish and P. Thornton, Quarterly Reviews, 20, 441, (1966)

S.J. Gregg, J.Chem.Soc. 561 (1946)

S.J. Gregg, J.Chem.Soc. 3940 (1953)

S.J. Gregg, J.Chem.Soc. 1438, (1955)

S.J. Gregg and K.S.W. Sing, 'Adsorption, Surface Area and Porosity', Academic Press, London, (1967).

S.J. Gregg and G.W. Winsor, Analyst, London, 70, 336, (1945)

R.W. Grimshaw, E. Heaton and A.L. Roberts, Trans Ceram.Soc. 44, 76, (1945)

G. Hägg - Z.Physik.Chem. $\frac{B6}{B7}$ 221 (1929) 33 (1931)

H. Hamijan and W. Lidman, J.Amer.Ceram.Soc. 35, 44, (1952)

M.R. Harvey, Diss.Abs. 25, 6510, (1965)

H. Hashimoto & Y. Toibana, Bull.Gov.Ind.Res.Inst. Osaka, Japan, 20, (1), 1, (1969)

C. Herring - J.Appl.Phys. 21, 437, (1950)

N.F. Hiester, F.A. Ferguson and N. Fishman, Chem.Eng. 237 (1957)

D.L. Hildenbrand and W.F. Hall, J.Phys.Chem. 68, 989, (1964)

P.B. Hirsh, A. Howie, R.B. Nicholson, D.W. Pashley and M.J. Whelan, 'Electron Microscopy of thin crystals' Butterworth, London, (1965)

Hitachi Company, Japan, B.P. 1,023,292 (1966)

Hitachi Company, Japan, B.P. 1,026,931 (1966)

J.L. Hoard and R.E. Hughes - 'Element Boron and Compounds of High Boron Content' in E.L. Muetterties, Ed. 'The Chemistry of Boron and its Compounds'. John Wiley, N.Y. (1967)

H.S. Houldsworth and J.W. Cobb, Trans.Ceram.Soc. 22, 111, (1922-23)

J.S. Jackson, Powder Met. 8, 73, (1961)

R.E. Jaeger and L. Egerton - J.Amer.Ceram.Soc. 45, 209, (1962)

JANAF Thermochemical Tables, Dow Chemical Co., N.Y. (1960-65)

S.Janes and J. Nixdorf, Ber.Dtsch.Keram.Ges. 43, H2, 136, (1966)

F.W. Jones, Proc.Roy.Soc. 166A, 16, (1938)

J.A. Jones, Patent Application No. 45939/69.

D.H. Kay (Ed.) 'Techniques for Electron Microscopy', Blackwell, Oxford, (1965)

R. Kieffer, F. Benesovsky and E. Honak - Z.Anorg.Chem. 268, 191, (1952)

W.D. Kingery, 'Proprty Measurements at High Temperature', J. Wiley, N.Y. (1959)

W.D. Kingery and M. Berg - J.Appl.Phys. 26, 1205, (1955)

H.P. Klug and L.E. Elexander, 'X-ray Diffraction Procedures' J. Wiley, N.Y. (1954)

W.A. Knarr, Diss.Abstr. 20, 4541, (1960)

J.A. Kohn, J. Katz and A. Giardini, Z.Krist. 111, 53, (1948)

J.A. Kohn and D.W. Eckart - Z.Krist. 111, 53, (1958)

J.A. Kohn and D.W. Eckart, Z.Krist. 116, 134, (1961)

J.A. Kohn, W.F. Nye and G.K. Gaule (eds), 'Boron-synthesis, Structure and Properties', Plenum Press, N.Y. (1960)

M.S. Koval'chenka and G.V. Samsonov, Proshkovaya Metallurgiya, 1, (2), 3, (1961)

H. Kramer - Anal.Chem. 27, 144, (1955)

O.H. Kriege, 'Analysis of Refractory Borides, Carbides, Nitrides and Silicides', Rept. No. LA-2306, Contract No. W-7405-ENG-36. (Mar. 1959)

W. Kroll, Z.Anorg.Chem. 101, 1, (1918)

G.C. Kuczynski - J.Appl.Phys. 21, 632, (1950)

N.A. Lange, 'Handbook of Chemistry', Handbook Publishing Co. (1946)

S. LaPlace and B.Post, Planseeber. Pulvermetal, 9, 109, (1961)

D. Lenzi and P.L. Pellegrini, Gazz.Chim.Ital. 89, 1725, (1959)

B. Lersmacher and S. Scholz, Arch.Eisenhuttenwesen, 32, 421, (1961)

B. Lersmacher, E. Roeder and S. Scholz, Naturwiss. 49, 35, (1962)

A. Lipp and M. Roder, Z.Anorg.Chem. 344, 225, (1966)

W.N. Lipscombe, Adv.inorg.Radiochem. 1, 117, (1959)

W.N. Lipscombe and D. Britton - J.Chem.Phys. 33, 275, (1960)

L.M. Litz and R.A. Mercuri - J.Electrochem.Soc. 110, 921, (1963)

H.C. Longuet-Higgins and M. deV. Roberts - Proc.Roy.Soc. 230A, 110, (1955)

C.E. Lowell, J.Amer.Chem.Soc. 50,(3), 142, (1967)

J.D. McElland and D.L. Whitney, Planseeber.Pulvermet. 10, 131, (1962)

J.K. Mackenzie and R. Shuttleworth - Proc.Phys.Soc. B62, 833, (1949)

A.D. McQuillan and M.K. McQuillan, 'Metallurgy of the Rarer Metals-Titanium', Butterworths, London, (1956)

G.E. Mangsen, W.A. Lambertson and B. Best - J.Amer.Ceram.Soc. 43, 55, (1960)

B. Magnusson and C. Brosset - Acta.Chem.Scand. 16, 449, (1962)

V.I. Matkovich - Acta.Cryst. 13, 679, (1960

V.I. Matkovich - J.Am.Chem.Soc. 83, 1804, (1961)

V.I. Matkovich - Acta.Cryst. 14, 1048, (1962)

V.I. Matkovich et al. - J.Amer.Chem.Soc. 86, 2337, (1964)

G.A. Meerson et al. - Izv.Akad.Nauk.SSSSR. 4, 90, (1961)

R.A. Mercuri, J.M. Finn, Jr. and E.M. Nelson - U.S. Pat. 2,998,302 (1959)

K. Moers, Z.Anorg.Chem. 198, 243, (1931)

H. Moissan, Compt.Rend. 114, 392, (1892)

H. Moissan, Compt.Rend. 120, 173, (1895)

H. Moissan, Compt.Rend. 121, 290, (1895)

H. Moissan, Ann.Chim.Phys.(7), 6, 296, (1895)

H. Moissan, Compt.Rend. 122, (1896)

H. Moissan, Ann.Chim.Phys. 7, 229, (1896)

H. Moissan and A. Stock. Compt.Rend. 131, 139, (1900)

P. Murray et al - Trans.Brit.Ceram.Soc. 53, 474, (1954)

F.R.N. Nabarro - 'The Strength of Solids', Physical Society (1948)

A.E. Palty, H. Margolin and J.P. Nielsen, Trans.Amer.Soc. Metals, 46, 312, (1954)

R.A. Pasternack - Acta.Cryst.12, 612, (1959)

H.S. Peiser, H.P. Rooksby, A.J.C. Wilson (Ed.), 'X-ray diffraction by Polycrystalline Materials', Part I, Chapman & Hall, London, 1960.

B. Ya. Pines - J.Tech.Phys. U.S.S.R., 16, 737, (1946)

B. Post - 'Refractory Binary Borides' in Roy M. Adams. Ed. 'Boron, Metalloboron Compounds and Boranes'. Interscience Publishers, N.Y. (1964.)

E. Podszus, Z.Anorg.Chem. 211, 41, (1933)

P. Popper and T.A. Inglis, Nature, 179, 1075, (1957)

C.F. Powell, J.H. Oxley and J.M. Blocher, Vapour Deposition, p.359, J. Wiley, London, (1966)

J.N. Pring and W. Fielding - J.Chem.Soc. 95, 1497, (1909)

L. Ramqvist - Powder Met. 9, 17, 1, (1966)

F.D. Richardson and J.H.E. Jeffes, J.Iron and Steel Inst. 160, (3), 261, (1948)

R.R. Ridgway - Trans. Am.Electrochem.Soc. 56, 117, (1934)

H.F. Rizzo and L.R. Bidweel - J.Amer.Ceram.Soc. 43, 550, (1960)

H.E. Robson and P.W. Gilles - J.Phys.Chem. 68, 983, (1964)

G.V. Samsonov and I.L. Zagyanskii and N.V. Popova, Dan.SSSR., 74, 723, (1950)

G.V. Samsonov, DAN.SSSR. 93, 689, (1953)

G.V. Samsonov, K.I. Portnoi and L.A. Solonikova, Dokl.Akad. Nauk.SSSR. 125, 823, (1955)

G.V. Samsonov, N.N. Zhuravlev and I.G. Amnuel, Fiz.Metal. i Metalloved Akad.Nauk.SSSR., Ural.Filial., 3, 309, (1956)

G.V. Samsonov, Abstr.Doctoral Diss.Moscow (1956a)

G.V. Samsonov and V.P. Latysheva, Fizika Metalloveden. 2, 309, (1956b)

G.V. Samsonov, K.I. Portnoi and L.A. Solonikova, Z.Neorg.Khim. 5, 203, (1960a)

G.V. Samsonov et al 'Boron ego Soendineniya i Splavy' Akad. Nauk.Ukr.SSSR Kiev (1960b available in U.S. translation; A.E.C. AEC-tr 5032 (Book 1 and 2)

G.V. Samsonov, 'Refractory Transition Metal Compounds', Academic Press, N.Y. (1964a)

G.V. Samsonov, 'High Temperature Materials, No2, Properties Index', Plenum Press, N.Y. (1964b)

G.V. Samsonov, Ukrain, Zhurnal, 31, (10), 1005, (1965)

V.T. Serebryanskii and V.A. Epel'Baum, Z. Strukt.Khim. No.2, 748, (1961)

H.L. Schick. T.D. of Certain Refractory Compounds, Academic Press (1966).

S. Scholz and B. Lersmacher, Arch. Eisenhuttenwesen, 41, 98, (1964)

S. Scholz, Planseeber.Pulvermet., 11, 83, (1963)

P. Schwarzkopf and R. Kieffer, Refractory Hard Metals, Macmillan. N.Y. (1953)

P. Schwarzkopf and R. Kieffer, Cemented Carbides, Macmillan, N.Y. (1960)

P.T.B. Shaffer, 'High Temperature Materials, No. 1, Materials Index', Plenum Press, N.Y. (1964)

A.J. Shaler and J. Wulff - Indust. and Eng. Chem. 40, 838, (1948)

A.H. Silver and P.J. Bray - J.Chem.Phys. 31, 247, (1959)

S. Sindeband and P. Shwarzkopf - Powder Met.Bull. 5, 42, (1950)

M.P. Slavinskii, Physico-Chemical Properties of the Elements, Metallurgizdat, Moscow, (1952)

D. Smith, A.S. Dworkin and E.R. Van Artsdalen - J.Am.Chem.Soc. 77, 2654, (1955)

E.K. Storms, The Refractory Carbide, Refract.Mater.Monogrs. Ed. J.L. Margrave, Academic Press, London, (1967).

R. Thompson and A.A.R. Wood - Chem.Eng. CE51, (1965)

R. Thompson - Borides 'Their Chemistry and Applications', R.I.C. Lecture Series, London, No. 5 (1965)

R. Thompson - Progress in Boron Chemistry, Ed. R.J. Brotherton and H. Steinberg, Pergamon Press, Oxford, (1969)

C.W. Tucker, Jr. and P. Senio - Acta.Cryst. 7, 456, (1954)

C.W. Tucker, Jr. and P. Senio - Acta.Cryst. 8, 371, (1955)

A.C. Van Dorsten, H. Niewdorf, A. Verhoeff, 'Philips Tech. Rev. 12, (2), 33, (1950)

T. Vasilos, J.Amer.Ceram.Soc. 43, 517, (1960)

T. Vasilos and R.M. Spriggs - J.Amer.Ceram.Soc. 46, 493, (1963)
G. Verhaegen et al. Nature, 193, 1280 (1962)
G. Vuillard - Comp.Rend., 257, (25), 3927, (1963)

J.M. Warde - Technical Bulletin No. 94, Refractories Institute, Pittsburgh, (1950)

E. Wedekind, Ber.46, 1198, (1913)

E. Wedekind, Ber. 76, 1885, (1913)

R.H. Wentorg, Jr. - J.Chem.Phys. 26, 956, (1957)

F. Weintraub, Trans.Electrochem.Soc. 21, 167, (1909)

F. Weintraub, Ind.Eng.Chem. 3, 2, (1911)

F. Weintraub, Ind.Eng.Chem. 5, 106, (1913)

J.H. Westbrook (ed) Intermetallic Compounds. J. Wiley. N.Y (1966)

G. Will - J.Amer.Chem.Soc. 85, 2335, (1963)

M. Yamazaki - J.Chem.Phys. 27, 746, (1957)

W.H. Zachariasen - J.Amer.Chem.Soc. 54, 3841, (1932)

G.S. Zhdanov and N.G. Sevast'yanov - Dokl.Akad.Navk. S.S.R. 32, 432, (1941)

V.K. Zworykin, G.A. Morton, E.G. Ramberg, J. Hillier and A.W. Vance - 'Electron Optics and the Electron Microscope', J. Wiley, N.Y. (1945)

A P P E N D I C E S

I. Janaf thermochemical tables

(a) boron carbide, B_4C
(b) diboron trioxide, B_2O_3
(c) carbon monoxide, CO
(d) carbon dioxide, CO_2
(e) magnesium oxide, MgO
(f) titanium monoboride, TiB
(g) titanium diboride, TiB_2
(h) titanium carbide, TiC
(i) titanium nitride, TiN

II. IBM 1130 Computer programme for B.E.T. gas sorption data.

III. Reprints of published papers -

'Formation and Reactivity of Borides, Carbides and Silicides'

I. Review and Introduction, J.appl. Chem. 19 (1969), 125

II. Production and sintering of boron carbide, J.appl. Chem. 19 137 (1969)

A P P E N D I X I

Reprints of

JANAF Thermochemical Tables

T, °K.	C_p° (cal. mole^{-1}deg.$^{-1}$)	S° (cal. mole^{-1}deg.$^{-1}$)	$-(F^\circ-H^\circ_{298})/T$ (cal. mole^{-1}deg.$^{-1}$)	$H^\circ-H^\circ_{298}$ (kcal. mole^{-1})	ΔH_f° (kcal. mole^{-1})	ΔF_f° (kcal. mole^{-1})	Log K_f
0	.000	.000	INFINITE	- 1.363	- 12.623	- 12.623	INFINITE
100	1.220	.191	13.524	- 1.313	- 12.631	- 12.619	27.577
200	6.570	2.703	7.448	- .949	- 12.645	- 12.601	13.769
298	12.545	6.482	6.482	.000	- 12.700	- 12.567	9.212
300	12.700	6.560	6.482	.023	- 12.701	- 12.565	9.193
400	18.450	11.108	7.063	1.617	- 12.701	- 12.518	6.839
500	21.400	15.582	8.325	3.628	- 12.689	- 12.475	5.453
600	23.750	19.655	9.879	5.865	- 12.726	- 12.430	4.528
700	24.580	23.345	11.544	8.261	- 12.819	- 12.373	3.863
800	25.640	26.699	13.232	10.773	- 12.962	- 12.302	3.361
900	26.530	29.772	14.901	13.383	- 13.147	- 12.208	2.964
1000	27.320	32.608	16.532	16.076	- 13.368	- 12.092	2.643
1100	28.040	35.247	18.115	18.845	- 13.614	- 11.951	2.374
1200	28.730	37.716	19.646	21.684	- 13.879	- 11.790	2.147
1300	29.380	40.042	21.127	24.590	- 14.154	- 11.603	1.951
1400	30.000	42.242	22.557	27.559	- 14.429	- 11.395	1.779
1500	30.610	44.332	23.940	30.589	- 14.699	- 11.168	1.627
1600	31.210	46.327	25.277	33.680	- 14.958	- 10.929	1.493
1700	31.800	48.237	26.572	36.831	- 15.197	- 10.688	1.371
1800	32.380	50.071	27.827	40.040	- 15.415	- 10.395	1.262
1900	32.951	51.837	29.044	43.307	- 15.610	- 10.112	1.163
2000	33.520	53.542	30.227	46.630	- 15.772	- 9.817	1.073
2100	34.088	55.191	31.376	50.011	- 15.906	- 9.516	.990
2200	34.650	56.790	32.495	53.447	- 16.005	- 9.206	.914
2300	35.205	58.342	33.588	56.940	- 34.468	- 8.897	.845
2400	35.760	59.852	34.649	60.488	- 34.515	- 7.786	.709
2500	36.315	61.323	35.686	64.092	- 34.507	- 6.675	.583
2600	36.870	62.758	36.700	67.751	- 34.447	- 5.564	.468
2700	37.420	64.160	37.691	71.466	- 34.332	- 4.457	.361
2800	37.970	65.531	38.661	75.235	- 34.164	- 3.349	.261
2900	38.520	66.873	39.611	79.060	- 33.943	- 2.254	.170
3000	39.070	68.188	40.542	82.939	- 33.669	- 1.158	.084
3100	39.614	69.478	41.454	86.874	- 33.340	- .077	.005
3200	40.160	70.744	42.350	90.862	- 32.960	.988	- .067
3300	40.709	71.989	43.229	94.906	- 32.526	2.030	- .134
3400	41.260	73.212	44.093	99.004	- 32.039	3.073	- .198
3500	41.800	74.416	44.942	103.157	- 31.499	4.104	- .256

Dec. 31, 1960; June 30, 1963

TETRABORON MONOCARBIDE (B_4C) (CRYSTAL) MOL. WT. = 55.291

$S^\circ_{298.15}$ = 6.48 ± 0.03 cal. deg.$^{-1}$ mole^{-1}

T_m = [2743 ± 20]°K.

$\Delta H_{f\ 0}^\circ$ = -12.6 ± 2.4 kcal. mole^{-1}

$\Delta H_{f\ 298.15}^\circ$ = -12.7 ± 2.4 kcal. mole^{-1}

ΔH_m° = [25] kcal. mole^{-1}

Heat of Formation.

The heat of formation was calculated from ΔH_f° = -683.3 ± 2.2 kcal. mole^{-1} for the reaction $B_4C(c) + 4O_2(g) = 2B_2O_3(amorph.) + CO_2(g)$ reported by D. Smith, A. S. Dworkin, and E. R. Van Artsdalen, J. Am. Chem. Soc. 77, 2654 (1955). The heat of formation for B_2O_3(amorph.), -300.98 ± 0.30 kcal. mole^{-1}, was obtained from W. H. Evans, National Bureau of Standards, private communication, October 6, 1960.

Heat Capacity and Entropy.

The low temperature heat capacities, 54-295°K., were taken from K. K. Kelley, J. Am. Chem. Soc., 63, 1137 (1941). High temperature heat capacities were reported by E. G. King, Ind. Eng. Chem. 41, 1298 (1949). $S^\circ_{298.15}$ was calculated based on the low temperature heat capacities measured by K. K. Kelley, loc. cit., using $S^\circ_{53.1}$ = 0.047 cal. deg.$^{-1}$ mole^{-1}.

Melting Data.

T_m was determined by Dolloff, WADD Tech. Rept. 60-143, 1960 and ΔH_m° was estimated.

T, °K	$C_p°$	S°	$-(G°-H°_{298})/T$	$H°-H°_{298}$	$\Delta H_f°$	$\Delta G_f°$	Log K_p
	cal mole⁻¹ deg⁻¹			kcal mole⁻¹			
[illegible]	[illegible]	[illegible]	[illegible]	[illegible]	- 299.786	- 282.115	206.786
[illegible]	[illegible]	[illegible]	19.719	.038	- 299.782	- 282.009	205.433
[illegible]	18.350	[illegible]	[illegible]	1.712	- 299.308	- 276.264	150.926
[illegible]	20.430	[illegible]	[illegible]	[illegible]	- 299.271	- 270.491	118.222
[illegible]	[illegible]	[illegible]	[illegible]	[illegible]	- 298.061	- 264.739	96.426
[illegible]	[illegible]	[illegible]	[illegible]	[illegible]	- 298.104	- 259.100	80.891
[illegible]	[illegible]	[illegible]	[illegible]	[illegible]	- 297.108	- 253.593	69.275
[illegible]	[illegible]	[illegible]	[illegible]	15.603	- 296.971	- 248.102	60.265
[illegible]	[illegible]	49.191	[illegible]	18.566	- 295.478	- 242.877	53.078
[illegible]	[illegible]	[illegible]	[illegible]	[illegible]	- 294.673	- 237.617	47.212
[illegible]	[illegible]	[illegible]	[illegible]	[illegible]	- 294.364	- 232.449	[illegible]
[illegible]	[illegible]	[illegible]	[illegible]	[illegible]	- 293.881	- 227.314	38.212
[illegible]	[illegible]	59.775	[illegible]	[illegible]	- 293.414	- 222.245	[illegible]
[illegible]	[illegible]	62.882	[illegible]	34.036	- 292.989	- 217.137	[illegible]
[illegible]	[illegible]	[illegible]	[illegible]	[illegible]	- 292.594	- 212.491	28.969
[illegible]	[illegible]	[illegible]	[illegible]	[illegible]	- 292.234	- 207.070	26.619
[illegible]	[illegible]	[illegible]	[illegible]	[illegible]	- 291.912	- 202.071	[illegible]
[illegible]	[illegible]	[illegible]	[illegible]	[illegible]	- 291.606	- 197.388	[illegible]
[illegible]	[illegible]	[illegible]	[illegible]	40.207	- 291.320	- 192.120	20.993
[illegible]	[illegible]	[illegible]	[illegible]	52.351	- 291.054	- 187.165	19.478
[illegible]	[illegible]	[illegible]	[illegible]	[illegible]	- 290.808	- 182.225	18.101
[illegible]	[illegible]	[illegible]	[illegible]	58.650	- 290.578	- 177.297	[illegible]
[illegible]	[illegible]	[illegible]	[illegible]	[illegible]	- 290.367	- 172.373	[illegible]
[illegible]	[illegible]	[illegible]	[illegible]	[illegible]	- 300.947	- 167.247	14.620
[illegible]	[illegible]	[illegible]	[illegible]	67.421	- 300.791	- 161.903	13.609
[illegible]	[illegible]	[illegible]	[illegible]	[illegible]	- 300.566	- 156.565	12.672
[illegible]	[illegible]	[illegible]	[illegible]	73.720	- 300.384	- 151.238	11.804
[illegible]	[illegible]	[illegible]	[illegible]	[illegible]	- 300.212	- 145.939	10.995
[illegible]	[illegible]	[illegible]	[illegible]	[illegible]	- 300.048	- 140.593	10.242
[illegible]	[illegible]	[illegible]	[illegible]	[illegible]	- 299.889	- 135.281	9.537
[illegible]	[illegible]	[illegible]	[illegible]	[illegible]	- 299.738	- 129.975	8.876
[illegible]	[illegible]	[illegible]	[illegible]	[illegible]	- 299.593	- 124.672	8.256
[illegible]	[illegible]	[illegible]	[illegible]	[illegible]	- 299.456	- 119.372	7.673
[illegible]	[illegible]	[illegible]	[illegible]	[illegible]	- 299.329	- 114.084	7.123
[illegible]	[illegible]	[illegible]	[illegible]	[illegible]	- 299.196	- 108.787	[illegible]
[illegible]	[illegible]	[illegible]	[illegible]	[illegible]	- 299.075	- 103.500	6.113
[illegible]	[illegible]	[illegible]	[illegible]	[illegible]	- 298.958	- 98.210	5.648
[illegible]	[illegible]	[illegible]	[illegible]	[illegible]	- 298.846	- 92.935	[illegible]
[illegible]	[illegible]	[illegible]	[illegible]	[illegible]	- 541.098	- [illegible]	4.555

BORON OXIDE (B_2O_3) (LIQUID)

$S°_{298.15}$ = 18.?59 cal. deg.⁻¹ mole⁻¹

T_m = 723 ± 2°K.

T_b = 2316°K.

$\Delta H_{f\,298.15}°$ = [illegible] kcal. mole⁻¹

$\Delta H_m°$ = [illegible].26 ± [illegible] kcal. mole⁻¹

$\Delta H_v°$ = [illegible] kcal. mole⁻¹

Heat of Formation.

$\Delta H_{f\,298.15}°$ for B_2O_3(1) was obtained from $\Delta H_{f\,298.15}°$ for B_2O_3(c) by adding $\Delta H_m°$ and the difference between $H°_{T_m} - H°_{298.15}$ for crystal and liquid.

Heat Capacity and Entropy.

The heat content ($H°_T - H°_{298.15}$) measurements on B_2O_3(glass) and B_2O_3(l) were determined, from [illegible] to [illegible]°K., by J. C. Southard, J. Am. Chem. Soc. 63, 3147 (1941) and, from 1015 to [illegible]°K., by R. M. Krasovitskaja, [illegible] Kantor, L. [illegible] Kon, V. V. Kandyba, L. M. Kutsyna and E. N. Fomichev, Russ. J. Phys. Chem. 35, 727 (1961). Based on these data the corresponding heat capacities (C_p) were derived. The C_p values thus obtained were plotted and joined smoothly, assuming a glass transition temperature at 550°K. The heat capacities above [illegible]°K. were estimated by graphical extrapolation. The entropy was obtained in a manner analogous to that of the heat of formation. The heat capacities of B_2O_3 glass and liquid have also been measured between 35 and 550°K with a radiation calorimeter by [illegible] Thomas and G. S. Parks, J. Phys. Chem. 35, 2091 (1931). The heat capacity curves obtained have been compared and discussed.

Melting Data.

See the B_2O_3(c) table.

Vaporization Data.

The boiling point (T_b) was calculated as the temperature at which the difference in $\Delta F_f°$ values for B_2O_3(g) and B_2O_3(l) becomes zero. The corresponding difference in $\Delta H_f°$ values at T_b is the heat of vaporization ($\Delta H_v°$).

B_2O_3

T, °K.	cal. mole^{-1}deg.$^{-1}$ C_p°	S°	$-(F^\circ-H^\circ_{298})/T$	kcal. mole^{-1} $H^\circ-H^\circ_{298}$	ΔH_f°	ΔF_f°	Log K_p
0	.000	.000	INFINITE	- 2.077	- 27.200	- 27.200	INFINITE
100	6.956	39.613	53.401	- 1.379	- 26.876	- 28.741	62.809
200	6.957	44.435	47.451	- .683	- 26.599	- 30.718	33.566
298	6.965	47.214	47.214	.000	- 26.417	- 32.783	24.029
300	6.965	47.267	47.214	.013	- 26.414	- 32.823	23.910
400	7.013	49.765	47.488	.711	- 26.318	- 34.975	19.109
500	7.121	50.841	48.006	1.417	- 26.296	- 37.144	16.235
600	7.278	52.152	48.491	2.137	- 26.332	- 39.311	14.318
700	7.450	53.287	49.182	2.873	- 26.400	- 41.468	12.946
800	7.624	54.291	49.759	3.627	- 26.514	- 43.612	11.914
900	7.786	55.200	50.314	4.397	- 26.637	- 45.744	11.108
1000	7.931	56.028	50.845	5.183	- 26.771	- 47.859	10.459
1100	8.057	56.790	51.351	5.983	- 26.914	- 49.962	9.926
1200	8.168	57.496	51.834	6.794	- 27.062	- 52.049	9.479
1300	8.263	58.154	52.295	7.618	- 27.218	- 54.126	9.099
1400	8.346	58.769	52.736	8.446	- 27.378	- 56.189	8.771
1500	8.417	59.348	53.158	9.285	- 27.537	- 58.241	8.485
1600	8.480	59.893	53.562	10.130	- 27.700	- 60.284	8.234
1700	8.535	60.409	53.950	10.980	- 27.865	- 62.315	8.011
1800	8.583	60.898	54.322	11.836	- 28.032	- 64.337	7.811
1900	8.626	61.361	54.681	12.697	- 28.201	- 66.349	7.631
2000	8.664	61.807	55.026	13.561	- 28.372	- 68.353	7.469
2100	8.698	62.230	55.359	14.430	- 28.544	- 70.346	7.321
2200	8.728	62.635	55.680	15.301	- 28.719	- 72.335	7.185
2300	8.756	63.024	55.991	16.175	- 28.894	- 74.311	7.061
2400	8.781	63.397	56.292	17.052	- 29.074	- 76.282	6.946
2500	8.804	63.756	56.584	17.931	- 29.254	- 78.247	6.840
2600	8.825	64.102	56.866	18.813	- 29.438	- 80.202	6.741
2700	8.844	64.435	57.140	19.696	- 29.623	- 82.153	6.649
2800	8.863	64.757	57.407	20.582	- 29.810	- 84.093	6.563
2900	8.879	65.069	57.666	21.469	- 30.001	- 86.028	6.483
3000	8.895	65.370	57.917	22.357	- 30.194	- 87.957	6.407
3100	8.910	65.662	58.163	23.248	- 30.388	- 89.878	6.336
3200	8.924	65.945	58.401	24.139	- 30.586	- 91.795	6.269
3300	8.937	66.220	58.634	25.032	- 30.786	- 93.707	6.206
3400	8.949	66.487	58.861	25.927	- 30.988	- 95.609	6.145
3500	8.961	66.746	59.083	26.822	- 31.192	- 97.509	6.088
3600	8.973	66.999	59.299	27.719	- 31.399	- 99.400	6.034
3700	8.984	67.245	59.511	28.617	- 31.608	- 101.286	5.982
3800	8.994	67.485	59.717	29.516	- 31.818	- 103.164	5.933
3900	9.004	67.718	59.919	30.416	- 32.031	- 105.039	5.886
4000	9.014	67.946	60.117	31.316	- 32.247	- 106.908	5.841
4100	9.024	68.169	60.311	32.218	- 32.464	- 108.774	5.798
4200	9.033	68.387	60.501	33.121	- 32.684	- 110.630	5.756
4300	9.042	68.599	60.687	34.025	- 32.906	- 112.483	5.717
4400	9.051	68.807	60.869	34.930	- 33.130	- 114.333	5.679
4500	9.059	69.011	61.047	35.835	- 33.356	- 116.177	5.642
4600	9.068	69.210	61.223	36.741	- 33.584	- 118.012	5.607
4700	9.076	69.405	61.395	37.649	- 33.814	- 119.845	5.573
4800	9.084	69.596	61.564	38.557	- 34.046	- 121.672	5.540
4900	9.092	69.784	61.729	39.465	- 34.280	- 123.497	5.508
5000	9.100	69.967	61.892	40.375	- 34.516	- 125.315	5.477
5100	9.107	70.148	62.052	41.285	- 34.755	- 127.132	5.448
5200	9.115	70.325	62.210	42.196	- 34.995	- 128.941	5.419
5300	9.123	70.498	62.365	43.108	- 35.237	- 130.741	5.391
5400	9.130	70.669	62.517	44.021	- 35.480	- 132.542	5.364
5500	9.138	70.836	62.667	44.934	- 35.727	- 134.336	5.338
5600	9.145	71.001	62.814	45.849	- 35.974	- 136.129	5.312
5700	9.153	71.163	62.959	46.763	- 36.225	- 137.919	5.288
5800	9.160	71.322	63.102	47.679	- 36.476	- 139.698	5.264
5900	9.167	71.479	63.242	48.595	- 36.730	- 141.473	5.240
6000	9.175	71.633	63.381	49.513	- 36.985	- 143.249	5.218

March 31, 1961

CARBON MONOXIDE (CO) (IDEAL GAS) MOL. WT. = 28.011

D_0° = 255.76 ± 0.43 kcal. mole^{-1} $\Delta H_{f\ 298.15}^\circ$ = -26.4165 ± 0.62 kcal. mole^{-1}

Ground State Configuration $^1\Sigma^+$ $S_{298.15}^\circ$ = 47.21 ± 0.01 cal. deg.$^{-1}$ mole^{-1}

ω_e = 2169.52 cm.$^{-1}$ $\omega_e x_e$ = 13.453 cm.$^{-1}$ D_e = 6.43 X 10^{-6} cm.$^{-1}$

B_e = 1.9302 cm.$^{-1}$ α_e = 0.01746 cm.$^{-1}$ r_e = 1.1281 Å σ = 1

Heats of Formation

The value given for the heat of combustion, equation I, by F. D. Rossini, J. Research Nat. Bur. Standards 22, 407 (1939) was changed to account for the presently accepted molecular weight of CO_2. The heat of formation is obtained by means of the following cycle:

I $CO_{(g)} + 1/2\ O_{2(g)} = CO_{2(g)}$ -67.6365 kcal. mole^{-1}

II $C_{(c)} + O_{2(g)} = CO_{2(g)}$ -94.0540 kcal. mole^{-1}

For details of equation II see $CO_{2(g)}$ sheet.

Heat Capacities and Entropies

Using the spectroscopic constants listed by G. Herzberg, Diatomic Molecules, D. Van Nostrand, New York, 1950, J. Belzer, L. G. Savedoff and H. L. Johnston, Ohio State Univ. Res. Found. Proj. 516, report no. 6, 1953, calculated the thermodynamic functions for $C^{12}O^{16}$. The spectroscopic constants listed above are for the naturally occurring isotopic composition given by D. Strominger, J. M. Hollander and G. T. Seaborg, Rev. Mod. Phys. 30, 585 (1958).

The dissociation energy had been selected by L. Brewer and A. W. Searcy, Ann. Rev. Phys. Chem. 7, 259 (1959). Belzer et al used a lower value for the dissociation energy in their calculations. However, their summations converge rapidly and this introduces no sensible error in the functions.

T, °K.	cal. mole⁻¹ deg.⁻¹ C_p°	S°	$-(F^\circ-H^\circ_{298})/T$	kcal. mole⁻¹ $H^\circ-H^\circ_{298}$	ΔH_f°	ΔF_f°	Log K_p
0	.000	.000	INFINITE	-2.239	-93.965	-93.965	INFINITE
100	6.981	42.758	58.188	-1.543	-93.907	-94.100	205.665
200	7.734	47.769	51.940	-.816	-94.028	-94.101	102.972
298	8.874	51.072	51.072	.000	-94.254	-94.765	69.095
300	8.896	51.127	51.072	.018	-94.255	-94.767	68.670
400	9.877	53.830	51.434	.948	-94.270	-94.335	51.540
500	10.668	56.122	52.148	1.987	-94.091	-94.399	41.260
600	11.310	58.126	52.981	3.087	-94.124	-94.458	34.405
700	11.846	59.910	53.865	4.249	-94.169	-94.510	29.506
800	12.293	61.522	54.706	5.469	-94.218	-94.556	25.830
900	12.667	62.992	55.486	6.732	-94.270	-94.596	22.970
1000	12.980	64.344	56.199	7.984	-94.321	-94.628	20.680
1100	13.243	65.594	57.143	9.208	-94.371	-94.658	18.806
1200	13.466	66.756	57.836	10.612	-94.419	-94.681	17.249
1300	13.656	67.841	58.620	11.988	-94.469	-94.701	15.920
1400	13.815	68.859	59.315	13.362	-94.515	-94.716	14.785
1500	13.953	69.817	59.984	14.740	-94.562	-94.728	13.801
1600	14.074	70.722	60.627	16.152	-94.607	-94.739	12.940
1700	14.177	71.578	61.246	17.565	-94.650	-94.746	12.180
1800	14.269	72.391	61.843	18.987	-94.694	-94.750	11.504
1900	14.352	73.165	62.418	20.418	-94.742	-94.751	10.898
2000	14.426	73.901	62.974	21.847	-94.789	-94.752	10.353
2100	14.489	74.608	63.512	23.303	-94.834	-94.746	9.860
2200	14.547	75.284	64.031	24.749	-94.885	-94.744	9.411
2300	14.600	75.931	64.535	26.212	-94.936	-94.735	9.001
2400	14.648	76.554	65.023	27.674	-94.991	-94.724	8.625
2500	14.692	77.153	65.496	29.141	-95.048	-94.714	8.280
2600	14.734	77.730	65.956	30.613	-95.107	-94.698	7.960
2700	14.771	78.286	66.402	32.088	-95.170	-94.683	7.654
2800	14.807	78.824	66.836	33.567	-95.234	-94.662	7.388
2900	14.841	79.344	67.258	35.049	-95.305	-94.639	7.132
3000	14.873	79.848	67.670	36.535	-95.377	-94.615	6.892
3100	14.902	80.336	68.071	38.024	-95.451	-94.587	6.668
3200	14.930	80.810	68.461	39.515	-95.530	-94.560	6.458
3300	14.956	81.270	68.843	41.010	-95.611	-94.531	6.260
3400	14.982	81.717	69.215	42.507	-95.696	-94.495	6.074
3500	15.006	82.151	69.578	44.004	-95.784	-94.462	5.898
3600	15.030	82.574	69.933	45.508	-95.874	-94.421	5.732
3700	15.053	82.986	70.280	47.012	-95.968	-94.379	5.574
3800	15.075	83.388	70.620	48.518	-96.064	-94.331	5.425
3900	15.097	83.780	70.953	50.027	-96.162	-94.285	5.283
4000	15.119	84.162	71.278	51.538	-96.261	-94.237	5.149
4100	15.139	84.536	71.597	53.051	-96.367	-94.186	5.020
4200	15.159	84.901	71.909	54.566	-96.473	-94.130	4.898
4300	15.179	85.258	72.216	56.082	-96.583	-94.072	4.781
4400	15.197	85.607	72.516	57.601	-96.694	-94.015	4.670
4500	15.216	85.950	72.811	59.122	-96.807	-93.954	4.563
4600	15.234	86.286	73.100	60.644	-96.923	-93.885	4.460
4700	15.254	86.611	73.384	62.169	-97.040	-93.818	4.362
4800	15.272	86.933	73.663	63.695	-97.160	-93.748	4.268
4900	15.290	87.248	73.937	65.223	-97.281	-93.673	4.178
5000	15.308	87.557	74.206	66.753	-97.404	-93.603	4.091
5100	15.327	87.860	74.471	68.284	-97.530	-93.528	4.008
5200	15.349	88.158	74.731	69.819	-97.656	-93.450	3.927
5300	15.371	88.451	74.988	71.355	-97.784	-93.361	3.850
5400	15.393	88.738	75.239	72.893	-97.912	-93.280	3.775
5500	15.415	89.021	75.488	74.433	-98.042	-93.190	3.703
5600	15.437	89.299	75.732	75.976	-98.173	-93.104	3.633
5700	15.459	89.572	75.972	77.521	-98.305	-93.017	3.566
5800	15.481	89.841	76.209	79.068	-98.438	-92.918	3.501
5900	15.503	90.106	76.442	80.617	-98.572	-92.820	3.438
6000	15.525	90.367	76.672	82.168	-98.707	-92.724	3.377

March 31, 1961

CARBON DIOXIDE (CO_2) (IDEAL GAS) MOL. WT. = 44.011

$\Delta H_f^\circ_0 = -93.966 \pm 0.03$ kcal. mole^{-1} $\Delta H_f^\circ_{298.15} = -94.0540 \pm 0.03$ kcal. mole^{-1}

Point Group $D_{\infty h}$ $S^\circ_{298.15} = 51.07 \pm 0.01$ cal. deg.$^{-1}$ mole^{-1}

Vibrational Levels and Multiplicities

ω, cm.$^{-1}$	
1342.94	(1)
667.3	(2)
2349.30	(1)

Bond Lengths r = C-O = 1.226 Å

Moments of Inertia $I_A = I_B = 7.1517 \times 10^{-39}$ g. cm.^{2} $I_C = 0$ $\sigma = 2$

Heats of Formation

The value selected by E. J. Prosen, R. S. Jessup and F. D. Rossini, J. Research Natl. Bur. Standards 33, 447 (1944) was corrected for the change in the molecular weight of CO_2.

Heat Capacities and Entropies

H. W. Woolley, J. Research Nat. Bur. Standards 52, 289 1954) calculated the thermodynamic functions by means of a direct summation for the naturally occurring isotopic composition. The spectroscopic constants used are essentially those selected by T. Wentink, Jr., J. Chem. Phys. 30, 109 (1959). A slightly different set of constants was obtained by C. P. Courtoy, Mem. soc. roy. Liege 18, 496 (1957).

T, °K.	C_p° (cal. mole^{-1}deg.$^{-1}$)	S° (cal. mole^{-1}deg.$^{-1}$)	$-(H^\circ-H^\circ_{298})/T$ (cal. mole^{-1}deg.$^{-1}$)	$H^\circ-H^\circ_{298}$ (kcal. mole^{-1})	ΔH_f° (kcal. mole^{-1})	ΔF_f° (kcal. mole^{-1})	Log K_p
0	.000	.000	INFINITE	- 1.235	-142.702	-142.702	INFINITE
100	1.965	.808	1.484	- 1.188	-143.156	-140.918	307.961
200	6.780	3.369	3.184	- .763	-143.559	-138.501	151.340
298	8.906	6.439	6.439	.000	-143.700	-135.981	99.672
300	8.939	6.496	6.439	.017	-143.701	-135.933	99.022
400	10.148	9.252	6.807	.978	-143.705	-133.340	72.850
500	10.854	11.598	7.517	2.031	-143.654	-130.755	57.150
600	11.323	13.621	8.386	3.141	-143.581	-128.181	46.688
700	11.656	15.393	9.283	4.291	-143.513	-125.619	39.218
800	11.905	16.966	10.132	5.469	-143.457	-123.067	33.619
900	12.098	18.380	10.969	6.670	-143.425	-120.521	29.265
1000	12.251	19.663	11.775	7.888	-145.541	-117.790	25.744
1100	12.375	20.837	12.546	9.119	-145.529	-115.025	22.852
1200	12.478	21.918	13.283	10.362	-145.538	-112.252	20.443
1300	12.565	22.920	13.986	11.614	-145.567	-109.478	18.404
1400	12.638	23.854	14.659	12.874	-176.047	-106.235	16.583
1500	12.701	24.728	15.301	14.141	-175.712	-101.261	14.753
1600	12.756	25.550	15.916	15.414	-175.375	- 96.309	13.155
1700	12.804	26.325	16.505	16.692	-175.034	- 91.378	11.747
1800	12.845	27.058	17.071	17.975	-174.693	- 86.467	10.498
1900	12.882	27.753	17.616	19.261	-174.351	- 81.574	9.383
2000	12.915	28.415	19.139	20.551	-174.008	- 76.699	8.381
2100	12.945	29.046	18.644	21.844	-173.665	- 71.844	7.477
2200	12.971	29.648	19.132	23.140	-173.321	- 67.004	6.656
2300	12.994	30.225	19.603	24.438	-172.979	- 62.178	5.908
2400	13.016	30.779	20.056	25.739	-172.636	- 57.368	5.224
2500	13.035	31.311	20.494	27.041	-172.295	- 52.572	4.596
2600	13.052	31.822	20.920	28.346	-171.955	- 47.790	4.017
2700	13.068	32.315	21.333	29.652	-171.616	- 43.018	3.482
2800	13.082	32.791	21.734	30.959	-171.280	- 38.264	2.986
2900	13.095	33.250	22.123	32.268	-170.945	- 33.518	2.526
3000	13.107	33.694	22.501	33.578	-170.613	- 28.785	2.097

December 31, 1960.

Magnesium Oxide (MgO) (Solid)

Mol. Wt. = 40.32

$\Delta H_{f\ 298.15}^\circ$ = -143.[illegible] ± 0.3 kcal. mole^{-1}

$S_{298.15}^\circ$ = 6.439 cal. deg.$^{-1}$ mole^{-1}

Data from National Bureau of Standards Report No. 6928, "Preliminary Report on the Thermodynamic Properties of Selected Light-Element Compounds", July, 1960.

T, °K	C_p°	S°	$-(F^\circ-H^\circ_{298})/T$	$H^\circ-H^\circ_{298}$	ΔH_f°	ΔF_f°	Log K_p
	←— cal. mole^{-1} deg^{-1}	—→		←— kcal. mole^{-1}		—→	
0							
100							
200							
298	7.400	7.200	7.200	.000	-41.000	-40.546	29.720
300	7.440	7.246	7.200	.014	-41.002	-40.543	29.534
400	9.500	9.666	7.519	.867	-41.106	-40.373	22.058
500	10.850	11.965	8.184	1.891	-41.151	-40.183	17.563
600	11.570	14.046	9.088	3.017	-41.172	-39.987	14.565
700	11.920	15.832	9.940	4.195	-41.204	-39.788	12.422
800	12.140	17.446	10.691	5.405	-41.253	-39.583	10.813
900	12.223	18.887	11.523	6.628	-41.332	-39.368	9.559
1000	12.360	20.184	12.325	7.859	-41.443	-39.145	8.555
1100	12.450	21.367	13.094	9.100	-41.579	-38.909	7.730
1200	12.543	22.454	13.829	10.349	-42.088	-38.623	7.034
1300	12.639	23.462	14.532	11.608	-42.865	-38.276	6.435
1400	12.738	24.402	15.204	12.877	-43.058	-37.917	5.919
1500	12.840	25.284	15.847	14.156	-43.263	-37.542	5.470
1600	12.896	26.115	16.463	15.443	-43.487	-37.153	5.075
1700	12.944	26.898	17.054	16.735	-43.715	-36.752	4.725
1800	12.998	27.640	17.621	18.033	-43.960	-36.335	4.411
1900	13.044	28.344	18.167	19.335	-44.219	-35.904	4.130
2000	13.087	29.014	18.693	20.641	-48.163	-35.366	3.864
2100	13.126	29.653	19.200	21.952	-48.384	-34.720	3.613
2200	13.162	30.265	19.689	23.266	-48.606	-34.063	3.384
2300	13.195	30.850	20.162	24.584	-53.429	-33.397	3.173
2400	13.226	31.413	20.619	25.905	-53.658	-32.523	2.961
2500	13.253	31.953	21.061	27.229	-53.884	-31.637	2.766
2600	13.273	32.473	21.490	28.555	-54.108	-30.745	2.584
2700	13.292	32.974	21.906	29.883	-54.330	-29.842	2.415
2800	13.309	33.459	22.310	31.213	-54.550	-28.930	2.258
2900	13.321	33.925	22.703	32.545	-54.768	-28.011	2.111
3000	13.335	34.377	23.085	33.877	-54.985	-27.083	1.973
3100	13.341	34.814	23.456	35.211	-55.202	-26.147	1.843
3200	13.353	35.238	23.918	36.545	-55.418	-25.210	1.722
3300	13.359	35.649	24.170	37.881	-55.632	-24.262	1.507
3400	13.368	36.048	24.519	39.217	-55.846	-23.311	1.498
3500	13.375	36.436	24.849	40.554	-56.059	-22.348	1.395
3600	13.382	36.812	25.176	41.892	-158.733	-19.640	1.210
3700	13.387	37.179	25.495	43.231	-158.964	-16.078	.950
3800	13.392	37.536	25.807	44.570	-159.209	-12.211	.702
3900	13.397	37.884	26.113	45.909	-159.468	-8.343	.468
4000	13.400	38.223	26.411	47.249	-280.879	-2.928	.160

$S^\circ_{298.15}$ = [7.2 ± [illegible]] cal. deg.$^{-1}$ mole^{-1}

T_d = (2500°K)

ΔH°_{d} = Unknown

$\Delta H^\circ_{f\ 298.15}$ = [illegible] ± [illegible] kcal. mole^{-1}

Heat of Formation.

P. O. Schissel and W. [illegible] Trulson [illegible] [illegible] (1962) determined the equilibrium vapor pressure [illegible] TiB [illegible] a mass spectrometer and obtained ΔH_{subl} ([illegible]°K) = [illegible] kcal. mole^{-1}. [illegible] ΔH°_f [illegible] = [illegible] ± [illegible] kcal. mole^{-1}, [illegible] kcal. mole^{-1} of the uncertainty is due to the heat of [illegible] of boron. [illegible] is reduced to 298°K one obtains ΔH°_f = -41.0 ± 9.0 kcal. mole. This value implies [illegible] high stability for TiB and this is also indicated by the phase studies of H. Nowotny, P. Benesovsky, [illegible] and [illegible], Monatshefte fur Chemie, 92, 403 (1961).

Heat Capacity and Entropy.

The heat capacity from 298 to 1200°K was estimated from that of TiB_2 [illegible] difference [illegible] same as that between CrB and CrB_2 as determined by H. Mozaki, [illegible] Tillcox, [illegible] Barnes, and [illegible] (Paper presented at the International Symposium on Nuclear Materials, Vienna, [illegible]). Above [illegible] were extrapolated smoothly so as to reach 13.4 at 4000°K. The entropy was [illegible] by averaging the [illegible] obtained from two approaches. It was assumed that entropy changes are additive [illegible] the heat capacities [illegible] [illegible] per atom. The reactions $1/2\,TiB_2 + 1/2\,Ti \rightarrow TiB$ and $TiB_2 - B \rightarrow TiB$ [illegible] at [illegible] for TiB.

[illegible] Data.

The phase diagram given in, "The Metallurgy of the Rarer Metals - [illegible]" [illegible] and [illegible] McQuillan, Academic Press, New York ([illegible]) was used to estimate the [illegible] temperature. [illegible] shows the decomposition to TiB_2 and Ti_2B. However, Nowotny et al. [illegible] have shown [illegible] to be non-existent and so the decomposition products are not defined. [illegible] of TiB and TiB_2 [illegible]

T, °K.	C_p°	S°	$-(F^\circ-H^\circ_{298})/T$	$H^\circ-H^\circ_{298}$	ΔH_f°	ΔF_f°	Log K_p
	cal. mole⁻¹ deg.⁻¹			kcal. mole⁻¹			
0							
100							
200							
298	[illegible]	[illegible]	[illegible]	[illegible]	-7[illegible]	-68.0[illegible]	50.[illegible]
300	10.740	[illegible]	[illegible]	.03[illegible]	-[illegible]	-68.945	50.22[illegible]
400	[illegible]	[illegible]	7.0[illegible]	[illegible]	-[illegible]	-68.[illegible]	37.46[illegible]
500	[illegible]	[illegible]	[illegible]	[illegible]	-[illegible].154	-58.195	29.90[illegible]
600	15.890	[illegible]	[illegible]	[illegible]	-74.218	-57.793	24.6[illegible]
700	[illegible].72[illegible]	19.[illegible]	[illegible].B[illegible]	5.9[illegible]	-[illegible].346	-67.376	[illegible]
800	17.445	2[illegible]	[illegible]	7.[illegible]	-70.445	-66.945	18.280
900	[illegible]	2[illegible]	[illegible]	[illegible]	-[illegible]	-6[illegible]	16.[illegible]48
1000	[illegible].595	2[illegible].8[illegible]	1[illegible]	[illegible]	-[illegible].059	-66.044	14.[illegible]
1100	[illegible]	2[illegible].5[illegible]	14.6[illegible]	[illegible].0[illegible]8	-[illegible].774	-55.577	13.028
1200	[illegible].61[illegible]	21.[illegible]49	15.905	1[illegible].04[illegible]	-71.837	-65.06[illegible]	11.8[illegible]
1300	2[illegible].[illegible]59	29.946	16.97[illegible]	[illegible].329	-71.948	-64.473	1[illegible]
1400	2[illegible].477	[illegible]	17.109	18.[illegible]	-72.0[illegible]	-63.316	[illegible].477
1500	22.830	[illegible].874	18.359	[illegible]	-72.[illegible]	-63.331	9.[illegible]
1600	2[illegible].289	[illegible].235	1[illegible]	2[illegible].132	-7[illegible].247	-62.74[illegible]	8.5[illegible]
1700	[illegible].675	35.537	2[illegible]	25.28[illegible]	-72.328	-62.144	7.999
1800	[illegible]	3[illegible].787	[illegible].529	[illegible]	-72.397	-61.5[illegible]	7.[illegible]
1900	[illegible].405	37.[illegible]89	22.3[illegible]	[illegible].089	-72.4[illegible]5	-5[illegible].938	7.[illegible]
2000	22.75[illegible]	33.147	[illegible]	31.9[illegible]	-76.172	-5[illegible].237	6.582
2100	[illegible]	[illegible].28[illegible]	2[illegible]	[illegible]	-75.144	-59.44[illegible]	6.13[illegible]
2200	[illegible]	[illegible].247	[illegible].725	[illegible]	-76.[illegible]	-58.6[illegible]	5.82[illegible]
2300	[illegible].759	[illegible].196	2[illegible]	[illegible]	-85.212	-57.853	5.[illegible]
2400	[illegible].083	[illegible]	25.169	[illegible]	-85.12[illegible]	-56.658	5.[illegible]
2500	[illegible]	[illegible]	[illegible]	[illegible]	-8[illegible].[illegible]6	-55.48[illegible]	4.85[illegible]
2600	[illegible]	4[illegible]	[illegible]	[illegible]	-84.840	-54.31[illegible]	4.565
2700	[illegible]	[illegible].705	29.[illegible]	[illegible]	-84.6[illegible]	-53.129	[illegible]
2800	[illegible]	[illegible].20	23.9[illegible]	[illegible]	-84.437	-51.9[illegible]	4.[illegible]57
2900	[illegible].605	[illegible].113	2[illegible]	[illegible]	-84.[illegible]	-5[illegible].819	3.63[illegible]
3000	[illegible].892	[illegible]	[illegible]	[illegible]	-83.916	-49.659	3.[illegible]18
3100	[illegible]	[illegible]	3[illegible]	[illegible]	-8[illegible]	-48.530	3.[illegible]
3200	[illegible]	[illegible].575	[illegible].419	[illegible]	-8[illegible].282	-47.[illegible]7	3.[illegible]
3300	[illegible]	[illegible].[illegible]93	[illegible]	[illegible]	-82.[illegible]25	-46.29[illegible]	3.[illegible]
3400	2[illegible].971	[illegible]	[illegible]	[illegible]	-82.5[illegible]	-45.192	2.[illegible]
3500	2[illegible].225	[illegible].680	[illegible]	[illegible]	-82.[illegible]1	-44.095	2.753
3600	[illegible]	[illegible].850	[illegible]	[illegible]	-184.[illegible]58	-41.5[illegible]	2.52[illegible]
3700	[illegible]	[illegible]	[illegible]	[illegible]	-183.[illegible]18	-37.6[illegible]	[illegible]
3800	2[illegible].9[illegible]	[illegible]	34.8[illegible]3	[illegible]	-18[illegible]	-33.6[illegible]	[illegible].[illegible]36
3900	[illegible].1[illegible]8	5[illegible]	35.[illegible]	[illegible]	-18[illegible].0[illegible]	-29.7[illegible]	1.66[illegible]
4000	23.40[illegible]	[illegible]	[illegible]	[illegible]	-[illegible]24.624	-2[illegible].7[illegible]	1.243

Titanium Diboride (TiB_2)

Mol. wt. = 69.5[illegible]

$\Delta H^\circ_{f\,298.15}$ = -7[illegible] ± [illegible] kcal. mole⁻¹

$S^\circ_{298.15}$ = [6.6 ± 0.5] cal. deg.⁻¹ mole⁻¹

T_m = 3193°K.

ΔH_m = [[illegible] ± 3] kcal. mole⁻¹

Heat of Formation. The only combustion reported was by V. A. Epel'baum and [illegible] Fomenko, [illegible] Khim. Bora i Ego Soedinenii p. 97 (1958), published (1958). This gives a heat of formation of [illegible] ± [illegible] kcal. mole⁻¹. The only other calorimetric determination was that of [illegible] and W. S. Williams, Rev. Sci. Instr. 32, 1120 (1961). This was a direct reaction calorimeter and gave ΔH_f° = -[illegible] ± 5 kcal. mole⁻¹. W. S. Williams, J. Phys. Chem. 65, 2213 (1961) gives an excellent evaluation of the reported heats of formation and shows them to be based on erroneous data. Williams also thoroughly studied the reaction $TiN + 2BN \rightarrow TiB_2 + 3/2N_2$ and determined that the free energy change was zero at 2150°K. When this value is reduced to 298°, one obtains $\Delta H^\circ_{f\,298}$ = -73.6 ± 4.5 kcal. mole⁻¹.

P. O. Schissel and C. Trulson, J. Phys. Chem. 66, 1492 (1962) investigated the decomposition vapor pressure using a mass spectrometer. When their values are recalculated using the present free energy functions for TiB_2 one obtains an average $\Delta H^\circ_{f\,298}$ = -[illegible].2 ± [illegible] with an additional uncertainty of ± [illegible] kcal. mole⁻¹ due to the very real uncertainty in ΔH_{sub} of boron, and ± 1 kcal. mole⁻¹ due to the uncertainty in the entropy of TiB_2.

A plot of their data indicates that the data taken in the presence of [illegible] does not fit with the data for TiB_2 alone and TiB_2 + Ti. This indicates that the pressure of B [illegible] was incorrect. A value of $\Delta H_{[illegible]\,298}B$ = 12[illegible] would bring these points into agreement and would [illegible] ΔH°_f TiB_2 = -[illegible].4 ± [illegible] kcal. mole⁻¹. M. J. Linevsky, pvt. comm., General Electric Company has calculated ΔH°_f [illegible] = -[illegible] ± [illegible] kcal. mole⁻¹ using resonance line absorption. Using the present functions this corresponds to $\Delta H^\circ_{f\,298}$ = -6[illegible] ± 3.5 kcal. mole⁻¹.

We adopt a value of -[illegible].0 ± [illegible] kcal. mole⁻¹ because the equilibrium work of Williams would indicate this as the least negative value, while the vapor pressure data would fit if the heat of sublimation of boron was ~ 1[illegible] kcal. mole⁻¹, a very real possibility.

Heat Capacity and Entropy. The heat capacity has been measured by [illegible] and N. S. [illegible], Sbornik Nauch. Trudov. Moskov Inst. Tsvetnoi Metal i Zolota No. [illegible], 42[illegible] ([illegible]) [illegible] at 1100°K. E. F. Walker, [illegible] T. Ewing, and R. R. Miller, J. Phys. Chem. 61, 1682 (19[illegible]) and R. Mezaki, [illegible] Thesis, Univ. of Wisconsin (1961) have also covered the same range. H. Prophet, private communication, Dow Chemical Co. (1962) has measured the heat capacity from 1300°K to 2[illegible]°K. A smooth curve was drawn through [illegible] and extrapolated [illegible] above 2150°K. The entropy was estimated from the entropy of zirconium diboride [illegible] measured by E. F. Westrum and [illegible] Feick, Technical Documentary Rept No. ASD-TDR-62-204 Part I, April, [illegible] Armed Services Tech. Info. Agency AD 27[illegible].

Melting. The melting point was measured by B. Post, F. Glaser, and D. [illegible], Acta. Met. 2, [illegible] (19[illegible]). The value of 3203 ± 60°K by G. V. Samsonov and G. V. Petrosn, Metalloved [illegible] Metallov, No. [illegible], 19 (1956) is in good agreement. The heat of melting was estimated from the heat of melting of the elements.

T, °K.	C_p°	S°	$-(G^\circ-H^\circ_{298})/T$	$H^\circ-H^\circ_{298}$	ΔH_f°	ΔG_f°	Log K_p
	cal. mole⁻¹ deg⁻¹			kcal. mole⁻¹			
0	.000	.000	INFINITE	-1.[illegible]	-44.2[illegible]	-44.[illegible]	INFINITE
100	1.791	.[illegible]	11.[illegible]	-1.[illegible]	-44.[illegible]	-44.147	96.470
200	[illegible]	[illegible]	[illegible]	-.[illegible]01	-44.[illegible]	-43.821	47.[illegible]
298	8.11[illegible]	[illegible]	[illegible]	[illegible]	-44.[illegible]	-43.[illegible]	31.987
300	8.145	5.852	5.832	.015	-44.[illegible]	-43.636	31.786
400	9.[illegible]	8.410	6.141	.911	-44.4[illegible]	-43.[illegible]	23.[illegible]
500	10.609	[illegible]	[illegible]	1.9[illegible]	-44.421	-4[illegible]	18.92[illegible]
600	11.[illegible]	12.678	7.[illegible]	3.022	-44.378	-42.[illegible]	15.[illegible]
700	11.[illegible]	14.449	8.409	4.172	-44.[illegible]	-42.[illegible]	13.294
800	12.[illegible]	16.036	9.[illegible]	5.[illegible]	-44.[illegible]	-42.204	11.[illegible]
900	12.294	17.470	10.[illegible]	6.578	-44.[illegible]	-42.061	10.[illegible]
1000	12.444	18.77[illegible]	10.958	7.9[illegible]	-44.[illegible]	-41.787	9.1[illegible]
1100	12.[illegible]	19.966	11.72[illegible]	9.[illegible]	-44.[illegible]	-41.[illegible]	8.[illegible]
1200	12.[illegible]	21.06[illegible]	12.[illegible]	10.[illegible]	-45.[illegible]	-41.217	7.510
1300	12.[illegible]	[illegible].077	13.158	11.506	-45.408	-40.[illegible]	6.876
1400	12.[illegible]	[illegible]	13.[illegible]	12.[illegible]	-45.[illegible]	-40.541	[illegible]
1500	12.[illegible]	[illegible].991	14.[illegible]	14.[illegible]	-45.[illegible]	-40.19[illegible]	[illegible]
1600	12.[illegible]	24.709	[illegible]	15.[illegible]	-45.[illegible]	-39.921	5.[illegible]
1700	12.[illegible]	25.478	15.[illegible]	16.[illegible]	-45.[illegible]	-39.452	5.[illegible]
1800	12.690	26.[illegible]	1[illegible].239	17.[illegible]	-45.[illegible]	-39.[illegible]	4.[illegible]44
1900	12.[illegible]	[illegible].999	[illegible]	19.[illegible]	-4[illegible].110	-38.684	4.450
2000	12.[illegible]	[illegible]	[illegible]	[illegible]	-49.0[illegible]	-38.197	4.174
2100	12.[illegible]	28.157	17.[illegible]	21.[illegible]	-4[illegible].080	-37.[illegible]	[illegible]
2200	12.[illegible]	28.747	18.790	23.[illegible]	-[illegible]	-37.0[illegible]	[illegible]
2300	12.[illegible]	30.311	18.[illegible]	24.[illegible]	-[illegible].327	-3[illegible]	[illegible]
2400	12.[illegible]	[illegible]	19.208	25.542	-[illegible].454	-35.795	[illegible]
2500	12.[illegible]	[illegible]	19.[illegible]	[illegible]	-[illegible]	-35.182	[illegible]
2600	12.[illegible]	[illegible]	20.0[illegible]	29.[illegible]	-[illegible]	-34.[illegible]	2.925
2700	12.[illegible]	[illegible]	[illegible]	30.[illegible]	-[illegible]	-33.063	2.747
2800	12.[illegible]	31.[illegible]	20.[illegible]	[illegible]	-50.0[illegible]	-33.[illegible]	2.[illegible]
2900	12.[illegible]	32.2[illegible]	21.[illegible]	31.892	-51.116	-3[illegible]	2.[illegible]
3000	12.[illegible]	[illegible]	[illegible]	33.169	-51.251	-32.[illegible]42	2.[illegible]
3100	12.[illegible]	33.[illegible]	21.[illegible]	34.[illegible]	-51.380	-31.[illegible]	2.21[illegible]
3200	12.[illegible]	33.409	22.[illegible]	35.[illegible]	-51.520	-30.751	2.1[illegible]
3300	12.[illegible]	33.988	22.600	36.[illegible]	-51.671	-3[illegible].009	1.99[illegible]
3400	12.690	34.267	23.025	38.[illegible]	-51.[illegible]	-29.445	1.[illegible]03
3500	12.68[illegible]	34.[illegible]	23.[illegible]	40.[illegible]	-51.050	-29.785	1.797
3600	12.690	34.99[illegible]	23.[illegible]	[illegible]	-154.567	-[illegible]	1.[illegible]
3700	12.680	[illegible]	2[illegible].08[illegible]	42.[illegible]	-154.735	-21.127	1.[illegible]
3800	12.[illegible]	[illegible]	[illegible]	4[illegible].204	-154.918	-19.558	1.125
3900	12.[illegible]	[illegible]	24.[illegible]	44.562	-155.117	-1[illegible].005	.8[illegible]
4000	12.680	[illegible]	24.[illegible]	45.[illegible]	-15[illegible].320	-12.429	.[illegible]79
4100	12.690	[illegible].641	25.[illegible]	47.[illegible]	-155.[illegible]	-9.054	.[illegible]
4200	12.680	[illegible]	[illegible]	4[illegible]	-155.[illegible]	-5.[illegible]	.[illegible]
4300	12.680	37.244	[illegible]	[illegible]	-15[illegible]	-1.696	.[illegible]
4400	12.[illegible]	37.536	[illegible]	[illegible]	-15[illegible].110	1.[illegible]	-.[illegible]
4500	12.[illegible]	37.821	[illegible]	[illegible]	-15[illegible]	[illegible]	-.[illegible]
4600	12.[illegible]	38.130	2[illegible]	[illegible]	-15[illegible].091	[illegible].114	-.[illegible]
4700	12.[illegible]	38.[illegible]	[illegible]	[illegible]	-157.105	12.774	-.[illegible]
4800	12.[illegible]	38.[illegible]	[illegible]	[illegible]	-157.511	1[illegible]	-.744
4900	12.[illegible]	[illegible]	27.[illegible]	57.242	-157.837	1[illegible].069	-.[illegible]
5000	12.[illegible]	39.157	27.[illegible]	[illegible].513	-158.173	23.402	-1.0[illegible]
5100	12.680	39.[illegible]	2[illegible]	[illegible]	-158.521	27.2[illegible]	-1.1[illegible]
5200	12.[illegible]	39.654	27.91[illegible]	[illegible]	-15[illegible].877	[illegible]	-1.298
5300	12.680	39.[illegible]	28.133	62.[illegible]	-1[illegible].242	[illegible].542	-1.424
5400	12.[illegible]80	40.113	28.359	63.[illegible]	-1[illegible].616	38.202	-1.5[illegible]
5500	12.[illegible]	40.[illegible]	28.[illegible]	64.85[illegible]	-1[illegible].000	41.[illegible]	-1.[illegible]
5600	12.[illegible]	40.594	2[illegible]	[illegible].118	-1[illegible].380	[illegible].560	-1.7[illegible]
5700	12.690	40.819	2[illegible]	[illegible]	-1[illegible].787	49.212	-1.[illegible]
5800	12.690	41.[illegible]	29.2[illegible]	[illegible]	-161.192	52.903	-1.993
5900	12.[illegible]80	41.256	29.[illegible]	[illegible]	-161.[illegible]	[illegible]	-2.097
6000	12.[illegible]80	41.469	29.[illegible]	[illegible]	-162.020	[illegible]	-2.19[illegible]

$S^\circ_{298.15}$ = [illegible].8 ± 0.1 cal. deg.⁻¹ mole⁻¹

T_m = [illegible] °K.

ΔH_f° [illegible] kcal. mole⁻¹

ΔH_f° [illegible] kcal. mole⁻¹

ΔH_m° = [illegible] kcal. mole⁻¹

Heat of Formation.

The heat of formation was selected [illegible] consideration of the following data.

Investigator	Method	ΔH_f° [illegible] kcal. mole⁻¹
[illegible][1]	Equilibrium pressure of Ti[illegible]	[illegible]
[illegible][2]	ΔH°_{298} = -183.[illegible]	[illegible]
[illegible][3]	ΔH°_{298} = [illegible]	[illegible]
[illegible][4]	[illegible] of Ti[illegible]	[illegible]
[illegible][5]	Direct reaction of the elements	[illegible]
	[illegible] =	-4[illegible].8

(1) [illegible] and M. [illegible], J. Phys. Chem. 6[illegible], [illegible] (19[illegible]). ΔH°_{298} = [illegible] kcal. mole⁻¹ [illegible] third law method yields $\Delta H^\circ_{f\,298}$ = [illegible] kcal. mole⁻¹.

(2) M. I. Morozova, M. K. [illegible], and [illegible], [illegible] ([illegible]).

(3) [illegible] L. Humphrey, J. Am. Chem. Soc. [illegible], [illegible] (1951).

(4) [illegible] L. [illegible], Missile and Space Vehicle Department, General Electric [illegible].

(5) [illegible] and [illegible] Williams, [illegible] Instr. [illegible], 112 [illegible].

[illegible] et al. point out that Humphrey's sample was [illegible] [illegible] at [illegible]°K. Humphrey's sample [illegible] part of the sample used [illegible] temperature [illegible] measurements, and his value of $\Delta H^\circ_{f\,298.15}$ = [illegible] kcal. mole⁻¹ was adopted.

Heat Capacity and Entropy.

[illegible] capacity data in the temperature range [illegible]° to [illegible]°K. were reported by [illegible], [illegible]. Heat content data from [illegible]° to [illegible]°K. were reported by [illegible], J. Am. Chem. Soc. [illegible] (19[illegible]). The tabulated values up to [illegible]°K. are the result of a [illegible] of the two sets of data. [illegible] data above [illegible]°K. [illegible] $H_T - H_{298}$ = [illegible] T [illegible] cal. mole⁻¹ deg.⁻¹ [illegible] S°_{298} [illegible] cal. deg.⁻¹ mole⁻¹.

Melting Data.

E. Friederich and L. Sittig, Z. Anorg. [illegible] Chem. [illegible], [illegible] (192[illegible]) and [illegible], Z. Anorg. Chem. [illegible], [illegible] (1951) reported T_m of TiC to be 34[illegible] ± 100°K. and [illegible] ± [illegible]°K. respectively. Recently, [illegible] L. [illegible], J. Phys. Chem. 6[illegible], [illegible] (1961) has reported a value of 34[illegible]°K. The average of these values was adopted. The heat of melting is derived from an estimated ΔS_m = 2.5 cal. deg.⁻¹ gm. atom⁻¹.

MONOTITANIUM MONONITRIDE (TiN) (Solid)

Mol. Wt. = 61.91

$\Delta H^\circ_{f\ 298.15} = -80.5 \pm 1.5$ kcal. mole^{-1}

$S^\circ_{298.15} = 7.193$ cal. deg.$^{-1}$ mole^{-1}

$T_m = 3200°K.$

$\Delta H_m = 16$ kcal. mole^{-1}

T, °K.	C_p°	S°	$-(F^\circ-H^\circ_{298})/T$	$H^\circ-H^\circ_{298}$	ΔH_f°	ΔF_f°	Log K_p
	cal. mole^{-1}deg.$^{-1}$			kcal. mole^{-1}			
0	.000	.000	INFINITE	- 1.311	- 79.625	- 79.625	INFINITE
100	2.572	1.020	14.368	- 1.235	- 80.029	- 78.028	170.521
200	6.531	4.107	7.940	- .767	- 80.367	- 75.879	82.913
298	8.966	7.193	7.193	.000	- 80.500	- 73.637	53.975
300	9.000	7.249	7.193	.017	- 80.501	- 73.595	53.611
400	10.430	10.854	7.566	.995	- 80.491	- 71.292	38.950
500	11.190	12.472	8.311	2.080	- 80.406	- 69.001	30.159
600	11.650	14.555	9.182	3.224	- 80.292	- 66.729	24.305
700	11.960	16.376	10.083	4.405	- 80.168	- 64.479	20.130
800	12.190	17.988	10.972	5.613	- 80.042	- 62.247	17.004
900	12.390	19.436	11.833	6.842	- 79.917	- 60.028	14.576
1000	12.550	20.750	12.660	8.089	- 79.798	- 57.826	12.637
1100	12.690	21.942	13.451	9.351	- 79.684	- 55.635	11.053
1200	12.830	23.062	14.206	10.627	- 80.524	- 53.416	9.728
1300	12.950	24.094	14.928	11.916	- 80.418	- 51.161	8.601
1400	13.070	25.058	15.617	13.217	- 80.318	- 48.915	7.636
1500	13.180	25.964	16.277	14.530	- 80.219	- 46.676	6.800
1600	13.290	26.818	16.910	15.854	- 80.125	- 44.441	6.070
1700	13.400	27.627	17.516	17.188	- 80.033	- 42.215	5.427
1800	13.510	28.396	18.100	18.534	- 79.942	- 39.993	4.856
1900	13.610	29.129	18.661	19.890	- 79.854	- 37.775	4.345
2000	13.710	29.830	19.202	21.256	- 83.441	- 35.469	3.876
2100	13.810	30.501	19.724	22.632	- 83.296	- 33.073	3.442
2200	13.910	31.146	20.229	24.018	- 83.143	- 30.686	3.048
2300	14.010	31.767	20.717	25.414	- 82.981	- 28.304	2.689
2400	14.110	32.365	21.190	26.820	- 82.810	- 25.931	2.361
2500	14.210	32.943	21.649	28.236	- 82.631	- 23.565	2.060
2600	14.310	33.502	22.094	29.662	- 82.443	- 21.207	1.783
2700	14.400	34.044	22.526	31.097	- 82.247	- 18.856	1.526
2800	14.500	34.569	22.947	32.542	- 82.042	- 16.510	1.289
2900	14.600	35.080	23.357	33.997	- 81.828	- 14.174	1.068
3000	14.690	35.576	23.756	35.462	- 81.605	- 11.845	.863
3100	14.790	36.060	24.145	36.936	- 81.374	- 9.521	.671
3200	14.880	36.531	24.525	38.419	- 81.134	- 7.211	.492
3300	14.980	36.990	24.896	39.912	- 80.885	- 4.901	.325
3400	15.070	37.439	25.258	41.415	- 80.626	- 2.606	.168
3500	15.170	37.877	25.612	42.927	- 80.360	- .315	.020
3600	15.260	38.306	25.959	44.449	-182.546	3.413	- .207
3700	15.360	38.725	26.298	45.980	-182.281	8.575	- .506
3800	15.450	39.136	26.631	47.520	-182.022	13.733	- .790

December 31, 1960.

Data from National Bureau of Standards Report No. 6928, "Preliminary Report on the Thermodynamic Properties of Selected Light-Element Compounds", July, 1960.

A P P E N D I X II

IBM 1130 Computer Programme for the determination of Specific Surfaces by the B.E.T. Method using least squares method to determine the intercept and slope of the isotherm.

```
TYPE  :
// JOB
LOG DRIVE   CART SPEC   CART AVAIL  PHY DRIVE
   0000        0AAA        0AAA        0000

V2 M06   ACTUAL  8K  CONFIG  8K

// FOR
*LIST SOURCE PROGRAM
*       ONE WORD INTEGERS
        SUBROUTINE PONI(SX,AN,SY,SXX,SXY,A,C)
C       SPECIFIC SURFACES BY B.E.T. METHOD   USING LEAST SQUARES METHOD TO
C       DETERMINE THE INTERCEPT AND SLOPE OF THE ISOTHERM
C       TO SOLVE TWO SIMULTANEOUS EQUATIONS IN TWO UNKNOWNS BY ELIMINATION
   12   FORMAT(/1X,'COEFFICIENTS'//(2F12.4))
   13   FORMAT(/1X,'CONSTANTS'//F12.4)
   14   FORMAT(/3X,'A=',F12.4,3X,'C=',F12.4)
   15   FORMAT(/1X,'CHECK'//2F10.4)
        WRITE(3,12)SX,AN,SXX
        WRITE(3,13)SY,SXY
C       MAKE COEFFICIENTS OF C UNITY
        SX1=SX/AN
        SXX1=SXX/SX
        SY1=SY/AN
        SXY1=SXY/SX
C       ELIMINATE C
        SX2=SX1-SXX1
        SY2=SY1-SXY1
C       CALCULATE A AND C
        A=SY2/SX2
        C=SY1-SX1*A
        WRITE(3,14)A,C
C       CHECK
        CH=SXX*A+SX*C
        WRITE(3,15)CH,SXY
        RETURN
        END

FEATURES SUPPORTED
 ONE WORD INTEGERS

CORE REQUIREMENTS FOR PONI
 COMMON       0  VARIABLES     16  PROGRAM     182

 END OF COMPILATION
```

```
PAGE    1
// JOB
LOG DRIVE   CART SPEC   CART AVAIL  PHY DRIVE
   0000         0AAA        0AAA        0000

V2 M05   ACTUAL  8K  CONFIG  8K

// FOR
*LIST SOURCE PROGRAM
*        ONE WORD INTEGERS
         SUBROUTINE PON1(SX,AN,SY,SXX,SXY,A,C)
C        SPECIFIC SURFACES BY B.E.T. METHOD   USING LEAST SQUARES METHOD TO
C        DETERMINE THE INTERCEPT AND SLOPE OF THE ISOTHERM
C        TO SOLVE TWO SIMULTANEOUS EQUATIONS IN TWO UNKNOWNS BY ELIMINATION
      12 FORMAT(/1X,'COEFFICIENTS'//(2F12.4))
      13 FORMAT(/1X,'CONSTANTS'//F12.4)
      14 FORMAT(/3X,'A=',F12.4,3X,'C=',F12.4)
      15 FORMAT(/1X,'CHECK'//2F10.4)
         WRITE(3,12)SX,AN,SXX
         WRITE(3,13)SY,SXY
C        MAKE COEFFICIENTS OF C UNITY
         SX1=SX/AN
         SXX1=SXX/SX
         SY1=SY/AN
         SXY1=SXY/SY
C        ELIMINATE C
         SX2=SX1-SXX1
         SY2=SY1-SXY1
C        CALCULATE A AND C
         A=SY2/SX2
         C=SY1-SX1*A
         WRITE(3,14)A,C
C        CHECK
         CH=SXX*A+SX*C
         WRITE(3,15)CH,SXY
         RETURN
         END

FEATURES SUPPORTED
 ONE WORD INTEGERS

CORE REQUIREMENTS FOR PON1
 COMMON       0  VARIABLES     16  PROGRAM     182

 END OF COMPILATION
```

```
PAGE    1

// JOB

LOG DRIVE    CART SPEC    CART AVAIL   PHY DRIVE
  0000          0AAA         0AAA         0000

V2 M06   ACTUAL  8K   CONFIG  8K

// FOR
*LIST SOURCE PROGRAM
*IOCS(DISK,CARD,1132 PRINTER,TYPEWRITER,KEYBOARD,PLOTTER)
*ONE WORD INTEGERS
C
C      G=WEIGHT NITROGEN ABSORBED. W=WEIGHT OF SAMPLE. AT=ATMOSPHERIC
C      PRESSURE. P=PRESSURE READ. GG=WEIGHT OF NITROGEN ABSORBED PER GRAM
C      OF SAMPLE PO=SATURATION VAPOUR PRESSURE
C
C
C      THIS PROGRAM PLOTS THE OBSERVATIONS FOR X AND Y AND ALSO THE
C      CALCULATED REGRESSION LINE  FOR EACH SET OF INPUT DATA
C
C      THE DATA IS READ IN THE FOLLOWING ORDER.
C      FIRST CARD    YMAX AND YMIN IN THAT ORDER IN FORMAT 2F8.0
C      SECOND CARD   N IN FORMAT I4
C      THIRD CARD AT AND W IN FORMAT F10.2 AND F12.4
C      THEN  READ G AND P ONE PAIR PER CARD IN FORMAT F12.5 AND F10.2
C      THESE CARDS CONSTITUTE A SET
C      THE FINAL CARD MUST BE BLANK
C
C
C
C
C
```

```
      DIMENSION X(10),Y(10)
    1 FORMAT(I4/F10.2,F12.4)
    2 FORMAT(1H1,'AT=',F10.2,'MM.HG. W=',F12.4,'GMS PO=',F10.2,'MMS.HG'
     1)
    3 FORMAT(F12.5,F10.2)
    4 FORMAT(5X,'X',10X,'Y'//(2F12.5))
  777 READ(2,100) YMAX,YMIN                                          IN 1
  100 FORMAT(2F8.0)                                                  IN 2
      READ(2,1)N,AT,W
      IF(N)9,9,6
    6 PO=2814.-(760.-AT)*3.
      WRITE(3,2)AT,W,PO
      DO 8 I=1,N
      READ(2,3)G,P
      GG=G/W
      Y(I)=P/(GG*(PO-P))
      X(I)=P/PO
      WRITE(3,4)X(I),Y(I)
    8 CONTINUE
C     X=P/PO AND Y=P/X(PO-P). SLOPE=A AND INTERCEPT=C
   21 FORMAT(/1X,'MONOLAYER CAPACITY IS',F9.6,'G.NITROGEN/G.SAMPLE')
   22 FORMAT(/1X,'SPECIFIC SURFACE IS',F10.3,'SQ.M./G.')
C     OBTAIN TWO EQUATIONS IN A AND C
      SX=0
      SY=0
      SXX=0
      SXY=0
      DO 23 K=1,N
      SX=SX+X(K)
      SY=SY+Y(K)
      SXX=SXX+X(K)**2
   23 SXY=SXY+X(K)*Y(K)
      AN=N
C     SOLVE EQUATIONS
      CALL PON1(SX,AN,SY,SXX,SXY,A,C)
      XM=1./(A+C)
      WRITE(3,21)XM
      S=XM*3650.0
      WRITE(3,22)S
      CALL SCFOR(1,8.,8.,1.,0)
      CALL SCFOR(3,0.,0.32,8.,0.)
      CALL SCFOR(4,YMIN,YMAX,8.,0.)
      DO 10 I=1,N
   10 CALL SCFOR(5,X(I),Y(I),235.,0)
```

```
PAGE   9

      IF(C-YMIN) 33,30,30
   30 TFD1=C0.
      TFD2=C0.
      FOFD1=0.32
      FOFD2=0.32*A+C
      IF(FOFD2-YMAX) 35,35,40
   40 TFD1=(YMAX-C)/A
      TFD2=YMAX
      GO TO 35
   33 TFD1=(YMIN-C)/A
      TFD2=YMIN
      FOFD1=(YMAX-C)/A
      FOFD2=YMAX
      IF(FOFD1-0.32) 35,35,45
   45 TFD1=0.32
      TFD2=0.32*A+C
   35 CALL SCFOR(5,TFD1,TFD2,224.,0)
      CALL SCFOR(5,FOFD1,FOFD2,224.,0)
      CALL SCFOR(6,TFD1,TFD2,FOFD1,FOFD2)
      XSC=1./0.32
      YSC=1./(YMAX-YMIN)
      CALL PCHAR(2.9/XSC,YMIN-0.6/YSC,0.1,0.1,0.)
      WRITE(7,900) A,C
  900 FORMAT('(Y = ',F7.2,' X + (',F7.2,'))')
      GO TO 777
    0 CALL EXIT
      END

FEATURES SUPPORTED
 ONE WORD INTEGERS
 IOCS

CORE REQUIREMENTS FOR
 COMMON       0  VARIABLES      96  PROGRAM     598

 END OF COMPILATION
```

A P P E N D I X III

Reprints of published papers:-

Formation and Reactivity of Borides, Carbides and Silicides

I. Review and Introduction

II. Production and sintering of boron carbide

FORMATION AND REACTIVITY OF BORIDES, CARBIDES AND SILICIDES

I. REVIEW AND INTRODUCTION

By D. R. GLASSON and J. A. JONES

Borides, carbides and silicides are reviewed with special reference to newer production methods and fabrication techniques. Crystal structures and types of bonding in binary and ternary compounds are classified and discussed. The scope and limitations of the Pauling–Rundle theory, molecular orbital treatment and the Ubbelohde–Samsonov theory are examined critically and appropriate experimental evidence is summarised.

Information so far available on the sintering of borides, carbides and silicides is summarised in relation to their chemical reactivity. The sintering is influenced by additives or impurities such as oxides formed by partial hydrolysis and oxidation. Resistance to oxidation is increased by sintering and hot pressing the refractories, but since the affinity of the metals is exclusively higher for oxygen, exchange reactions diminish the quality of the materials. Boride and carbide coatings generally have poor resistance in air or oxygen, but some silicides are more suitable. The kinetics and products of oxidation of borides, carbides and silicides so far studied depend mainly on the intrinsic reactivity of the material and the available surface at which oxidation can occur.

Introduction

Increasing industrial requirements for refractory materials have enhanced research on borides, carbides and silicides. Important properties of these materials now include melting point and thermal stability, hardness and brittleness, as well as specific electrical and magnetic properties. Thus, modern refractories are not necessarily of high m.p., yet possess suitable groups of other properties such as great hardness, low vapour tensions and evaporation rates, low reactivity towards normally corrosive chemicals, etc. Such properties are determined by the electronic structure of the compounds, arising from the position of their components in the periodic system of the elements.[1]

The metallic components of the refractory borides, carbides and silicides include elements of the odd (A) subgroups of Groups III to VII, Group VIII, lanthanides, actinides and aluminium.[2,3] The chemical bond in the lattices of these compounds (in addition to the *s*- and *p*-electrons of the metallic and non-metallic components, respectively) is formed also by the electrons of the incomplete *d*- and *f*-levels of the transition metals. Isolated atoms of metals of the odd subgroups of Group II, the alkaline-earth metals, do not have any electrons in the *d*- and *f*-shells, but in compounds with non-metals, energy states corresponding to these shells may occur.[3,4] The 'metal-like' refractory compounds have heteroesmic chemical bonding, the proportion of each type of bond depending on the crystal structure. Hard-cast alloys, e.g. cemented carbides,[5] are formed with binder metals such as chromium, cobalt and nickel.

A second class of borides and carbide refractories consists of so-called non-metallic refractory compounds, i.e., compounds of B and C with each other, or with other non-metals such as N, S, P and Si. Their bond character is also heteroesmic, but with covalent bonding predominating. This confers semi-conductor properties as well as high electrical resistance at room temperature. They generally have layer, chain or skeletal structural groups or patterns, and either melt with decomposition or decompose below the m.p.

The three elements, Be, Mg and Al (typical elements of Groups II and III) are intermediate in their ability to form refractory metal-like and non-metallic borides and carbides. Thus, their borides and carbides are moderately refractory semi-conductors.

The remaining borides and carbides are classified generally as ionic or 'salt-like'. They are formed by the more strongly electropositive metals, and are colourless, transparent, crystalline solids, non-conductors of electricity, which are decomposed by water or dilute mineral acids.[1,4]

Methods of boride, carbide and silicide production

Larger-scale production methods

Borides,[2,6–9] carbides[2,10] and silicides[2,11,12] can be produced by direct combination of their elements. Variations on this method, governed thermodynamically by heats of formation, include heating the metal hydrides or reducing the metal oxides with boron, carbon or silicon. Alternatively, carbides are obtainable by reducing the metal oxides with carbon[2,10] and a readily oxidisable metal,[10] e.g. Ca or Mg, or with its carbide only,[10] e.g. CaC_2. For silicides, the metal oxides are reduced with Si or by mixtures of SiO_2 with C, Al or Mg.[2] Similarly, borides are formed by co-reduction of metal oxides and boric oxide at high temperatures, usually with carbon, aluminium or a Group I or II metal,[2,8,9] e.g., $V_2O_5 + B_2O_3 + 8C \rightarrow 2VB + 8CO$. This carbon reduction is not usually satisfactory because of considerable losses of B_2O_3 by volatilisation and contamination of the product with boron, carbon and boron carbide. Reduction of the metal oxide is improved by using carbon in the presence of boron carbide or the boride of another metal, e.g. CaB_6. The boron carbide is a good source of boron and will react with most metals or their oxides, e.g. production of rare-earth metal borides such as MB_6 (thermionic emitters): $M_2O_3 + 3B_4C \rightarrow 2MB_6 + 3CO$. The carbon (or the additional B_2O_3) ensures complete removal of the oxygen or carbon as carbon monoxide, e.g. $7Ti + 3B_4C + B_2O_3 \rightarrow 7TiB_2 + 3CO$; this contrasts with the reaction $8Mg + 3B_4C \rightarrow 6MgB_2 + Mg_2C_3$, which gives a mixed product in alkaline-earth metal boride manufacture.[13]

Nevertheless, the direct syntheses from the elements give the purer borides required for special applications or research; both synthesis and fabrication proceed during hot pressing.[2] The purity of the product largely depends on that of the parent metal, since the impurities in boron are usually more volatile. Contamination by the crucible material is minimised by using boron nitride which has been heated in hydrogen to remove oxygen. However, exact stoicheiometry is difficult to attain, particularly with very volatile metals.[9]

Reductions of B_2O_3, oxides of carbon or SiO_2 with metals are generally less satisfactory, as the products often contain large quantities of the metal oxides. Relatively pure silicides of definite composition are produced by reacting the metals with silicon in a copper menstruum.[2,14]

Smaller-scale production methods

Small amounts of pure borides, carbides and silicides are deposited (a) by hydrogen reduction of mixed vapourised B, C or Si compounds and appropriate metal compounds at a heated surface, or (b) by decomposing volatile B, C or Si compounds at the heated surfaces of appropriate metals.[15] Boride coatings, e.g., Ti, Zr, Nb, and V diborides and B_4C, may be applied by plasma-jet methods, normally using argon as the carrier gas.[8] A ZrB_2–$MoSi_2$ plasma-applied coating is claimed to withstand 2000° in an oxidising atmosphere.[8] Finely-divided non-pyrophoric carbides have been produced recently[16] by subjecting a volatile halide (e.g., chlorides of B, Si, Ti, Zr, Hf, V, Nb, Ta, Mo, W, Th and U) and a gaseous hydrocarbon (e.g. CH_4, C_3H_8, C_4H_{10}, C_2H_2, C_2H_4 or C_6H_6) to the action of a hydrogen plasma jet (at 2000—5000° for 10^{-4}—10^{-2} sec.). The powdered carbide is sintered in a rotating drum at 900—1000°. Mixed carbides are obtainable from mixtures of metal halides, preferably chlorides. Some carbides, e.g. Cr_3C_2, are deposited on metal surfaces which have been oxidised with CO or CO_2 at higher temperatures.[17]

Other methods include fused-salt electrolysis of the metal oxides, e.g. TiO_2, ZrO_2, V_2O_5, Nb_2O_5, Ta_2O_5, Cr_2O_3, MoO_3, WO_3 and U_3O_8, with boric oxide or borax, usually in an electrolyte flux of an alkali or alkaline-earth halide or fluoroborate.[2,8,9,18] Elemental boron impurities in the products are separated partly by flotation. Under appropriate conditions, fused salt electrolysis of carbonates can produce free carbon to form carbides with metals present,[18] e.g. Mo and W. Well developed crystals of silicides, e.g. of Ti, Zr and Co, are formed by electrolysing fused alkali fluorosilicates and the respective metal oxides or fluorides.[19,20]

Small amounts of carbides, mainly of alkali or alkaline-earth metals, are produced by passing acetylene into solutions of the metals in liquid ammonia.[10] Initial products such as CaC_2, C_2H_2, $4NH_3$; Na_2C_2, C_2H_2; KC_2, C_2H_2; or LiC_2, C_2H_2, $2NH_3$, all decompose to simple carbides *in vacuo* at temperatures up to 300°. The carbides of the heavier metals, notably of even Group I B, are obtained usually by passing acetylene into metal salt solutions.[10]

Thermodynamics of boride, carbide and silicide formation

The stability of borides, carbides and silicides and their production at various temperatures are related to their standard free energies of formation, ΔG°_T;[1,21] more negative values of ΔG°_T indicate stabler compounds. These are compared for some of the more important compounds on an Ellingham diagram[22] (Fig. 1), showing the temperature variation of ΔG°_T per g-atom of boron (a), carbon (b) and silicon (c). Of the metal diborides, Fig. 1(a), those of the fourth and fifth odd (A) subgroups, e.g. TiB_2, have the greatest stability. This progressively decreases for diborides in the lower groups, e.g. MgB_2, and for transition metal diborides in Groups VI to VIII, e.g. CrB_2. Disilicides show a similar trend, Fig. 1(c). Further information[23] shows that the diborides are the most stable borides of the Group IV transition metals, but for metals of the sixth group, the monoborides appear more stable than the diborides. For Group V, the different boride phases exhibit about equal thermal stability regardless of composition. On the basis of m.p., the strength of the M-B bond is increasing with the atomic weight of the metals with each Group (IV, V and VI) and decreasing with the atomic weight within each period.

The generally lower stability of boron carbide, Fig. 1(a), makes it an excellent source of boron, and it reacts with most metals or their oxides, alone or in the presence of B_2O_3. However, although energetically feasible, these reactions may be kinetically unfavourable. The solid state reactions are facilitated by fine grain sizes and pressing of well homogenised materials as in reactive sintering. Thus, Glaser[24] obtained borides of Ti, Zr, Nb and Ta by hot-pressing mixtures of boron with the respective metal hydrides or carbides, and borides of V, Cr, Mo and W by hot-pressing boron with metal or carbide powders. Later, boron carbide was hot-pressed with metals or their hydrides or carbides. Likewise, silicon combines with metals only at relatively high temperatures, and silicide formation is accelerated by using mixtures of components in finest dispersion.[25] Silicon is able as well to reduce metal oxides under analogous conditions to carbon. At high temperatures (above 1700°), SiO rather than SiO_2 is formed under reducing conditions. Use of temperatures above the m.p. of SiO_2 is recommended, to facilitate ultimate separation of silica.

The carbides of the fourth and fifth odd (A) subgroups also have the greatest stability, e.g., SiC and TiC in Fig. 1(b). This progressively decreases for carbides in the lower groups, e.g. CaC_2, and Al_4C_3, and for transition-metal carbides in Groups VI to VIII, e.g. WC.

The relative affinities of metals for boron, carbon and silicon are compared in Fig. 2. The borides are of greater stability and more readily formed than the corresponding carbides and silicides. This is ascribed to the relatively open structure of elemental boron compared with that of carbon or silicon. Elemental groupings (B_{12}-icosahedra) are retained in boron, whereas the carbon (graphite) and silicon (diamond) lattices are disrupted completely, thus allowing ready ingress of the metal component in the formation of binary borides, e.g. AlB_{10} (but not AlB_{12});[26] ScB_{12} and YB_{12} have B_{12}-cubo-octahedra.[27,28] On the other hand, the solubilities of boron and silicon in solid transition metals are usually small,[29–31] except where the metals have substitutionally dissolved boron (Mo and W–B alloys) or silicon (Mn, Fe, Co and Ni–Si alloys) with unit cell shrinkage. Slight increases in cell dimensions of other transition metals indicate that boron and silicon are dissolved interstitially, unless the increases have been caused by uptake of nitrogen or oxygen. The latter elements are more electronegative but are usually small enough to be dissolved interstitially. The free energy of the intermediate phases greatly influences the homogeneity range of the primary solid solution. Thus, the very great stability of ZrB_2 and HfB_2 vitiates an extended interstitial solid solution of boron in Zr and Hf although the size relationships are not too unfavourable. Electronic factors also govern the extent to which the different non-metals are accommodated interstitially in solid metals, and these are discussed in the next sections.

Relationship between bonding and crystal structure of borides, carbides and silicides

Hägg[32,33] suggested that the binary refractory borides and carbides of the transition elements had simple 'normal' structures when the radius ratio, $r_x:r_m$, of the non-metal and

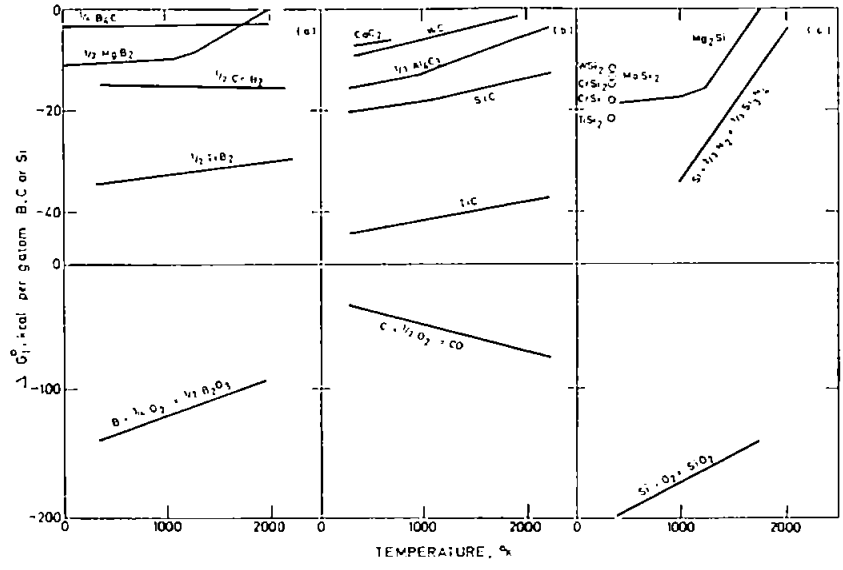

Fig. 1. *Variation of free energies of formation (per g atom of B, C or Si) of borides, carbides and silicides with temperature* (Single points for silicides are estimated values at 298°K from ΔH_f, 298° value, assuming $\Delta S_f \sim 0$)

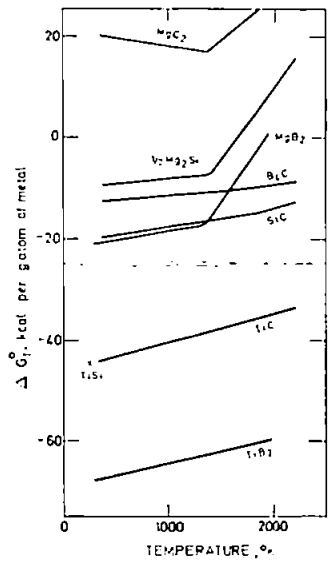

Fig. 2. *Variation of free energies of formation (per g atom of metal) of borides, carbides and silicides with temperature*

metal atoms was less than 0·59 (corresponding to a metal to non-metal radius ratio of over 1·70). Higher non-metal concentrations increase the unit cell dimensions of the interstitial phases, effectively making the radius ratio less favourable for normal structures. Nevertheless, many of these compounds are still metallic in character, but their structures become more complex with decreasing size of the metal atom. Later research[2] indicates that this limiting radius ratio rule is valid only for carbides.

Kiessling[34] ascribes the deviation of borides to the tendency of B atoms to form chains, sheets or three-dimensional networks. Hägg's rule seems restricted to phases not containing directly interconnected non-metal structure elements. Accordingly, 8 different types of boride crystal structures have been described by Schwarzkopf & Kieffer[2] for boride phases ranging in composition from M_2B to MB_{12}. Further variations are included in later reviews[35–37] covering phases from M_4B to MB_{12}, and possibly MB_{70}. In transition-metal silicides, the comparatively large radius of the Si atom (1·17 Å) ensures that Hägg's critical ratio is exceeded.

General theories

Many of the refractories first investigated[32,33] were monocarbides and mononitrides (MX-type) having radius ratios within the range 0·41—0·59. These had rock-salt structures irrespective of whether the original metal had a cubic close-packed structure or not. Rundle[38] considered that there was octahedral metal to non-metal bonding, and developed Pauling's basic concept[39–41] of the resonance of the 4-covalent C or N bonds amongst the 6 positions. Physical properties such as hardness, high m.p. and electrical conductivity were interpreted partly on the basis of resonating bond structures and on ionic structures, involving essentially homopolar and heteropolar forces.

A different theory, first advanced by Ubbelohde[42,43] and Umanskiy,[44,45] has been developed by Samsonov & Neshpor,[3,12,46–48] and reviewed recently for nitrides.[49] Bonding is provided by transfer of non-metal valence electrons into the electron cloud of the compound, at least partially filling the electron defect of the metal atoms. The additional forces of the donor–acceptor interaction greatly strengthen the interatomic bond. Therefore, heats of formation of borides, carbides and silicides (and nitrides) increase uniformly with greater 'acceptor ability', $1/Nn$, of the atoms of the metallic components, where N is the principal quantum number of the partially filled *d*- (or *f*-) shell and n is the number of electrons in this shell.[46] Likewise, the lattice energy and the hardness of the metallic compounds increase. Their electrical resistance decreases with a rise in $1/Nn$,[12] whereas the work function of the electrons increases in this direction in the case of thermionic emission.[50] The electron density also depends on the ionisation potentials of the non-metal atoms, their electron-donor ability increasing in the direction of O, N, C, B, Si. The latter concept is repudiated by Rundle,[38] but Schwarzkopf & Kieffer[2] consider that sufficiently strong metal to non-metal bonds can be formed if the lighter atoms in the refractory compounds assume the metallic state. The Ubbelohde–Samsonov theory provides a wider and more quantitative interpretation of physical properties and chemical reactivity. Its scope in rationalising existing knowledge for borides, carbides and silicides is illustrated now; types of experimental data which may extend its applicability are indicated.

Borides

The relative electronegativities of boron and transition metals suggest that electron transfer in borides should occur always from metal to boron. This accords with Pauling's calculations (using his relation between bond length and order[41]) that in borides of the type, MB, one-third to one-quarter of an electron would be transferred to the boron. However, the actual electronic structures depend considerably on the types of boron and metal lattices present. Nevertheless, more recent molecular orbital treatment of intermediate and higher borides (MB_2 to MB_{12}) also indicates electron transfer to the boron lattice. The Ubbelohde–Samsonov theory confirms the latter findings, but contradicts

Pauling's conclusions by indicating electron transfer from boron to metal for the lower (metal-rich) borides. It extends the molecular orbital treatment by explaining the inability of the even (B) subgroup metals to form higher borides. Appropriate experimental evidence is summarised in relation to boride crystal structures.

Binary metallic phases

Lower borides (Isolated atoms, pairs or chains)

Boron has a small ionisation potential. Hence, in compounds where the B atoms are isolated from one another (M_4B to M_2B),[9] the boron valence electrons are mainly in the free *d*-levels of the transition-metal atom if the latter has a sufficiently high acceptor ability.[51,52] This gives typical metallic phases, similar to intermetallic compounds.

Electron transfer from boron to metal is confirmed by magnetic measurements on CrB, MnB, CoB, NiB,[53,54] Fe_2B[55] and Co_2B,[56] and Mössbauer measurements for the isomer shift and hyperfine magnetic field for the two iron borides.[57] The latter decreases from Fe to Fe_2B to FeB, more greatly than expected through distortion or expansion of the metal lattice alone. Other metal-rich borides have not been studied, but Mössbauer measurements on Fe–Si and Fe–Al systems crystallographically similar to Fe–B again accord with electron transfer from the non-metal to the iron atoms.[58,59]

In the formation of pairs (M_3B_2), and single chains (MB), double chains (M_3B_4), and extended 2- or 3-dimensional networks of B atoms, as in MB_2, M_2B_5, MB_4, MB_6 etc.,[9] a considerable proportion of the *p*-electrons of the boron forms covalent B–B bonds, with a smaller proportion going into the electron cloud resulting in a metallic bond. The degree of metallic bonding decreases as the B/M ratio increases.

The essentially metallic character of the interatomic bond is comparable with the Hume-Rothery electron phases, the nature of the crystal structure depending on the electron concentration. Increasing concentration produces a sequence of crystal lattices, viz. body-centred cubic, base-centred hexagonal, face-centred cubic, simple hexagonal, for similar atomic radii ratios $r_x:r_m$, where X = B, Si, C, N. The face-centred cubic lattice, most characteristic of Groups IV and V metal carbides and nitrides, corresponds to an electron concentration of 5·5 to 6 electrons per atom.

Intermediate borides (Two-dimensional boron networks)

This group includes some of the best electrically conducting borides of highest melting point, and hardest of all the borides. Metal diborides, MB_2, represent the transition between the metal-rich and the boron-rich types of boride. Interpretations of Hall coefficient and resistivity measurements have been based on transfer of boron electrons to the metal-band system,[60] making any boron–boron bonding very weak. This is refuted by thermal expansion and variations in lattice constants suggesting considerable rigidity in the boron lattice.[36] The axial ratio, *c*/*a* (the '*a*'-axis is in the plane of the boron lattice), increases as the size of the metal atom increases.

Molecular orbital treatment of diborides is based on MgB_2 as the closed-shell prototype of the transition-metal diborides.[61] This is more satisfactory in that the transfer of the two electrons from the metal to the boron atoms (in the formulation $M^{2+}(B^-)_2$) makes the boron layers isoelectronic with graphite.[62] Nuclear magnetic resonance measurements are consistent with π-bonding in the boron layer, possibly achieved by electron transfer from metal to boron.[63,64] The excess valence electrons of the transition metals account for the metallic properties, and the conductivity of YB_2 accords with one free electron per metal atom.[65] There are insufficient experimental data to extend this interpretation to consider possible effects of unfilled inner orbitals in the metal atoms and to account for the inability of most Group B metals to form borides.

The hexagonal close-packed metal lattice in diborides permits considerable metal–metal bonding which might stabilise transition-metal diborides. However, formation of crystal structures characteristic for metallic compounds does not necessarily arise from the transitional nature of their atomic components. Thus, aluminium diboride, AlB_2, is not a metallic conductor, in contrast with the isomorphic diborides of the Group III–IV transition metals.[3] This boride, although isomorphic, does not form solid solutions with transition-metal diborides.[60]

Higher borides (Three-dimensional boron networks)

Tetragonal tetraborides, MB_4, are formed by Ca,[66] Y,[67] Th,[68] U,[68–70] Pu,[71] rare-earth elements,[68,72–76] Mo and W.[77] Their crystal structure is a hybrid of MB_2 and MB_6.[36] Metal hexaborides, MB_6, (cubic lattice-type CaB_6, O^5_h) are formed by *d*- and *fd*-transition metals (Y, La, Ce, Pr etc.) and non-transition metals (Ca, Sr, Ba).[3,36] Quantitative treatment of the bonding in metal hexaborides has been based initially on molecular orbital calculations (for isolated B_6-octahedra) using the 2*s* and 2*p* boron orbitals.[78,79] This suggests that 2 electrons must be provided by the metal atoms to give a configuration $M^{2+}(B_6)^{2-}$. More detailed calculations involving the 3*s*, 3*p* and 3*d* orbitals[80] are more in accord with the semiconducting properties of CaB_6, SrB_6 and BaB_6 with small energy gaps of 0·1–0·4 eV.[65] The magnetic properties of the rare-earth hexaborides suggest tervalent metal atoms.[81] Their conductivity data indicate generally one conduction electron per metal atom, with probable transfer of the other two electrons to the boron lattice.[3,82] The borides with the larger cell constants, e.g. EuB_6 and YbB_6, have almost zero conduction electrons per metal atom, but the properties of the pure metals suggest a possible decrease in the effective valency from 3 to 2. The other exception, SmB_6, has anomalous electrical and magnetic properties.[7] Hall-constant measurements for lanthanum hexaboride are interpreted on the availability of one 'excess' valence electron per La as a negative current carrier in stoicheiometric LaB_6.[83] This implies a theoretical lower limit of homogeneity of $La_{0.67}B_6$ with each La contributing all 3 valence electrons to the boron net. Then the phase should be an electrical insulator, but mechanical instability caused by the large number of metal vacancies restricts the observed lower limit to $La_{0.82}B_6$.[66]

Molecular orbital treatment of the bonding in the dodecaborides, MB_{12}, is in accord with a 'closed-shell' configuration requiring 38 electrons, giving a probable $M^{2+}(B_{12})^{2-}$ arrangement.[84] Therefore, divalent metals should give dodecaborides which are insulators or at least poor conductors. In ZrB_{12}, the 4 metal valence electrons confer metallic properties similar to those in rare-earth dodecaborides.[36]

Samsonov & Neshpor have suggested that cubic hexaborides are formed only by metals having first and second ionisation potentials less than about 6·7 and 12 eV.[58] This excludes the transition metals (6·5–9 and 12–20 eV) and

Be (9·3 and 18·2 eV) and accounts for the failure of B subgroup metals such as Ga, In, Tl, Ge, Sn, and Pb to form borides, through inability to transfer electrons to the boron lattice.[86] Substitution of sodium in CaB_6 and ThB_6 up to concentrations of $Ca_{0.57}Na_{0.43}B_6$ and $Th_{0.23}Na_{0.77}B_6$[87] could require the equivalent of 1·57 and 1·69 electrons to be transferred to the boron. The relative importance of electronic or structural factors may be ascertained if further alkali-metal hexaborides similar to NaB_6[88] and KB_6[89] can be isolated. However, the ionisation-potential criterion[85] does not hold for diborides. Since these are formed by metals of all types, e.g., AgB_2 and AuB_2,[90] complete transfer of 2 electrons may not be necessary, nevertheless, some metal to boron electron transfer is still highly probable in contrast to the reverse transfer in monoborides and metal-rich borides. Studies of the spectrum of electrons are limited and include investigations of the *X*-ray spectra of La, Ti, V, Nb, Mo and Cr borides,[3,91–94] and electron paramagnetic resonance studies of rare-earth hexaborides.[95]

Binary non-metallic phases

These phases include non-metallic refractory compounds of boron with C, N, Si, P and S, or analogues with As and possibly oxygen. They are characterised by covalent bonds in the crystal lattices, and either melt with decomposition or decompose below the m.p.[1,3] They have semiconducting properties and high electrical resistance at room temperature, and become *p*- or *n*-type conductors when normal sites of their crystal lattices are replaced by atoms of foreign metals. Their crystal structures generally consist of linear, lamellar or three-dimensionally extended structural groups.

Lower borides (Isolated boron atoms)

The most important of the MB-type compounds is boron nitride. Its hexagonal form ('white' graphite or lampblack) has unit cell dimensions very similar to those of the isoelectronic graphite.[36] In both crystal structures, the planar hexagonal nets of atoms are separated by half the length of the *c* spacing. The B atoms are situated directly above the N atoms in the adjacent layers, in contrast to the C atoms in graphite being directly above the centres of the hexagonal rings in successive layers.[96] B and N atoms alternate in the rings giving the structure with B–N bond lengths of 1·45 Å. The basic skeleton bonds are formed by sp^2 hybrid orbitals of the B and N atoms; the remaining electrons exist in delocalised π-orbitals extending above and below the whole plane, but there is an energy gap of sufficient magnitude to make BN non-conductive, cf. graphite.

Higher borides (Three-dimensional boron networks)

The most important compound of this group is boron carbide, $B_{12}C_3$. The remainder, viz. $B_{12}Si_3$, $B_{12}P_2$, $B_{12}As_2$, $B_{12}S$ and $B_{12}O_2$, have crystal structure analogous to boron carbide and α-boron.[97] The boron carbide unit cell is rhombohedral with one $B_{12}C_3$ structural unit.[98,99] The B atoms at the vertices of compact, nearly regular, icosahedra are linked by B–B bonds to form a three-dimensional network. In each unit cell, 3 C atoms are arranged linearly (parallel to the 3-fold axis of the rhombohedral cell) in large holes formed by the approximately close-packed large boron icosahedra. The crystal structure of α-boron is approximately that of boron carbide with the C atom omitted from the large interstitial holes.[100] Since boron carbide is stable over a wide range of composition,[101] this suggests a possible extended range of carbon content, from pure B to B_4C, cf. B to $B_{12}Be$ to B_6Be.[102] In the higher boron phase, $B_{13}C_2$, one B atom apparently replaces a C atom in the linear triad. More recently, Hoard & Hughes[103] indicate that the $B_{12}C_3$ has a structure of this type B_{12}(C–B–C) where a C atom has replaced a B atom in the icosahedron. In contrast, excess C in $B_{12}C_3$ is manifested as intercrystallite graphite.

Ternary phases

These are formed sometimes in systems of borides with other borides, carbides, nitrides and silicides.[2] Isomorphous borides, e.g., simple hexagonal diborides, should form continuous series of solid solutions where the radius ratios of the metal atoms are favourable. By analogy with conditions in carbide systems, e.g., TiC–WC, solid solutions are formed possibly between separately non-isomorphous borides. Thus, the high-temperature modification of MoB (β) is stabilised by solid solution with CrB;[104] at least 50 wt.-% MoB is soluble in CrB. Likewise, small amounts of titanium boride are effective, and both MoB and WB dissolve in ZrB_2 with an excess of boron.[105,106] The compounds Mo_2CoB_2, Mo_2NiB_2, Mo_2FeB_2, Mo_2CoB_4 and Mo_2NiB_4 have properties suitable for cutting-tool materials[107,108] where the low B/M ratios are consistent with high degrees of metallic bonding. In some ternary and multiple $M_2'M''B_2$ borides ($r_{M'} > r_{M''}$) the smaller M'' atoms probably occupy the cubic holes between the A-layers in the U_3Si_2-type structures.

More recent research also suggests that the cubic-F type structure of the so-called monoborides, TiB, ZrB, HfB and PuB may be stabilised by O, N or C impurities which could form ternary or quaternary phases.[31,74,109–111] TiBN has been described and its infra-red radiation has been studied.[112] A number of rare-earth MB_x phases, with *x* varying from 3 to 4 and with simple tetragonal structures, have been prepared only in the presence of carbon.[73] Hence, they are probably borocarbides of unspecified and possibly variable B and C content. Several borosilicides crystallise with the Cr_5B_3 structure,[37] and in the ternary phases which are isomorphous with W_5Si_3, the B atoms replace the Si atoms only in the antiprismatic holes giving M_5Si_2B, e.g., $Fe_{4.8}Si_2B$ and $Co_{4.7}Si_2B$. There is increasing deviation from stoicheiometry in the series Cr_5Si_3, $Fe_{4.8}Si_2B$, $Co_{4.7}Si_2B$ (W_5Si_3-structure) and the Nowotny phases[113] Zr_5Si_3 (C), $Ta_{4.8}Si_3$ (C), $Mo_{4.0}Si_3C$ (Mn_5Si_3-structure), which requires explanation in terms of fundamental electronic interactions. Ternary non-metallic boron carbonitrides probably exist in some crucible materials[114] and electrical insulators protecting metal thermocouples.[115]

Carbides

The more conventional classification of carbides,[116,117] as (A) salt-like or ionic, (B) covalent, (C) interstitial and (D) Fe_3C-type, has been defined more precisely by Samsonov[4] in terms of the electronic and crystal structures of the carbide phases. The carbide-forming elements are those with (1) valence *s*-electrons with complete or incomplete deeper shells, (2) valence *sp*-electrons and (3) valence *sd*- or *sfd*-electrons, i.e. with completed *d*- and *f*-shells. Classes (1) and (3) have been subdivided, giving 5 groups altogether.

Binary carbides

Salt-like or ionic carbides

These are formed by non-transition metals having valence *s*-electrons (with completely occupied or built-up internal

electron shells) with first ionisation potentials from 3 to 7 eV, i.e. carbides of alkali or alkaline-earth metals. The formation of strong covalent links between the carbon atoms is ascribed to the stabilisation of the *sp*-electron configuration by the *s*-electrons of the alkali metals. Carbide phases with relatively large carbon contents are formed, especially for metals with the lowest first ionisation potentials. Thus, lithium (5·57 eV) forms only one stable carbide, Li_2C_2, but sodium (5·09 eV) and potassium (4·32 eV) form polycarbides.[118,119] NaC_3, NaC_{13}, NaC_{16}, KC_3, KC_{16} (or KC_9 and KC_{19}). The potassium dicarbide, K_2C_2, is formed only with difficulty and Rb (4·19 eV) and Cs (3·86 eV) do not form dicarbides but give polycarbides, MC_3 and MC_{16}.

The higher ionisation potentials of the alkaline-earth metals restrict the tendency to form complex anions, and only carbide phases of type MC_2 are given. Carbides of Be and Mg are intermediate in character between this group of carbide phases and the covalent carbides.

Covalent-metallic carbides

These are formed by metals having outer *s*-electrons with first ionisation potentials of 7 to 11 eV, such as Cu and Zn in Groups I B and II B. Under the usual conditions, these carbides are not formed because of the isolation of the stable electronic configuration of metals and carbon;[51] the metal atom configurations $d^{10}s^1$ and $d^{10}s^2$ de-stabilise by *s*-electrons the lattices of configuration d^{10} and sp^3.

Covalent carbides

These are formed by elements having outer *sp*-electrons in the state of the isolated atoms. Group III elements, B, Al, Ga, In and Tl have a characteristic s^2p configuration which is convertible to sp^2. The latter can be stabilised up to sp^3 or in disturbance to the sp^3 configuration of the C atoms. Boron produces the most stable *sp* configuration, giving very stable carbide phases, particularly $B_{12}C_3$. Electron transfer from carbon to stabilise the boron configuration leads to the formation of linear chains of C atoms similar to the allenic groups. The separation of two very stable configurations in boron carbide explains the large energy breakdown,[120] semiconductivity, decomposition on melting,[121] high chemical stability, great hardness, etc.[122] The overlap between the electronic configurations is greater in Al_4C_3 causing lower stability and greater chemical reactivity; Al_4C_3 is decomposed by water to form CH_4 similar to Be_2C. Gallium carbide, Ga_2C_2, is extremely unstable (heat of formation only 6 kcal mole.$^{-1}$), while In and Tl carbides are apparently unknown.[123]

Group IV elements, C, Si, Ge, Sn and Pb, have an s^2p^2 configuration tending to acquire the sp^3 stable configuration for the tetrahedral structure of diamond (carbon carbide). Again, increased overlap reduces the hardness of the SiC compared with diamond and decreases the width of the forbiden zone.[124] There are numerous modifications of SiC based on combinations of the bond functions of sp^3, sp^2 for Si and the sp^3-carbon.[124] The statistical weight of the configuration is much higher for SiC than B_4C. Thus, SiC generally has higher chemical stability in various media, but it decomposes even before melting through its inability to form completely independent electron configurations. Ge, Sn and Pb do not form carbides, as the configurations of sp^3 and of a lower order become even less energetically stable.[125]

Group V elements, N, P, As, Sb and Bi, have an s^2p^3 configuration convertible to sp^2 and sp^3+e, with the electron capable of transferring to acceptor partners or ensuring the formation of electron pairs. This indirectly explains the formation of gaseous cyanogen and solid covalent carbides such as P_2C_6 of low thermal stability but acid and alkali resistant.[126]

Metal-like (or metallic) carbides of the sd*-transition metals*

Metals with up to 5 electrons in the *d*-shell form less stable d^0 and more stable d^5 configurations.[127-129] Metals with over 5 *d*-electrons form d^5 and d^{10} configurations. The statistical weights of the larger configurations increase with more *d*-electrons. Hence, the energetic stabilities and m.p. of TiC, ZrC and HfC increase with the greater statistical weight of the most stable d^5 configurations; accordingly, NbC and TaC have the highest m.p. On the other hand, the hardness depends primarily on the antibonding action of the collective *s*-electrons, so that TiC (m.p. 3150° and hardness 3000 kg mm^{-2}) is harder than NbC (3480°, 1950 kg mm^{-2}) and TaC (3880°, 1600 kg mm^{-2}).[122] The state of the collective electrons also specifies the type of conductivity,[130] the moderate thermo-electromotive forces[131] and the characteristic crystal structures.[132]

The simpler and the Fe_3C-type complex interstitial phases (conventional (C) and (D) classes) are formed by transition metals having fewer or more than 5 *d*-electrons, respectively. In the latter case, the high statistical weight of the d^5 configurations for Fe (d^6s^2), Co (d^7s^2) and Ni (d^8s^2) allows part of the *s*-electrons to convert to the collective state. This ensures completeness of the electronic configuration of the carbon atoms which are isolated in the centres of triangular prisms of metal atoms in the cementite lattices. It also agrees with the endothermicity of the formation of such carbides.[1] The isolation of complex covalently bonded groups of metal atoms is indicated by *X*-ray spectrum investigations showing larger numbers of trapped electrons with increasing statistical weight of the d^5 states.[133,134]

Where the d^0 and d^5 stable configurations can vary widely, as in TiC or ZrC, there is only one carbide and it has a wide range of homogeneity.[135] Larger numbers of carbide phases with narrower homogeneity ranges are given, as d^5 becomes the more probable configuration.[132] Thus, V and Nb form 2 phases, MC and M_2C, Cr forms 3 phases with high metal content, $M_{23}C_6$, M_7C_3 and M_3C_2, while Mn gives 5 phases, M_4C, $M_{23}C_6$, M_3C, M_5C_2 and M_7C_3. Similar patterns are observed in other periods and series. The homogeneity ranges progressively narrow from about 20–30 at.-%C for Ti, Zr and Hf (d^2s^2), to 8–15% for Nb and Ta (d^4s^1), to 2–4% for Mo and W (d^5s^1, d^4s^2), to 1·2% for Fe (d^6s^2)-type metals. Further comparison of the hardness[1,122,135] and electrical conductivity[1,130] of the *d*-transition metal carbides shows an uninterrupted trend from simpler interstitial phases to carbides of the cementite type that previously were classified separately.

Salt-like covalent metallic carbides of the sdf*-transition metals*

This group of transition metals, which includes lanthanides and actinides, forms several types of carbide phases: M_3C, MC, M_2C_3 and MC_2.[135-138] The phases M_3C and MC are typical interstitial phases with isolated C atoms, but the M_2C_3 and the MC_2 phases (Pu_2C_3 and CaC_2 structural types) contain paired C atom arrangements.

The M_3C carbides resemble Be_2C by hydrolysing only to CH_4 and H_2.[139] The carbides MC and M_2C_3 hydrolyse to hydrocarbons, mainly acetylene, and hydrogen. More acetylene and less hydrogen are evolved from the dicarbides, MC_2, suggesting that the bonds in MC and M_2C_3 are covalent-metallic with a larger proportion of the covalent bonds

in the MC_2 carbides. The quantity of hydrogen evolved seems to be related to the number of electrons present in the *d*-states. The probability of $f \rightarrow d$ transitions increases with decreasing number of possible terms.[140] The very probable $4f \rightarrow 5d$ transition in La and Ce compared with the other rare-earth metals gives dicarbides forming more hydrogen.

As the carbon content increases in the series M_3C, MC, M_2C_3, MC_2, the relative proportion of ionic to covalent bonds increases, and the metallic bonds accomplished by collective electrons are decreased. Hence, the more salt-like carbides of high carbon content have some semiconductor properties while the lower carbides have high electrical conductivity, distinguishing this group from the salt-like and the metallic carbides. Carbides of yttrium and scandium are intermediate between metallic and salt-like covalent metallic carbides.

Ternary phases

Formation of continuous series of solid solutions by isomorphous carbides and carbide–nitride systems depends mainly on differences in atomic dimensions being less than 15%.[2,141] However, in NbC–ZrN no solid solutions form, although the size factor is favourable, and there is limited solubility in VC–ZrN where the radius difference exceeds 15%. This suggests that the state of the collective *s*-electrons may be of additional importance, and their antibonding action would specify the properties of cemented carbides,[5] i.e. readily sintered materials where metals have alloyed with binary and ternary carbides. The alloying metal may form a separate carbide, e.g., cementite, Fe_3C, in sintered compositions of TiC with iron or steel.[142] In carbide–boride systems, the borides generally are more stable than the corresponding carbides; some monoborides, e.g. Ti, Ta, become unstable and form the respective diborides and monocarbides.[104]

Silicides

Binary silicides

The Cu–Si system exemplifies wide variations often found in composition and crystal structures of silicides. Phases Cu_5Si (β-Mn structure), $Cu_{31}Si_8$ ($\gamma-$) and Cu_3Si ($\varepsilon-$) conform with the Hume-Rothery rules[143] and the general theory of metals,[144] and are analogous to Cu_5Sn (β-brass), $Cu_{31}Sn_8$ ($\gamma-$) and Cu_3Sn ($\varepsilon-$). Magnesium silicide, Mg_2Si, is analogous to Mg_2Ge, Mg_2Sn, Mg_2Pb and Be_2C which all crystallise in the fluorspar structure.[116] This enables the first Brillouin zone to just accommodate the 8/3 electrons per atom in all these compounds, which are in fact either insulators or semiconductors. The molten compounds are good conductors, since the ordered crystal structure is now absent. Higher silicides (up to MSi_2 and also $BaSi_3$) are given by the other alkaline-earth and the rare-earth metals for which improved methods of preparation have been reported recently.[145–147] The silicides of Groups IV A, V A and VI A also have widely varied crystal structures.[2] There are 6 different structures for the disilicides, whereas all of the diborides are isomorphous and most of the monocarbides and nitrides are isomorphous with each other. The comparatively large diameter of the Si atom precludes formation of interstitial structures, yet some of the silicides are metallic in character and are therefore classifiable as hard metals.

In different silicides of *d*- and *fd*-transition metals, variations in Si content and atomic radii ratios produce different classes of structure.[148] In the lower M_3Si phases, the Si atoms are isolated. The higher silicides, like the borides, contain chains, two-dimensional layers or three-dimensional frameworks of Si–Si bonds. However, all of the borides have metallic conductivity, whereas several transition metal silicides are either semiconductors ($CrSi_2$, $FeSi_2$, $ReSi_2$) or have a conductivity between that of metals and semiconductors ($MoSi_2$, WSi_2).[149] A theoretical analysis of the electron structure of $MoSi_2$ indicated that the *d*-state of the metal (and its corresponding energy bands) in $MoSi_2$ has vacant sites, just as in metallic Mo.[150] Tungsten disilicide of similar structure, also exhibits *p*-type conductivity, whereas in the remaining metallic disilicides of Groups IV–VI transition metals the current carriers are electrons.[149] Nevertheless, vacant *d*-states are probably still present in metallic disilicides with *n*-type conductivity and in lower silicides, according to the correlation between resistivity, 'acceptor ability' of the metals[46] and current carrier mobility.

The *X*-ray absorption spectra of silicides of Ti[151] and V[152] confirm that the higher silicides have fewer free electrons and greater conductivity, but the semiconducting $CrSi_2$ has lower conductivity.[3] Crystallochemical calculations using Pauling's method[153] give approximately similar Cr valencies (5·5—5·7) for Cr_3Si, Cr_5Si_3 and $CrSi_2$. This indicates an essentially homopolar Cr–Si bond in keeping with the semiconductivity properties of $CrSi_2$.[3,154,155] There is also spectrum evidence of a heteropolar component in the M–Si bond in higher silicides[150] and of directed covalent M–M bonds in lower silicides (where the disilicide has metallic conductivity).[154] The high-temperature form of iron disilicide, α-leboite, has metallic conductivity but the low-temperature β-leboite is semiconducting, having a Si lattice analogous to pure Si and Ge.[3] At 0–400°, the *n*-type conductivity of the ζ_β-phase is changed to *p*-type by 0·1% Al impurities. Ordered solid solutions are characterised by a significantly higher temperature coefficient of resistance than for alloys of low Si content;[156] the coefficient remains almost constant up to the Curie point, but it is negative in the paramagnetic state.

Ternary phases

Thermodynamic data so far available[157] suggest that the decrease in heat of formation, i.e. stability, with increasing metal group number from IV A to VIII becomes less marked in the sequence: nitrides, carbides, borides and silicides. In the ternary systems M′–M″–X, the metal with the lower group number is almost invariably concentrated in the phase most rich in non-metals.[37] Similar trends in stability are shown in the M–X′–X″ systems, e.g. the M–Si–B systems are dominated by the diborides and disilicides of metals of lower and higher group numbers respectively. Information on M–Si–C, M–Si–N and M–B–N systems[157] demonstrates the great stability of the Group IV A and V A metal carbides and nitrides. The latter phases dominate the ternary systems of these metals, but borides and silicides occur over much larger fractions of the ternary systems of the later group transition metals. The M–B–N and M–Si–N systems are complicated by the comparatively great stability of B and Si nitrides which may form 2-phase equilibria with the metal-rich phases, including elementary metals.

Kinetics of boride, carbide and silicide formation

Vapour-phase deposition of borides, carbides and silicides has been extensively studied by Powell and Campbell and their co-workers.[15,158] The kinetics are interpreted more easily than those of the preparative methods involving completely solid state reactions, where the mechanisms are more

complex. As with nitride deposits,[49] two methods exist for producing borides, carbides and silicides: (a) direct deposition from an atmosphere containing either B, C or Si and the metal components both as volatilised compounds, and (b) boriding, carbiding or siliciding the surface layer of an object by heating it in an atmosphere of a volatile B, C or Si compound. For borides and carbides, process (a) deposits coatings at a faster rate than (b), where the rate of interdiffusion of B or C and the base metal limits the boride or carbide formation rate. Process (a) generally yields the purer deposits, since the B or C to metal ratios can be controlled better. As most metals form more than one boride, the practicable control of relative rates of diffusion and deposition is usually insufficient to avoid appreciable simultaneous formation of several boride phases, causing wide variations in the properties of the coatings. The carbides require temperatures to be sufficiently high for the interdiffusion of the deposited carbon or metal (from the decomposed hydrocarbon or metal halide vapours) with the metal or carbon substrates respectively. On the other hand, silicon diffuses so readily into most materials at comparatively low temperatures, which makes process (b) more convenient in the instances so far examined.

Vapour deposition of borides

Borides directly deposit most readily when hydrogen reduces mixed vaporised chlorides of boron and the desired metal component at a heated surface, i.e. process (a).[15,159] However, Nb, Ta, Mo and W borides are not deposited suitably by reduction of the mixed halides because the free metals are deposited rapidly at temperatures below those required for boride formation. The impure boride deposits either contain much free metal or are non-adherent powders, and process (b) becomes preferable. Deposition often is discontinuous when halides without a common ion or atom are used, e.g. VCl_4 and BBr_3. Limited studies on the thermal decomposition of metal borohydrides, e.g., $Th(BH_4)_4$,[160] suggest that such a method generally would produce boride deposits having excess uncombined boron. The deposition reaction is rendered inefficient by some decomposition of the borohydrides at the vaporisation temperature and the inflammability of some of them in dry air.

The boronising or boriding process (b) essentially requires deposition of free boron at a lower temperature before its diffusion into the base material at a higher temperature; otherwise the temperature must be high enough for deposition and diffusion at comparable rates. Kinetics of boron deposition by low-temperature pyrolysis of boranes and organoboron compounds have been determined by Schlesinger *et al.*[161] However, there have been no comprehensive studies of rates of boron diffusion and formation of boride layers on various metals.

Vapour deposition of carbides

Extensive studies of carbon deposition from pyrolysis of hydrocarbons show that thermodynamics, kinetic, transport and nucleation characteristics of the systems are closely interrelated.[15] In process (b), the carburisation rate depends on the specimen temperature, the hydrocarbon content in the surrounding gases, the rate of gas flow and the geometry of the specimen. The factors also affect the adhesion of the carbide layer. In general, the thinner carbide layers are the most adherent. As found for nitrides[49] and oxides,[162] the formation of non-uniform, i.e. porous or cracked, scales depends partly on the Pilling–Bedworth rule,[163] which seems less significant for scales that grow by outward migration of matter.[164] It is more important for scales where the diffusion is from the surface towards the metal/scale interface. Apart from fractional volume differences between the metals and their carbides, there is sometimes dissolution of free C in the carbides, e.g. in Mo carbide.[15] Formation of mixed carbides, carboborides or carbonitrides often improves the hardness of the coatings, e.g. boronised 0·3% carbon steel is harder than boronised iron, particularly at higher boronising temperatures.[165] Gas mixtures and temperatures must be controlled carefully to equalise the reaction velocities for the deposition of each component.[166] The range of mixed carbide coatings might be increased by carburising alloy-vapour deposits, or by diffusing superposed carbide deposits at high temperatures.

Vapour deposition of silicides

Free silicon is deposited usually by hydrogen reduction of silicon tetrachloride, but the reaction is sensitive to impurities.[167] Deposits on quartz or ceramic bases[168] below 1000° tend to be grainier, but they are smooth and hard above 1100°. The deposition rate is independent of time and proportional to the $SiCl_4$ concentration, within limits. Silicide deposits rich in Si on the outside are obtained by successively coating Ta and momentarily flashing each layer to the m.p. of Si; the products have the most suitable mechanical and electrical properties for electrical translating materials.[169] Detailed investigation of silicide formation by diffusion of Si coatings appears to be confined so far to Ti, Zr, Nb, Ta, Cr, Mo, W, Fe, Ni and several alloy steels;[15] coatings can be applied also to Cu, Ag, Be, Al, Hf, Th, V, Mn, rare-earth metals, Co and Pt-group metals. Minimum Si-deposition temperatures are about 900–1000° for H_2-reduction methods, unless the base materials are sufficiently reactive for Si diffusion to cause deposition by displacement at lower temperatures,[167] e.g., Fe, W at 800°, or Mo at 800–900°. At low deposition rates, the maximum deposition temperature is limited by the m.p. of any eutectic or peritectic compositions formed between the base and the coating. At high deposition rates, it is limited by the m.p. of Si unless this is higher than the m.p. of any eutectics. The silicides formed are not usually homogeneous in composition, but comprise most of the silicide phases that can exist in a given system at the deposition temperature.[15] Silicon also has some solid solubility in most metals. Thinner silicide deposits are usually more adherent, e.g. Mo silicide up to 80 μm thick, but the adhesion of the thicker deposits (> 200 μm) is improved by successive short-stage depositions and intermittent heating in hydrogen to diffuse the coating into the substrate.

Solid state preparative reactions

In the production of borides, carbides and silicides by direct combination of their elements (or close variations of these methods), the reactions are accelerated by using mixtures of components in finest dispersion.[2,170] Rational grain-size composition is of special interest now because of newer methods of grinding materials (vibratory grinding, fluid-energy mills, etc.). The uniformity and degree of grinding influences the following parameters:[171] (a) surface area and energy of the grains, (b) temperature, heat of fusion and solution, (c) intensity of heat exchange with surroundings, (d) rate of solution, sublimation, dissociation and chemical

reaction with other reagents, (e) thickness of the product layer developing on the grains during chemical reaction, and governing diffusion rates through the layer, (f) properties of the crystalline reaction products, e.g. mechanical and thermal, (g) effectiveness of reaction accelerators between solids, and (h) the economics of the process. The kinetics are determined mainly by (d) and (e). For mixtures with components with similar grain sizes, Jander & Hoffmann[172] have shown that the thickness of the product layers around the grains is proportional to the square root of the calcination time. In the sintering of each product, Berezhnoi[173] has established that the minimum porosity is given by a mixture of fine and coarse fractions having a grain size ratio of 0·3, and contents of 30–40% and 60–70% respectively. The successful production of borides by hot pressing (reactive sintering) of metals, hydrides and carbides with boron or boron carbide powders[24,174] illustrates the general applicability of the above parameters. However, there are only detailed kinetic data available[175] on the average solid solution rates (1400–2400°) for the 50/50 TiB_2–ZrB_2 composition. In the production of carbides and silicides, most metals and their oxides react with C and Si far below their m.p. (1200–2200°). The lowest possible carburisation temperatures are used to avoid any deleterious grain growth.[2]

Reactivity of borides, carbides and silicides

Sintering of borides, carbides and silicides

The chemical reactivity of borides, carbides and silicides is controlled considerably by the extent to which they have been sintered during their formation and any subsequent calcination. At present, there is much more information available on the sintering of oxides and a limited amount on nitrides.[49] Theories of sintering have been developed by Hüttig,[176] Kingery,[177] Coble,[178,179] Kuczynski,[180] White[181] and Fedorchenko & Skorokhod.[182] Sintering is enhanced by compacting the powdered materials before calcining them *in vacuo* to prevent possible hydrolysis and oxidation.[183,184]

Hot pressing often extensively densifies materials,[2] giving almost the theoretical densities for oxides such as MgO, CaO and Al_2O_3.[185–187] Development is limited by impurities, particularly gas-producing contaminants such as hydroxides and carbonates. Also, nitrogen reacts extensively with some carbides, e.g., TiC[188,189] and ZrC,[141] and produces carbide–nitride solid solutions. Hence, often vacuum hot pressing is preferred.[190] Sintering is accelerated generally by additives of low melting point,[191] but these may cause serious reductions in optical and mechanical properties. However, extremely brittle borides, carbides and silicides may be sintered with metals such as Co to give satisfactory cermets,[5] or may be used as surface coatings.[15]

Hydrolysis and oxidation of borides, carbides and silicides

The resistance of borides, carbides and silicides to the action of water and aqueous acids and alkalis has been summarised by Shaffer & Samsonov.[1] The materials listed by Campbell *et al.*[158] for high-temperature coatings include several metals such as Zr, Th, Nb and Ta which all have m.p. above 1700° and generally reasonable ductility, but their oxidation resistance is poor. The numerous carbides of high melting-point, e.g. TiC, ZrC, NbC, Mo_2C, W_2C, SiC, also have generally poor oxidation resistance, and their ductility is inferior to that of the metals. The affinity of the metals is exclusively higher for oxygen than for carbon, cf. Figs 1 and 2, and consequently exchange reactions diminish the quality of the coatings. Similar considerations apply to borides, but silicides partly possess suitable combinations of the desired properties.

The only interstitial boride and carbide oxidations that have been studied in any detail are those of TiB_2 and TiC. They illustrate factors to consider and problems to be encountered in further investigations of other transition-metal boride and carbide oxidations. Reactions having parabolic kinetics between 600–1000° for TiB_2[192–194] and 450–1000° for TiC[192–196] produce scales consisting essentially of rutile. A cubic relationship with time, found by Münster[193] for the oxidation of TiB_2 at 900°, was not observed by Samsonov & Golubeva.[192] *X*-ray and metallographic examination[192,194] shows that at 700° the rutile is dispersed in vitreous B_2O_3, but between 800–1000° the B_2O_3 forms a top layer covering a rather porous rutile layer with coherent rutile adjoining the metal boride. Platinum marker experiments[193] suggest that the oxide/boride interface moves away from the oxide/gas interface, but at higher temperatures the B_2O_3 flows outwards (over the markers) to form a separate layer; at 1100°, most of the B_2O_3 volatilises and the scale consists almost entirely of rutile. This indicates that oxygen rather than Ti diffusion is rate-determining at least in the parabolic stage of the oxidation, cf. diffusion of anion vacancies in the TiO_2 (*n*-type conductor)[197,198] which controls oxidation of Ti between 600–700° and gives a similar energy of activation.[196,199] Therefore, the oxidation mechanism would be essentially the same as for TiC and TiN, where the rutile scales are separated from the carbide and nitride by thin films of TiO–TiC and TiO–TiN solid solutions.[192] The carbon formed in the reaction $TiC + O_2 = TiO_2 + C$, is thought to diffuse to the scale surface where it reacts with oxygen to form carbon oxides,[200] cf. oxidation of UC which finally gives UO_3 containing residual CO_2.[201] Some carbon may be assimilated by the TiC lattice, especially at lower temperatures, for commercial TiC is usually C-deficient.[202] Effects of temperature and oxygen partial pressures on TiC oxidation have been investigated further,[203] and also the reactivity with water[204] and the related oxidations of Zr and Hf carbides.[205] TiC–Co aggregates containing 18% Co also oxidise parabolically in air between 600–1000°,[206] and WC oxidises more readily than TiC.[207] The hard metals TiC–WC–Co oxidise linearly for high WC-contents (as found for TiC at very low temperatures, 300–400°). Re-entrant edges in the product scales are typical of uninhibited oxidation at the hard metal-oxide interface. In contrast, the parabolic curve for oxidation of TiC–Co–Cr hard metal produces much thinner scales, which are tenaciously adherent and protective; chromium carbide improves the oxidation resistance.[208]

Atmospheric oxidation of transition metal silicides has been studied systematically by Kieffer and his co-workers, mainly between 1100–1500°. The maximum oxidation resistance in the systems Ti–Si,[209] Zr–Si,[210] V–Si,[211] Nb–Si,[212] Cr–Si[213] and Mo–Si[214] is exhibited by compositions of approximately MSi_2, or higher Si contents of about 30 wt.-% in the systems Ta–Si[209] and W–Si.[215] However, $NbSi_2$ oxidises rapidly compared with the Nb_5Si_3 phase stabilised with Cr.[212] When oxidised at 1200°, $TiSi_2$ (m.p. 1540°), VSi_2 (1670°), $MoSi_2$ (2030°) and WSi_2 (2160°) form vitreous well-adhering scales which are highly protective. $MoSi_2$ is especially resistant to oxidation and the scales are self-healing.[216] The mechanism of the low ionic diffusion in these vitreous silicate scales is not yet established. $ZrSi_2$ and

Ta silicides of lower Si content than $TaSi_2$ form scales which are vitreous but brittle, tending to flake off during temperature fluctuations.[209,210] These silicides are more oxidation-resistant than those of Cr and Nb which form porous, loosely adherent scales. More recently, the continuous solid solution at 50% $ReSi_2$–$MoSi_2$ is claimed as a composition of extreme oxidation resistance at high temperatures,[217] but poor oxidation resistance for $ReSi_2$ has been reported.[218] Improvements generally would seem to depend on the mutual alloying of transition metal silicides (and borides) to produce ternary phases of new and independent structures, the stabilities being controlled by electron relations.[219] The new structures would be unlike those of the end members, but isomorphic to other single silicides with the best oxidation resistances. Further improvements in protective performance will depend on slight ductility possessed by some silicides, e.g., $NbSi_2$, $TaSi_2$, $MoSi_2$, WSi_2, matching of lattice volumes, eutectic and melting temperatures, and the extent of sintering of the oxidised overlayers.

Experimental techniques

Materials

Borides, carbides and silicides usually contain impurities introduced during their production by the initial reactants and apparatus materials or surrounding gases. Purification is required before determination of physical properties such as m.p., hardness, electrical conductivity etc.[219] The thermochemistry of interactions of metals and refractory materials commonly used for containers has been reviewed recently by Kubaschewski,[220] who emphasises the lack of accurate thermochemical data for the nonstoicheiometric compositions in refractory systems, particularly non-stoicheiometric metal–non-metal phases of high affinity. Purer boride, carbide and silicide products are obtained by using high frequency heating *in vacuo* or in argon, as developed by Brewer *et al.* for borides[221] and silicides[222] and Agte & Moers for carbides.[223] Agte & Moers embed the sintering carbide bars in carbide powders to protect against carburisation, oxidation and nitridation. Extremely high temperatures of final sintering give self-purification, by evaporation of the oxides, metals and other impurities with vapour pressures higher than those of the carbides.

Additives promoting sintering, e.g. 0·2–1·5% Cr, Fe, Co, Ni or their oxides, often form liquid phases and promote self-purification through diffusion processes, particularly for carbides of Groups IV and V.[224,225] The auxiliary metal additives can be completely vacuum-evaporated in high-frequency furnaces at pressures of about 0·1 mm Hg at 2000–2500°. The refractories are hot pressed by the present authors using apparatus designed by Scholtz,[226] Roeder & Scholtz[227] and Oudemans.[228] Pressure sintering bonds compacts of ceramic friction materials on to metal backplates, for which special types of furnace are required.[229]

Production of finely divided and more reactive materials by milling can produce considerable strain.[230] This may be increased by impurities, e.g. the presence of oxygen in the lattice causes some carbides to lose cubic symmetry and deform more isotropically.[231] Modern apparatus for closely controlling the milling of materials[232–236] can give products having narrow particle size distributions. Changes in crystallite and aggregate sizes during sintering and milling of the borides, carbides and silicides are determined by the methods described below.

Procedure

Hydrolysis and oxidation of the borides, carbides and silicides are followed by weight changes on vacuum[237–239] and thermal[240] balances. Samples are outgassed usually at 200° *in vacuo* before determination of their surface areas by the B.E.T. procedure[241] from nitrogen (or occasionally oxygen) isotherms recorded at −183° on an electrical sorption balance. The deduced average crystallite sizes (equivalent spherical diameters) are compared with particle size ranges determined by optical or electron microscope or sedimentation balance. Where necessary, particle size fractions of the materials are sintered or hot pressed for further periods at fixed temperatures.

Phase composition identification

Samples are examined for phase composition and crystallinity using an *X*-ray powder camera and a Solus–Schall *X*-ray diffractometer with Geiger counter and Panax rate-meter. The average crystallite size of some of the phases can be determined from *X*-ray line- or peak-broadening.[242] Certain samples are further examined by optical and electron microscopes (Philips EM-100). More detailed investigation involves determination of pore size distribution in refractories, where the microscopic examination may be supplemented advantageously by methods based on mercury penetration, expulsion of water from a saturated specimen and electrical detection of capillary penetration.[243] Electron-probe microanalysis often provides further information.[244]

Acknowledgments

The authors thank Dr. S. J. Gregg for his interest and encouragement in this work; Mrs. M. A. Sheppard for her assistance in the translation and classification of the chemical literature; the University of London, Imperial Chemical Industries Ltd., and the Science Research Council for grants for apparatus and a S.R.C. Research Technicianship (for M.A.S.).

John Graymore Chemistry Laboratories,
College of Technology,
Plymouth

see also "Special ceramics", (B.C.R.A.), 1970.

References

[1] Shaffer, P. T. B., & Samsonov, G. V., 'High temperature materials', 1964, Handbooks 1 and 2 (New York: Plenum)
[2] Schwarzkopf, P., & Kieffer, R., 'Refractory hard metals', 1953 (New York: Wiley)
[3] Samsonov, G. V., 'Refractory transition metal compounds', 1964 (London: Academic Press)
[4] Samsonov, G. V., *Ukr. khim. Zh.*, 1965, **31** (10), 1005 (N.L.L. translation, RTS 4233: Dec. 1967); summarised in *Izv. Akad. Nauk SSSR*, 1967, **58** (10), 76
[5] Schwarzkopf, P., & Kieffer, R., 'Cemented carbides', 1960 (London: Macmillan)
[6] Samsonov, G. V., & Markovskii, L. Ya., *Usp. Khim.*, 1956, **25**, 190 (Associated Technical Services translation RJ 631)
[7] Samsonov, G. V., *Usp. Khim.*, 1959, **28**, 189 (U.K.A.E.A. translation, report AERE, Trans. 849)
[8] Thompson, R., & Wood, A. A. R., *Chem. Engr.*, 1965, p. CE51
[9] Greenwood, N. N., Parish, R. V., & Thornton, P., *Q. Rev. chem. Soc.*, 1966, **20** (3), 441
[10] Mellor, J. W., 'Comprehensive treatise on inorganic and theoretical chemistry', Vol. 5, p. 844 (London: Longmans)
[11] Samsonov, G. V., *Zh. teor. Fiz.*, 1956, **26**, 216
[12] Samsonov, G. V., & Neshpor, V. S., 'Subjects of powder metallurgy and strength of materials', 1959, Issue 7, p. 99 (Kiev: Izdvo Akad. Nauk SSSR)
[13] Elektroschmelzwerk Kempten, B.P. 1,070, 325

[14] Lebeau, P., & Figueras, J., *C. r. hebd. Séanc. Acad. Sci., Paris*, 1903, **136**, 1329
[15] Powell, C. F., Oxley, J. H., & Blocher, J. M., 'Vapour deposition', 1966, p. 343 (New York: Wiley)
[16] Ciba Ltd., B.P. 1,069,748
[17] Leach, H. F., Thesis, Univ. Exeter, 1964; Glasson, D. R., Gregg, S. J., Lakey, B., Leach, H. F., & Maude R., unpublished work
[18] Andrieux, L., & Weiss, G., *Bull. Soc. chim. Fr.*, 1948, **15**, 598
[19] Andrieux, L., *Revue Métall., Paris*, 1948, **45**, 49
[20] Dodero, M., Thesis, Univ. Grenoble, 1937
[21] JANAF thermochemical tables, 1960-65, P.B. 168,370 (New York: Dow Chemical Co.)
[22] Ellingham, H. J. T., *J. soc. chem. Ind.*, 1944, **63**, 125
[23] Schwarzkopf, P., & Glaser, F. W., *Third Int. Cong. Electroheat. Electro-chem., Paris*, 1953, paper 4
[24] Glaser, F. W., *J. Metals, N.Y.*, 1952, **4**, 391
[25] Wallbaum, H. J., *Z. Metallk.*, 1941, **33**, 778
[26] Will, G., *Nature, Lond.*, 1966, **212**, 175
[27] Matkovich, V. I., Giese, R. F., jun., & Economy, J., *Z. Kristallogr. Kristallgeom.*, 1965, **122**, 116
[28] Matkovich, V. I., Giese, R. F., jun., Economy, J., & Barrett, R., *Acta crystallogr.*, 1965, **19**, 1056
[29] Hansen, M., & Anderko, K., 'Constitution of binary alloys', 1958, p. 14 *et seq.* (New York: McGraw-Hill)
[30] Pearson, W. B., 'A handbook of lattice spacings and structures of metals and alloys', 1958, p. 7 *et seq.* (Oxford: Pergamon)
[31] Aronsson, B., *Ark. Kemi.*, 1960, **16**, 379
[32] Hägg, G., *Metallwirt., Metalwiss., Metalltech.*, 1931, **10**, 387
[33] Hägg, G., *Z. phys. Chem.*, 1931, (B), **12**, 33
[34] Kiessling, R., *Acta chem. scand.*, 1950, **4**, 209
[35] Kieffer, R., & Benesovsky, F., 'Hartstoffe', 1963, (Wien: Springer-Verlag)
[36] Post, B., in 'Boron, metallo-boron compounds and boranes', (Ed. R. M. Adams), 1964, p. 301 (New York: Interscience)
[37] Aronsson, B., Lundstrom, T., & Rundqvist, S., 'Borides, silicides and phosphides', 1965, (London: Methuen)
[38] Rundle, R. E., *Acta crystallogr.*, 1948, **1**, 180
[39] Pauling, L., 'Nature of the chemical bond', 1940, p. 420 (Ithaca, N.Y.: Cornell Univ. press)
[40] Pauling, L., *J. Am. chem. Soc.*, 1947, **69**, 542
[41] Pauling, L., *Proc. R. Soc.* [A], 1949, **196**, 343
[42] Ubbelohde, A. R., *Trans. Faraday Soc.*, 1931, **28**, 284
[43] Ubbelohde, A. R., *Proc. R. Soc.* [A], 1937, **159**, 295
[44] Umanskiy, Y. S., *J. phys. Chem., Wash.*, 1943, **26**, 127
[45] Samsonov, G. V., & Umanskiy, Y. S., 'Solid compounds of refractory metals', 1957, p. 1 (Moscow: Metallurgizdat)
[46] Samsonov, G. V., *Zh. fiz. Khim.*, 1956, **30**, 2058
[47] Samsonov, G. V., & Neshpor, V. S., *Dokl. Akad. Nauk SSSR*, 1958, **122**, 1021
[48] Samsonov, G. V., Neshpor, V. S., & Paderno, Y. B., *Ukr. fiz. Zh.*, 1959, **4**, 509
[49] Glasson, D. R., & Jayaweera, S. A. A., *J. appl. Chem., Lond.*, 1968, **18**, 65
[50] Samsonov, G. V., Neshpor, V. S., & Kudnitseva, G. A., *Radiotekh. Elektron.*, 1957, No. 5, p. 119
[51] Samsonov, G. V., *Dokl. Akad. Nauk. SSSR.*, 1953, **83**, 689; *Neorg. Mater.*, 1967, No. 1, p. 17
[52] Samsonov, G. V., Markovskiy, L. Ya., Zhigach, A. F., & Valyashko, M. G., 'Boron, its compounds and alloys', 1960, p. 6 (Kiev: Izdvo Akad. Nauk Ukr. SSR)
[53] Lundquist, N., & Myers, H. P., *Ark. Fys.*, 1961, **20**, 463
[54] Lundquist, N., Myers, H. P., & Westin, R., *Phil. Mag.*, 1962, **7**, 1187
[55] Weiss, P., & Forrer, R., *Phys. Ber.*, 1929, **12** (10), 279
[56] Fruchart, R., *C.r. hebd. Séanc. Acad. Sci., Paris*, 1963, **256**, 3304
[57] Cooper, J. D., Gibb, T. C., Greenwood, N. N., & Parish, R. V., *Trans. Faraday Soc.*, 1964, **60**, 2097
[58] Stearns, M. B., *Phys. Rev.*, 1963, **129**, 1136
[59] Stearns, M. B., *J. appl. Phys.*, 1964, **35**, 1095
[60] Juretschke, H. J., & Steinitz, R., *J. phys. Chem. Solids*, 1958, **4**, 118
[61] Lipscomb, W. N., & Britton, D., *J. chem. Phys.*, 1960, **33**, 275
[62] Muetterties, E. L., *Z. Naturf.*, 1957, **12**, (B), 411
[63] Silver, A. H., & Bray, P., *J. chem. Phys.*, 1960, **32**, 288
[64] Silver, A. H., & Kushida, T., *J. chem. Phys.*, 1963, **38**, 865
[65] Johnson, R. W., & Daane, A. H., *J. chem. Phys.*, 1963, **38**, 425
[66] Johnson, R. W., & Daane, A. H., *J. phys. Chem., Ithaca*, 1961, **65**, 909
[67] Gschneider, K. A. 'Rare earth alloys', 1961, p. 63 (New York: Van Nostrand)
[68] Zalkin, A., & Templeton, D. H., *Acta crystallogr.*, 1953, **6**, 269
[69] Andrieux, L., *Annls Chim. Phys.*, 1929, **12**, 423
[70] Bertaut, F., & Blum, P., *C.r. hebd. Séanc. Acad. Sci., Paris*, 1949, **229**, 666
[71] McDonald, R. J., & Stuart, W. J., *Acta crystallogr.*, 1960, **13**, 447
[72] Felten, E., Binder, I., & Post, B., *J. Am. chem. Soc.*, 1958, **80**, 3479
[73] Post, B., Moskowitz, D., & Glaser, F. W., *J. Am. chem. Soc.*, 1956, **78**, 1800
[74] Eich, M. A., & Gilles, P. W., *J. Am. chem. Soc.*, 1959, **81**, 5030
[75] Paderno, Y. B., & Samsonov, G. V., *Zh. strukt. Khim.*, 1961, **2**, 213
[76] Zhuravlev, N. N., Stepanova, A. A., Paderno, Y. B., & Samsonov, G. V., *Kristollografiya*, 1962, **6**, 636
[77] Chretien, A., & Helgorsky, J., *C.r. hebd. Séanc. Acad. Sci., Paris*, 1961, **252**, 742
[78] Longuet-Higgins, H. C., & Roberts, M. de V., *Proc. R. Soc.* [A], 1955, **224**, 336
[79] Yamakazi, M., *J. phys. Soc. Japan*, 1957, **12**, 1
[80] Flodmark, S., *Ark. Fys.*, 1959, **14**, 513; *ibid.*, 1960, **18**, 49
[81] Benoit, R., *J. Chim. phys.*, 1955, **52**, 119
[82] Paderno, Y. R., & Samsonov, G. V., *Dokl. Akad. Nauk SSSR*, 1960, **137**, 646
[83] Lafferty, J. M., *J. appl. Phys.*, 1951, **22**, 299
[84] Lipscomb, W. N., & Britton, S., *J. chem. Phys.*, 1960, **33**, 275
[85] Neshpor, V. S., & Samsonov, G. V., *Russ. J. inorg. Chem.*, 1959, **4**, 893
[86] Samsonov, G. V., & Grodshtein, A. E., *Zh. fiz. Khim.*, 1956, **30**, 379
[87] Blum, P., & Bertaut, F., *Acta crystallogr.*, 1954, **7**, 81
[88] Hagenmuller, P., & Naslain, R., *C.r. hebd. Séanc. Acad. Sci., Paris*, 1963, **257**, 1294
[89] Naslain, R., & Etourneau, J., *C.r. hebd. Séanc. Acad. Sci., Paris*, 1966, **263**, (C), 484
[90] Obrowski, W., *Naturwissenschaften*, 1961, **48**, 428
[91] Vaynshteyn, E. Y., & Zhurakovskiy, Y. A., *Zh. neorg. Khim.*, 1959, No. 1, p. 4; *Dokl. Akad. Nauk SSSR*, 1959, **127**, 534; *Izv. Akad. Nauk SSSR. O. Khim. neorg.*, 1959, No. 3, p. 1
[92] Zhuravlyov, N. N., Manelis, R. M., Gramm, N. V., & Stepanova, A. A., *Poroshkovaya Metall.*, 1967, No. 2 (50), 95
[93] Nemnonov, S. N., & Men'shikov, A. Z., *Izv. Akad. Nauk SSSR. seriya fiz.*, 1959, **23**, 587
[94] Korsunskiy, M. I., & Genkin, Y. Y., 'Heat resisting materials seminar', 1958, Bull. No. 5 (Kiev: Izdvo Akad. Nauk SSSR)
[95] Vlasova, M. V., Sorin, L. A., & Shcherbina, V. I., *Poroshkovaya Metall.*, 1967, No. 1 (49), 70
[96] Pease, R. S., *Acta crystallogr.*, 1952, **5**, 356
[97] LaPlaca, S., & Post, B., *Planseeber. Pulv. Metall.*, 1961, **9**, 109
[98] Zhdanov, G. S., & Sevast'yanov, N. G., *Dokl. Akad. Nauk SSSR*, 1941, **32**, 432
[99] Clark, H. K., & Hoard, J. L., *J. Am. chem. Soc.*, 1943, **65**, 2115
[100] Decker, B. F., & Kasper, J. S., *Acta crystallogr.*, 1959, **12**, 503
[101] Glasser, F. W., Moskowitz, D., & Post, B., *J. appl. Phys.*, 1953, **24**, 731
[102] Sands, D., Cline, C. F., Zalkin, A., & Hoenig, C. L., *Acta crystallogr.*, 1961, **14**, 309
[103] Hoard, J. L., & Hughes, R. E., 'Chemistry of boron and its compounds' (Ed. E. L. Muetterties), 1967, p. 25 (New York: Wiley)
[104] Steinitz, R., *Powder Metall. Bull.*, 1951, **4**, 54
[105] Kisliy, P. S., & Kuzenova, M. A., *Neorg. Mater.*, 1966, No. 12, p. 2139
[106] Voroshilov, U. G., *Neorg. Mater.*, 1967, No. 9, p. 1597
[107] Steinitz, R., & Binder, I., *Powder Metall. Bull.*, 1953, **6**, 123
[108] Kuzma, Y. B., Nish, O. V., & Skolozdra, R. V., *Neorg. Mater.*, 1966, No. 11, p. 1975
[109] Post, B., & Glaser, F. W., *J. chem. Phys.*, 1952, **20**, 1050
[110] McDonald, R. J., & Stuart, W. J., *Acta crystallogr.*, 1960, **13**, 447
[111] Aronsson, B., 'Modern materials' (Ed. H. Hausner), 1960, Vol. II, p. 54 *et seq.* (New York: Academic Press)
[112] Grenis, A. F., & Levitt, A. P., *J. Am. Ceram. Soc.*, 1966, **49** (12), 629
[113] Nowotny, H., 'Electronic structure and alloy chemistry of the transition elements' (Ed. R. A. Beck), 1963, p. 179 (New York: Interscience)
[114] Degtyarev, V. S., *Refractories, Wash.*, 1966, 31 (5), 305

[115] Dubrovik, T. V., & Struk, L. I., *Poroshkovaya Metall.*, 1966, No. 5 (41), 107
[116] Emeléus, H. J., & Anderson, J. S., 'Modern aspects of inorganic chemistry', 1943, p. 450 (London: Routledge)
[117] Meerson, G. A., *Kratkaya khimicheskaya entsiklopediya*, 1963, 2, 424
[118] Ostroushko, Yu. I., Buchikhin, P. I., *et al.*, 'Litii, ego khimiya i tekhnologiya', Gosatomizdat, 1960, p. 40
[119] Alabyshev, A. Ya., Grachev, K. Ya., Zaretskiy, S. A., & Lantratov, M. F., 'Natrii i kalii', Goskhimizdat, 1959, p. 44
[120] Samsonov, G. V., & Sinel'nikova, V. S., *Ukr. fiz. Zh.*, 1961, 6, 687
[121] Samsonov, G. V., Markovskiy, L. Ya., Zhigash, A. F., & Valyashko, M. G., 'Bor, ego soedineniya i splavy', 1960, p. 179 (Kiev: Izdvo Akad. Nauk Ukr. SSR)
[122] Samsonov, G. V., & Stassovskaya, V. V., *Poroshkovaya Metall.*, 1966, No. 12 (48), 95
[123] Sheka, I. A., Chaus, I. B., & Mityureva, T. T., 'Galii', Gostekhizdat, Ukr. SSR., 1963, p. 36
[124] Doborolezh, S. A., Zubkova, S. I., *et al.*, 'Karbid kremniya', Gostekhizdat, Ukr. SSR., 1963, p. 75
[125] Scace, R., & Slack, G., *J. chem. Phys.*, 1959, **30**, 1551
[126] Samsonov, G. V., & Vereikina, L. I., 'Fosfidy', 1961, p. 4 (Kiev: Izdvo Akad. Nauk Ukr. SSR)
[127] Samsonov, G. V., *Poroshkovaya Metall.*, 1966, No. 12 (48), 49
[128] Pryadko, I. F., *Poroshkovaya Metall.*, 1966, No. 12 (48), 61
[129] Kozlova, I. F., Gurin, V. N., & Obukhov, A. P., *Poroshkovaya Metall.*, 1966, No. 12 (48), 68
[130] L'vov, S. N., Nemchenko, V. F., & Samsonov, G. V., *Dokl. Akad. Nauk SSSR.*, 1960, **135**, 577
[131] Samsonov, G. V., & Strel'nikov, N. S., *Ukr. Fiz. Zh.*, 1958, **3**, 135
[132] Kuchima, A. Ya., & Samsonov, G. V., *Neorg. Mater.*, 1966, No. 11, p. 1970
[133] Korsunskiy, M. I., & Genkin, Ya. E., *Dokl. Akad. Nauk SSSR.*, 1962, **142**, 1276
[134] Korsunskiy, M. I., & Genkin, Ya. E., *Izv. Akad. Nauk SSSR., seriya fiz.*, 1964, **28**, 832
[135] Storms, E. K., 'The refractory carbides', Refractory materials monogrs (Ed. J. L. Margrave), 1967, Vol. II (London: Academic Press)
[136] Samsonov, G. V., 'High-melting compounds of the rare-earth metals', 1964, p. 1 (Moscow: Metallurgizdat)
[137] Paderno, Yu. B., Yupko, V. L., Rud, B. M., Kvas, O. F., & Makarenko, G. N., *Neorg. Mater.*, 1967, No. 2, pp. 395, 398
[138] Makarenko, G. N., & Kvas, O. F., *Poroshkovaya Metall.*, 1967, No. 8 (56), 34
[139] Spedding, P., Gschneider, K.A., & Daane, A.H., *J. Am. chem. Soc.*, 1958, **80**, 4499
[140] Samsonov, G. V., & Neshphor, V. S., *Dokl. Akad. Nauk SSSR.*, 1958, **122**, 1021
[141] Duwez, P., & Odell, F., *J. electrochem. Soc.*, 1950, **97**, 299
[142] Sededa, N. N., & Kovalchenko, M. S., *Poroshkovaya Metall.*, 1967, No. 9 (57), 42
[143] Hume-Rothery, W., 'The structure of metals and alloys', 1936, p. 16 (London: Institute of Metals)
[144] Mott, N. F., & Jones, H., 'The theory of the properties of metals and alloys', 1936 (Oxford: Clarendon Press)
[145] Dvorina, L. A., *Poroshkovaya Metall.*, 1966, No. 6 (42), 92
[146] Vaynshteyn, E. Y., Bril, M. N., Stariy, I. B., Gladyshevskiy, E. I., & Kripyakevich, R. I., *Neorg. Mater.*, 1967, No. 4, p. 644
[147] Rud, B. M., & Paderno, Yu. B., *Poroshkovaya Metall.*, 1967, No. 1 (49), 81
[148] Umanskiy, Ya., & Samsonov, G. V., *Zh. fiz. Khim.*, 1956, **30**, 1526
[149] Neshpor, V. S., & Samsonov, G. V., *Dokl. Akad. Nauk SSSR.*, 1960, **133**, 317; *ibid.*, 1960, **134**, 1337
[150] Schenk, U., & Dehlinger, U., *Acta metall.*, 1956, **4**, 7
[151] Zhurakovskiy, Ye. A., & Vaynshteyn, E. Ye., *Izv. Dokl. Akad. Nauk SSSR, O. Khim. Neorg.*, 1959, No. 3, p. 1
[152] Vaynshteyn, E. Ye., Zhurakovskiy, Ye. A., Neshpor, V. S., & Samsonov, G. V., *Dokl. Akad. Nauk SSSR.*, 1960, **134**, 68
[153] Pauling, L., *Proc. R. Soc.* [A], 1949, **196**, 343
[154] Guseva, L. N., & Ovechkin, B. I., *Dokl. Akad. Nauk SSSR*, 1957, **112**, 181
[155] Voronov, B. K., Dudkin, L. D., Kiryukhina, N. I., & Trusova, N. N., *Poroshkovaya Metall.*, 1967, No. 1 (49), 75
[156] Avraamov, Y. S., & Naumani, G., *Neorg. Mater.*, 1967, No. 7, 1170
[157] Schick, H. L., 'Thermodynamics of certain refractory compounds', 1966, Vols I and II (London: Academic Press)
[158] Campbell, I. E., Powell, C. F., Nowicki, D. H., & Gonser, B. W., *J. electrochem. Soc.*, 1949, **96**, 318
[159] Walther, H., U.S.P. 2,313,410
[160] Hoekstra, H. R., & Katz, J. J., *J. Am. chem. Soc.*, 1949, **71**, 2488
[161] Schlesinger, H. I., Schaeffer, G. W., & Barbaras, G. D., *USAEC Rep.*, 1944, No. MDDC-1338
[162] Kubaschewski, O., & Hopkins, B. E., 'Oxidation of metals and alloys', 1962, p. 40 (London: Butterworths)
[163] Pilling, N. B., & Bedworth, R. E., *J. Inst. Metals*, 1923, **29**, 529
[164] Vermilyea, D. A., *Acta metall.*, 1957, **5**, 492
[165] Samsonov, G. V., & Tseitiva, N. Ya., *Fizika Metall.*, 1955, **1**, 303
[166] Moers, K., *Z. anorg. Chem.*, 1931, **198**, 243
[167] Hölbling, R., *Z. angew. Chem.*, 1927, **40**, 655
[168] Teal, G. K., Fisher, J. R., & Treptow, A. W., *J. appl. Phys.*, 1946, **17**, 879
[169] Storks, K. H., & Teal, G. K., U.S.P. 2,441,603
[170] Colton, E., *J. inorg. Nucl. Chem.*, 1961, **17**, 108
[171] Budnikov, P. P., 'Solid state chemistry', 1966, p. 75, translated Shaw, K., 1968 (London: MacLaren)
[172] Jander, W., & Hoffmann, E., *Z. anorg. Chem.*, 1934, **218**, 211
[173] Berezhnoi, A. S., *Ogneupory*, 1954, No. 7, p. 307
[174] Kieffer, R., Benesovsky, F., & Honak, E. R., *Z. anorg. Chem.*, 1952, **268**, 191
[175] Glaser, F. W., & Ivanik, W., *Powder Metall. Bull.*, 1953, **6**, 126
[176] Hüttig, G. F., *Kolloidzeitschrift*, 1941, **97**, 281
[177] Kingery, W. D., 'Introduction to ceramics', 1960, p. 353 (New York: Wiley)
[178] Coble, R. L., *J. appl. Phys.*, 1961, **32**, 787, 793
[179] Coble, R. L., 'Fundamental phenomena in material sciences', 1964, Vol. I (New York: Plenum Press)
[180] Kuczynski, G. C., 'Theory of solid state sintering', 1961 (New York: Wiley; Interscience)
[181] White, J., 'Science of ceramics', *Proc. Br. Ceram. Soc.*, 1962, **1**, 305; *ibid.*, 1965, **3**, 155
[182] Fedorchenko, I. M., & Skorokhod, V. V., *Poroshkovaya Metall.*, 1967, No. 10 (58), 29; 'Progress in inorganic materials', 50th Anniversary Publication, *Akad. Nauk SSSR*, October, 1967, p. 1
[183] Chiotti, P., *J. Am. Ceram. Soc.*, 1952, **35**, 123
[184] Geguzin, Y. E., & Partskaya, L. N., *Poroshkovaya Metall.*, 1967, No. 1 (49), 20; No. 5 (53), 31
[185] Carruthers, T. G., & Wheat, T. A., *Proc. Br. Ceram. Soc.*, 1965, No. 5, p. 259
[186] Wheat, T. A., & Carruthers, T. G., 'Science of ceramics', 1968, Vol. IV, p. 34 (Stoke-on-Trent: British Ceramic Society)
[187] Rice, R., *Proc. Br. Ceram. Soc.*, in the press
[188] Zelikman, A. N., & Loseva, S. S., *Tsvet Metally, Mosk.*, 1947, **20** (4), 41
[189] Zelikman, A. N., & Gorovits, N. N., *Zh. prikl. Khim. SSSR*, 1950, **23**, 689
[190] Wheildon, W. M., & King, A. G., *Ceramic Ind.*, 1967, **88** (6), 56
[191] Glasson, D. R., *J. appl. Chem., Lond.*, 1967, **17**, 91
[192] Samsonov, G. V., & Golubeva, N. K., *Zh. fiz. Khim.*, 1956, **30**, 1258
[193] Münster, A., *Z. Elektrochem.*, 1959, **63**, 807
[194] MacDonald, N. F., & Ransley, C. E., *Powder Metall. Bull.*, 1959, No. 3, p. 172
[195] Webb, W. W., Norton, J. T., & Wagner, C., *J. electrochem. Soc.*, 1956, **103**, 112
[196] Nikolaiski, E., *Z. phys. Chem., Frankf. Ausg.*, 1960, **24**, 405
[197] Hauffe, K., *Wiss. Z. Univ. Greifswald*, 1951–2, **1**, 1
[198] Grunewald, H., *Annln Phys., Lpz.*, 1954, **14**, 121, 129
[199] Tylecote, R. F., & Mitchell, T. E., *J. Iron Steel Inst.*, 1960, **196**, 445
[200] Pollard, F. H., & Woodward, P., *Trans. Faraday Soc.*, 1950, **46**, 190
[201] Dell, R. M., Wheeler, V. J., & McIver, E. J., *Trans. Faraday Soc.*, 1966, **62**, 3591
[202] Kubaschewski, O., *Z. Elektrochem.*, 1959, **63**, 823
[203] Stewart, R. W., & Cutler, I. B., *J. Am. Ceram. Soc.*, 1967, **50** (4), 176
[204] Avgustinik, A. I., Drozdetskaya, G. V., & Ordanyan, S. S., *Poroshkovaya Metall.*, 1967, No. 6 (54), 53
[205] Berkowitz-Mattuck, Joan B., *J. electrochem. Soc.*, 1967, **114**, 1030
[206] Kinna, W., & Rudiger, O., *Arch. Eisenhütt Wes.*, 1953, **24**, 535

[207] Newkirk, A. E., *J. Am. chem. Soc.*, 1955, 77, 4521
[208] Hinnuber, J., & Rudiger, O., *Arch Eisenhüttenwes.*, 1953, **24**, 267
[209] Kieffer, R., Benesovsky, F., Nowotny, H., & Schnachner, H., *Z. Metallk.*, 1953, **44**, 242
[210] Kieffer, R., Benesovsky, F., & Maschenschalk, R., *Z. Metallk.*, 1954, **45**, 493
[211] Kieffer, R., Benesovsky, F., & Schmid, H., *Z. Metallk.*, 1956, **47**, 247
[212] Lublin, P., & Sama, L., *Bull. Am. Ceram. Soc.*, 1967 (Nov.), p. 1083
[213] Kieffer, R., Benesovsky, F., & Schroth, H., *Z. Metallk.*, 1953, **44**, 437
[214] Kieffer, R., & Cerwenka, E., *Z. Metallk.*, 1952, **43**, 101
[215] Kieffer, R., Benesovsky, F., & Gallistl, E., *Z. Metallk.*, 1952, **43**, 284
[216] Fitzer, E., & Schwab, J., *Metall*, 1955, **9**, 1062
[217] Neshpor, V. S., & Sansonov, G. V., *Fizika Metall.*, 1961, **11**, 638
[218] Knapton, A. G., *3rd Plansee Seminar* (1958), 1959, p. 412
[219] Goldschmidt, H. J., 'Interstitial alloys', 1967 (London: Butterworth)
[220] Kubaschewski, O., *Rev. hautes Temp. Refract.*, 1966, **3**, 229
[221] Brewer, L., Sawyer, D. L., Templeton, D. H., & Dauben, C. H., *J. Am. Ceram. Soc.*, 1951, **34**, 173
[222] Brewer, L., Searcy, A. W., Templeton, D. H., & Dauben, C. H., *J. Am. Ceram. Soc.*, 1950, **33**, 291
[223] Agte, C., & Moers, K., *Z. anorg. Chem.*, 1931, **198**, 233
[224] Nowotny, H., & Kieffer, R., *Metallforschung*, 1947, **2**, 257
[225] Norton, J. T., & Mowry, A. L., *Trans. Am. Inst. Min. metall. Engrs*, 1949, **185**, 133
[226] Scholtz, S., 'Special ceramics', *Proc. Symp. Br. Ceram. Res. Ass.*, 1962, p. 293 (London: Academic Press)
[227] Roeder, E., & Scholtz, S., 'Special ceramics', *Proc. Symp. Br. Ceram. Res. Ass.*, 1964, p. 269 (London: Academic Press)
[228] Oudemans, G. J., *Proc. Br. Ceram. Soc.*, 1967, in the press
[229] Dubek, V., Navratil, A., & Miculek, J., *Powder Metall.*, 1966, **9**, 18
[230] Gammage, R. B., & Glasson, D. R., *Chemy Ind.*, 1963, p. 1466; Gammage, R. B., Thesis, Univ. Exeter, 1964
[231] Gillies, D. C., & Lewis, D., *J. less-common Metals*, 1967, **13** (2), 179
[232] Kirk, A., *Chemy Ind.*, 1967, p. 1378
[233] Rose, H. E., *Chemy Ind.*, 1967, p. 1383
[234] Smith, E. A., *Chemy Ind.*, 1967, p. 1436
[235] Podmore, H. L., & Beasley, E. S. C., *Chemy Ind.*, 1967, p. 1443
[236] Groshev, V. I., Maskayev, A. S., Nezhevenko, L. B., & Poltoratsky, N. I., *Poroshkovaya Metall.*, 1967, No. 1 (49), 108
[237] Gregg, S. J., *J. chem. Soc.*, 1946, p. 561
[238] Sartorius-Werke, 'Electrono-vacuum balances', 1963 (Göttingen: Sartorius-Werke, A.-G.)
[239] C. I. Electronics, 'Microforce balances', 1966 (Wimborne, Dorset, England: C. I. Electronics Ltd.)
[240] Gregg, S. J., & Winsor, G. W., *Analyst, Lond.*, 1945, **70**, 336
[241] Brunauer, S., Emmett, P. H., & Teller, E., *J. Am. chem. Soc.*, 1938, **60**, 309
[242] Glasson, D. R., *J. appl. Chem., Lond.*, 1964, **14**, 121
[243] Clements, J. F., & Vyse, J., *Trans. Br. Ceram. Soc.*, 1968, **67**, 285
[244] Ruddlesden, S. N., *Trans. Br. Ceram. Soc.*, 1967, **66**, 587, 599, 607

FORMATION AND REACTIVITY OF BORIDES, CARBIDES AND SILICIDES

II.* PRODUCTION AND SINTERING OF BORON CARBIDE

By D. R. GLASSON and J. A. JONES

The principal methods of boron carbide production are compared and their thermodynamics are examined. Mechanism of carbide formation and sintering of the products are discussed and investigated further.

High-purity stoicheiometric B_4C of submicron size was produced on a semi-technical scale by reduction of diboron trioxide with carbon and magnesium. Rates of sintering were determined from changes in surface areas and average crystallite and aggregate sizes.

Sintering of boron carbide was enhanced by increased temperature and time of calcination. Addition of chromium accelerated sintering at temperatures above 1600 and especially at 1800 . For more extensive sintering, submicron powders from the magnesium reduction process were more suitable than the coarser samples given by the electro-thermal carbon reduction; the latter required ballmilling to provide suitable grain size composition for effective hot pressing.

Introduction

Manufactured boron carbide is an extremely wear-resistant crystalline material (Mohs' hardness 8–9) which can be used as an abrasive.[1] Other applications include neutron absorption by the boron component and as a precursor in the production of metal borides, cf. Part I.[2] Resistance of boron carbide to oxidation is improved by the presence of 15—85% graphite, and such products have been used recently in oxygen process steel converters.[3]

Comparison of production methods

Principal methods for producing boron carbide[2] involve reactions between elemental boron and carbon, boron compounds (such as the oxide) and carbon, alone or partly replaced by magnesium, and boron halides with hydrogen and carbon compounds.

The production of boron carbide from the elements, empirically $4B + C = B_4C$, has a standard free energy $\Delta G^\circ = -14{,}367 + 2{\cdot}275\,T$ cal mole^{-1} B_4C between $T = 800$ and 2500°K.[4] Since both reactants and product are refractory, the reaction proceeds by solid-state diffusion over a wide temperature range; it is slow despite the favourable ΔG and the exothermicity of the reaction. However, ΔG is zero at 3100°K and the carbide loses boron as vapour.

* Part I: preceding paper.

In the reduction of B_2O_3, viz., $2B_2O_3+7C = B_4C+6CO$, $\Delta G^\circ = +397{,}193-215{\cdot}22\,T$ cal mole^{-1} B_4C, making the theoretical initiating temperature 1845°K. This temperature will be reduced at lower pressures since $\Delta G_T = \Delta G^\circ_T + RT \ln p_{CO}$ and ΔG° has a negative variation with T. In practice, the reactants are heated to temperatures above 2400° in an electrical furnace, the reaction being endothermic. When part of the carbon is replaced by magnesium, the reaction $2B_2O_3+6Mg+C = B_4C+6MgO$, has $\Delta G^\circ = -478{,}333+195{\cdot}67\,T$ cal mole^{-1} B_4C, above the b.p. of Mg, 1378°K. A reversal of the reaction is feasible above 2445°K ($\Delta G^\circ = 0$ at 2445°K), but since $\Delta G_T = \Delta G^\circ_T - RT \ln p_{Mg}$, this diminishes as the reaction continues, as ΔG° has a positive temperature variation. After the highly exothermic reaction is initiated, it is self-propagating if there is adequate thermal contact between the magnesium fragments.

The last production method may proceed by alternative routes: (i) $4BCl_3+4H_2+CH_4 = B_4C+12HCl$, (ii) $4BCl_3+8H_2+CCl_4 = B_4C+16\,HCl$, or (iii) $4BCl_3+6H_2+C = B_4C+12HCl$. All are highly exothermic, and once initiated are subsequently self-propagating; carbide formation is favoured at lower pressures.

Mechanism of formation

General information on the kinetics of vapour phase deposition of borides and carbides has been summarised in Part I.[2] Pring & Fielding[5] reduced BCl_3 vapour with an excess of H_2 and deposited boron on a carbon surface at 1500—1750°. At higher temperatures, 1750—1950°, carbide coatings (reported as B_6C) were obtained which became more crystalline and non-adherent as the deposition temperatures were increased further to 2200°. Powell *et al.*[6] also obtained adherent deposits superficially resembling B_4C on Mo and C bases from 1:1 BCl_3 and H_2 mixtures containing about 2 vol.-% toluene vapour at specimen temperatures of 800—1200°. There have been no comprehensive studies of rates of boron diffusion and formation of boride layers on carbon or various metals. Empirically, the coefficient of diffusion of boron in graphite, $D = 3{\cdot}02\exp(-28{,}625/T)$, which indicates that the diffusion of carbon in boron is correspondingly much slower.[7,8] Although B (0·9 Å) is larger than C (0·7 Å), the former has the higher polarisability (first ionisation potentials: B, 8·28 eV; C, 11·41 eV).

In the reduction of B_2O_3 by an excess of C, Samsonov *et al.*[8,9] have demonstrated that there are two consecutive processes: $B_2O_3+3CO = 2B+3CO_2$ above 1640°K, and $4B+C = B_4C$. The newly formed B diffuses through the boron carbide layers progressively formed on the surface of the graphite particles, finally giving boron carbide particles retaining the original shape of the graphite, i.e. there is no penetration of liquid B_2O_3 through the carbide layers. The equilibrium temperature for boron carbide formation according to the total reaction $2B_2O_3+7C = B_4C+6CO$ is about 1400° at 1 atm pressure of CO, allowing for fusion and evaporation of B_2O_3.[10] Volatilisation of boron from boron carbide at higher temperatures, 2300—2500°, leaves carbon as fine filaments and graphite inclusions in the carbide grains. This substantially reduces the abrasiveness and hinders sintering of the material.

Sintering of materials

Sintering of solids is enhanced by increases in temperature and time of calcination, which promote surface and crystal lattice diffusion.[11] These processes are assisted further by the presence of comparatively low-melting additives[12] and by application of pressure (hot pressing).[13] The importance of rational grain-size composition has been discussed also in Part I.[2]

In the present work, finely-divided boron carbide was prepared by reduction of B_2O_3 with C and Mg. Rates of sintering were determined from changes in surface areas and average crystallite and aggregate sizes. These are correlated with temperature conditions during and after boron carbide production. Also, effects of additives and hot pressing were determined.

Experimental

Production of boron carbide

The materials used were magnesium technical grade (Magnesium Elektron), diboron trioxide (Borax Consolidated) and carbon black (Cabot's).

Stoicheiometric proportions of the boron oxide and carbon black were mixed thoroughly by ballmilling. The mixing was continued with an additional stoicheiometric excess of magnesium powder. The completely mixed powder was transferred to an open reaction vessel, and a volatile fuel oil was added to bind the powder and prevent sifting. The mixture was ignited by a glowing fuse wire and the reaction was allowed to continue spontaneously. The burning fuel oil provided a non-oxidising blanket for the reaction and assisted in the propagation; temperatures reached a maximum of 1600°. After complete reaction, the products were allowed to cool overnight. The top crusts of the product were discarded and the remainder were crushed to small size before the magnesia was leached out with dilute sulphuric acid. The boron carbide powder was filtered, washed free of sulphate ion with hot water and finally dried at 120° for 2 h. The yield (allowing for the crust) was better than 90% for batches of about 3 kg.

Sintering of boron carbide

Since boron carbide is oxidised in air at higher temperatures, the samples were sintered *in vacuo*. The furnace consisted of a fused silica tube connected to a high-vacuum system, a single-stage rotary pump and a 3-stage oil diffusion pump. Pressures were monitored using a Penning gauge, and vacuum conditions of better than 2×10^{-5} torr were possible during the heating cycle. The sample was in a pyrolytic graphite crucible inductively heated by a 4 kW radiofrequency heater operating at 450 kHz. The temperature was measured by a disappearing filament pyrometer. Slight outgassing during the first minutes of heating became almost negligible when samples were reheated, particularly at the higher temperatures.

The samples were calcined (A) for fixed times at different temperatures, (B) for various times at each of a number of fixed temperatures. The cooled samples were removed and outgassed at 200° *in vacuo* (where necessary) before determination of their surface areas by the B.E.T. procedure[14] from nitrogen isotherms recorded at −183° on an electrical sorption balance.[15,16]

More extensive sintering, up to 90% of the theoretical density, was achieved by hot pressing. The powder was compacted into a graphite mould fitted with graphite pistons and heated inductively by a 32 kW heater at 450 kHz, while continuous pressure up to a maximum of 3000 kg cm^{-2} was applied during the heating cycle of 1 h. The mould was insulated by a packing of burnt lime. Temperatures up to

1900° were recorded by a thermocouple. The cooled compact was removed easily from the mould and sectioned with a diamond-impregnated saw, before determination of its phase composition and density. For more detailed studies, hot presses designed by Scholtz *et al.* are referenced and discussed in Part I.[2]

Phase composition identification

Samples were examined for phase composition and crystallinity using an emission spectrograph, an *X*-ray powder camera and a Solus-Schall *X*-ray diffractometer (Cu Kα-radiation) with Geiger counter and Panax ratemeter. Certain samples were examined further by optical and electron-microscopes (Philips EM-100).

Results

Emission spectrographic and *X*-ray analysis indicated that the boron carbide was a high-purity stoicheiometric B_4C; batches contained less than 1% free carbon. Trial hot pressings showed a material capable of being sintered to better than 90% theoretical density without any additives. Particle size and shape analysis by *X*-ray line-broadening[17] and electron-micrography indicated sub-micron sizes ranging from 0·01–1 μm and regular shape. This was in accord with gas sorption and surface area measurement.

In Fig. 1, variations in specific surface, *S*, and average crystallite size (equivalent spherical diameter) are shown for boron carbide samples calcined *in vacuo* for different lengths of time at each of a number of fixed temperatures, (a) and (c), and for fixed times of 2 h and 5 h at different temperatures, (b) and (d).

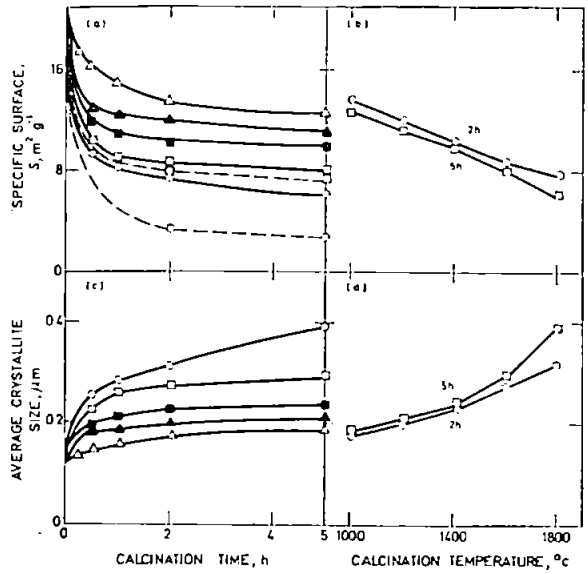

Fig. 1. *Variation of average crystallite size and specific surface of boron carbide with calcination time and temperature*

(a) and (c): △ 1000°, ▲ 1200°, ■ 1400°, □ 1600°, ○ 1800°. Addition of 10% Cr shown by broken lines for 1600° and 1800°
(b) and (d): ○ 2 h, □ 5 h calcinations

Discussion

Formation of boron carbide

Boron carbide from the magnesium reduction method gave an extremely fine powder of submicron size. Nevertheless, the material could be filtered readily after acid leaching and washing. It tended to aggregate in acidic or neutral media, probably because of some acidic oxide coating of the particles. Accordingly, the material could be dispersed readily in alkaline media and then became impossible to filter. The extremely fine granularity is ascribed to the simultaneous and rapid formation of two refractory products, boron carbide and magnesium oxide, at temperatures well below their m.p. (2350° and 2800° respectively). The magnesium oxide inhibits any subsequent sintering of the boron carbide. On the other hand, boron carbide produced by the electro-thermal carbon reduction at very high temperatures is coarse crystalline material, which requires ball-milling to give suitable grain-size compositions for hot pressing effectively. This material has irregular shape and is compacted only with difficulty, requiring much higher temperatures for sintering without additives.

Sintering of boron carbide

The changes in specific surface, *S*, and average crystallite size in Fig. 1 show that sintering of boron carbide was enhanced by increased temperature and time of calcination. Addition of 10% chromium (broken-lined curves) accelerated sintering at temperatures above 1600° and especially at 1800°.

Although boron carbide has approximately the same m.p. as calcium oxide, it sintered much less extensively at 1000–1200°, which is near the Tammann temperature (half m.p. in °K) for lime.[12] Other related ionic compounds also show appreciable crystal lattice diffusion at temperatures of about half m.p. (in °K).[11] The covalent-bond character and crystal structure of boron carbide (discussed in Part I[2]) confer low plasticity and great resistance to sliding on the grain boundaries up to temperatures near to the m.p., combined with a low surface tension in the solid state. At about 1800°, chromium metal completely wets the boron carbide surface.[18] The adhesion between the metal and the carbide is weak, for the chromium can be removed readily from the surface of the carbide cakes. However, it is sufficient to accelerate carbide sintering. No zone of interaction of boron carbide with chromium was found previously,[18] and no crystalline chromium boride or carbide has been detected by *X*-ray examination in the present work. Some graphitisation of carbon has been noted at 1800°, which could have left some boron in solid solution with the remaining boron carbide or chromium. This behaviour of chromium contrasts with that of iron which forms zones of interaction when it accelerates sintering of boron carbide. Other transition metals, e.g. Co and Ni, give similar zones, apparently consisting of carbide and boride alloys of the corresponding metals.[18]

More extensive sintering of boron carbide requires hot pressing, i.e. heating under a pressure exceeding the critical stresses at temperatures relatively close to the m.p.[19,20] Fine powders of less than 0·5–1 μm grain size, as in Fig. 1, hot pressed to almost zero porosity even at 1650—1700° and pressures of about 200 kg cm.$^{-2}$ The boron carbide grains increased to 3–15 μm. The extra cost of the magnesium required to replace part of the carbon for reducing B_2O_3 can be counterbalanced mainly by the simplification of the plant equipment and the elimination of ball milling, besides producing a superior material for sintering.

Acknowledgments

The authors thank Dr. S. J. Gregg and Mr. L. Bullock for their interest and encouragement in this work, and for facilities at the Bullock Research Laboratories; Mrs. M. A. Sheppard for her assistance in the *X*-ray analytical work; the University of London, Imperial Chemical Industries Ltd., and the Science Research Council for grants for apparatus and a S.R.C. Research Technicianship (for M.A.S.).

John Graymore Chemistry Laboratories,
College of Technology,
Plymouth

Received 7 November, 1968

References

[1] Boulton, J. F., & Eardley, R. P., *Analyst, Lond.*, 1967, **92**, 271
[2] Glasson, D. R., & Jones, J. A., *J. appl. Chem., Lond.*, 1969, **19**, 125
[3] Storms, E. K., 'The refractory carbides', Refractory materials monogrs (Ed. J. L. Margrave), 1967, p. 225 (London: Academic Press): U.S.P. 3,284,178
[4] JANAF thermochemical tables, 1960-65, P.B. 168,370 (New York: Dow Chemical Co.)
[5] Pring, J. N., & Fielding, W., *J. chem. Soc.*, 1909, **95**, 1497
[6] Powell, C. F., Oxley, J. H., & Blocher, J. M., 'Vapour deposition', 1966, p. 359 (London: Wiley)
[7] Lowell, C. E., *J. Am. Ceram. Soc.*, 1967, **50** (3), 142
[8] Samsonov, G. V., Markovskiy, L. Ya., Zhigash, A. F., & Valyashko, M. G., 'Bor ego soedineniya i splavy', 1960 (Kiev: Akad. Nauk Ukr. SSR). USAEC translation, 1962, No. 5032 (1), p. 179
[9] Samsonov, G. V., Zagyanskiy, I. L., & Popova, N. V., *Dokl. Akad. Nauk SSSR*, 1950, **74**, 723
[10] Fajana, C., & Barber, S., *J. Am. chem. Soc.*, 1952, **74**, 2761
[11] Hüttig, G. F., *Kolloidzeitschrift*, 1941, **97**, 281
[12] Glasson, D. R., *J. appl. Chem., Lond.*, 1967, **17**, 91
[13] Wheildon, W. M., & King, A. G., *Ceramic Ind.*, 1967, **88** (6), 56
[14] Brunauer, S., Emmett, P. H., & Teller, E., *J. Am. chem. Soc.*, 1938, **60**, 309
[15] Gregg, S. J., *J. chem. Soc.*, 1946, p. 561
[16] Sartorius-Werke, 'Electrono-vacuum balances', 1963 (Göttingen: Sartorius-Werke, A.-G.)
[17] Glasson, D. R., *J. appl. Chem., Lond.*, 1964, **14**, 121
[18] Hamijan, H., & Lidman, W., *J. Am. Ceram. Soc.*, 1952, **35**, 44
[19] Dawihl, W., *Z. Metallk.*, 1952, **43**, 138
[20] Bryjan, E., Missol, W., & Bojarski, Z., *Hutnik, Katowice*, 1956 **23**, 117